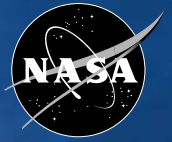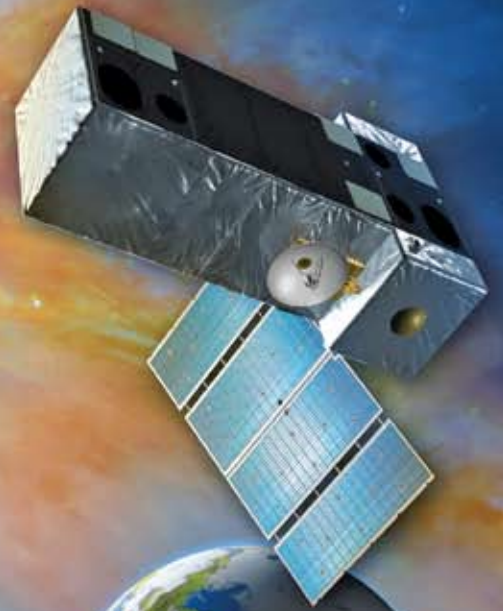National Aeronautics and Space Administration

SIMLite

Astrometric Observatory

From Earth-Like Planets To Dark Matter

NASA

ON THE COVER

The front cover picture is a montage illustrating the project's key science themes.

SIM Lite will search for Earth-like planets, examining over 60 nearby stars for evidence of habitable worlds, and will conduct a survey of young stars as part of a larger effort to map the birth, evolution, and architectures of planetary systems.

SIM Lite will probe the nature of dark matter and its role in the formation of galaxies. Dwarf spheroidal galaxies will be used as test particles to validate models of dark matter distribution in the Milky Way and the Local Group.

SIM Lite will make ultraprecise measurements of stellar masses, luminosities, and ages, testing models of stellar evolution with heightened fidelity and strengthening the theoretical foundation for understanding cosmological galaxy evolution, as we enter the era of the James Webb Space Telescope and large adaptive-optics ground-based telescopes.

SIM Lite will peer into the hearts of active galactic nuclei, probing to within light-days of the supermassive black holes at their cores. This unprecedented accuracy will shed new light on the nature of the accretion disks that surround the core and the relativistic jets that propagate away from them.

The SIM Lite Astrometric Observatory is a 6-m Michelson stellar interferometer. It will be launched into an Earth-trailing solar orbit where it will operate for a mission lifetime of five years.

The back cover shows a framed sextant much like the one used by Tycho Brahe for his astrometric measurements.

SIMLite

EDITORS

John Davidson, *Jet Propulsion Laboratory*

Stephen Edberg, *Jet Propulsion Laboratory*

Rolf Danner, *Northrop Grumman*

Bijan Nemati, *Jet Propulsion Laboratory*

Stephen Unwin, *Jet Propulsion Laboratory*

CONTRIBUTING AUTHORS

Rachel Akeson, *NASA Exoplanet Science Institute*
Ronald Allen, *Space Telescope Science Institute*
Oscar Alvarez-Salazar, *Jet Propulsion Laboratory*
Charles Beichman, *NASA Exoplanet Science Institute*
G. Fritz Benedict, *University of Texas*
David Boboltz, *United States Naval Observatory*
James Bullock, *University of California at Irvine*
Andreas Burkert, *Universitäts-Sternwarte München*
Joseph H. Catanzarite, *Jet Propulsion Laboratory*
Brian Chaboyer, *Dartmouth College*
Rolf Danner, *Northrop Grumman*
John M. Davidson, *Jet Propulsion Laboratory*
Frank G. Dekens, *Jet Propulsion Laboratory*
Stephen J. Edberg, *Jet Propulsion Laboratory*
Alan L. Fey, *United States Naval Observatory*
Debra A. Fischer, *San Francisco State University*
Eric Ford, *University of Florida*
B. Scott Gaudi, *Ohio State University*
Ralph Gaume, *United States Naval Observatory*
Brad Gibson, *University of Central Lancashire*
Douglas R. Gies, *Georgia State University*
Oleg Y. Gnedin, *University of Michigan*
Andrew Gould, *Ohio State University*
Eva Grebel, *University of Basel*
Puragra Guhathakurta, *University of California at Santa Cruz*
Inseob Hahn, *Jet Propulsion Laboratory*
Hugh C. Harris, *United States Naval Observatory*
Amina Helmi, *University of Groningen*

Contributing Authors

Todd J. Henry, *Georgia State University*

Philip A. Ianna, *University of Virginia*

Wei-Chun Jao, *Georgia State University*

Kathryn V. Johnston, *Columbia University*

Kenneth Johnston, *United States Naval Observatory*

Dayton L. Jones, *Jet Propulsion Laboratory*

Pavel Kroupa, *Universität Bonn*

Shrinavas Kulkarni, *California Institute of Technology*

Steven R. Majewski, *University of Virginia*

Valeri Makarov, *NASA Exoplanet Science Institute*

Geoffrey W. Marcy, *University of California at Berkeley*

David L. Meier, *Jet Propulsion Laboratory*

Manuel Metz, *Universität Bonn*

Ben Moore, *University of Zurich*

Mauricio Morales, *Jet Propulsion Laboratory*

David W. Murphy, *Jet Propulsion Laboratory*

Matthew W. Muterspaugh, *University of California at Berkeley*

Bijan Nemati, *Jet Propulsion Laboratory*

Fabien Nicaise, *Jet Propulsion Laboratory*

Roopesh Ohja, *United States Naval Observatory*

Robert Olling, *University of Maryland*

Xiaopei Pan, *Jet Propulsion Laboratory*

Richard J. Patterson, *University of Virginia*

B. Glenn Piner, *Whittier College*

Lisa Prato, *Lowell Observatory*

Andreas Quirrenbach, *University of Heidelberg / NASA Exoplanet Science Institute*

I. Neill Reid, *Space Telescope Science Institute*

Adric R. Riedel, *Georgia State University*

Stuart B. Shaklan, *Jet Propulsion Laboratory*

Michael Shao, *Jet Propulsion Laboratory*

Edward Shaya, *University of Maryland*

Michal Simon, *State University of New York at Stony Brook*

Louis E. Strigari, *Stanford University*

John P. Subasavage, *Georgia State University*

Angelle Tanner, *Santa Barbara Applied Research*

John R. Thorstensen, *Dartmouth College*

John A. Tomsick, *University of California at Berkeley*

Wesley A. Traub, *Jet Propulsion Laboratory*

Stephen C. Unwin, *Jet Propulsion Laboratory*

Roeland van der Marel, *Space Telescope Science Institute*

Ann E. Wehrle, *Space Science Institute*

Guy Worthey, *Washington State University*

Jason Wright, *Cornell University*

Norbert Zacharias, *United States Naval Observatory*

Preface

We are entering a new golden age in astrometry. The European Hipparcos mission measured precision distances and luminosities beyond the closest stars for the first time, and the Gaia survey mission promises to extend our reach out into the Galaxy.

Sky survey telescopes and powerful targeted telescopes play complementary roles in astronomy. The SIM Lite Astrometric Observatory, as a flexibly pointed instrument capable of high astrometric accuracy even on faint targets, is an ideal complement to the astrometric surveys. Under development for more than 10 years, SIM Lite is poised to push the frontier of precision astrometry well out into the Local Group of galaxies.

What has changed since the 1999 predecessor to this volume?

The field of exoplanet research has quickly developed into an amazingly rich field for observers, modelers, and theoreticians alike. Known exoplanets, now numbering over 300, are predominantly gas giants, and we have a few dozen multiple-planet systems. SIM Lite will search for Earth-like planets down to 1.0 $M_\oplus$, examining over 60 nearby stars for evidence of habitable worlds, and will conduct a survey of young stars as part of a larger effort to map the birth, evolution, and architectures of planetary systems.
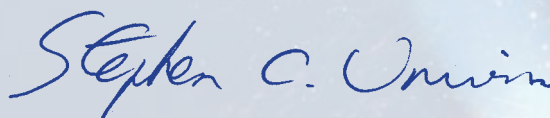
In cosmology and physics, there is now compelling evidence that only 4 percent of the energy density in the Universe can be seen directly. Of the remainder, about 22 percent is thought to be composed of dark matter, nonbaryonic material of unknown character that does not interact with the electromagnetic force but whose presence can be inferred from its gravitational effect on visible matter. SIM Lite will probe the nature of dark matter and its role in the formation of galaxies. Dwarf spheroidal galaxies will be used as test particles to validate models of dark matter distribution in the Milky Way and the Local Group.

As we enter the era of the James Webb Space Telescope and the new ground-based, adaptive-optics-enabled large telescopes, SIM Lite will deliver ultra-precise measurements of stellar masses, luminosities, and ages that will enable astronomers to test stellar evolution models with heightened fidelity. This will strengthen the theoretical foundation for understanding cosmological galaxy evolution based on the findings from these great telescopes.

Active galactic nuclei are now known to have supermassive black holes at their cores, but we still lack a detailed understanding of the nature of the accretion disks that surround the core, or the relativistic jets that propagate away from them. SIM Lite will peer into the hearts of active galactic nuclei, probing to within light-days of the massive black holes at their centers. Precision optical astrometry will shed new light on this mystery.

The SIM Lite Astrometric Observatory will be the first separated-element, phase-stable, visible-wavelength Michelson stellar interferometer operating in space. SIM Lite is a new implementation — more compact, reduced in mass, and more cost-effective — of the concept formerly known as the Space Interferometry Mission (SIM).

Read the original Preface by John Bahcall starting on the next page. The science questions he posed still remain as challenges for observers. To answer them requires a next-generation astrometry mission. The most ancient discipline in astronomy is new again.

Stephen C. Unwin

Stephen C. Unwin
SIM Lite Deputy Project Scientist

Jet Propulsion Laboratory,
California Institute of Technology
Pasadena, California
January 2009

J. N. Bahcall's Preface to the first edition.

The Decade Survey for Astronomy and Astrophysics in the 1990s recommended the development of an interferometric mission to "...achieve a 1,000-fold improvement in our ability to measure celestial positions." The design goal was to measure positions of widely separated objects to visual magnitude 20 with an accuracy of 30 microarcseconds. Our futuristic hope was that the mission might ultimately achieve a precision of 3 µas.

Whatever you do in astronomy, you need to know distances to what you study. Precise distances enable fundamental science that is otherwise impossible. This is the reason the Decade Survey placed such a high priority on the development of a space interferometry mission. I have to confess that this interferometric project was the Decade Survey's most ambitious and challenging recommendation and that many of us wondered if we were not asking for too great a leap from our engineers and scientists. Somewhat to my surprise, an extraordinarily talented team of astronomers and engineers has developed a mature and robust design, informed by ground-based tests, that more than satisfies the Decade Survey recommendations. This achievement guarantees, in my view, great science.

An improvement of a factor of 10 in instrumental sensitivity or precision often leads to major discoveries in astronomy. A thousand-fold improvement in precision is extremely rare and, if recent astronomical history is any guide, seems almost certain to lead to revolutionary discoveries.

This book provides a clear and simple statement of how SIM will work and describes some of the major areas for the scientific studies. Just glance at the topics listed—there is almost certainly something close to your own personal wish list. Here are just a few that make my mouth water: calibrating stellar evolution theory by measuring precisely the distances to stars of many different types with accurately known masses, luminosities, and pulsation characteristics; measuring the masses to better than 1 percent of stars in binary systems; determining the size, rotation rate, and mass distribution of the Galaxy; establishing direct distance measurements to nearby spiral galaxies independent of all intermediate distance indicators; and measuring the peculiar velocities of nearby galaxies that reflect the initial perturbation spectrum and the distribution of mass, dark and visual, in our own neighborhood.

May I offer a suggestion? If you teach a course in astronomy, use this book as a reference text and point out how the accepted theories that you present will be rigorously tested by SIM. Ask the students to propose new research topics that cannot be carried out today because of limitations in astrometric precision. If you do research in astrophysics, take this book as a personal challenge and consider how SIM can be used to resolve fundamental questions in your subject area that today appear unanswerable.

The precision provided by SIM promises to open a vast frontier of precision science.

J. N. BAHCALL
School of Natural Sciences,
Institute for Advanced Study
Princeton, New Jersey,
March 1999

Contents

Executive Summary

Astrometry is the foundation of classical astronomy and modern astrophysics. It is the first step in the transformation of the field from phenomenology to a science that is rooted in precise measurements and physical theory. The history of astrometry spans more than two millennia — from Hipparchus (circa 130 BC) and Ptolemy (150 AD) to the modern CCD-based sky surveys. The improvements in accuracy match this historic time scale. Today, astronomers take for granted resources such as the U.S. Naval Observatory's UCAC survey (2000) with a precision of around 10 milliarcseconds (mas), and the ESA Hipparcos mission, which yielded a catalog of over 100,000 stellar positions measured to an accuracy of 1 mas.

With NASA's SIM Lite mission, we are now ready to take another giant leap in astrometric accuracy, pushing the state of the art by more than two orders of magnitude beyond what is possible today. With this breakthrough in precision, astronomers will be able to secure the rungs of the distance ladder by which they extend their reach throughout the observable Universe.

SIM Lite is a targeted precision astrometric telescope with a single-measurement accuracy of 1.0 microarcsecond (μas) in narrow-angle mode and a *minimum detectable astrometric signature* of 0.21 μas, from magnitude –1.5 to 20. In the wide-angle mode, SIM Lite has an end-of-mission accuracy of 4 μas. It contrasts with survey instruments in that it delivers ultra-high precision on targets that are selectable

Precision Astrometry

SIM Lite will take astrometry from the milliarcsecond (mas) level to the microarcsecond (μas) level. Here are a few benchmarks to relate astrometric precision to astronomical quantities that astronomers care about, such as distance, luminosity, mass, and velocity.

Parallax distance
- A star at 10 pc: 100,000 μas (SIM Lite measures to ~0.04 percent)
- Globular cluster at 10 kpc: 100 μas (SIM Lite measures to ~4 percent)
- M31 (730 kpc): 1.4 μas

Stellar luminosity (assuming perfect photometry)
- Star at 1 kpc: parallax to 5 μas delivers 1 percent accuracy

Astrometric reflex motion of a planet orbiting a G star at 10 pc
- Earth at 1 AU: 0.3 μas (SIM Lite instrument noise floor ~0.035 μas)
- Jupiter at 5 AU: 500 μas
- "Hot Jupiter" at 0.05 AU: 5 μas

Stellar motion
- Velocity of 1 m/s at 10 pc: 21 μas/yr proper motion
- Velocity of 10 km/s at 1 Mpc: 2.1 μas/yr proper motion

and can be observed on a schedule that is matched to the science objectives. In this sense, it has more in common with observatory missions like HST and Spitzer than the survey missions that precede it. This book describes SIM Lite.

In this book, we show the breadth of research areas in astronomy for which precision astrometry is an important and, in some cases, enabling tool for science. Topics range from the search for Earth-like planets orbiting nearby Sun-like stars to uncovering the mysteries of dark matter — and many problems in stellar and galactic astrophysics in between. Astrometry at high precision will surely enable SIM Lite to make some unexpected discoveries among individual objects and classes of objects that it observes.

The SIM Lite Astrometric Observatory

The SIM Lite Astrometric Observatory (hereafter SIM Lite) will be the first separated-element, phase-stable, optical-wavelength Michelson stellar interferometer operating in space. Designed specifically for ultra-high-precision astrometry, SIM Lite will contribute in fundamental ways to a wide range of astro-physical problems. Paramount among these are searching for Earth-mass planets around nearby stars,

SIM Lite Mission and Instrument Performance

SIM Lite instrument and mission parameters

- Baseline length: 6 m
- Wavelength range: 450 to 900 nm
- Telescope aperture: 50 cm
- Mission duration: 5 years
- Orbit: Heliocentric, Earth-trailing

Wide-angle (global) astrometric performance (1σ)

- Reference grid accuracy: 4 µas
- Faint target limit: 20 mag
- Number of grid stars: 1302
- Grid-quasar frame-tie accuracy: 2 µas
- Grid star selection: K-giants at ≈ 1 kpc, V ≈ 10
- Wide-angle field of regard: 15 deg

Narrow-angle (differential) astrometric performance (1σ)

- Single-measurement accuracy: 1.0 µas
- Differential-measurement accuracy: 1.4 µas
- Narrow-field diameter: 2 deg
- Instrument noise floor: 0.035 µas
- Minimum detectable astrometric signature: 0.21 µas at SNR = 5.8
- Minimum detectable planet mass at 10 pc from the Sun: 0.7 $M_\oplus$
    — For a star of 1.0 solar mass orbited by a planet at 1.0 AU
- Planet search capability: at least 60 of the closest FGK stars for 1 $M_\oplus$ planets orbiting in the habitable zone (0.7 to 1.5 AU for a G star)

establishing the locations and architectures of nearby multiple-planet systems, mapping the distribution of dark matter in the Galaxy and the Local Group, and tracing the assembly of the Milky Way over cosmic time. In addition, SIM Lite will inaugurate an era of precision stellar astrophysics, provide a fundamental stellar reference frame, and measure the motions of quasar jets in visual wavelengths. These and many other problems in modern astrophysics will be addressed by SIM Lite and are described in the chapters to follow.

SIM Lite has an impressive historical pedigree. When the 1990 Decadal (Bahcall) Report laid out the science case for an "Astrometric Interferometer Mission," it was not certain that the required optical precision was achievable, though the prospects for stellar astrophysics and giant-planet discovery were strong motivations. Ten years later, a carefully crafted technology development plan was not only in full swing, it had already shown us the way to exceed the goals of the Bahcall Report. This encouraged the 2000 Decadal (McKee-Taylor) committee to recommend a mission that could find not only giant planets but also rocky planets. SIM Lite will have the capability not just to detect rocky planets but to conduct an exhaustive search of the nearest 60 or so nearest Sun-like stars for planets as small as one Earth mass orbiting in the "habitable zone."

Is the astrometric science advocated by the Bahcall and McKee-Taylor reports still waiting to be done? Is it still interesting? The science themes laid out in this book emphatically answer "yes" to both questions. Astrometric science at the microarcsecond level is a new and incredibly rich field; SIM Lite will explore, but certainly not exhaust, the science in this huge discovery space.

Why space astrometry? Because the distortions inherent in propagation of light through the atmosphere present a fundamental limitation in reaching microarcsecond accuracy, especially over wide fields. The next advance in astrometry requires the stable environment offered by a space-based platform, with limitations imposed only by the design of the instrument, its sensing and control algorithms, and observing and calibration techniques.

SIM Lite started in 1996 as a mission concept, and is now a fully mature design, having nearly completed NASA's Formulation Phase: it is essentially ready to enter Implementation Phase. This design is a new implementation — more compact, reduced in mass, and more cost-effective — of the concept formerly known as the Space Interferometry Mission (SIM). It was made possible by the success of a technology development program carried out over 10 years and involving five hardware major testbeds. The technology program, with a series of milestones that were independently reviewed, was formally completed in 2005.

Six Themes Spanning Science and Technology

This book is organized into six "Themes," spanning the science and technology of SIM Lite. The first four themes summarize the main science topics for SIM Lite. The fifth theme describes a General Observer Program through which new investigators will share in the promise of SIM Lite, and it includes representative "design reference missions" for possible programs. The sixth theme explains the SIM Lite instrument, and shows how the completed technology program validates the expected performance of the instrument.

SIM Lite Science Investigations

Theme I. The Search for Habitable Worlds

- A Search for Earth-Mass Planets in the Habitable Zones of Nearby Stars (Chapter 1)
- Young Stellar Systems, Their Birth and Evolution (Chapter 2)
- Planetary System Architectures (Chapter 3)

Theme II. Dark Matter and the Assembly of Galaxies

- The Distribution of Dark Matter in the Milky Way and Local Group (Chapter 4)
- The Role of Dark Matter in the Formation of Galaxies (Chapter 4)
- Dark Matter: What Is It? (Chapter 4)
- Measuring Masses of Compact Galactic Objects with Microlensing (Chapter 5)
- Rotational Parallax: Luminosity-Independent Extragalactic Distance Measurement (Chapter 6)
- The Formation History of the Milky Way (Chapter 7)

Theme III. Precision Stellar Astrophysics

- The Physics of Exceptional Stars, from Massive Type O Stars to White Dwarfs (Chapter 8)
- Compact Object Astrophysics: Black Holes, Neutron Stars, and X-Ray Binaries (Chapter 9)
- Cepheid Science and the Extragalactic Distance Scale (Chapter 10)

Theme IV. Supermassive Black Holes and Quasars

- What Powers Quasars? (Chapter 11)
- Inertial Stellar Reference Frame Science (Chapter 12)

Theme V. Charting the Uncharted Waters

- New Concepts for Research with Ultra-Precise Astrometry (Chapter 13)
- A General Observer Program: Sharing the Promise of SIM Lite (Chapter 14)

Theme I. The Search for Habitable Worlds

SIM Lite will conduct a definitive search for Earth-mass planets in the "habitable zone" of solar-type stars. It will have the ability to search at least 60 of the closest such stars. The mass of a planet is of course its most fundamental property, and SIM Lite measures masses definitively, resolving the sin *i* ambiguity in RV measurements. Searching the closest stars is important, because these are the stars for which follow-up spectroscopy of their planets will be possible. Spectroscopy is the next step after discovery, and the challenges of imaging and spectroscopy will be greatly eased by a verified target list resulting from SIM Lite's survey. SIM Lite will also determine precision orbits; these are especially interesting for multiple-planet systems, which may not be coplanar — factors that bear on questions of their origins and the habitability of their planets. SIM Lite will chart the full suite of planets from Earth-size rocky bodies through ice giants

SIM Lite will search for Earth-mass planets in the habitable zones around the nearest 60 solar-type stars — a capability unmatched by any existing instrument or instruments currently in development.
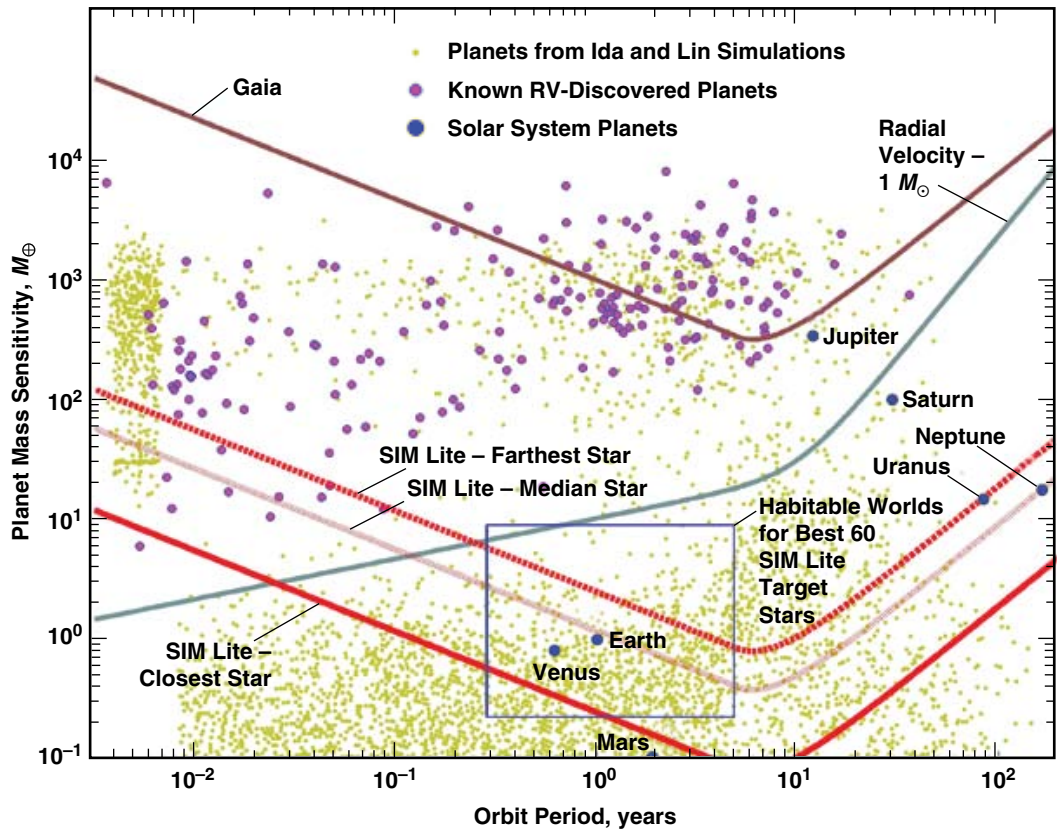
to gas giants and it will provide extensive architectural details for planetary systems around the nearby stars. In this field, SIM Lite has no competition; not now, not in the coming decade. In addition, SIM Lite is also the technology precursor to future missions to image the planetary systems SIM Lite will discover.

SIM Lite will also search for planets around young stars. SIM Lite's ability to measure 12th- to 14th-magnitude stars with a single-measurement accuracy of 4 μas will provide a unique and urgently needed probe of protoplanetary systems. The study of planets orbiting stars that are considerably younger than the Sun bears directly on questions of the genesis of planetary systems. Rapid rotation and active photospheres of the young stars themselves largely preclude planet detection by the Doppler and transit techniques that have been so fruitful for more mature stars. Astrometry with SIM Lite offers our best observational opportunity to find gas giants and icy planets orbiting stars ranging in age from 2 to 100 Myr at distances from 30 to 140 pc. SIM Lite will survey classical and weak-lined T Tauri stars looking for such giants at orbital distances from 1 to 5 AU. It provides the determination of mass and orbital properties needed to confront theories of planet formation with new data.

Recently, a few objects that have been imaged are located many tens of AU from their hosts. They are certainly substellar, but their masses are highly uncertain (planet or brown dwarf) since little dynamical information is possible at such great orbital separations and the estimates are subject to large uncertainties in model assumptions. Microarcsecond measurements made over SIM Lite's mission duration can help reduce these uncertainties.

Multiple-planet systems are expected to be common, and sorting out their constituents is an essential requirement for any planet detection technique. SIM Lite has been subjected to an extensive series of "double-blind" simulations designed to test its ability to find multiple planets and, in particular, to detect Earths in the presence of other planets. Four independent teams worked on realistic data generated by a

fifth team. The most successful of the teams detected essentially every planet that they should have, from a signal-to-noise perspective. The results are summarized in Chapter 3, but the important conclusion is that SIM Lite is not limited in capability for most multiple-planet systems. No other mission in a similarly advanced state of readiness as SIM Lite will provide this kind information on multiple planet systems. Furthermore, with a flexibly pointed instrument, the observer always has the option of allocating additional resources to the most "interesting" systems. A true analog of our Solar System would be worth the investment to characterize masses and orbits fully.

SIM Lite will not only discover rocky planets and ice giants orbiting within a few AU of nearby stars (complementing the gas giants found around those same stars by RV and transit surveys), it will provide masses and full 3-D orbits for planets in each system, including orbital inclinations and eccentricities, thus establishing the major components and structure of planetary systems. Full orbital parameters are essential inputs to any study of the stability and evolution of multiple-planet systems: co-planarity is a convenient but unjustified assumption in current analyses. SIM Lite will also provide a statistically meaningful census of typical planetary system architectures around stars within 20 pc of the Sun.

Theme II. Dark Matter and the Assembly of Galaxies

What is the dark matter made of? How is it distributed in galaxies and groups of galaxies and how did it get that way? How does this distribution differ from that of the luminous matter and why? Is the process of galaxy formation from luminous and dark matter complete, or is it still ongoing? These important questions lie at the heart of modern cosmology and galaxy formation. SIM Lite will play an essential role in providing answers to them.

The concordance Cold Dark Matter (CDM) model for the formation of structure in the Universe has been remarkably successful at describing the observations of structure on large scales. However, it does not do as well with observations on galaxy scales. Fortunately, CDM models and their various proposed alternatives offer a rich variety of testable predictions that make the Local Group and our own Milky Way galaxy key laboratories for exploring dark matter (DM) in this regime. Some of the most definitive tests of local DM require measurements of proper motions to microarcseconds per year on distant faint stars moving under the influence of gravity from both luminous and dark matter — measurements that are uniquely the domain of SIM Lite.

SIM Lite will constrain dark matter particle mass by measuring the motions of stars in Local Group dwarf spheroidal (dSph) galaxies. These are critical laboratories for testing CDM on galactic scales. Astrometric motions measured with SIM Lite, combined with RV, probe the shape of the gravitational potential. A cusp is indicative of cold and massive particles, indicative of CDM. A core is indicative of the warm light particles of "WDM." Radial velocities alone cannot resolve the problem. Determining the dark matter density profile requires measuring velocity anisotropy of stars, with proper motions to about 7 km/s on roughly 200 stars per galaxy. These translate to roughly 15 µas/yr measurements at 19th mag. SIM Lite candidates include the Draco, Sculptor, Ursa Minor, Sextans, and Boötes dSph galaxies for these measurements.

Hypervelocity stars are another probe of dark matter, but on the scale of the potential of our Milky Way. A handful have been found recently, and with galactocentric velocities of >> 600 km/s they must have been ejected from close to a supermassive black hole at the center of the Galaxy. Their 3-D motions provide a means of measuring the shape of the total mass distribution to large distances. SIM Lite will provide the

Precision proper motions of stars in dwarf spheroidal galaxies made by SIM Lite will distinguish between the signatures of competing models of cold and warm dark matter. Only SIM Lite can measure these faint stars to sufficient precision.
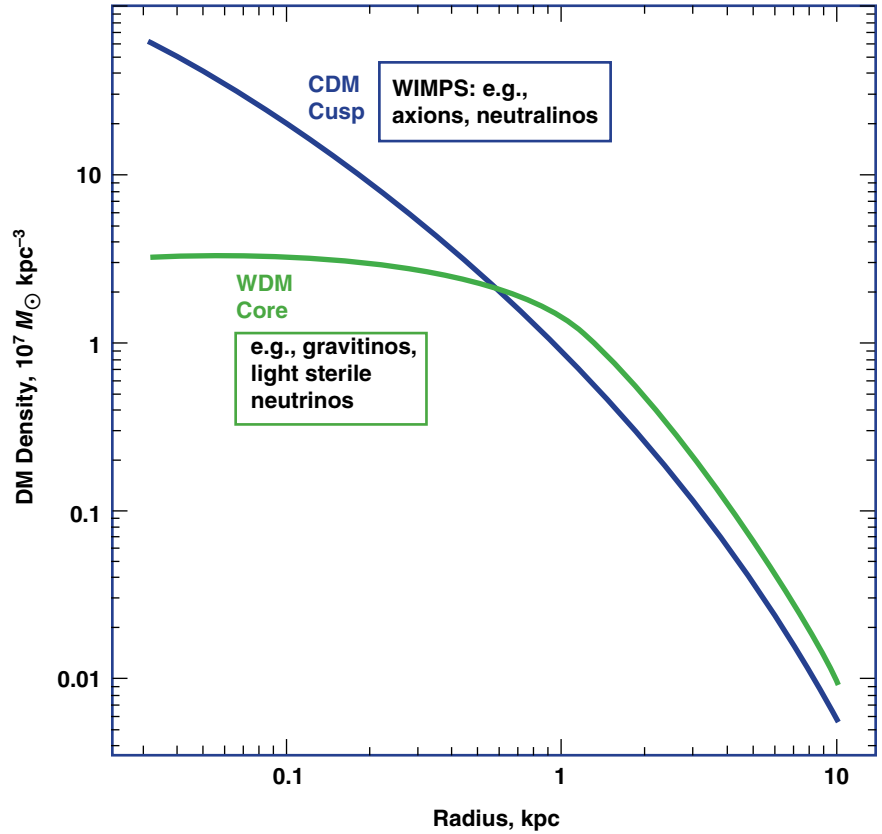
Tidal tails of dwarf spheroidal galaxies encode the history of encounters with the Milky Way. SIM Lite measurements of proper motions in these dynamically cold systems can be used to test our understanding of the formation and evolution of galactic halos.
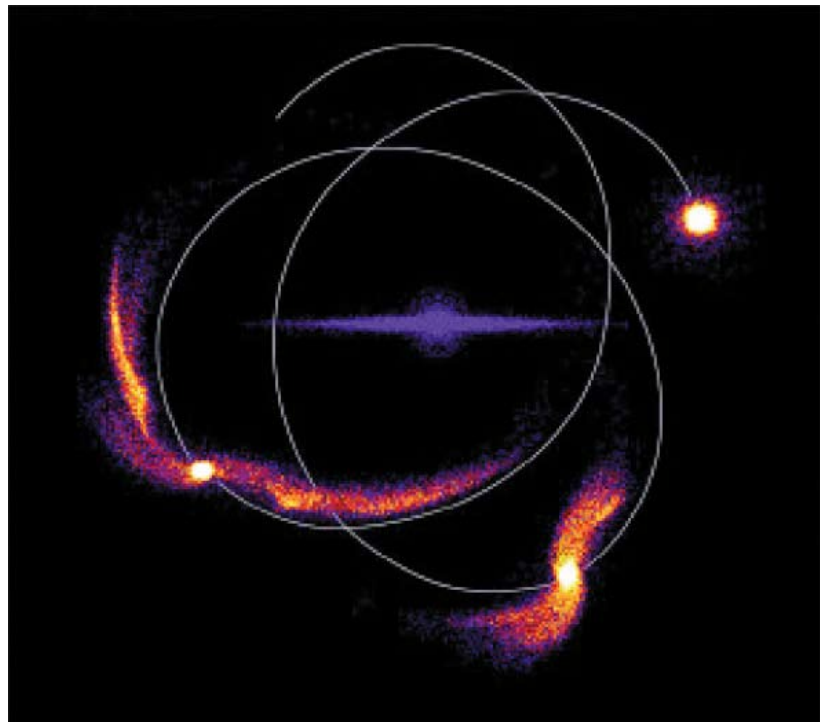
precision distances and proper motions on the individual stars needed for this determination. SIM Lite could extend such a study to the LMC and M31 and identify supermassive black holes if they are also present in those galaxies.

SIM Lite will study the assembly of galaxies by measuring stellar motions in tidal streams around the Galaxy. Streams have already been identified out as far as 100 kpc and they trace the total mass distribution at all radii in the Galaxy. In some, the motions may be irregular, due to clumping of dark matter. These clumps may be a new structural feature of the dark matter distribution. SIM Lite will also measure the motions of newly discovered ultra-faint satellite galaxies of the Milky Way. CDM predicts that these dSph galaxies fell into the Local Group recently, and as such, their motions should be different from those of older accretion events.

We have a reasonable census of luminous objects in the Galaxy, from giant stars at the top to very nearly the bottom of the main sequence. But the populations of dark or very dim objects in the Galactic disk and bulge remain poorly constrained. SIM Lite observations of Galactic gravitational microlensing events will directly probe this unseen population, conducting a representative census of all compact Galactic objects from brown dwarfs to black holes, including white dwarfs, neutron stars, and main-sequence stars. The masses of these objects will be derived from a combination of precise measurements of the tiny astrometric deflections that are generated by all microlensing events and a photometric "microlens parallax" (see Chapter 5). The latter is possible because SIM will be in solar orbit, which means that it measures a "different" photometric event compared to what is seen from the ground.

Globular clusters and Population II stars are the fossil remnants of the first major epoch of star formation in the Milky Way. SIM Lite will determine precise distances to selected Pop II objects to define a reliable distance scale and thereby establish reliable absolute and relative ages. Those ages set a minimum age for the Universe and permit us to map the early formation history of the Milky Way (see Chapter 7). SIM Lite will establish absolute distances for 35 globular clusters, especially distant clusters, spanning a range of metallicity. This will allow age measurements with accuracy better than 10 percent and constrain both the absolute age and the distribution of ages of globular clusters.

Theme III. Precision Stellar Astrophysics

What is the mass of the largest star? The smallest one? What is the mass of a neutron star? Can we directly measure the mass of a stellar-remnant black hole? SIM Lite's reach across the Galaxy will provide precise distance measurements of objects that are rare, and SIM Lite's ability to stare at its targets provides precision distances to objects that are faint. SIM Lite will provide fundamental data at both of these extremes and usher in a new era of precision stellar astrophysics.

Stellar astronomy relies primarily upon two "maps": the Hertzsprung-Russell (HR) diagram and the Mass-Luminosity Relation. Because of its reach into the Galaxy and its flexible observing modes and timing, SIM Lite can add great details to both of these crucial stellar maps. For the HR diagram, SIM Lite will pinpoint the distances to the rare, massive O/B stars, to supergiants and variable stars, and to the central stars of planetary nebulae. For the Mass-Luminosity Relation, SIM Lite will provide unparalleled mass determinations for stars in fundamental clusters, from the massive O/B stars to subdwarfs and white dwarfs. With a high-quality distance in hand, astronomers will finally have accurate luminosities and can place O stars on the HR diagram with confidence. The goal for SIM Lite is stellar masses to 1 percent, needed for any serious challenge to models of stellar structure. Current errors are much larger — embarrassingly
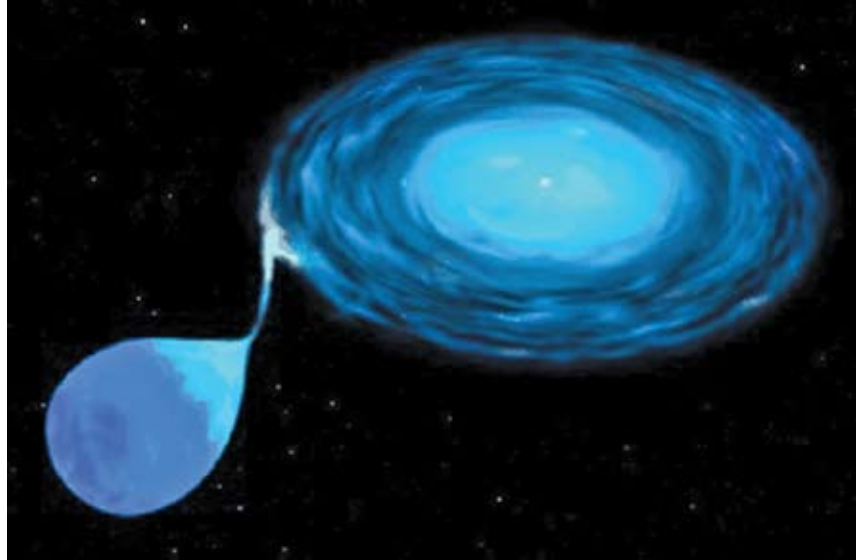
large, really, for such a simple parameter — and they preclude tests of models that distinguish the effects of age and metallicity on the luminosity of a star of given mass. Fundamental stellar astrophysics is enabled by precise measurements of the relevant quantities — in this case, stellar masses and distances with SIM Lite.

Black holes and neutron stars are fascinating objects with great potential for testing physical theories in extreme conditions. The gravitational fields near these objects provide an opportunity for tests of General Relativity in the strong-field limit and the properties of matter at the remarkably high densities that exist within neutron stars are unknown. Many of these objects are in binary systems where accreting matter from the stellar companion provides a probe of the compact object. But a main difficulty in making measurements that lead to definitive tests has been uncertainty about basic information such as distances to the sources, orientations of their binary orbits, and masses of the compact objects. Through astrometry, SIM Lite will, for the first time, be able to obtain precise distances and proper motions for dozens of these systems and will also be capable of mapping out orbital motion, leading to direct compact object mass measurements.

Obtaining such information is critical for a wide variety of investigations that range from probing the space-time around the compact object to constraining the origin and evolution of the systems themselves. SIM Lite will make fundamental contributions to establishing the neutron star equation of state, determining the properties of accretion disks around black holes and neutron stars to probe strong gravity, and determining where X-ray binaries were born and how their compact objects were formed. Only SIM Lite can provide accurate distances to these optically faint (V > 17) and distant (5 to 10 kpc) targets, as well as proper motions to the required precision.

Theme IV. Supermassive Black Holes and Quasars

Giant black holes in the central regions of galaxies push out enormous bursts of matter into jets that are visible at a wide range of wavelengths from X-ray to radio. The mechanism, which lies at the heart of this phenomenon, operates deep in the nuclear regions of the galaxy where a giant black hole is thought to be in some way responsible. Studying the details of the structures surrounding the black hole requires a

SIM Lite and Gaia

SIM Lite and Gaia are both astrometric missions. Gaia is an all-sky survey mission currently under development by the European Space Agency. Are both needed? The answer is emphatically yes, for two reasons. First, the advent of microarcsecond-level astrometric precision opens up a wide array of topics in astrophysics for which astrometry can now play a major role. Far from being a specialist technique, astrometry is once again becoming a fundamental tool for astronomy. Second, these missions are complementary in a way that every astronomer appreciates: Gaia is a broad-survey instrument and will fly first. SIM Lite is a powerful, sensitive, pointed instrument that will build on the results from Gaia.

Is there science overlap between SIM Lite and Gaia? The simple answer is — surprisingly little (see figure). This is because the SIM Lite science program is designed to complement, not duplicate, Gaia science. In general, Gaia will pursue those programs for which the science is derived from measurements of an ensemble of a very large number of targets. SIM Lite will focus on science that requires the highest precision on individually selected targets. Many examples can be found in this book. Two of these are the search for Earth-like planets orbiting the closest Sun-like stars and probing the Galactic potential by measuring the trajectories of individual hypervelocity stars.

This book concentrates on the SIM Lite science case, but discusses the role of Gaia and other missions in each section where the contributions of each are explained in more detail and in the proper scientific context.

Wide-Angle SIM Lite Measurements by Object Type
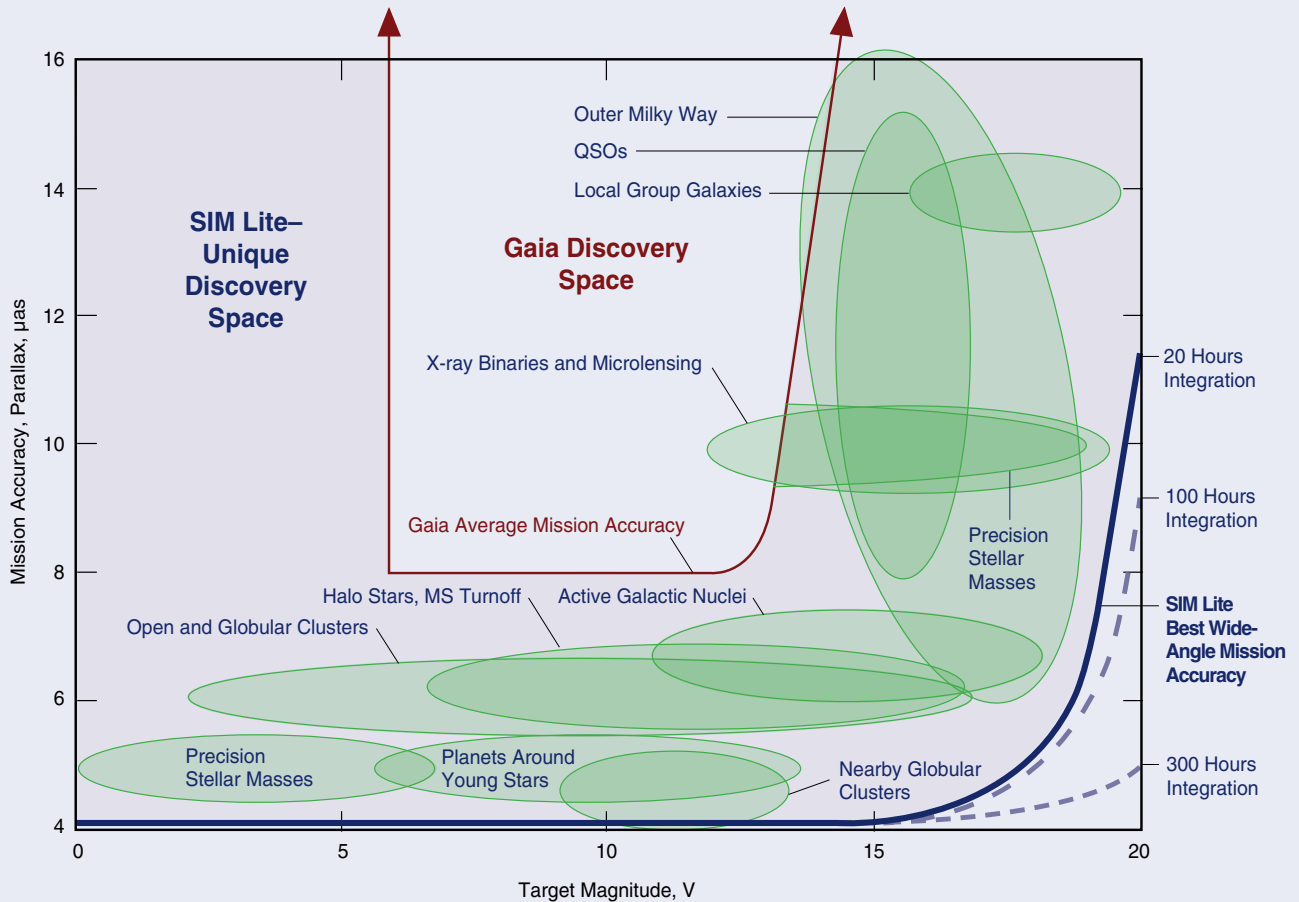
level of angular resolution that is presently reached only with difficulty using VLBI — very long baseline interferometry — in the radio. Measurements on these size scales at vastly shorter wavelengths (optical) would provide fundamental new insight into the emission mechanism, and its spatial extent.

SIM Lite is capable of such measurements, not through direct imaging of the quasar, but via precision astrometry of the quasar's nucleus. The same instrument that can measure the reflex motion of a star due to an orbiting planet can detect the apparent position shift due to activity in, say, a quasar. Taking advantage of SIM Lite's flexible schedule allows correlations between various measurements to be made, which in turn provide stringent tests of physical models. Multiband photometry, polarimetry, VLBI imaging, X-ray and gamma-ray monitoring — and SIM Lite astrometry — all play a role. Proper motions of the brightness centroids are related to the origin of relativistic jets and the accretion disk around the central supermassive black hole.

SIM Lite can also measure an astrometric color shift, itself a vector quantity on the sky, and possibly variable. Its direction and orientation form a direct test of the relative contributions of different physical components in an active galactic nucleus (AGN) as they have very different spectra.

SIM Lite will permit the establishment of an optical inertial reference frame based on a grid of Galactic stars anchored to distant quasars, allowing for the first time the direct detection of the motion of the Solar System within the Milky Way as well as the motion of the Local Group toward the Virgo cluster. By establishing an accurate link between SIM Lite's optical inertial reference frame and the present standard radio frame, high-resolution imaging data at these different wavelengths can be accurately lined up for comparison, at an accuracy of about 2 to 4 µas; the current state of the art is around 300 µas. The final reference frame will supersede the current ICRF standard, and will remain as a lasting legacy of the mission.

Theme V. Charting the Uncharted Waters

SIM Lite will have a substantial General Observer (GO) program. Approximately half of the science observing time will be allocated in this way. The SIM Science Team, selected through a NASA AO in 2000, has Key Projects that address many, but by no means all, aspects of the astrometric science described in this book. Indeed, one of the objectives of this book is to encourage members of the community to think of how they can use precision astrometry with SIM Lite in their research.

The General Observer (GO) program will enable researchers in the astronomy community to share in the promise of precision astronomical science by carrying out their own research projects with SIM Lite. A proposal call is expected one to two years before launch. The GO program will likely encompass a range of proposed programs, from projects comparable in size to the Key Projects, down to studies of just a handful or even a single object. For simple parallax or proper motion measurements, the scheduling and data analysis would largely be provided as a service to the user by the NASA Exoplanet Science Institute (NExScI). The program will operate in a fashion similar to those put in place for other NASA missions of comparable cost and capability.

What new science is there for SIM Lite to do? In April 2008, the SIM Lite Project and NExScI issued a proposal call for studies to answer exactly this question. The objective was to enhance the science return from SIM Lite by supporting studies that will lead to new concepts and approaches for research using SIM Lite. The results are summarized in Chapter 13. An independent peer-review panel selected a total of 19 one-year studies, spanning a wide range of science topics including truly novel experiments that SIM Lite could perform.

We describe three versions of a possible SIM Lite GO program, understanding that a peer-reviewed competition will of course determine the actual use. These variants arise from different assumptions about science priority. The first takes a broad view of the science of precision astrometry, with about half the available science time, about 31 percent of the five-year mission, set aside for a GO program. Another version commits most of the available science time to the quest for habitable worlds, with about 10 percent of the mission set aside for an unrestricted GO program. The preferred version also places its emphasis on exoplanets, but preserves the astrophysics Key Projects. The GO program remains at 31 percent of the five-year mission, but a majority of this time is earmarked for exoplanet studies. With several years to launch, and with anticipated science advances in the intervening time, these three variants should be regarded as illustrative of the strength of SIM Lite's expected contributions to astrophysics.

Theme VI. Project Technology Readiness

Based on the NRC recommendations of the 1991 and 2000 Decadal Surveys, astrometric measurement requirements and goals were specified. In response, a challenging technology program was established by NASA that included technology milestones with specific, measurable objectives and due dates. The milestones were all met with performance at or exceeding that required to achieve NRC goals and were completed on schedule. The program was so successful that the expected performance of the original SIM PlanetQuest exceeded the NRC goals by 40 percent in single-measurement and mission accuracy. This allowed implementation of the design in the more compact form of SIM Lite, while retaining performance at the level of the NRC goals.

The highlights of this amazing technology story are told in Theme VI of this book, where a description is presented of the design of the SIM Lite instrument and the laboratory subsystem testbeds on which the demonstrations of performance took place. Although SIM Lite is a complex mission, the completion of this development program has demonstrated that project technology is ready for entry into Phase C/D.

The STB-3 testbed, one of a series of testbeds in the SIM Lite technology program, emulates the full instrument functionality and features a realistic flight-like flexible structure.
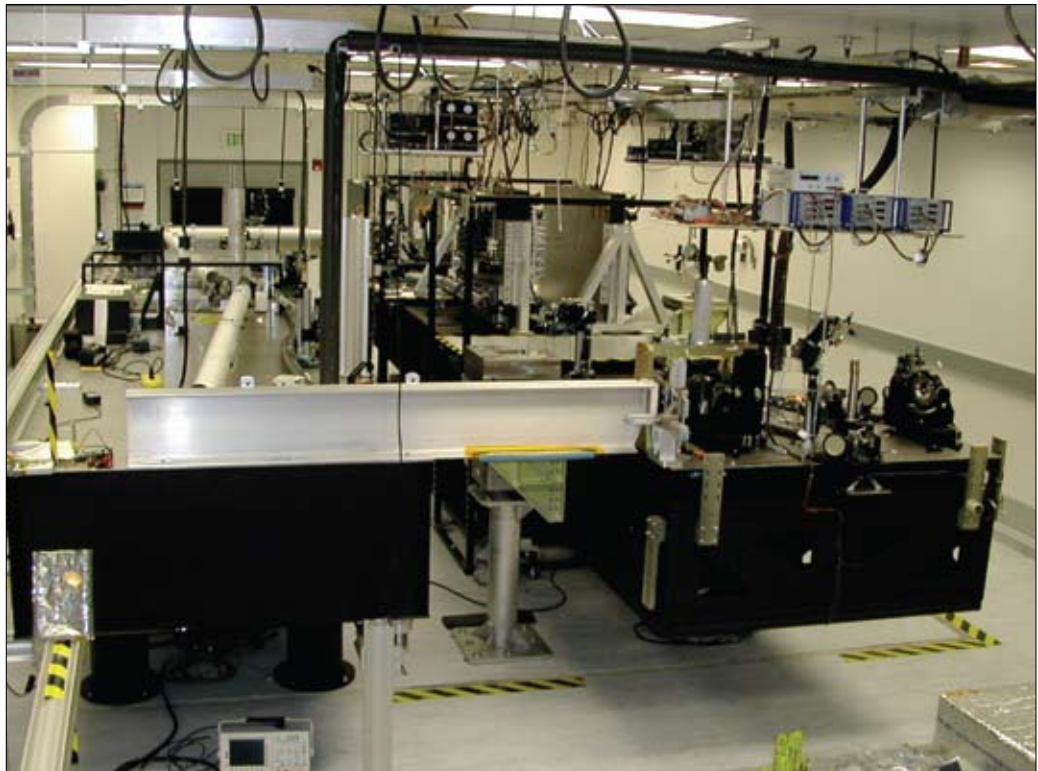
SIM Lite and the Future of Space Astrophysics

Fifty years ago, the new science of radio astronomy faced "Grand Challenge" problems that required order-of-magnitude improvements in the angular resolution achievable with radio telescopes. These included understanding the cosmology of the Universe using counts of radio sources and understanding the physical origin and evolution of radio galaxies. Only phase-stable, separated-element interferometry was capable of providing the required angular resolution, sensitivity, and imaging capability. Major new instruments like the Cambridge One-Mile and 5-km radio telescopes, the Westerbork Synthesis Radio Telescope, and the Very Large Array were built to address these Grand Challenges. These instruments in turn were used to investigate a wide range of astrophysical problems, some of which even eclipsed the original grand challenges themselves.

In the same spirit, we presently face new grand challenges of equal importance. These include the search for habitable worlds and understanding the nature and distribution of dark matter and its role in the assembly of galaxies. No space- or ground-based instrumentation presently available can provide either the astrometric precision or the imaging angular resolution ultimately required to effectively address these challenges. A phase-stable, scalable, precision optical interferometer in space is needed to address them. SIM Lite is just such an interferometer.

Besides its essential role in addressing the grand challenge problems of astrophysics today, SIM Lite is also a technology pathfinder for the future. In the next decade, SIM Lite will demonstrate routine, long-term operation of a phase-stable, separated-element, optical interferometer in space and pave the way for new generations of telescopes for space astrophysics in the decades to come.

Major instruments such as the Very Large Array have investigated a wide range of astrophysical problems. SIM Lite will address a new series of questions, including the search for habitable worlds and understanding the nature and distribution of dark matter.
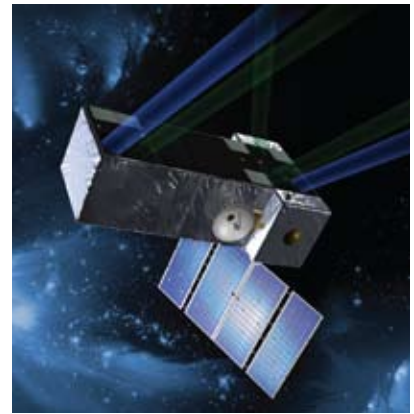
The Search for Habitable Worlds

Do Earth-like planets exist in the habitable zones of Sun-like stars within 20 pc?

What are the masses and mass distributions of exoplanets?

Are planetary orbits co-planar?

How do multiplanet systems evolve?

What is the frequency of planets for stars of different mass? Among binary stars? Stars with dust disks? Evolved stars and white dwarfs? Stars with planets found with radial velocity surveys?

Is a high abundance of heavy elements correlated with giant planet formation? With rocky planets?

Are multiple fragmentation events or core accretion in a dense disk responsible for the formation of planets?

Detecting
1 Earth-Like Planets

Geoffrey W. Marcy (UC Berkeley), **Michael Shao** (JPL), **Matthew W. Muterspaugh** (UC Berkeley), **Charles Beichman** (NExScI), **Debra A. Fischer** (SFSU), **Eric Ford** (University of Florida), **Joseph H. Catanzarite** (JPL), **Robert Olling** (University of Maryland), **Shrinavas Kulkarni** (Caltech), and **Stephen C. Unwin** (JPL)

ABSTRACT

Astrometry is the only known technique for detecting planets of Earth mass in the habitable zone around solar-type stars within 20 pc. These Earths are close enough for follow-up observations to characterize both the planets and dust disks by infrared imaging and spectroscopy with planned future missions such as the James Webb Space Telescope (JWST) and the Terrestrial Planet Finder/Darwin. Employing a demonstrated astrometric precision of 1 μas and a noise floor under 0.1 μas, SIM Lite can make multiple astrometric measurements of the nearest 60 F,- G-, and K-type stars during a five-year mission to detect the ~0.3 μas amplitude induced by a benchmark Earth-mass planet orbiting in the habitable zone (1 AU) about a solar-mass star at 10 pc. SIM Lite can detect rocky planets in a broad range of masses and orbital distances, and it will measure their masses and three-dimensional orbital parameters, including eccentricity and inclination, to provide the properties of terrestrial planets in general. The masses of both the new planets and the known gas giants can be measured unambiguously, allowing a direct calculation of the gravitational interactions, both past and future. Such dynamical interactions inform theories of the formation and evolution of planetary systems, including the Earth-like planets. Thus, SIM Lite directly tests theories of rocky planet formation and evolution around Sun-like stars and identifies the nearest potentially habitable planets for later spaceborne imaging, e.g., with Terrestrial Planet Finder and Darwin. SIM was endorsed by the two recent Decadal Surveys and it meets the highest-priority goal of the 2008 AAAC Exoplanet Task Force.

1.1 Introduction to Exoplanets: Toward Rocky Worlds

The past decade has seen the discovery of over 300 exoplanets, found by precise Doppler measurements, transits, and microlensing. The known exoplanets have masses from ~10 $M_{Jupiter}$ down to nearly 5 $M_{\oplus}$. The M sin (i) distribution of Doppler-detected exoplanets (Figure 1-1) reveals increasing numbers of planets with decreasing mass in the Jovian domain. But for lower masses, below a Saturn-mass (0.3 M_{Jup}), there is an apparent decline in the number of planets with decreasing mass. This apparent paucity of low-mass planets is almost certainly an artifact of sensitivity, as the Doppler technique struggles to detect lower-mass planets. Thus, we have reached a roadblock in planetary science and astrobiology. Without knowledge of the occurrence rate or properties of terrestrial planets, the confluence of geology, astrophysics, and biology remains poorly informed.

Figure 1-1. Distribution of minimum masses, M sin (i), for known exoplanets, on a log mass scale. The rise of jovians toward lower masses is real, implying more Saturns than super-Jupiters. But the decline in the sub-Jupiter domain toward lower masses is likely an artifact of the declining sensitivity to low-mass planets by the Doppler technique. Detecting Earth-like planets around nearby Sun-like stars requires a space-borne astrometric mission. Blue represents planets orbiting within 0.1 AU; red represents planets beyond 0.1 AU.
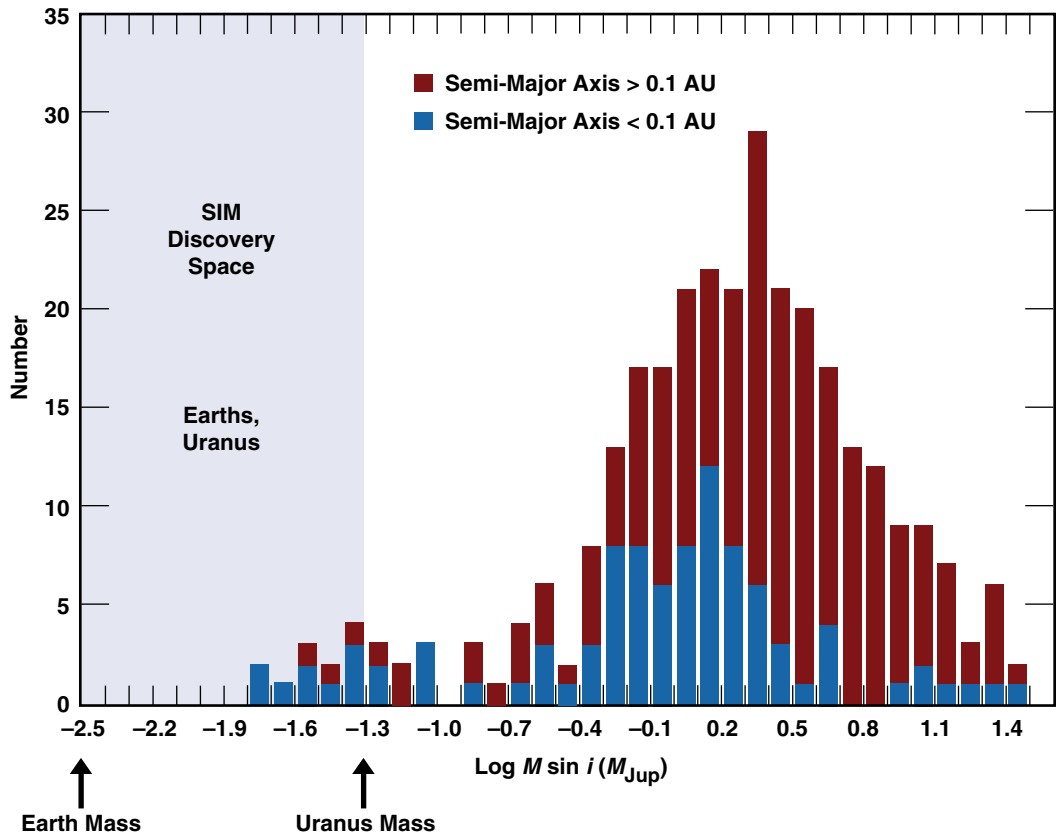
The study of exoplanets is driven in part by a fundamental question of the human desire to better understand life and our role in the Universe: is the phenomenon of life unique to Earth or frequent elsewhere? A reasonable starting point is to search for life similar to that found on Earth. Life as we know it appears to require a few crucial ingredients that guide this search, including liquid water on relatively small, rocky planets. Only a small range of star–planet separations result in planet temperatures suitable for liquid water; our search for candidate life-hosting planets requires the ability to find planets in the regime (near 1 AU for Sun-like stars). While some planets have been found at this separation around other stars, they are gas giants like Jupiter. Current techniques are insensitive to the smaller signatures that result from smaller Earth-like planets. Once candidate planets are found, the next logical step will be to confirm whether water (and other life-related chemicals) exists on those planets. This will require isolating the spectrum of the planet's light from that of the bright star it orbits. Only for the closest systems to the Sun will it be feasible for future missions to detect the light from a faint planet near a bright star. To reliably interpret the spectrum, it will be important to know the planet's mass. Thus, the path to finding candidate habitable planets requires a new observatory capable of simultaneously addressing four search criteria:

It must (1) search the stars closest to the Sun with enough sensitivity to (2) detect Earth-sized planets at (3) star–planet separations that allow for liquid water, and (4) measure their masses.

Existing techniques do not meet these four criteria. Only spaceborne astrometry is capable of detecting Earth-mass, rocky planets around nearby Sun-like stars while simultaneously measuring their masses, a key property of planets. The technology development of SIM Lite during the past decade has established an instrument architecture that is thoroughly tested and reviewed, demonstrating the crucial sub-µas astrometric precision to detect rocky planets. Having met all technology milestones, SIM Lite's historic search for other Earths can begin as soon as funding becomes available.

A recent 15-year strategy for detecting Earth-like planets was developed in a study conducted by the Astronomy and Astrophysics Advisory Committee's Exoplanet Task Force commissioned by NASA and NSF. The final report from the task force recommends that in the 6- to 10-year time frame, the U.S. should "Launch and operate a space-based astrometric mission capable of achieving 0.2 µas sensitivity to detect planet signatures around 60 to 100 nearby stars."

This recommendation agrees with the past three Decadal Surveys, notably the Field, Bahcall, and McKee-Taylor Reports, that have strongly promoted development of a µas astrometric program for detecting and characterizing extrasolar planets.

1.2 Basic Astrometric Physics and SIM Lite Detectability

The semi-amplitude of the angular wobble, α, of a star of a given mass, M_*, and distance, D, due to a planet of a given mass, M_p, orbiting with a semi-major axis, a, is given by:

$$\alpha = 3.00 \, \frac{M_\odot}{M_*} \, \frac{M_p}{M_\oplus} \, \frac{a}{(1 \text{ AU})} \, \frac{(1 \text{ pc})}{D} \, \mu\text{as}$$

The benchmark case is an Earth-mass planet orbiting 1 AU from a solar-mass star located 10 pc away. For such a planet, the astrometric semi-amplitude, α, is 0.3 µas. Using specially chosen and vetted reference stars located within a degree of the target star, SIM Lite achieves an astrometric precision of 0.82 µas per observation. (Note that this "narrow-angle" mode of SIM Lite yields higher astrometric precision than the "wide-angle" mode by using angularly nearby reference stars rather than generic grid stars for reference.) With SIM Lite's narrow-angle astrometric precision of 0.82 µas per observation, many observations are needed to detect the benchmark signal, as described below.

The intrinsic periodicity of the astrometric signals from planets greatly enhances their detectability. In contrast, errors, both photon-limited and systematic, are unlikely to be strictly periodic (except near 1.0 year). If any periodic errors did occur, they would be quickly revealed in the astrometry of the ensemble of target stars and reference stars, allowing such periodicities to be ignored (and perhaps removed). Thus, planet signals increase, relative to noise, with the square root of the number of observations because of the strict temporal coherence orbital motion obeys.

Standard time-series analysis provides a quantitative measure of the increasing signal-to-noise ratio (and decreasing false alarm probability) that accrues with an increasing number of observations. A periodogram analysis of simulated astrometric data from planets shows that the signal rises over the noise in Fourier space with the square root of the number of observations, as expected (Catanzarite et al. 2006). Figure 1-2 shows one such example in which the astrometric signature of a 1.5 $M_\oplus$ planet is inferred from 200 simulated SIM Lite observations. The periodograms of the simulated astrometry in both RA and DEC reveal the 1.5 $M_\oplus$ planet with a false-alarm probability (FAP) under 1 percent (Unwin et al. 2008).

Figure 1-2. Simulation of the astrometric detection of a planet with SIM Lite. The simulation assumes 100 measurements in RA and 100 in DEC over a mission of five years duration. The planet has a mass of 1.5 $M_\oplus$ orbiting at 1.16 AU from a 1.0 $M_\oplus$ star at a distance of 10 pc from Earth. This example was chosen to illustrate a system close to the limit of detectability with SIM Lite. (a) Sky plot showing the astrometric orbit (solid curve) and the individual SIM measurements with error bars. (b), (c) The same data as in (a) but shown as time series along with the astrometric signal projected onto RA and DEC. (d) Periodograms of the data plotted in (b) and (c). (e) Joint periodogram of data from (b) and (c). The horizontal lines in (d) and (e) show the level above which the false-alarm probability is less than 1 percent. The peak near $P = 1.2$ years is the astrometric signal of the 1.5 $M_\oplus$ planet. Note that the planet is not detected in RA or DEC alone, but is detected with a false-alarm probability of well below 1 percent in the joint periodogram.
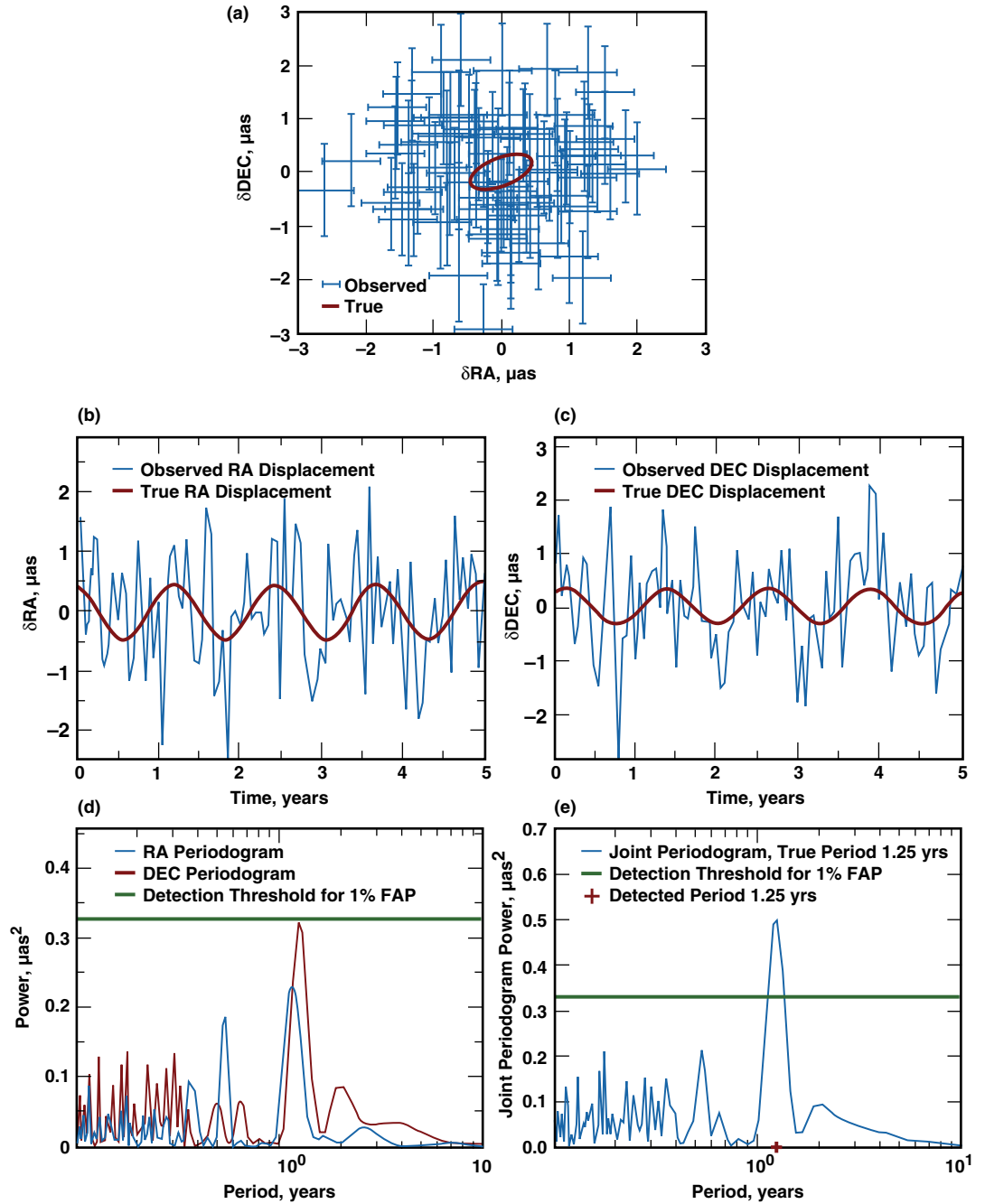
For the benchmark case of an Earth-mass planet orbiting at 1 AU around a solar-mass star at 10 pc, roughly 500 measurements at 0.82 µas accuracy are needed to attain a signal-to-noise ratio (SNR) of 5.8, the approximate threshold for detection. In general, if σ is the one-axis RMS noise per differential measurement, N is the number of SIM Lite visits, and α_{THRESH} is the threshold astrometric amplitude detectable with a probability of 50 percent, we have:

$$\alpha_{THRESH} = SNR \times \sigma / N^{1/2}$$

SIM Lite offers the astrometric precision and duration (five years), along with a noise floor below 0.1 µas, to detect Earth-mass planets around the ~60 nearest FGK stars.

1.3   SIM Lite: Making the First Catalog of Earth-Like Planets

SIM Lite remains the only technically demonstrated method for identifying rocky, Earth-mass planets around Sun-like stars within 20 pc, during the 2010 to 2020 decade. A competitor, the Doppler technique, suffers from the intrinsic "jitter" of ~1 m/s due to photospheric spots, convection, and acoustic oscillations, preventing detection of the tiny radial velocity signature (0.1 m/s) of a habitable Earth-like planet around a Sun-like star. Another competitor, direct imaging, remains to be developed technically; and indeed, three architectures of the Terrestrial Planet Finder and the European counterpart, Darwin, remain to receive full technical vetting. Yet another approach, detecting transits of planets as they block starlight, works for the rare planets whose orbits are edge-on as seen from Earth. That probability is only 1 in 200 for planets in the habitable zones of Sun-like stars. Most nearby planetary systems would be missed. Other planet detection methods, such as microlensing, are not well suited for nearby stars. Figure 1-3 shows the detectability of rocky planets by a variety of techniques, none of which is competitive with SIM Lite in the domain of the habitable zone around solar-mass stars.

Nonetheless, a key long-term goal is to directly image and take spectra of Earth-like planets. The well-known challenge for imaging missions is to overcome the combination of the extreme contrast between, and the small angular separations of, the star and planet, along with the sheer intrinsic faintness of the planet. Rocky planets orbiting 1 AU from stars 10 pc away will have a V-band magnitude of V = 28 mag separated only 0.1 as from a magnitude 5 star. Astrometry is well optimized for discovering such low-mass planets around the nearest stars, to identify the best targets for later missions that can directly image the planets.

Indeed, the ExoPTF Report states on page 60, "The most promising way to mitigate the cost of space-based direct imaging is 1) to identify targets before the direct imaging mission is flown…." By first

Figure 1-3. Detectability of planets by SIM Lite, Gaia, and radial velocity (RV). The regions above each curve are accessible to the respective mission/technique. The two red curves show the detection thresholds for the closest and farthest among the 60 FGK stars to be probed by SIM Lite. Small rocky worlds circling in the habitable zones of these stars will fall within the box near the bottom of the figure. SIM Lite offers excellent detectability of these planets. In contrast, RV (accuracy ≈ 1 m/s) and Gaia lack the sensitivity to probe this region. The pale green dots show predicted planets from planet formation theory (Ida and Lin 2004), the purple dots show known planets, mostly from RV work, and the blue dots show the planets of our Solar System.
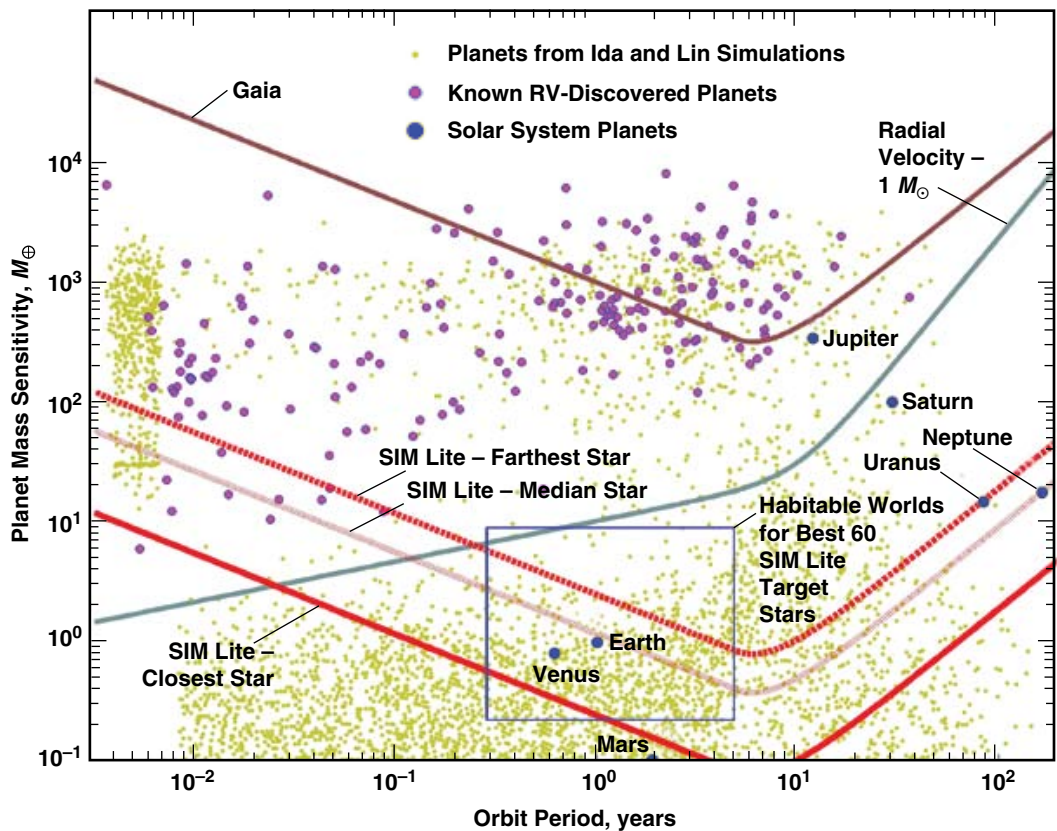
deploying SIM Lite to find and characterize Earth-like planets around nearby stars, the cost of a future direct-imaging mission is reduced and the scientific output increased. Moreover, the risk of failure is greatly reduced, and the specifications of any imaging system and a spectrometer are definable, based on the orbit and expected size of the planet, all stemming from SIM Lite observations.

1.3.1   Earths Are Detectable Despite the Presence of Other Planets

A significant question is whether SIM Lite can detect Earth-mass planets despite the astrometric "noise" contributed by other planets, both other terrestrials and gas giants. Terrestrials and asteroids located both inward and outward of the habitable zone will create a forest in the power spectrum, making the detection of one Earth-mass planet difficult. Giant planets orbiting well outside 1 AU will cause an astrometric curvature partially absorbed (incorrectly) in the solution for proper motion. As part of a comprehensive double-blind simulation (described in Chapter 3), 12 mock planetary systems were generated containing Earth-mass planets in the habitable zone, to carry out a "double-blind test" of detectability. Four systems were single-planet systems with a terrestrial planet in the habitable zone, and eight were solar system analogs with planets and orbit parameters within 10 percent of the corresponding solar system planets. The corresponding astrometric data and radial velocity data were generated for each mock system with realistic errors and cadence. The astrometric and velocity data were analyzed by four competent teams without knowledge of the input planets. The teams "discovered" virtually all of the Earth-mass planets (masses 0.3 to 10 $M_\oplus$) that should have been detectable had they been alone. (Section 1.2 shows that planets with astrometric amplitude greater than 5.8 σ / $N^{1/2}$ are detectable, where σ is the single-measurement error and N is the number of observations.) A major conclusion of the double-blind study is that the presence of additional planets in a planetary system causes almost no degradation in the detectability of Earth-mass planets. This double-blind test showed that SIM Lite is capable of detecting Earth-like planets embedded in multiple-planet systems. (See Chapter 3 for a more complete treatment of multiple-planet systems.)

1.3.2   Earth Search Yields

The exact expenditure of SIM Lite time spent searching for other Earths remains open to discussion (cf. Figure 1-4). To survey the nearest 64 stars to a threshold of 1 $M_\oplus$ at 1 AU scaled to stellar luminosity takes 40 percent of the nominal SIM Lite mission time, with a lifetime of five years. Among the 64 stars, the most distant 10 of them require 25 percent of that time due to their distance and the 1 $M_\oplus$ detection goal. An alternative plan is to observe only 54 stars, which requires only 30 percent of SIM Lite mission time, while adhering to the 1 $M_\oplus$ threshold. The saved time can be used to observe an additional 37 stars at a lower threshold of 2 $M_\oplus$ (photon-limited errors twice as large are achievable with one-fourth the exposure time). Such a relaxed threshold offers useful statistical advantages gleaned from the 37 stars, over the gains of 10 more stars surveyed at the highest precision. Simulations of actual planetary systems are needed to optimize the use of SIM Lite observing time.

1.3.3   Earth-Analog Characterization Facilitated by SIM Lite

Splitting the discovery and characterization of other Earths between two sequential missions — namely an easier indirect discovery program, i.e., SIM Lite, and a later imaging and spectroscopy program, i.e., Terrestrial Planet Finder/Darwin — allows for technology to be developed for the latter with specified detection thresholds. Such a two-step approach offers methodical, cumulative, and complementary information about other Earth-like planets. It should be noted that SIM Lite stands on its own, providing

Figure 1-4. The number of stars that can be searched for Earth-analogs depends strongly on the planet mass threshold adopted by SIM Lite. Top: Mass sensitivities are presented at the Inner Habitable Zone (IHZ), which is 0.8 AU scaled to the square root of luminosity. The flat plateau in the black curve exists because there are no more target stars that can be measured to 1 $M_\oplus$ in fewer than the maximum number of measurements set by the instrument noise floor. Bottom: Mass sensitivities are at the Earth Habitable Zone (EHZ), which is 1.0 AU scaled to the square root of luminosity. A differential measurement error of 1.4 μas for a 900 s "standard visit" and a mission lifetime of five years are assumed. Note that the ordinates have different scales. (Charts prepared by Joseph Catanzarite.)
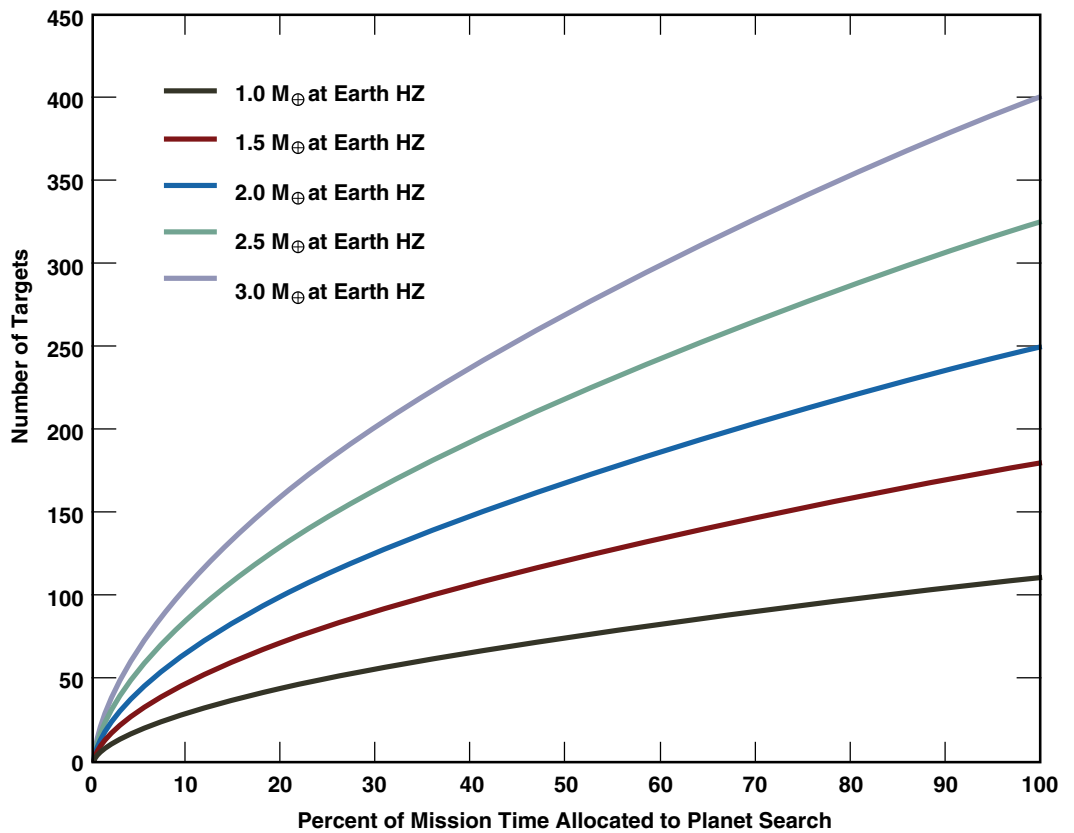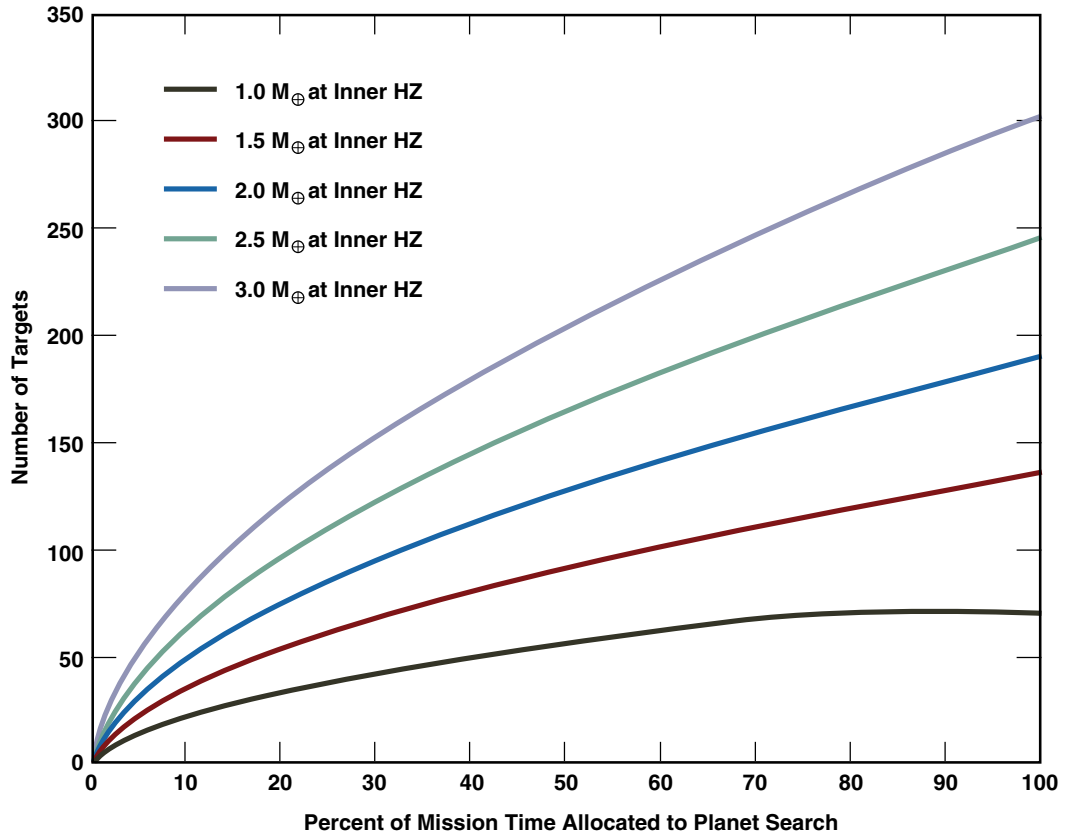
the detections of rocky planets, their masses, and their full, three-dimensional orbits in the habitable zone (1 AU) of the host star. Moreover, in combination with Doppler observations (see Chapter 3), SIM Lite data will permit the full characterization of all planets, rocky and giant, out to about 5 AU. This is an especially intriguing prospect, given that many of the stars that SIM Lite will examine are already known from Doppler measurements to have one or more giant planets. If archival Hipparcos data are also included, it may be possible to infer the presence of giant planets beyond 5 AU, although with less-complete characterization. Such an inventory of rocky and giant planets around individual nearby stars will offer valuable constraints on the formation and dynamical evolution of planetary systems in general.

1.4　Measuring Masses: A First Step Toward Characterizing Exoplanets

Determining planet mass by space-based astrometry is clearly necessary in conjunction with direct imaging. Because mass is a fundamental property of planets, the science return of a direct imaging mission would be reduced without SIM Lite and would suffer significant ambiguities. A dot does not a planet prove, and even a spectrum that reveals some particular molecular constituent (such as methane or carbon dioxide) cannot securely distinguish between rocky planets and ice giants. Using either transits (that provide radius) or spectroscopy (offering chemical assays of the atmosphere), the distinction between ice giants and rocky planets may not be solid. The uncertain albedos of ice giants and rocky planets will prevent a secure mapping of reflected light fluxes to planet radius, leaving the planetary masses even less secure. Thus, measuring a planet's mass will remain crucial for interpreting any spectrum of the planet's atmosphere, and certainly bears on its habitability. Only by measuring the gravitational effect of the planet on its host star can the planet's mass be measured, and only astrometry can do the job. A µas astrometric mission is required to empirically characterize Earth-like planets.

A precise measurement of the planet mass is important when attempting to understand the formation and dynamical evolution of any individual planetary system. Only with accurate measurements of mass, unencumbered by $\sin(i)$ ambiguities, can dynamical models be attempted securely. Not only may planet masses correlate with the mass or chemical composition of the host star, the mass of a particular planet having unexpected properties can spur theoretical research into its formation mechanisms (e.g., orbital migration, eccentricity excitation). Theorists will watch for planets having intriguing combinations of properties of their mass, orbits, and host star. Table 1-1 illustrates some of the possibilities for Earth-like planets. Thus, SIM Lite's ability to characterize individual planet systems, rather than just statistical averages, will help reveal the physical processes by which they formed.

Table 1-1. Planet properties enabled by SIM Lite plus visible and infrared spectra.

Parameter	Planet Property Derived	Planet Property Implied
Planet Mass	Density, Surface Gravity, Atmosphere	Likelihood of plate tectonics; atmospheric mass, scale height, lapse rate, and surface pressure and temperature
Orbit Semi-Major Axis	Temperature	Potential habitability, liquid water
Orbit Eccentricity	Variation of Temperature	Thermal time constant of the atmosphere, mass of the atmosphere
Orbit Inclination	Co-planar Planets?	
Orbital Period		

1.5   SIM Lite Contributions to the Theory of Rocky Planet Formation

The theory of the formation of rocky planets and super-Earths, along with their subsequent dynamical evolution, has been developed by Ida and Lin (2008) and Kennedy and Kenyon (2008) (and references therein). They start with a collection of thousands of rocky planetesimals having kilometer sizes similar to modern asteroids and comets. They simulate the collisions and sticking of these objects, allowing them to grow and gravitationally perturb each other until final planets emerge. The dynamical effects of the gas (drag, density inhomogeneities) and the condensation of ice are included in the calculation. Gas serves both as a dissipative medium to exchange angular momentum and energy with the planet (often causing inward migration) and also as the reservoir of material that can accrete onto the rocky cores, making ice and gas giants. Ice condensation also creates density discontinuities in the dust component of the disk, causing reversals in density and ionization gradients that can trap planetesimals.

Figure 1-5 shows the result of a recent simulation by Ida and Lin (2008), displaying the distribution of final planets in a two-parameter space of planet mass and orbital distance. Remarkably, planets of mass 1 to 30 $M_\oplus$ are predicted to be rare within 1.5 AU. That is, super-Earths and Neptunes are expected to be rare, largely because once inside the ice line they migrate inward quickly, destined to be lost in the star (or parked in a close-in orbit). More-massive rocky cores accrete gas quickly, becoming gas giants. Thus, this theory makes a remarkable prediction that planets in a decade range larger than Earth may be rare. Indeed, our Solar System has no such super-Earths. This remarkable prediction may be directly tested by SIM Lite, as planets orbiting within 0.5 to 1 AU, with masses of 5 to 30 $M_\oplus$, will be detected easily.

Figure 1-5. Predicted masses and orbital distances of planets from a Monte Carlo simulation of planet formation, from Ida and Lin (2008). The calculation includes growth of planetesimals and effects of gas drag. Note the predicted planet "desert" between 1 to 30 $M_\oplus$ within 1.5 AU. SIM Lite will test such predictions.
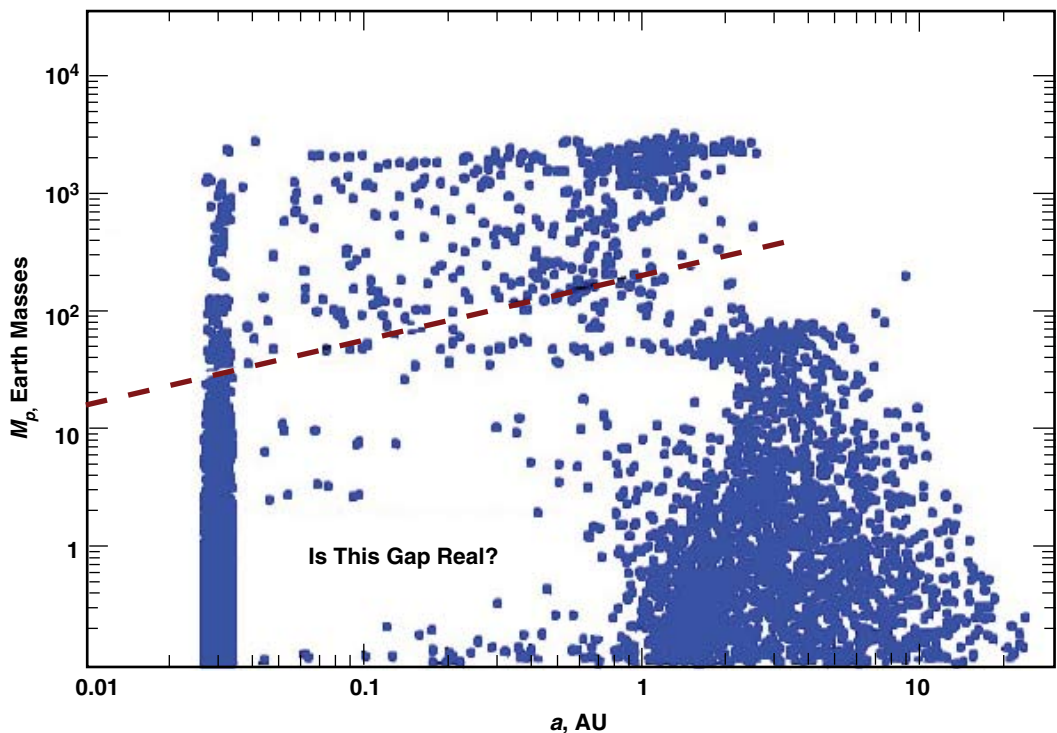
If the Ida and Lin prediction of a mass desert is contradicted by SIM Lite observations, the theory must be significantly modified with new physics. Successful theories will have to determine orbital stability of all planets over long time periods, include orbital resonances, and determine the interactions in multiple planet systems. The chemistry of both the gaseous and dust components will also require considerable care.

Indeed, theoretical work on planet formation mechanisms for the entire range of planet masses, from terrestrial planets, to ice giants, to gas giants, is necessary in order to place the exoplanet discoveries in the context of planetary system formation theories. Terrestrial planet formation is strongly influenced by gas giant planet formation and orbital evolution. A complete theory of planet formation is needed in order to understand the formation of any one component.

1.6   Other Exoplanet Research

1.6.1   Lifting the Mass-Inclination Ambiguity in RV Planets

The large majority of known exoplanets have ambiguous masses: their unknown inclination angles permit only lower-limit mass estimations. This mass ambiguity disappears in the astrometric determinations of dynamical mass, since astrometry determines the system inclination angles. Specific targets of interest where unambiguous masses are important include those with multiple planets where planet–planet interactions might become significant. The inclination ambiguity does not strongly affect the derived distributions of planet masses (i.e., Figure 1-5). However, for individual planetary systems, it is important to know the full specification of masses and orbits to compare with the structure of the systems predicted by theorists. Ida and Lin et al. (2004) demonstrate how the knowledge of the unambiguous dynamical masses guides the development of the theory. Unknown inclination angles (and hence masses) degrade the quality of the comparison between observation and theory, especially when planet–planet interactions are significant.

1.6.2   Follow-up of Kepler Candidate Earths

The candidate Earth-like planets revealed by Kepler will raise the question: Are they really Earths? Instead, they could be grazing-incidence eclipsing binaries with a brighter third star that dilutes the photometric dimming. SIM Lite offers a valuable way to check some of these potential false-positives. SIM Lite can detect the astrometric motion of the photocenter of the triple-star system, or indeed detect the confused interference fringes from the three stars. With a resolution of 10 µas, SIM Lite can also interferometrically resolve binaries in the Kepler field. The fractional dimming corresponding to an Earth-sized planet is 1 part in 10,000 around a Sun-sized star. If instead, the dimming is caused by a diluted, eclipsing binary, the astrometric shift will be 1 part in 10,000 of the angular separation between the eclipsing binary and the brighter, third star. Ground-based work will detect such "third" stars unless they are within ~0.5 as. For separations of ~0.5 as, the displacement will be 50 µas, easily detectable by SIM Lite. For separations of 0.1 as, the displacement will be 10 µas, still detectable by SIM Lite. Thus, SIM Lite offers one of the very few methods to determine the false-positive rate of the Kepler mission.

1.7   Future Research: Imaging Earths

Astrometric observations not only identify which stars host Earth-like planets but also yield the full orbital ephemeris of the planet, specifying the angular position of the planet relative to the star at all times. Knowing the angular position and separation of the planet as a function of time specifies the optimal observation times for any direct imaging programs. One would attempt imaging and spectroscopy of rocky

planets only when the planet is well outside the direct imaging instrument's inner working angle for the star. (The inner working angle is the radius within which the glare of the star, caused by diffraction and mirror microroughness, prevents detection of the planet.) This optimization is not possible without prior SIM Lite observations.

Such optimization can be quite valuable. A benchmark Earth-like planet resides only 0.1 as from the host star at maximum elongation. The inclination of the orbital plane flattens the apparent trajectory of the planet relative to the star. For a typical inclination of ~45 deg, the planet spends most of its time located well within 0.1 as of the star, only briefly poking out to ~0.1 as. There is no way to know when those favorable moments of maximum elongation occur without prior SIM Lite observations. For Earth-like planets 10 billion times fainter than the star, a high premium is placed on timing the imaging and spectroscopic effort to those moments when the elongation of the planet from the star is maximum.

SIM Lite will establish the planet orbital ephemeris, allowing imaging efforts to be timed when the planet is widely separated from the star. Indeed, the technical requirements of a direct imaging mission may be reduced because it need only detect planets when they are in optimal configurations relative to the star. Similarly, SIM Lite will establish the orientation of the orbit in space. This provides an additional increase in efficiency for any direct imaging mission that achieves its highest contrast for a limited range of angles and orientations. Such a mission could choose an observation time and roll-angle that would maximize the SNR for detecting the planet.

1.8   The Impact of Gaia

Gaia is a European astrometry mission with launch planned for 2011. It will achieve a precision of ~100 µas per measurement (to V = 15) on 30 million stars (and reduced precision for up to a billion fainter stars), with each star revisited 1 to 250 times (typically ~90 one-dimensional measurements) over the course of the mission. It is a survey mission without the capability of pointing at a particular object at a particular time. Thus, neither the timing nor cadence of revisits can be controlled for a high-priority target. Gaia will saturate for very bright stars (V $\lesssim$ 6), including the stars closest to Earth that are highest priority when looking for Earth-like planets.

Thus, Gaia will fall short of discovering Earth-like planets due to its limited precision and cadence. The 100× better precision, and the pointing optimization of SIM Lite, are required to achieve this goal. Furthermore, the number of repeated measurements for a given target is much larger for SIM Lite, with 200 to 500 (two-dimensional) measurements on high-priority targets, which yield higher sensitivity to lower mass planets, and better coverage of orbital phase to accurately measure the orbit. Good orbital coverage is necessary to adequately characterize a planet's orbit well enough to inform a future direct imaging mission about the optimal observing time.

References

Bahcall, J. et al., 1990, Astronomy and Astrophysics Survey Committee, National Research Council, The Decade of Discovery in Astronomy and Astrophysics, Washington, D.C.: National Academy Press.

Baraffe, I. et al., 2002, A&A, 382, 563.

Burrows, A. et al., 1997, ApJ, 491, 856.

Boss, A. P., 2001, ApJ, 551, L167.

Catanzarite, J., Law, N., and Shao, M., 2008, Proceedings of the 2008 SPIE Astronomical Instrumentation Meeting, Marseille, France.

Catanzarite, J. et al., 2006, Publications of the Astronomical Society of the Pacific (PASP), 118, 1319.

Cameron, P. B., Britton, M. C., and Kulkarni, S. R., 2008, arXiv:0805.2153 AJ, submitted.

Chauvin, G. et al., 2005, A&A, 438, Issue 2, L25.

Cumming, A., Butler, R. P., Marcy, G. W., Vogt, S. S., Wright, J. T., and Fischer, D. A., 2008, Publ. Astron. Soc. Pacific, 120, 531.

Field, G. B., 1982, Astronomy and Astrophysics for the 1980s, Report of the Astronomy Survey Committee,

National Research Council, Washington, D.C.: National Academy Press.

Ford, E. B., Lystad, V., and Rasio, F. A., 2005, Nature, 434, 873.

Ida, S. and Lin, D. N. C., 2004, ApJ, 604, 413.

Ida, S. and Lin, D. N. C., 2005, ApJ, 626, 1045.

Ida, S. and Lin, D. N. C., 2008, ApJ, 685, 584.

Kennedy, G. and Kenyon, S. 2008, ApJ, 682, 1264.

Lee, M. H. and Peale, S. J., 2002, ApJ, 567, 596.

Malhotra, R., 2002, ApJL, 575, L33.

Mayor, M. and Queloz, D., 1995, Nature, 378, 355.

McKee, C. and Taylor, J., 2000, Astronomy and Astrophysics Survey Committee, National Research Council. Astronomy and Astrophysics in the New Millennium (Washington, D.C.: National Academy Press).

Morbidelli, A., Chambers, J., Lunine, J. I., Petit, J. M., Robert, F., Valsecchi, G. B., and Cyr, K. E., 2000, Meteoritics and Planetary Science. 35, 1309.

Muterspaugh, M., Lane, B., Fekel, F., Konacki, M., Burke, B., Kulkarni, S. R., Colavita, M. M., Shao, M., and Wiktorowicz, S., 2008, AJ, 135, 766.

Muterspaugh, M., Lane, B., Kulkarni, S., Burke, B., Colavita, M., and Shao, M., 2006, ApJ, 653, 1469.

Neuhauser, R. et al., 2005, in Direct Imaging of Exoplanets: Science and Techniques, Proceedings of IAU Colloquium 200, eds. C. Aime and F. Vakili.

Pravdo, S. H., Shaklan, S. B., Henry, T., Benedict, G. F., 2004, ApJ, 617, 1323.

Pravdo, S. H., Shaklan, S. B., and Lloyd, J. P., 2005, ApJ, 630, 528.

Pravdo, S., Shaklan, S., Redding, D., Serabyn, E., and Mennesson, B., 2007, "Finding Exoplanets around Old and Young Low-Mass Stars," white paper submitted to the AAAC Exoplanet Taskforce.

Pravdo, S. H., Shaklan, S. B., Wiktorowicz, S. J., Kulkarni, S., Lloyd, J. P., Martinache, F., Tuthill, P. G ., and Ireland, M. J., 2006, ApJ, 649, 389.

Raymond, S. N., Mandell, A. M., and Sigurdsson, S., 2006, Science, 313, 1413.

Shao, M. et al., SIM PlanetQuest — The Most Promising Near-Term Technique to Detect and Find Masses and 3-D Orbits of Nearby Habitable Planets, April 2, 2007, white paper prepared for the Exoplanet Task Force.

Tsiganis, K., Gomes, R., Morbidelli, A., and Levison, H. F., 2005, Nature, 435, 459.

Unwin, S. Shao, M., Tanner, A., Allen, R. Beichman, C. A., Boboltz, D., Catanzarite, J., Chaboyer, B., Ciardi, D., Edberg, S. J., Fey, A., Fischer, D. A., Gelino, C., Gould, A., Grillmair, C., Henry, T., Johnston, K., Johnston, K., Jones, D., Kulkarni, S., Law, N., Majewski, S., Makarov, V., Marcy, G., Meier, D., Olling, R., Pan, X., Patterson, R., Pitesky, J., Quirrenbach, A., Shaklan, S., Shaya, E., Strigari, L., Tomsick, J., Wehrle, A., Worthey, G., 2008, PASP, 863, 38.

Wetherill, G. W., 1996, Icarus, 119, 219.

Wuchterl, G. and Tscharnuter, W. M., 2003, A&A, 398, 1081.

Young Planets and Star Formation

2
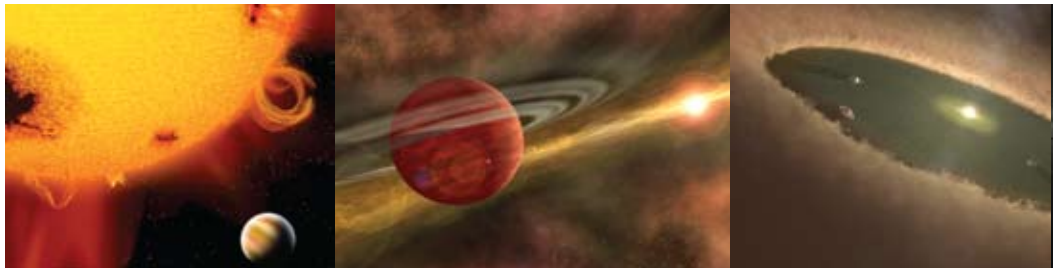
Charles Beichman (NExScI), **Angelle Tanner** (Santa Barbara Applied Research), **Michal Simon** (SUNY Stony Brook), and **Lisa Prato** (Lowell Observatory)

ABSTRACT

Despite the revolution in the detection of planets around mature stars, we know almost nothing about planets orbiting young stars because rapid rotation and active photospheres preclude detection by radial velocities or transits. Thus, our knowledge about the formation and evolution of planetary systems is rudimentary at best. Astrometry with SIM Lite offers our best observational opportunity to find gas giant (100 to 300 $M_{\oplus}$), icy giant (10 to 100 $M_{\oplus}$) planets, and even a few rocky, super-Earths (~10 $M_{\oplus}$) orbiting stars ranging in age from 2 to 100 Myr. SIM Lite's astrometry can also address more general questions of star formation, including the physical properties of young low-mass objects whose masses and evolutionary tracks are highly uncertain.

2.1 Young Systems: Beyond the Reach of RV, Transit, and Imaging

An astrometric survey using SIM Lite of 200 stars with ages from 2 to 100 Myr will help us to understand the formation and dynamical evolution of gas-giant planets. The majority of the host stars of the more than 300 exoplanets found to date are mature main-sequence stars (and a few giants) chosen for having quiescent photospheres to enable the measurement of small Doppler velocities ($\leq$10 m/s) or small photometric variations due to transits (millimagnitude precision). In this section, we contrast SIM Lite's astrometric capabilities with other techniques as well as with expectations for Gaia's performance.

2.2 The Challenge of RV

Many young stars are characterized by weak spectral features due to veiling, rotationally broadened line widths >> 1 km/s, large-scale radial velocity (RV) motions, and/or brightness fluctuations of many percent due to starspots (Carpenter et al. 2001). Thus, visible radial velocity measurements and photometric observations have been unable to detect planets around young stars. Setiawan et al. (2008) recently claimed an RV detection of a planet orbiting the young star TW Hya, but this claim has been called into serious question (Huélamo et al. 2008) as being due to large-scale photospheric variations. Similarly, Prato et al. (2008) initially identified potential "hot Jupiters" orbiting DN Tau and V836 Tau based on visible spectroscopy, but used follow-up IR spectroscopy to demonstrate that the RV variations were due to photospheric variability, not planets. While the near-IR is a promising wavelength region for RV and photometric searches of young stars due to the 2 to 5 times lower contrast between the photosphere and the starspots that are often the cause of the variability (Eiroa et al. 2002), there is no evidence that precisions less than 50 m s^{-1} will be possible. This limit precludes detections of all but the most massive, most closely orbiting "hot Jupiters" (<0.1 AU). As valuable as such detections would be, this technique cannot push into the interesting 1 to 5 AU area now well studied around main sequence stars and critical for understanding the formation of planetary systems.

2.3 The Challenge of Transits

There is a long history of the variability of young stars, from outbursts of FU Ori objects to rotational modulation of a few percent in relatively quiescent T Tauri stars. These variations make transit detections of even gas giant planets (~1 percent transit depth) highly unlikely in the visible. Transit detections may prove possible in the near-IR where the variability is a factor of 2 to 5 times lower (Eiroa et al. 2002), but transits are likely to remain a marginal technique for young stars also because the surface density of suitable stars is so low that it is difficult to build up adequate samples. A survey of ~10^4 objects is necessary given the low probability of alignment and of having a planetary system in the first place, i.e., total probability of 10^{-3}.

2.4 The Challenge of Imaging

A few objects of potentially planetary mass have been detected at 25 to 100 AU from young (<10 Myr) host stars by direct, coronagraphic imaging, e.g., 2MASSW J1207334-393254 (Chauvin et al. 2005) and GQ Lup (Neuhauser et al. 2005) and most recently around the stars Fomalhaut and HR8799 (Marios et al. 2009; Kalas et al. 2009). However, these companions are only inferred to be of planetary mass by comparison to uncertain evolutionary models that predict the brightness of young Jupiters as a function of mass and age (Wuchterl and Tscharnuter 2003; Baraffe et al. 2002; Burrows et al. 1997). Since dynamical determinations of mass are impossible for objects on such distant orbits, it is difficult to

be sure that these are planets and not brown dwarfs. Nor is it even clear that the origin of these distant young "Jupiters" is due to the same formation processes as planets found closer to their hosts. Multiple fragmentation events (Boss 2001), rather than core accretion in a dense disk (Ida and Lin 2005), may be responsible for the formation of these objects orbiting so far from their star.

Advanced coronagraphs on extremely large telescopes (~30 m) may one day explore as close to a host star as 3 AU (corresponding to an Inner Working Angle of 4 λ/D at 50 pc) down to a few M_{Jup} levels, and interferometers may probe comparable masses and regions in the youngest star forming regions (140 pc). But imaging cannot yield dynamical information, so even if objects can be detected by these instruments, critical information on masses will remain unknown in the absence of astrometry.

2.5   The Promise of Astrometry

As a consequence of the limits and selection biases of the radial velocity, transit, and direct imaging techniques, we know almost nothing about the incidence of planets around young stars, leaving us with many questions about the formation and evolution of gas giant planets. Astrometry with SIM Lite promises to remedy this situation. Table 2-1 gives typical astrometric signals for gas giants (Jupiter and Saturn) and icy giants (Uranus) at two orbital distances (1 and 5.2 AU), two distances from the Sun (140 and 30 pc [cf. Figures 2-1 and 2-2], representative of 2- to 10-Myr-old stars and 10- to 100-Myr-old objects, respectively), and orbiting 0.15 and 1.0 $M_\odot$ stars. The signatures cover a range of <1 to 1000 µas. The closest Jovian planets will be detectable by Gaia or ground-based interferometers (~50 µas), but most will require SIM Lite's precision.

Figure 2-1. Sensitivity of SIM Lite to planets in the mass–semi-major axis plane for young stars (<5 Myr) at a distance of 140 pc. A representative population of planets seen around nearby mature stars (data from a variety of RV surveys of main sequence stars, e.g., http://exoplanet.edu/) is shown to indicate what SIM Lite might find when looking at young (1 $M_\odot$) stars for the first time. SIM Lite sensitivity estimates are given for worst-case and best-case scenarios for starspot noise. Sensitivity estimates for Gaia, RV studies, a coronagraph on a 30-m Extremely Large Telescope (ELT) operating at 1.6 µm, and the 85-m Keck Interferometer operating in direct imaging mode are shown for comparison. To date there are no credible detections of young planets located within <25 AU of their parent stars, highlighting the need for SIM Lite.
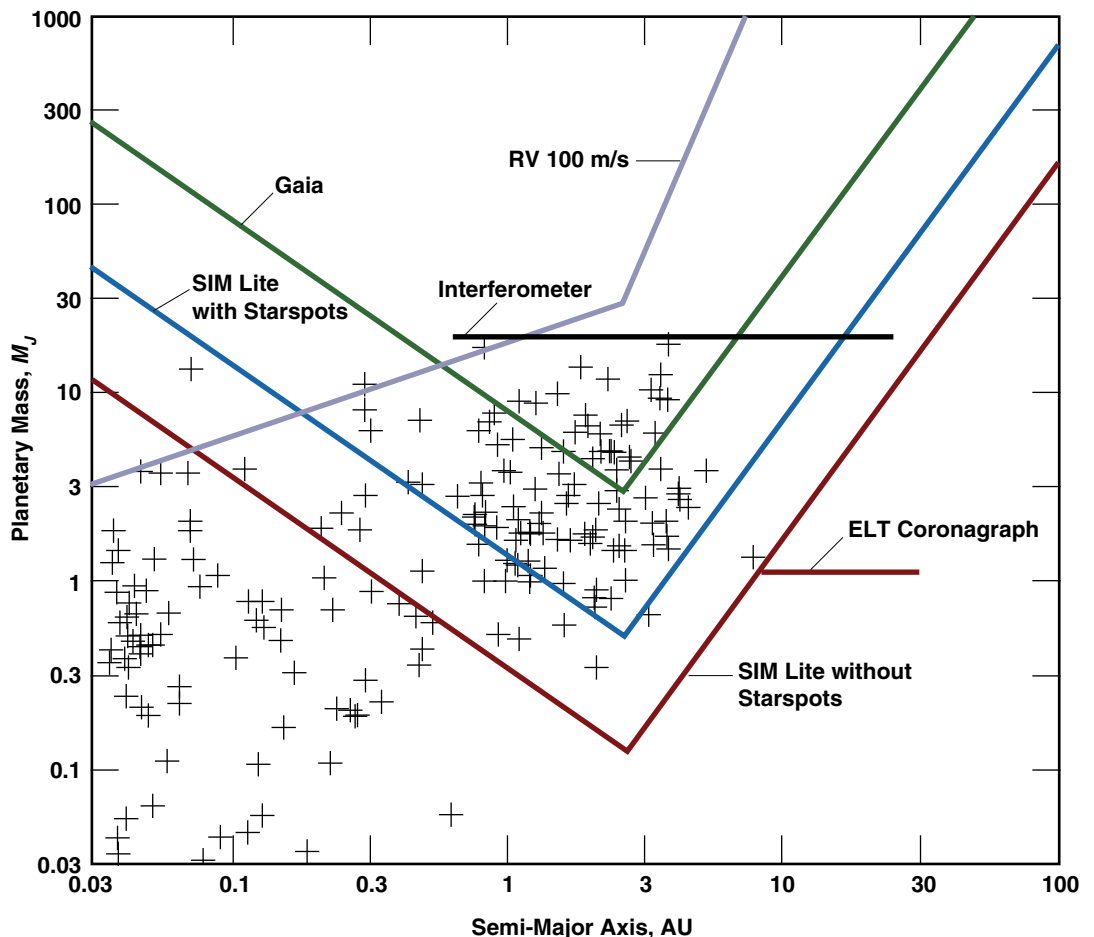
Table 2-1. Astrometric signal (µas) from planets at various distances, orbital locations, and stellar host mass. Entries indicated in blue (≥ 50 µas) would be detectable with Gaia or ground-based interferometers. Entries indicated in green require SIM Lite's sensitivity in either narrow- or wide-angle modes.

		1 $M_\odot$ Star				0.15 $M_\odot$ Star			
		Distance, pc				Distance, pc			
		30		140		30		140	
		Orbit, AU		Orbit, AU		Orbit, AU		Orbit, AU	
Planet	M_{Jup}	1	5.2	1	5.2	1	5.2	1	5.2
Jupiter	1	32	170	7	36	214	1110	46	240
Saturn	0.28	9	47	2	10	60	311	13	67
Uranus	0.023	0.7	4	0.2	0.8	5	26	1.1	6

Figure 2-2. Same as Figure 2-1, except for a planet orbiting a 0.15 $M_\odot$ star at a distance of 30 pc. Such stars have ages between 10 and 100 Myr.
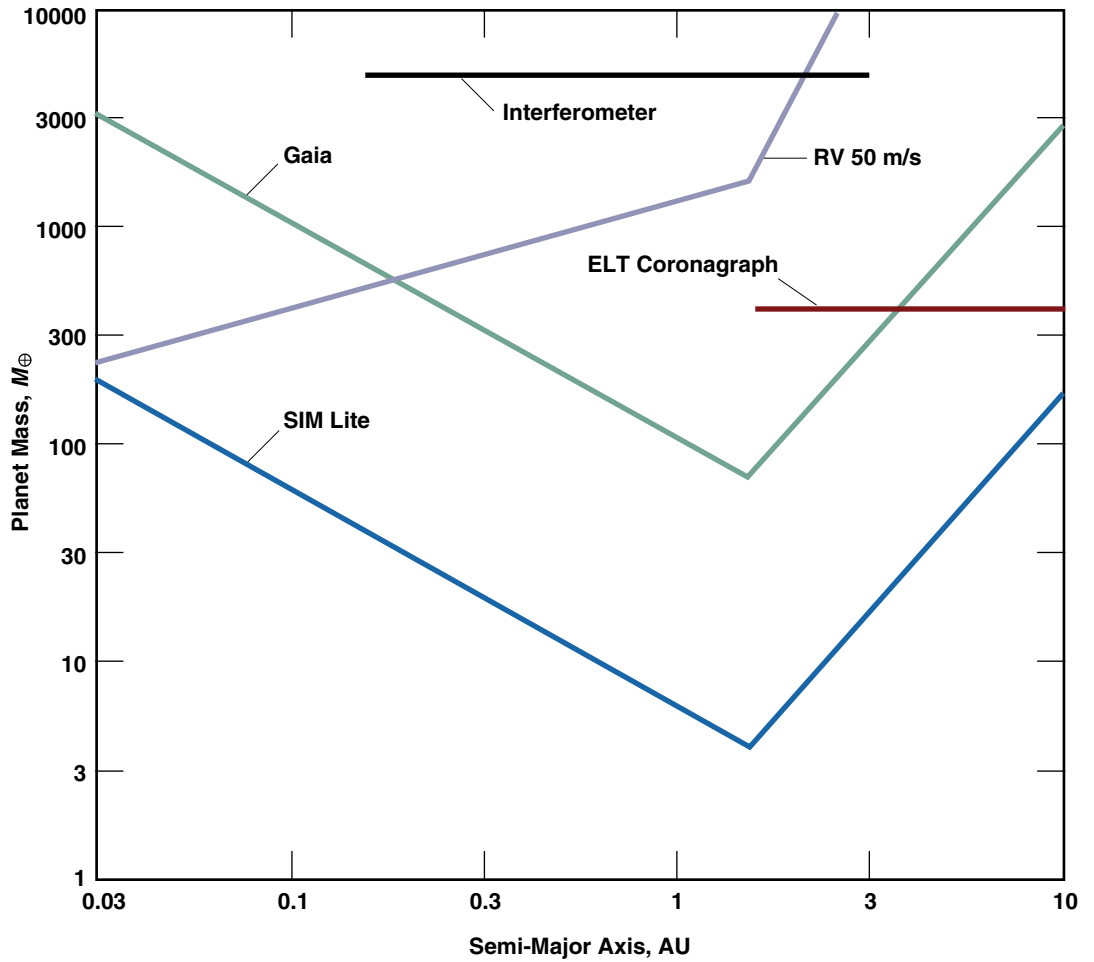
A Jupiter orbiting 5.2 AU away from a 1 $M_\odot$ star at the distance of the youngest stellar associations (1 to 10 Myr) such as Taurus (140 pc) and Chamaeleon (100 pc) would produce an astrometric amplitude of 36 µas. At the 25 to 50 pc distance of the nearest young stars (10 to 50 Myr), such as members of the β Pic and TW Hya groups, the same system would have an astrometric amplitude in excess of 100 µas. Moving a Jupiter into a 1 AU orbit would reduce the signal by a factor of 5.2, to 40 µas for a star at 25 pc and 7 µas for one in Taurus.

In its narrow-angle mode, SIM Lite will have a planet search accuracy of 2 to 3 µas with SNR = 5.8 at relevant magnitudes, V ~ 6 to 13 mag, and for reasonable integration times (cf. §2.6). A search for gas and icy giant planets, and even large rocky planets orbiting the closest, lowest-mass stars, falls well within SIM Lite's capabilities and forms the basis of the SIM–YSO Key Project (Beichman, PI; Beichman 2001; Tanner et al. 2007). Figure 2-1 and Figure 2-2 show SIM Lite's expected astrometric accuracy for the SIM–YSO survey as a function of planet mass and semi-major axis at distances of 140 and 30 pc. Also plotted is the expected RV accuracy achievable with infrared echelle spectrometers subject to the RV limitations (100 m s^{-1} for the youngest stars, 50 m^{-1} for somewhat older stars, >10 Myr) discussed in the preceding section. RV surveys will be limited to Jupiter-mass planets located very close to the star and coronagraphic imaging will be limited to planets located very far from the star. SIM Lite can detect planets throughout the critical distances of 1 to 5 AU around the snowline where gas giant planets are thought to form.

2.6 The Challenge of Astrometry

The photospheric activity that affects radial velocity and transit measurements also affects astrometric measurements, although to a lesser degree consistent with the secure detection of gas giant and smaller planets. From measurements of photometric variability (Bouvier and Bertout 1989; Bouvier et al. 1995) plus Doppler imaging (Strassmeier and Rice 1998), T Tauri stars are known to have active photospheres with large starspots covering significant portions of their surfaces (Schussler et al. 1996) as well as hot spots due to infalling accreting material (Mekkaden 1998). These effects can significantly shift the photocenter of a star. Using a simple model for the effect of starspots on the stellar photocenter (Beichman 2001; Tanner et al. 2007), the astrometric jitter for a typical T Tauri star at 140 pc with radius 3 $R_\odot$ is less than 3 µas (1 σ) for R-band variability less than 0.05 mag. Thus, the search for Jovian planets is plausible for young stars less variable than ~0.05 mag in the visible, even without making any assumption that the star spot noise will average down. If the spot noise averages down over many stellar rotational periods (typically of a few days, short compared with the observing sequence) with the square root of the number of observations, the mass detection limit will drop well below the gas giant limit.

If the Key Project survey is carried out with instrumental noise of 2.5 to 4 µas (single-measurement accuracy, depending on target brightness) and with astrophysical jitter of 3 µas (depending on stellar variability), then the limiting astrometric amplitude for reliable detection is given by a combination of instrumental and astrophysical noise sources:

$$\text{Amplitude} \sim 5.8 \, \sqrt{(\sigma^2(\text{SIM}) + \sigma^2\,(\text{astrophysical})) \, / \, N_{epoch}} \ \ \mu\text{as}$$

For σ (SIM Lite) = 3 µas (single-measurement accuracy), σ (Astrophysical) = 3 µas and N_{epoch} = 62 (125 one-dimensional measurements), the minimum detectable amplitude is 3 µas. For N_{epoch} = 125 (250 one-dimensional measurements), the minimum amplitude is 2 µas. In either case, SIM Lite's performance is consistent with detection of Saturns and Jupiters throughout nearly the entire the 1 to 5 AU region at 140 pc (Table 2-1). The value of 5.8 has been shown by extensive Monte Carlo simulations to be the correct value to ensure reliable detection (<1 percent false alarm probability; §1.2). If the astrophysical jitter does not scale with the square root of the number of observations, i.e., due to unfavorable "1/f" noise in the power spectrum of the astrometric noise, the SIM Lite limit will be astrophysical rather than

instrumental, roughly $3(R_*/3\,R_\odot)(D/140\text{ pc})$ µas. Even at this pessimistic limit, SIM Lite will be able to detect Jupiters and possibly Saturns in most of the 1 to 5 AU region. If, as expected, the astrometric jitter scales favorably, then much lower masses (discussed below) will be detected.

Note that since both the astrometric signal and the astrometric jitter scale inversely with distance, there is no advantage (from the jitter standpoint) to examining nearby stars despite their larger absolute astrometric signal — although the measurements will be easier for SIM Lite since the nearer targets will be brighter and the signal larger. Other astrophysical noise sources, such as offsets induced by the presence of nebulosity and stellar motions due to non-axisymmetric forces arising in the disk itself, are negligible for appropriately selected stars.

For searches for the lowest-mass planets around nearby low-mass stars, one can scale the astronomical jitter directly with the distance to the star and the stellar activity and inversely with the stellar radius. A 40-Myr-old star at a distance of 30 pc, with radius 0.28 $R_\odot$ and mass of 0.15 $M_\odot$, displays astrometric jitter at <0.5 µas, assuming that the stellar activity decreases from its level at ~3 Myr in Taurus to 40 Myr according to the Skumanich relation $\propto t^{-0.5}$ for calcium plage activity (Skumanich 1972). If this estimate for the astrometric noise of spotted stars is correct, then planets of super-Earth to Uranus masses will be detectable over the semi-major axis range of 1 to nearly 5 AU for these young, but not infant, stars.

2.7   The YSO Sample

The observational strategy of the existing SIM–YSO project is a compromise between the desire to extend the planetary mass function as low as possible and the essential need to build up sufficient statistics on planetary occurrence. About half of the sample will be used to address the where and when of planet formation. SIM Lite will study classical T Tauri stars (cTTs), which have massive accretion disks, as well as post-accretion, weak-lined T Tauri stars (wTTs). Preliminary studies suggest the sample will consist of ~30 percent cTTs and ~70 percent wTTs, driven in part by the difficulty of making accurate astrometric measurements toward objects with strong variability or prominent disks. The second half of the sample will be drawn from the closest young clusters with ages starting around 5 to 10 Myr, thought to mark the end-stage of prominent circumstellar disks, through targets of ~100 Myr, when theory suggests that the properties of young planetary systems should become indistinguishable from those of mature stars. The characteristics of the planets found around stars in these later age bins will be used to address the effects of dynamical evolution and planet destruction (Lin et al. 2000). Since we will also measure accurate parallaxes, we will have reliable luminosities for the host stars which can be used to help estimate ages.

The youngest stars in the sample will be located in well-known star-forming regions such as Taurus, the Pleiades, Scorpius-Centaurus, and TW Hydrae (Tanner et al. 2007). Somewhat older stars, such as those in the β Pictoris and TW Hydrae Associations, are only 25 to 50 pc away and can be observed with less mission time to the accuracy needed to identify Saturn- and Jupiter-mass planets. We have adopted the following criteria in developing our initial list of candidates: (a) stellar mass between 0.2 and 2.0 $M_\odot$; (b) R <12 mag for reasonable integration times; (c) distance less than 140 pc to maximize the astrometric signal to be greater than 6 µas; (d) no companions within 2" or 100 AU for instrumental and scientific considerations, respectively, (e) no nebulosity to confuse the astrometric measurements; (f) variability ΔR < 0.1 mag; and (g) a spread of ages between 1 and 100 Myr to encompass the expected time period of planet–disk and early planet–planet interactions. The variability program proved to be the most stringent filter with roughly 50 percent of the sample showing photometric dispersion in excess of 0.1 mag. A fully validated list of 75 stars meeting all of the above criteria now exists. More stars will be added to the precursor program to bring the total up to the desired number of ~200 stars.

SIM Lite will also look for the lowest-mass planets around the closest, lowest-mass young stars. More and more young stars (10 to 100 Myr) are being found in the vicinity of the Sun as members of the "nearby young moving groups (NYMGs)," associations of stars moving in the same approximate direction (Zuckerman and Song 2004). The stars in the NYMGs are much closer than those in the intensely studied Taurus and Ophiuchus star-forming regions. Hence, the NYMGs enable study of the processes of planet formation at higher resolution than has been possible. To date, the identified members of the NYMGs consist mostly of stars of spectral type F, G, or K; only a few low-mass stars of spectral type M have been confirmed as members. One would, however, expect the groups to contain many more low-mass members simply because the local field mass function strongly favors them. A program is presently underway (Lepine and Simon 2008) to identify new low-mass members in the β Pic and AB Dor groups.*

Figure 2-3 shows the distance distribution of the stars in these groups identified by Zuckerman and Song (2004). The median distances are similar, 35 pc for the ~12-Myr-old β Pic group, and 30 pc for the older, ~40-Myr-old, AB Dor group. Of the 14 candidates for membership in the β Pic NYMG, 11 are bona fide members of which eight are new identifications. Of the 14, eight are M stars, including two M4s. The one AB Dor candidate is also a new member. Even lower-mass group members should be observable in the β Pic and AB Dor moving groups.

Figure 2-3. Nearby moving groups (<35 pc) contain stars as young as 12 to 50 Myr that could be targets for SIM searches for very young, very low-mass planets.
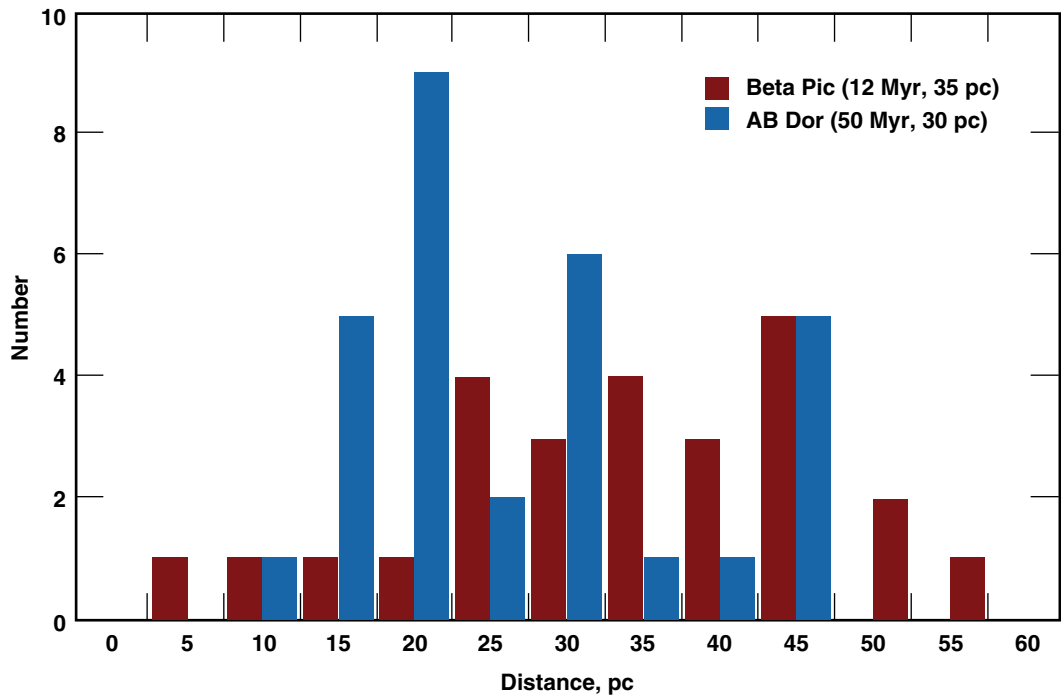
Figure 2-2 (Section 2.5) shows the sensitivity of SIM Lite (~4 µas in a single measurement) to planets with masses much less than Jupiter orbiting an AB Dor group member of M4 spectral type (0.15 $M_{\odot}$) at distance 30 pc. If the astrometric signal is not contaminated by positional jitter (or if, as expected, the noise averages down with square root of the number of visits), then planets with a few Earth masses might be detected at semi-major axes of ~1-5 AU. Certainly, Uranus-mass planets could be detectable.

---

* Low-mass members of the NYMG are also important targets for exoplanet surveys by high-resolution imaging techniques in the near-IR because, at ages of a few tens of Myr, the gas giants are still bright from their gravitational contraction.

2.8   The Young Planets Observing Program

With the nominal performance of SIM Lite, the observing time allocated to the SIM–YSO program (1600 hr), will suffice to make 62 two-dimensional visits to each of 200 stars (Table 2-2). Spread over five years, this would be enough to identify and characterize one or more planets per star, with periods of 1 to 2.5 years. With additional observations during a 10-year extended mission, it will possible to find planets out to 5 AU. The instrumental limit for appropriate observing parameters (http://mscws4.ipac.caltech.edu/simtools/portal/login/) is 2 to 3 µas in narrow-angle mode and 12 µas in wide-angle mode for the closer stars.

Table 2.2. Representative search for planets around young stars (observing estimates from SIM Lite time-estimation simulator).

Observing Mode	Scientific Goal	V Range	5.8σ Limiting Amplitude	No. Stars	Time, hr
Narrow Angle	Jupiter/Saturn search around youngest stars (1–2 Myr, 140 pc, e.g. Taurus) AND Lowest-mass planets around nearby, low-mass stars (10–50 Myr, 30–50 pc, e.g., Beta Pic, AB Dor groups)	6–13 mag	2–3 µas	100	1373
Wide Angle	Jupiter/Saturn search around nearby stars (10–50 Myr, 30–50 pc, e.g., Beta Pic, AB Dor groups)	6–13 mag	12 µas	100	227
Total (equal to allocation for Young Stars Key Project of 1600 hours)				200	~1600

In a SIM Lite survey of 200 young stars, we expect to find anywhere from 20 (assuming that only the presently known fraction of stars, 10 ~15 percent, have planets; Cumming et al. 2008) to 200 (all young stars have planets) planetary systems. We have set our sensitivity threshold to ensure the detection of Jupiter- and Saturn-mass planets in the critical orbital range of 1 to 5 AU. Depending on how well astrometric jitter due to starspots averages down with increasing number of observations, the mass limits could be significantly lower.

These observations, when combined with the results of planetary searches of mature stars, will allow us to test theories of planetary formation and early solar system evolution. By searching for planets around pre-main-sequence stars carefully selected to span an age range from 1 to 100 Myr, we will learn at what epoch and with what frequency giant planets are found at the water-ice "snowline" where they are expected to form (Pollack et al. 1996). This will provide insight into the physical mechanisms by which planets form and migrate from their place of birth, and about their survival rates.

With SIM Lite we will have the data to investigate a series of important questions: What processes affect the formation and dynamical evolution of planets? When and where do planets form? What is the initial mass distribution of planetary systems around young stars? How might planets be destroyed? What is the origin of the eccentricity of planetary orbits? What is the origin of the apparent dearth of companion objects between planets and brown dwarfs seen in mature stars? How might the formation and migration of gas-giant planets affect the formation of terrestrial planets? With a sample of 200 stars, perhaps increased by additional observing programs in an extended 10-year mission, SIM Lite will address directly these and many other questions.

References

Baraffe, I., Chabrier, G., Allard, F., and Hauschildt, P. H., 2002 A&A, 382, 563.

Beichman, C., 2001, Young Stars Near Earth: Progress and Prospects, in ASP Conference Series, Vol. 244, Young Stars Near Earth: Progress and Prospects, (San Francisco: ASP; eds. Jayawardhana, R. and Greene, T.), p. 376.

Bouvier, J. and Bertout, C., 1989, A&A, 211, 99.

Bouvier, J., Covino, E., Kovo, O., Martin, E. L., Matthews, J. M., Terranegra, L., and Beck, S. C., 1995, A&A, 299, 89.

Boss, A. P., 2001, ApJ., 562, 842.

Burrows, A. et al., 1997, ApJ., 491, 856.

Butler, R. P., Johnson, J. A., Marcy, G. W., Wright, J. T., Vogt, S. S., and Fischer, D. A., 2006, PASP, 118, 1685.

Carpenter, J. M. et al., AJ, 121, 3160.

Chauvin, G., Lagrange, A.-M., Dumas, C., Zuckerman, B., Mouillet, D., Song, I., Beuzit, J.-L., Lowrance, P., 2005, A&A, 438, L25.

Cumming, A., Butler, R. P., Marcy, G. W., Vogt, S. S., Wright, J. T., and Fischer, D. A., 2008, PASP, 120, 531.

Eiroa, C. et al., 2002, A&A 384, 1038–1049.

Huélamo, N. et al., 2008, A&A, 489, 9.

Ida, S. and Lin, D. C., 2005, ApJ., 626, 1045.

Kalas, P. et al., 2009, Science, in press.

Lepine, S. and Simon, M., AJ, in press.

Lin, D. N. C., Papaloizou, J. C. B., Terquem, C., Bryden, G., Ida, S., 2000 in Protostars and Planets IV (Tucson: University of Arizona Press, eds. Mannings, V., Boss, A. P., Russell, S. S.), p. 1111.

Marios, C. et al., 2009, Science, in press.

Mekkaden, M. V., 1998, A&A, 340, 135.

Neuhäuser, R., Guenther, E. W., Wuchterl, G., Mugrauer, M., Bedalov, A., and Hauschildt, P. H., 2005, A&A, 435, L13.

Pollack, J. B., Hubickyj, O., Bodenheimer, P., Lissauer, J. J., and Podolak, M., Icarus, 1996, 124, 62.

Prato, L., Huerta, M., Johns-Krull, C. M., Mahmud, N., Jaffe, D. T., and Hartigan, P., 2008, ApJ, in press. (arXiv:0809.3599)

Schussler, M., Caligari, P., Ferriz-Mas, A., Solanki, S. K., Stix, M., 1996, A&A, 314, 503.

Setiawan, J., Henning, Th., Launhardt, R., Müller, A., Weise, P., and Küster, M., 2008, Nature, 451, 38.

Skumanich, A., 1972, ApJ, 171, 565.

Strassmeier, K. G. and Rice, J. B., 1998, A&A, 339, 497.

Tanner, A. et al., 2007, PASP, 119, 747.

Wuchterl, G. and Tscharnuter, W. M., 2001, A&A, 398, 1081.

Zuckerman, B. and Song, I., 2004, ARAA, 42, 685.

3 Multiple-Planet Systems

Eric Ford (University of Florida), **Geoffrey W. Marcy** (UC Berkeley), **Michael Shao** (JPL), **Matthew W. Muterspaugh** (UC Berkeley), **Charles Beichman** (NExScI), **Jason Wright** (Cornell University), **Debra A. Fischer** (SFSU), **Joseph H. Catanzarite** (JPL), **Robert Olling** (University of Maryland), **Shrinivas Kulkarni** (Caltech), **Stephen C. Unwin** (JPL), and **Wesley A. Traub** (JPL)

ABSTRACT

SIM Lite will discover rocky planets and ice giants orbiting within a few AU of nearby stars, complementing the gas giants found around those same stars by radial velocity and transit surveys. A set of 60 stars within 20 pc are to be surveyed with the nominal SIM Lite mission, providing a statistically meaningful census of typical architectures of planetary systems. Results from radial velocity surveys suggest that multiple-planet systems are common. SIM Lite will provide the full three-dimensional orbits and the masses for planets in each system, including orbital inclinations and eccentricities, thus establishing the major components and architecture of each planetary system. By extending the census of nearby planetary systems to include terrestrial planets, SIM

Lite can test theories of planet formation and subsequent evolution that are desperately in need of further empirical constraints. By providing precision measurements of planetary masses and full three-dimensional orbits, SIM Lite can search for correlations between planet mass and other properties, providing tests of planet-formation models. Further, SIM Lite can characterize the long-term evolution of planetary eccentricities and inclinations, permitting tests of theories of the origins of multiple-planet systems, including orbital migration and planet–planet gravitational interactions. Mock multiplanet systems have been constructed and used as the basis for simulated SIM Lite and radial velocity measurements and a double-blind search for planets (using separate teams to generate input data and analyze mock observations) has been performed. Even when faced with multiple-planet systems, mock planets with masses as low as 1.0 $M_\oplus$ were "detected" by SIM Lite, as long as the astrometric signature (α) of the rocky planet was above the threshold for detection $\alpha_{THRESH} = 5.8\sigma / N^{1/2}$, where σ is the single-observation astrometric uncertainty and N is the number of astrometric observations. Thus, a combination of SIM Lite and radial velocity monitoring has been demonstrated to provide a powerful basis for detecting and characterizing the orbits of terrestrial-mass planets in realistic planetary systems. The proximity of these planetary systems will allow IR and mm-wavelength observatories (e.g., JWST, ALMA) to detect, measure, and resolve dust disks within these planetary systems, providing detailed assessments of the small-body populations (e.g., asteroids, Kuiper belt objects, comets) and their relationship to the arrangement of planets in the system. Finally, the proximity of the planetary systems discovered by SIM Lite will eventually allow coronagraphs and spaceborne observatories to study the planets themselves, using imaging, photometric variability, and spectroscopy.

3.1   Multiple-Planet Systems Are Common

Theoretical models of planetary formation predict the common occurrence of systems with multiple planets. Already, 27 multiplanet systems have emerged from Doppler surveys of nearby stars, as shown in Figure 3-1, despite a significant bias towards finding the most-massive planets on relatively short-period orbits. A complete description of known multiple-planet systems and their properties is given by Wright et al. (2008). Theoretical models of planetary systems undergoing dynamical relaxation predict that mature planetary systems typically contain two or three giant planets (e.g., Adams and Laughlin 2003; Juric and Tremaine 2008). The Doppler discovery of exoplanet systems with at least four planets (HD160691) and five planets (55Cnc), along with the eight major planets in our Solar System, suggests that multiple-planet systems may be the rule rather than the exception. Further, radial velocity (RV) surveys already suggest that 23 percent of surveyed stars show a significant excess of radial velocity variability that could be naturally explained by additional planets (Cumming et al. 2008). If one also accounts for long-term radial velocity trends, then 30 to 50 percent of giant exoplanet host stars show some evidence of additional companions (Wright et al. 2007, 2008). Both the number and fraction of planets in multiple-planet systems are likely to increase as planet searches become sensitive to planets with lower masses and longer orbital periods. In particular, some theoretical models of planet formation predict that low-mass planets will be significantly more numerous and find that even systems with short-period gas giants could contain several low-mass planets regardless of whether the gas giant planets migrated through the terrestrial planet region (Cresswell and Nelson 2006; Mandell and Raymond 2006). Since many, if not most, planets are members of multiple-planet systems, understanding the formation and evolution of multiple-planet systems is essential for understanding planet formation in general.

Figure 3-1. Display of semi-major axes and masses for the 27 known multiplanet systems. The diameters depicted for planets are proportional to the cube root of the planetary $m \sin (i)$. The periapsis to apoapsis excursion is shown by a horizontal line. Masses are in M_{Jup}. Despite a significant bias toward finding the most massive planets on relatively short-period orbits, most known multiple-planet systems contain a planet beyond 2 AU, suggesting that many systems currently known to contain a single planet may harbor additional planets at larger separations.
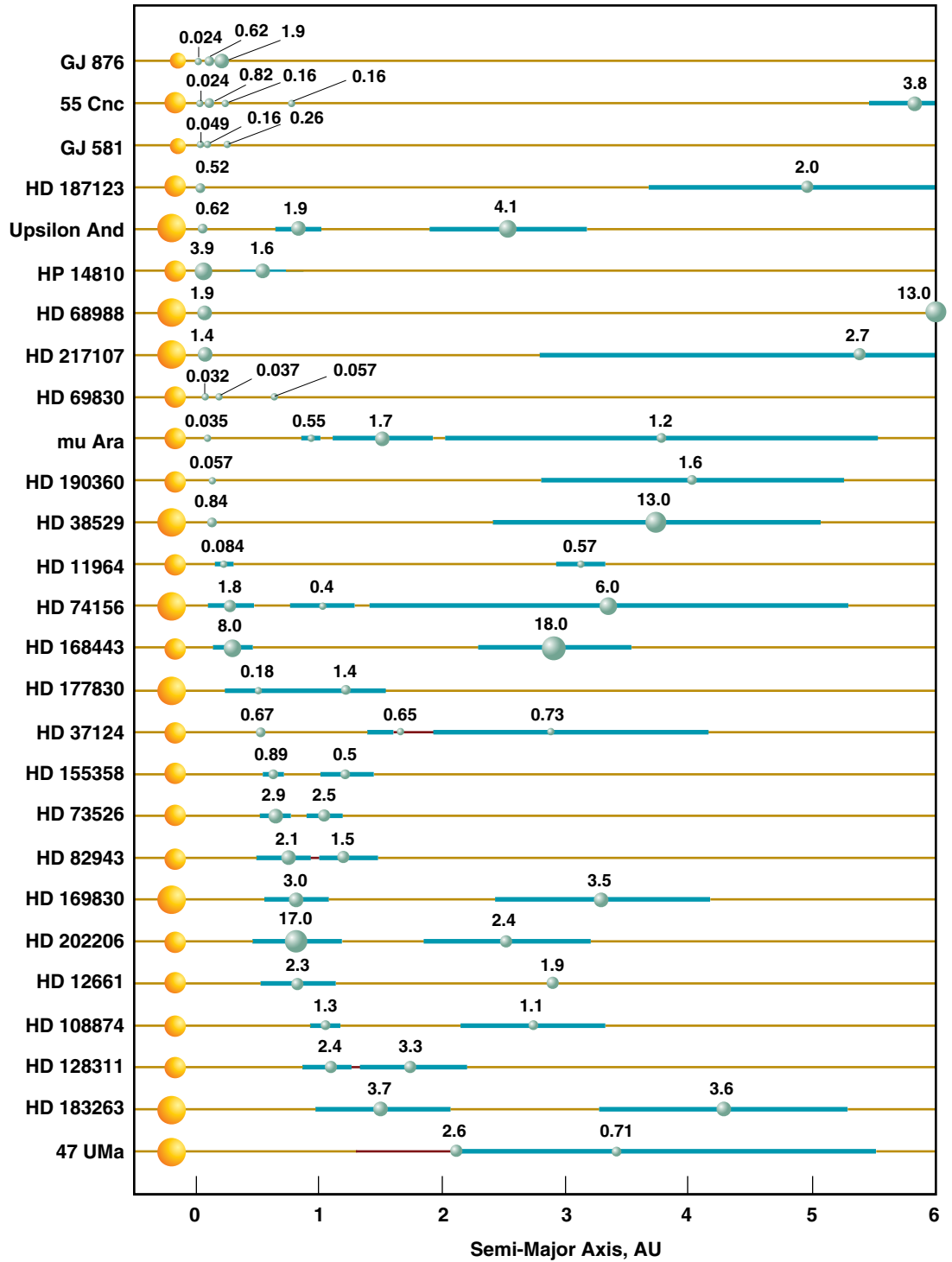
3.2   Observable Properties of Multiplanet Systems

Astrometric observations provide the opportunity to fully characterize the six phase-space coordinates (e.g., positions and velocities) for each planet detected, including all seven orbital parameters (i.e., the planet masses and the six osculating Keplerian orbital elements) for each planet. The combination of both radial velocity and astrometric observations is particularly powerful for studying multiple-planet systems, both to independently verify planets and to establish the full suite of planet masses and orbits. Radial velocity observations contribute by detecting and measuring most of the orbital parameters for short-period planets. Once radial velocities measure the period and phase of a short-period planet, adding astrometric observations can often constrain the planet's inclination and orientation, even if astrometry alone would not be able to detect the short-period planet. In contrast, astrometric observations are most sensitive to long-period planets (up to orbital periods comparable to the time span of astrometric observations). For planetary systems containing giant planets with orbital periods exceeding SIM Lite's mission lifetime, radial velocity observations can again contribute by constraining their orbital periods and modeling out their effects. Thus, the combination of SIM Lite and radial velocity observations is significantly more powerful for measuring the architecture of a planetary system than either method alone (Ford 2006).

While the dynamical signature for a single planet is relatively simple, the dynamical signature for multiple-planet systems can be much more complex and require detailed modeling. Fortunately, simulations have shown that SIM Lite will be able to precisely characterize most systems with multiple giant planets with orbital periods up to the mission lifetime (Sozzetti et al. 2003) and that SIM Lite's detection efficiency for terrestrial planets will only be slightly impacted by the presence of other planets (Ford 2006; §3.5). Those systems that are more challenging typically contain closely spaced planets and/or near mean-motion resonance. For such systems, there can be significant planet–planet interactions, and full *n*-body simulations may be necessary to achieve self-consistent orbital solutions (Laughlin and Chambers 2001). While significant planet–planet interactions complicate the analysis, they also provide an opportunity to measure the strength and time scale of such interactions. When early observations are consistent with multiple orbital solutions, dynamical models can identify which epochs are particularly powerful for constraining models, resulting in increased efficiency of observations (Loredo and Chernoff 2003; Ford 2008). Similarly, by assuming long-term dynamical stability, theorists can reject otherwise plausible orbital solutions and constrain the masses and orbital parameters (e.g., Rivera and Lissauer 2000). As more multiple-planet systems are discovered, dynamical research will play a symbiotic role in planning and deciphering observations.

3.3   Relationship of Giant and Terrestrial Planets

Doppler measurements show that 10.5 percent of stars harbor giant planets (with masses greater than a Saturn mass) within ~7 AU (Cumming et al. 2008). However, there are no firm constraints observationally or theoretically on the occurrence rate of Earth-mass planets. Using our Solar System as a guide, one might expect that long-period Jupiters could often be accompanied by inner terrestrial planets. The formation processes and typical structure of multiplanet systems, including both terrestrial and giant planets, remains poorly known. Currently, theories for the formation of rocky planets suggest that terrestrial planets should be commonplace, regardless of whether or not gas giant planets have had a chance to form (e.g., Wetherill 1996; Raymond et al. 2006). However, theory has a checkered history of predicting exoplanet properties. In particular, the diversity of known giant exoplanets casts doubt on the assumption that our Solar System represents a typical planetary system. By detecting both terrestrial and giant planets across a broad range of orbital separations, SIM Lite will characterize the typical architectures of planetary systems, so humankind can finally answer the fundamental question: "Is our Solar System special?"

Both the diversity of observed planetary systems and theoretical models of planet formation suggest that similar initial conditions can result in widely differing final planetary systems. While theoretical models do not predict the masses or orbits of individual systems, they can predict properties of the exoplanet population as a whole, such as the typical number of giant planets (e.g., Adams and Laughlin 2003), the eccentricity distribution (e.g., Ford and Rasio 2008; Juric and Tremaine 2008), and the correlation between stellar and planet properties (e.g., Robinson et al. 2006). SIM Lite will provide a statistically useful set of planetary systems that will demand theoretical explanations by a combination of deterministic and stochastic processes.

Moreover, protoplanetary disks will be observed directly by JWST, the Atacama Large Millimeter Array (ALMA), and other IR and mm-wavelength instruments. The observed properties of protoplanetary disks and models of planet formation and evolution must adequately predict the properties of exoplanets (Wolf et al. 2007). SIM Lite's ability to measure planet masses to 10 percent and their three-dimensional orbits is crucial for mapping JWST and ALMA observations to actual planets. Comparing these predictions with actual exoplanet detections can provide valuable constraints on models for the formation and evolution (e.g., orbital migration, eccentricity excitation) of planetary systems (e.g., Benz et al. 2006; Ida and Lin 2004ab, 2008ab; Kennedy and Kenyon 2008ab; Figure 3-4).

3.4   Architecture of Multiple-Planet Systems

Studying the architectures of multiple-planet systems can provide insights into planet formation processes, including formation, orbital migration, and subsequent gravitational interactions. Moreover, discovering and characterizing multiple-planet systems would add key information about the orbital properties and habitability of planets (Ford et al. 2008).

For example, it remains unknown if the co-planarity of planetary orbits in the Solar System is a common property of planetary systems in general. Already, spectroscopic observations during transit have measured the Rossiter-McLaughlin effect (the apparent change in radial velocity due to the transit) and constrained the spin-orbit alignment of several short-period giant planets. While existing observations suggest that most short-period, giant, transiting planets have orbital angular momentum nearly parallel to the stellar spin axis, at least one system appears to have a large misalignment (Hebrard et al. 2008). SIM Lite will be able to measure the orbital inclinations of giant planets relative to the inclinations of other planets, particularly at larger orbital separations where tides are not significant. SIM Lite will also be able to measure the relative inclinations of low-mass planets for which Rossiter-McLaughlin observations are impractical. If the low inclinations (and eccentricities) in our Solar System contributed to the habitability of Earth, then our human presence may have biased our ideas about planetary systems, which have long presumed that our Solar System is "normal." In fact, our Solar System could be a relatively rare type of planetary system that did not suffer close encounters between giant planets, allowing the terrestrial planets to form and persist on circular orbits for long enough to give rise to intelligent life (Thommes et al. 2008). Gravitational interactions may be so common among planets in a typical system that such co-planarity is rare. Modeling shows that the final distribution of inclinations of giant planets is influenced by strong planet–planet scattering. In some models, rocky planets might typically be accreted or ejected by giant planets that migrate through the "habitable zone" (Kasting 1993). SIM Lite will measure the co-planarity of planetary systems, a property directly tied to the origin and gravitational interactions of planets in general. Thus, SIM Lite will contribute to testing one variable of the "rare-Earth" hypothesis.

3.5 Origins of Planetary Systems from Dynamical Measurements

Studying the dynamical properties of specific planet systems can provide insights into planet formation processes. Dynamical research is particularly powerful when applied to observations of multiple-planet systems, since the current orbital configuration can provide clues to the dynamical history of these systems. By making precise measurements of the planet masses and their current orbits, SIM Lite will enable theorists to evolve systems forward and backward in time to study the long-term evolution of planets' eccentricities and inclinations. The presence of mean-motion resonances or significant long-term eccentricity evolution can provide strong constraints on the mechanisms involved in their formation, orbital migration, and subsequent gravitational interactions.

3.5.1 Mean-Motion Resonances

Detections of pairs of planets in or near mean-motion resonances provide empirical constraints on models of orbital migration. For example, the GJ876 system contains two giant planets with periods of 30 and 61 days. Long-term radial velocity monitoring of this system has provided empirical evidence that the two Jovian planets are in a 2:1 mean-motion resonance and participate in a secular apsidal lock (Laughlin et al. 2005), providing a wealth of information about the formation, migration, and eccentricity damping of the system during its formation stages. Figure 3-2 shows the velocities from the Keck telescope for GJ876 during the past decade. The odd envelope structure of the radial velocities is well understood in terms of a near commensurability of orbital periods and the precession of both orbits due to the planet–planet interactions. The long-term stability of the system is contingent upon the precise orbital separations that allow the two orbits to precess at the same rate, so as to avoid close encounters that would destabilize the system. The mere presence of such mean-motion resonances provides evidence for orbital migration that allowed the two planets to form on more widely separated orbits before becoming captured into the current resonant location. More-detailed modeling provides constraints on the rate and smoothness of the migration. For GJ876, the amplitude of oscillations about a precise resonance and the currently observed eccentricities place constraints on the mechanisms that caused the eccentricity damping and/or halting of migration (Lee and Peale 2002).

Figure 3-2. Top: Stellar reflex velocity from a self-consistent, coplanar, edge-on three-body integration compared to the GJ876 radial velocities. Bottom: Residuals to the orbital fit. (Figure from Laughlin et al. 2005)
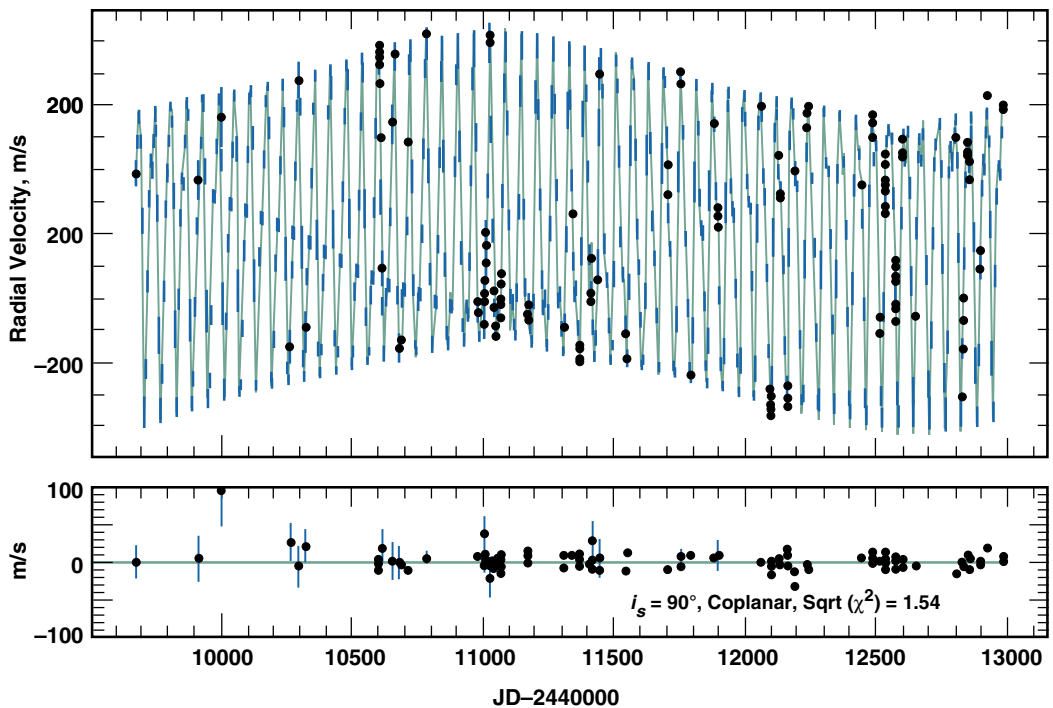
3.5.2 Long-Term Eccentricity Evolution

As another example, the secular evolution of the Upsilon Andromedae planetary system provides evidence for an impulsive perturbation, likely due to a previous close encounter by another planet (Malhotra 2002; Ford et al. 2005). Figure 3-3 (bottom) shows the variation in eccentricity of the outer two giant planets in this system implied by the current RV observations. The periodic recurrence of a very nearly circular orbit for one of the giant planets is unlikely to be a coincidence. It indicates a history in which both planets originally followed nearly circular orbits, but one planet suffered a close encounter with another Jovian planet. That close encounter impulsively perturbed the orbit of the outer planet, leading to the peculiar long-term evolution that is seen today. Such close encounters may be common, perhaps exciting the large eccentricities commonly observed for giant planets. If so, strong scattering of giant planets may play a significant role in sculpting planetary systems in general, with important consequences for the frequency and orbits of terrestrial planets.

The ability to directly measure orbit inclinations also opens the door to qualitatively new tests of planet formation models. Different models of planet migration and eccentricity excitation make different predictions for the secular evolution of planetary eccentricities and inclinations (e.g., Chatterjee et al. 2008). Therefore, testing models of planetary orbital evolution requires astrometric observations to determine if the long-term evolution of orbital inclination correlates with the eccentricity evolution.

Figure 3-3. Secular evolution of the outer two giant planets orbiting in the planetary system around υ Andromedae. The top panel shows the semi-major axes (thick lines), as well as the periastron and apastron distances (thin lines), for planets c (red) and d (blue). The lower panel shows the evolution of the orbital eccentricity for each planet. Note that both planet c (dashed) and planet d (dotted) have a significant eccentricity at the present time ($t = 0$), but that the eccentricity of planet c returns periodically to very small values near zero (Ford et al. 2005).
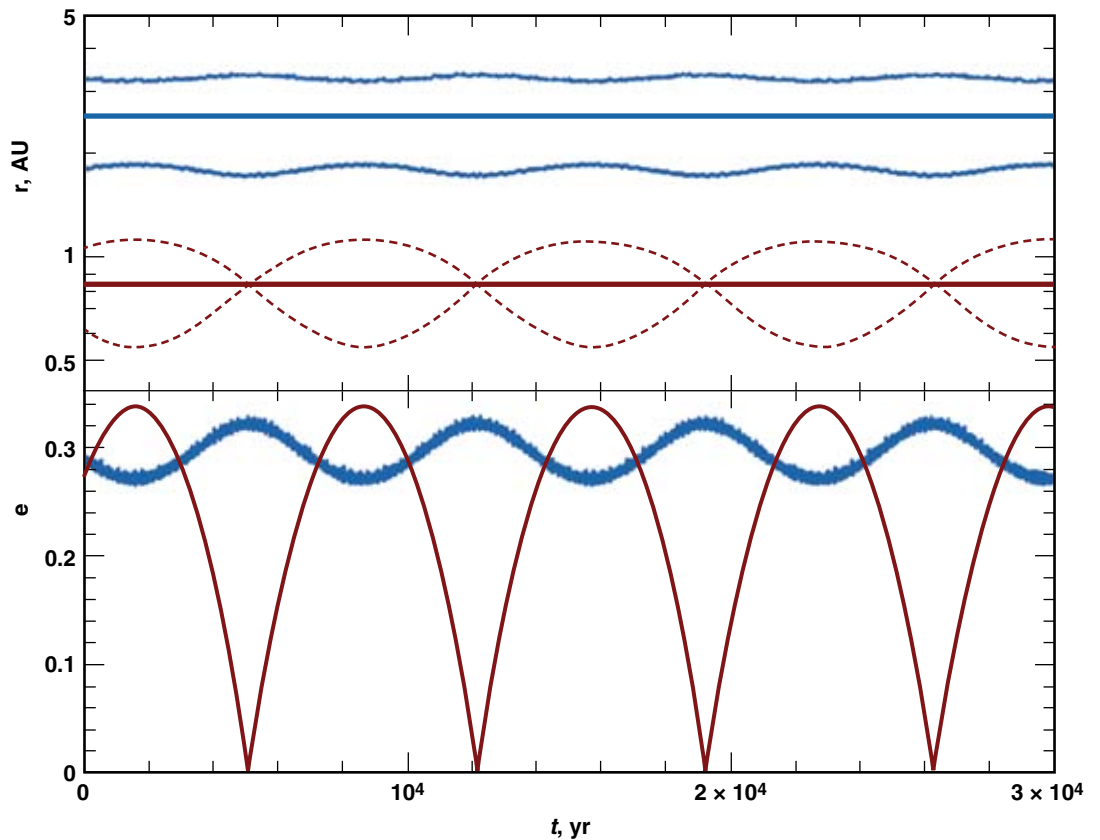
3.5.3   Long-Term Dynamical Stability and Long-Period Planets

For multiple-planet systems, the requirement of long-term orbital stability can provide strong constraints on the masses and orbits of planets throughout the entire system. Orbital analysis based only on radial velocities typically benefits from demanding long-term dynamical stability, thereby constraining the inclinations and providing upper limits to the planet masses. Unfortunately, such analyses often leave uncertainties of ~30 degrees in inclination and a factor of ~2 in the planet masses. These uncertainties can cause qualitative uncertainties in the dynamical state of the system. SIM Lite observations can resolve such degeneracies, establishing masses and orbits to better than ~10 percent accuracy, for planets with orbital periods less than the mission duration. For multiple-planet systems, the combination of SIM Lite observations, ground-based radial velocity observations, and long-term orbital stability can place constraints on the masses and orbits of long-period planets and thus provide improved constraints on the properties of other planets closer to the "habitable zone."

3.6   Detectability of Earth-Mass Planets in Multiple-Planet Systems

At first glance, it should not be difficult to extract the astrometric signal of an Earth-like planet from the composite signal of a system of planets around a star. Because each planet contributes an astrometric signal with a different frequency in time, a Fourier analysis of the total signal should reveal the signature of each planet provided there is a large number of observations with sufficient signal-to-noise ratio. However, in reality the case might be not so simple. For example, a planet in an eccentric orbit with a dominating signal (e.g., a Jupiter) might have harmonic terms that are not recognized as such but might look like a separate planet. Or a long-period planet observed over a time shorter than that period would have noise generated at many frequencies owing to the difficulty of distinguishing a proper motion on the sky from a part of an orbit. In order to address these potential concerns, we initiated a double-blind simulation to see how well Earth-like planets (i.e., terrestrial masses, habitable-zone periods) could be detected in multiple-planet systems with SIM Lite, with the help of RV. An additional goal was to see what accuracy by SIM Lite is necessary to achieve a goal of being able to detect Earth-like planets.

The simulation was organized with four teams of scientists, the planet modelers (Team A), the data simulators (Team B), the data analyzers (Team C), and the overall summarizers (Team D).

Team A comprised five groups of planetary system modelers. Each group generated about 150 planetary systems, using their own best estimate of the actual distribution of masses and periods in real systems. The constraints were that the frequency and orbital properties of Jupiter-like planets agree with the Cumming et al. (2008) analysis of a Jupiter-complete sample of RV observations. In addition, the systems were to be stable.

Team B was a single group that took input planetary models, rotated the systems at random, set up realistic observing schedules, generated synthetic astrometric and RV signals, and added noise. A total of 48 planetary systems were generated, of which 32 were random Team A systems, 8 were Solar System analogs (perturbed), 4 were single terrestrial HZ planets, and 4 had only planetesimals or planets below the threshold for detection. To focus on the key variables of planet mass and period, all simulations were for a single star at a fixed point in the sky and at 10 pc. The RV noise was 1 m/s rms, a value that includes expected instrumental as well as astrophysical noise. The astrometric noise for most of the data sets was the expected noise from SIM Lite, 1.0 µas per single observation per axis per star, and therefore a factor of about 1.4 larger for a differential measurement (target with respect to reference) per axis (RA or DEC). The timelines for half of the data were five years of astrometric and 15 years of RV observations. For the other half, the timelines were 10 years of astrometric and 20 years of RV observations. The orbits were calculated assuming independent Keplerian motion, i.e., *n*-body codes were not used.

Team C comprised five groups of data analyzers, competitively selected. Each group was given a set of practice data sets, with and without noise, to validate their code. The groups worked independently to develop their own analysis codes. The groups were given four weeks to analyze all 48 systems described above. The Team C groups were asked to report planet signals detected in the joint astrometric–RV data streams that had a false-alarm probability of less than 1 percent. The exercise was double-blind in the sense that the person distributing the simulated data to the analyzers did not know any details of the systems, so no hints could possibly be transmitted. A brief summary of the results follows.

Reliability of detections is defined as the ratio of true detections to the total of all detections, true plus false. A reliability of 100 percent would mean that no reported detections were false alarms. In the double-blind study, one group had a reliability of 100 percent. Two others were over 80 percent. A fourth was at about 40 percent. (One group was not able to complete the exercise on time.) In principle, this value should have been about 99 percent, if the false alarm rate had truly been 1 percent. However, the short amount of time for the exercise meant that only one group had enough experience to fully weed out false alarms. For this reason, the exercise is being repeated with extra statistical tests added.

Completeness of detections is defined as the ratio of true detections to the total of all detectable planets. A completeness of 100 percent would mean that all detectable planets were reported. (In the double-blind study, a planet with a combined astrometric and RV SNR of 5.8 was considered detectable, Figure 3-4.) Completeness was expected to be 100 percent if the SNR was well above that value. Here the SNR is defined as the amplitude of the true signal, divided by the noise for the entire observing campaign, which is the measurement noise per visit to the star divided by the square root of the number of visits. This definition applies to astrometric as well as RV observations. Over a range of SNR values from about 0.7 to 7000, we found that the completeness did indeed jump sharply from about 0 to 100 percent at a SNR of about 5.8, as expected theoretically. Completeness vs. planet type is shown in Figure 3-5.

The accuracy of results also was close to the theoretically expected values for the key parameters of period and mass. We calculated the expected accuracy using a minimum-variance bound method. Comparing the subjectively correct answers to the actual answers, and scaling that offset by the expected value of the offset, we found a roughly Gaussian distribution, with approximately the expected number (68 percent) of values lying in the range (–1, +1), no significant offset from zero (i.e., no bias), and very few values in the range between plus or minus 1 and 3. However, beyond the 3-sigma point, where essentially no points should fall, we found a handful of cases (about 14 percent); these appear to be situations where the expected error was very small (less than 1 percent in mass or period), and the actual error was more than three times that value. In other words, these were good measurements but not as perfect as theoretically expected.

In overall summary, this first phase of the simulation showed that the answers to our initial questions are: (1) Earths can be detected in realistic multiplanet systems, and (2) the sensitivity needed matches the projected capability of a five-year SIM Lite mission. The mission was defined to be using 40 percent of the available observing time, with the expected noise level and a 6-m baseline, plus the additional help (mostly with long-period planets) from 15 years of RV observations. The first phase of the study is being followed up with a second phase in which planetary systems will be simulated for the 60 best actual stars for planet searching — using actual distances, masses, and luminosities — instead of a hypothetical reference star of one solar mass at 10 pc. In this follow-up, all tentative detections will be subject to an additional statistical F-test and a stability test, as well as given additional time for the analysis, before being reported as probable detections.

Figure 3-4. Results on completeness from the SIM Lite double-blind study. Completeness is the detected fraction of planets. The curve is empirically determined for 1 percent false alarm probablility (Catanzarite et al. 2006). The plotted points are the (number of correct planets)/(number of total planets). The curve shows that at SNR >6, the measured completeness is excellent, as predicted. Here, SNR is the RV SNR and astrometric SNR combined in quadrature.
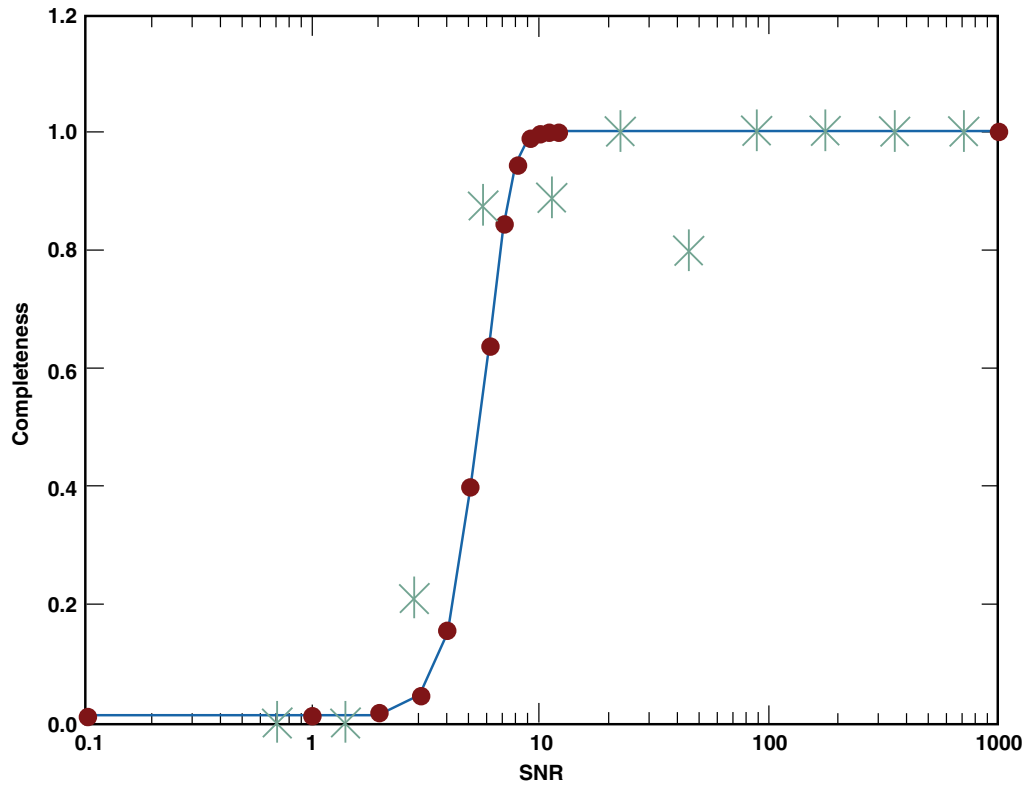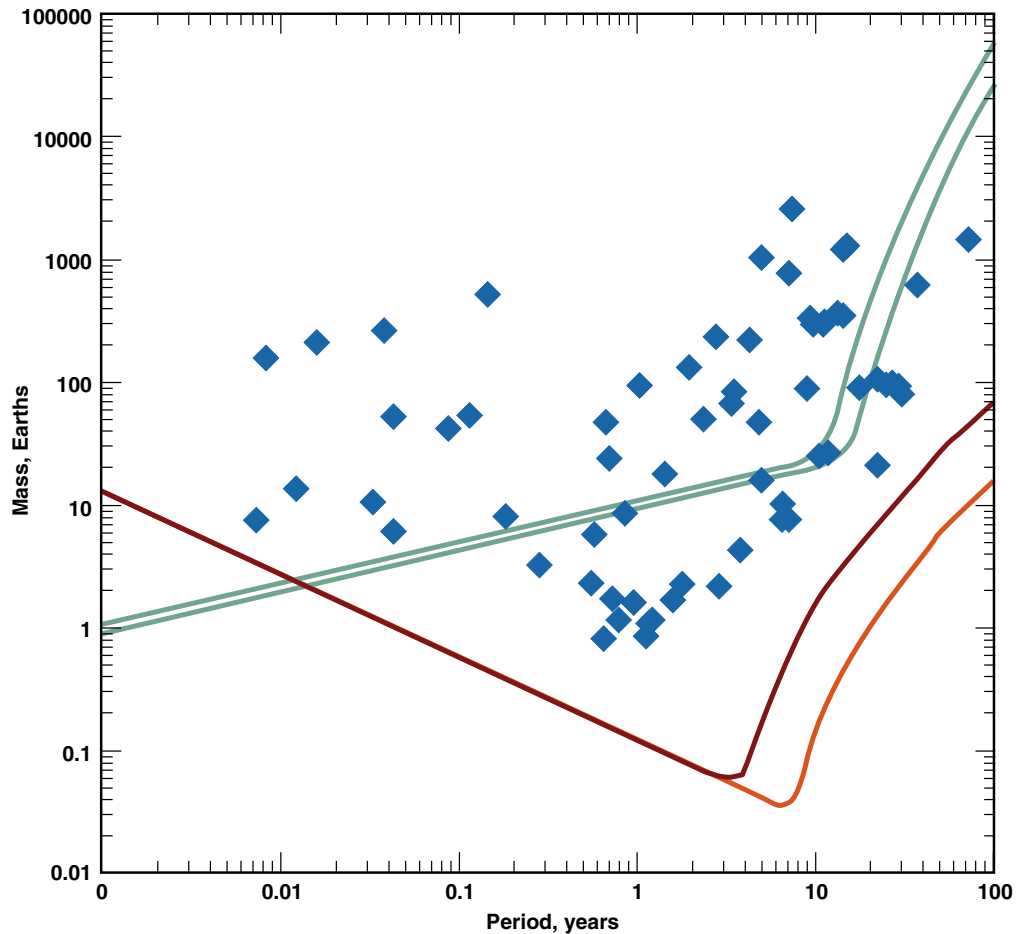

Figure 3-5. From the test systems, there are 70 high-SNR (>6) planets (plotted). Forty-eight of these have periods shorter than 10 years; all should have been detected and all were. The chart shows SNR-based detection limits for RV (blue; upper for 15 years of measurements, lower for 20 years) and SIM Lite (red, upper for a five-year mission, lower for a 10-year mission).

3.7   Relevance to Habitability and Search for Earth-Like Life

While previous exoplanet discoveries have revealed a diverse range of planetary systems, it is not yet clear if planetary systems resembling our Solar System are common or exceedingly rare. Future observational programs will search for planets increasingly similar to the Earth, in terms of their mass, orbital separation, host star, physical size, and atmospheric/surface properties.

The dynamical processes of planetary systems impact the habitability of any terrestrial planets and may have influenced the evolution of life on Earth. For example, in our Solar System, interactions between the giant planets and the planetesimal disk are believed to have triggered the late heavy bombardment of Earth (Tsiganis et al. 2005) and contributed to the delivery of Earth's oceans and of organic molecules to Earth's surface (Morbidelli et al. 2000). Thus, the detection of both the gas giants and the Earth-like planets will stimulate work on dynamical properties of the host planetary system that contribute to habitability. The combination of radial velocity and SIM Lite is uniquely capable of characterizing all major planets in an inner planetary system, allowing theorists to investigate their dynamical histories and implications for planet formation.

Periodic variations in both Earth's rotational and orbital state are believed to be a cause of variations in Earth's climate (Hays et al. 1976). Both the small eccentricities of the Solar System planets and the presence of a massive Moon that stabilizes Earth's obliquity contribute to a stable climate that may have been significant for the evolution of life on Earth. One wonders if typical terrestrial-mass planets maintain nearly constant eccentricities and obliquities, like Earth, or if their stellar irradiation and climate will vary much more widely due to large oscillations in orbital eccentricity and chaotic variations in the obliquity. In order to understand the habitability of a planet, Earth-like or otherwise, it is important to detect and characterize the orbits of all major planets orbiting that host star. For example, a detection of our Solar System that only identified Earth and Jupiter would not provide enough information to understand the secular orbital evolution of the Earth or the role of the giant planets in scattering Kuiper Belt objects and comets. Thus, when searching for planets near the habitable zone, it is important to have significant sensitivity for detecting additional planets at distances much closer and more distant than the habitable zone. The combination of long-term ground-based radial velocity (Tanner et al. 2007; §13.4) and astrometric observations (Cameron et al. 2008) and SIM Lite's high-precision astrometry will provide a unique capability to investigate the dynamical influence of long-period giant planets on potentially habitable planets.

3.8   Strategy for Maximizing Scientific Return of SIM Lite

The rich diversity of planetary systems with multiple giant planets discovered by radial velocity surveys raises the possibility of a comparable or even greater diversity among terrestrial planets. The combination of long-term radial velocity and astrometric observations is astronomers' most powerful method for characterizing the dynamical state of planetary systems. The detection of Earth-like planets will stimulate a variety of questions about the host planetary system:

- Are there signs of large-scale planetary migration, such as other planets in mean-motion resonances, or giant planets at small orbital separations?
- Are there signs of previous violent phases of evolution, such as eccentric or highly inclined planets?
- Will the orbits remain nearly constant or undergo significant long-term evolution?
- What are the implications for the planet's climate, the potential for liquid water, and the possibility of Earth-like life?

Addressing each of these questions will require identifying and characterizing the orbits of all other major planets in the planetary system. Therefore, detections of Earth-like planets by SIM Lite should be accompanied by significant astrometric and radial velocity follow-up observations to determine the architecture of the planetary system and to enable comparisons to our own Solar System. In order to achieve this goal, we offer the following recommendations to maximize SIM Lite's scientific return.

SIM Lite should search for and characterize a wide range of planetary systems, including planets and host stars both similar and dissimilar to our own. This is necessary to appreciate the significance of our Earth and Solar System. In particular, previous exoplanet discoveries have revealed many planets with very unexpected orbital properties. Therefore, SIM Lite should search for terrestrial planets in any location where they could survive — given the constraint of long-term orbital stability — regardless of the predictions of planet formation theories. As there is little dynamical significance to the habitable zone or one Earth-mass, SIM Lite can best contribute to improving our understanding of planet formation in general by observing many planetary systems with a range of planet masses and orbital properties.

Stars already known to host at least one planet should be included among SIM Lite targets. Since stars hosting one giant planet are more likely to harbor additional giant planets, increasing the observing cadence for observations of these target stars can simultaneously improve the dynamical constraints for known planets and increase the sensitivity for detecting additional planets.

In addition to discovering new planets, a significant portion of SIM Lite's observing time should be devoted to intensified follow-up observations that provide precision dynamical constraints for multiple-planet systems. Multiple-planet systems, especially those with significant planet–planet interactions, are typically much more valuable to theorists than several single-planet systems for providing insights into planet formation. Further, the power of dynamical studies increases with the number, time span, and precision of the observations for each particular planetary system. Thus, the SIM Lite observing schedule should allow for intensified observations of particularly interesting multiplanet systems that are identified early in the mission. Theorists should collaborate with observers to identify the most interesting systems to be targeted for intensive follow-up observations.

Coordinated long-term radial velocity monitoring will play an important and complementary role in SIM Lite's quest to characterize the architectures of multiple-planet systems, particularly those with hot Jupiters and/or long-period giant planets, such as Jupiter and Saturn. To understand the orbital evolution of a planet, it is important to detect and characterize the orbital parameters of the other major planets orbiting the host star. In particular, when searching for planets in or near the habitable zone, it is important to have significant sensitivity for detecting additional planets at distances much closer and more distant than the habitable zone.

Detecting Earth-like planets around Sun-like stars may require intensive observations (~250 SIM Lite visits) of a modest number of target stars (~60 in the nominal SIM Lite mission). At the same time, shallow and wide planet searches could provide significant statistical constraints for testing planet formation models. If prior missions/observations determine that terrestrial-mass planets are quite common, astronomers should consider a hybrid observing strategy, including both shallow-wide and narrow-deep planet searches.

Funding for data analysis and theoretical research is essential to maximize SIM Lite's scientific return. The 1991 and 2001 NRC Decadal Surveys concluded that significant funding of theoretical research is necessary to maximize the scientific return of new observatories. Theoretical research in planetary dynamics will play an essential role in the design, analysis, and interpretation of SIM Lite observations. Comparing theoretical models with planets discovered by SIM Lite will require a detailed understanding

of observational techniques and uncertainties. Frequent interactions between theorists and observers should provide opportunities for theorists to learn about the observational sensitivities, precisions, uncertainties, systematic effects, biases, etc., that should be considered when interpreting observations.

References

Adams, F. C. and G. Laughlin, 2003, Icarus, 163, 290.

Benz, W., Mordasini, C., Alibert, Y., and Naef, D., 2006, Tenth Anniversary of 51 Peg-b: Status of and prospects for hot Jupiter studies, eds. Arnold, L., Bouchy, F., and Moutou, C., 24. http://www.obs-hp.fr/www/pubs/Coll51Peg/proceedings.html.

Butler, R. P. et al., 2006, ApJ, 646, 505.

Cameron, P. B., Britton, M. C., and Kulkarni, S. R., 2008, arXiv:0805.2153 AJ, submitted.

Catanzarite, J. et al., 2006, PASP, 118, 1319.

Chatterjee, S., Ford, E. B., Matsumura, S., Rasio, F. A., 2008, ApJ, 686, 580.

Cresswell, P. and Nelson, R. P., 2006, A&A 450, 833.

Cumming, A., Butler, R. P., Marcy, G. W., Vogt, S. S., Wright, J. T., and Fischer, D. A., 2008, PASP, 120, 531-554.

Ford, E. B., 2006, PASP, 118, 364.

Ford, E. B., 2008, AJ, 135, 1008.

Ford, E. B. et al., 2008, white paper submitted to the Exo-Planet Task Force, arXiv:0705.2781.

Ford, E. B. and F. A. Rasio, 2006, ApJ, 638, L45.

Ford, E. B. and Rasio, F. A., 2008, ApJ, 686, 621.

Ford, E. B., Lystad, V., and Rasio, F. A., 2005, Nature, 434, 873.

Hays, J. D., Imbrie, J., and Shackleton, N. J., 1976, Science, 194, 1121.

Hebrard, G. et al., 2008, to be published in A&A, arXiv:0806.0719.

Ida, S. and Lin, D. N. C., 2004, ApJ, 604, 413.

Ida, S. and Lin, D. N. C., 2004, ApJ, 616, 567.

Ida, S. and Lin, D. N. C., 2008a, ApJ, 673, 487.

Ida, S. and Lin, D. N. C., 2008b, ApJ, 685, 584.

Juric, M. and Tremaine, S., 2008, ApJ, 686, 603.

Kasting, J. F., Whitmire, D. P., and Reynolds, R. T., 1993, Icarus, 101, 108.

Kennedy, G. and Kenyon, S., 2008a, ApJ, 673, 502.

Kennedy, G. and Kenyon, S. 2008b, ApJ, 682, 1264.

Laughlin, G., Butler, R. P., Fischer, D. A., Marcy, G. W., Vogt, S. S., and Wolf, A. S., 2005, ApJ, 622, 1182.

Laughlin, G. and Chambers, J. E., 2001, ApJ, 551, L109.

Lee, M. H. and Peale, S. J., 2002, ApJ, 567, 596.

Loredo, T. J. and Chernoff, D. F., 2003, "Bayesian Adaptive Exploration," in Statistical Challenges in Astronomy, p 57.

Malhotra, R., 2002, ApJL, 575, L33.

Morbidelli, A., Chambers, J., Lunine, J. I., Petit, J. M., Robert, F., Valsecchi, G. B., and Cyr, K. E., 2000, Meteoritics and Planetary Science, 35, 1309.

Muterspaugh, M., Lane, B., Fekel, F., Konacki, M., Burke, B., Kulkarni, S. R., Colavita, M. M., Shao, M., and Wiktorowicz, S., 2008, AJ, 135, 766.

Tanner, A. et al., 2007, PASP, 119, 747.

Thommes, E. W., Matsumura, S., and Rasio, F. A., 2008, Science, 321, 814.

Raymond, S. N., Mandell, A. M., and Sigurdsson, S., 2006, Science, 313, 1413.

Rivera, E. J. and Lissauer, J. J., 2000, ApJ, 530, 454.

Robinson, S. E., Laughlin, G., Bodenheimer, P., and Fischer, D., 2006, ApJ, 643, 484.

Sozzetti, A., Casertano, S., Brown, R. A., and Lattanzi, M. G., 2003, PASP, 115, 1072.

Tsiganis, K., Gomes,R., Morbidelli, A., and Levison, H. F., 2005, Nature, 435, 459.

Wetherill, G. W., 1996, Icarus, 119, 219.

Wolf, S., Moro-Martin, A., and D'Angelo, G., 2007, Planetary and Space Science, 55, 569.

Wright, J. T. et al., 2007, ApJ, 657, 533.

Wright, J., Upadyay, S., Marcy, G. W., Fischer, D. A., Ford, E., Johnson, J., 2008, submitted to ApJ.

II
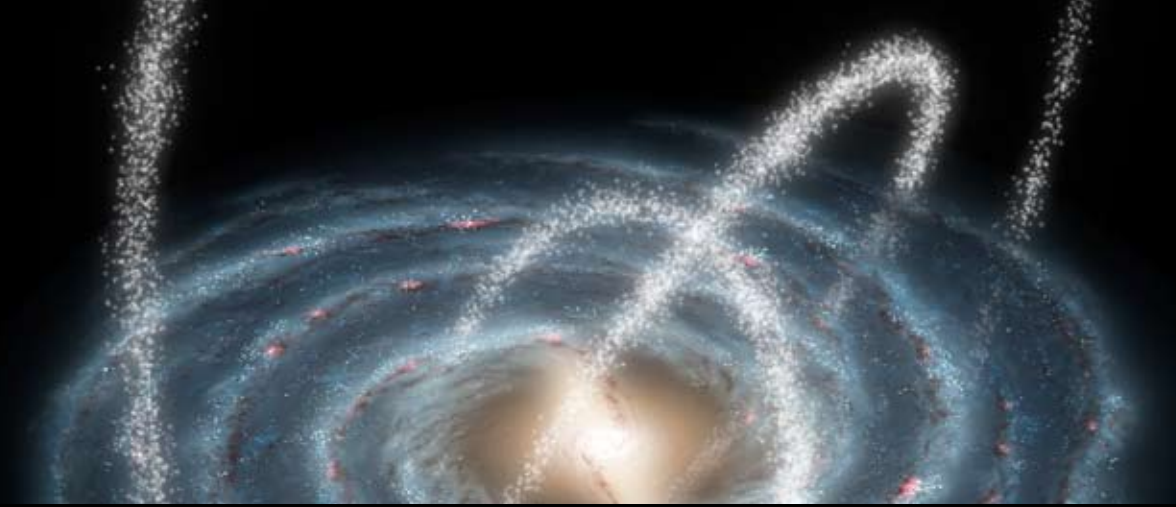
Dark Matter and the Assembly of Galaxies

The universe is made mostly of dark matter and dark energy, and we don't know what either of them is.

Saul Perlmutter

What is the history of galaxy formation?

How do the ages of metal-poor stars in the Milky Way halo and globular clusters constrain cosmological models?

What is the mass distribution of the Galaxy, including dark matter, and its rotation curve?

What is the nature of galactic dark matter?

What are the total masses of the individual galaxies and galaxy groups nearby?

What is the density of matter that is smoothly distributed across super-clusters or larger scales?

Galactic Dynamics and Local Dark Matter

4
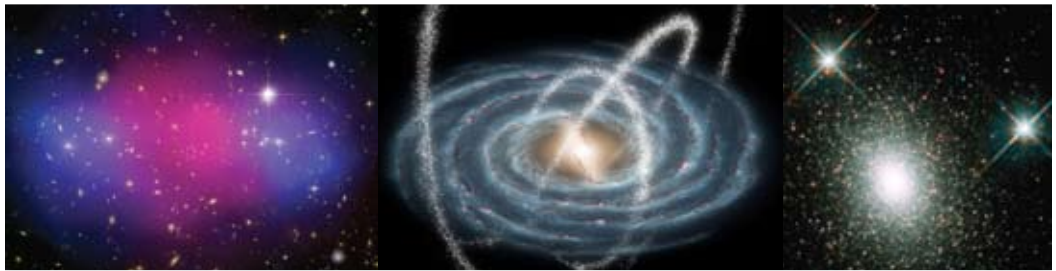
Steven R. Majewski (Univ. Virginia), **James Bullock** (UCI), **Andreas Burkert** (Univ.-Sternwarte München), **Brad Gibson** (Univ. of Central Lancashire), **Eva Grebel** (Univ. Basel), **Oleg Y. Gnedin** (Univ. Michigan), **Puragra Guhathakurta** (UCSC), **Amina Helmi** (Univ. Groningen), **Kathryn V. Johnston** (Columbia Univ.), **Pavel Kroupa** (Univ. Bonn), **Manuel Metz** (Univ. Bonn), **Ben Moore** (Univ. Zurich), **Richard J. Patterson** (Univ. Virginia), **Edward Shaya** (Univ. Maryland), **Louis E. Strigari** (Stanford Univ.), and **Roeland van der Marel** (STScI)

ABSTRACT

The concordance Λ Cold Dark Matter (ΛCDM) model for the formation of structure in the Universe, while remarkably successful at describing observations of structure on large scales, continues to be challenged by observations on galactic scales. Fortunately, CDM models and their various proposed alternatives make a rich variety of testable predictions that make the Local Group and our own Milky Way Galaxy key laboratories for exploring dark matter (DM) in this regime. However, some of the most definitive tests of local DM require μas astrometry of faint sources, an astrometric regime that is a unique niche of SIM Lite. This chapter explores the important and distinct contributions that can be made by SIM Lite in the exploration of galaxy dynamics and DM on galaxy scales and that have cosmological consequences. Key areas of potential SIM Lite exploration include (1) measuring the shape, orientation, density law, and lumpiness of the dark halo of the Milky Way and other nearby galaxies, (2) determining the orbits of Galactic satellites, which may be representatives of late infall from the hierarchical formation of the Milky Way, (3) ascertaining

the distribution of angular momentum and orbital anisotropy of stars and globular clusters to the outer reaches of the Galactic halo, dynamical properties that hold clues to the early hierarchical formation of the Galaxy, (4) measuring the physical nature of DM by placing strong constraints on the phase space density in the cores of nearby dSph galaxies, and (5) reconstructing the dynamical history of the Local Group through the determination of orbits and masses of its constituent galaxies.

4.1   Understanding Structure Formation on Galactic Scales

4.1.1   Pushing the Frontiers of Near-Field Cosmology

Empirical studies of the structure and evolution of the Universe must navigate a trade space that includes, at one extreme, surveys of galaxies to high redshift — which yield critical sampling of the luminous Universe in the time dimension but with ever-decreasing levels of detail as distances increase — and, at another extreme, exploration of galaxies in the local Universe — which can provide singularly detailed views of structure and dynamics, but with coarser time resolution. With the latter strategy, often called "near-field cosmology," we see galaxies only in the recent epoch, but they still harbor ancient stellar populations that formed at the earliest epochs of galaxy formation. The spatial, chemical and kinematical distributions of stars of different ages in a galaxy provide valuable information about the properties of the environment in which they formed and allow us archaeologically to reconstruct evolutionary histories.

Both of these strategies, far- and near-field cosmology, provide complementary constraints and contexts that successful theories of the evolving Universe must simultaneously satisfy and describe, and many recent advances in understanding the evolution of galaxies and the Universe are directly tied to great strides in the development of each approach. While technological advances have now allowed far-field cosmology to see galaxies (or at least their central quasar beacons) to $z \sim 6$, so too has the domain of near-field cosmology, most exquisitely realized through the study of resolved stars, been pushed out from the solar neighborhood to the remote reaches of the Milky Way, into the Local Group and beyond. SIM Lite will make a significant and unique contribution to expanding the frontiers of near-field cosmology across this realm by providing unprecedentedly accurate sensitivity to the motions of stars in galaxies on Mpc scales. New data on the dynamics of stars that SIM Lite can measure within the Milky Way and in galaxies in the Local Group — which we expect to be more or less typical of spiral galaxies and modest density galaxy groups at the current epoch — can provide critical leverage on still perplexing questions regarding the assembly of structure on small scales that cannot be gleaned from the simple snapshots and global dynamical measurements derived for galaxies at higher redshifts.

4.1.2   Testing CDM Models Within the Local Group

Since the seminal study of Searle and Zinn (1978), the notion of accretion of "subgalactic units," including "late infall," has been a central concept of Milky Way and galaxy evolution studies. Since then, large-scale *N*-body simulations of the formation of structure in the Universe in the presence of DM (and dark energy) have also shown galaxies like our Milky Way — as well as all large structures in the Universe — building up hierarchically (e.g., Figure 4-1; also see Figure 4-7). The predicted large-scale filamentary structure of the Universe is observed in the distributions of galaxies as mapped by extensive galaxy redshift surveys, while the presence of substructure within galaxies and galaxy clusters provides strong support for the merger hypothesis, so that bottom-up structure formation on all scales has become the commonly accepted paradigm.

Figure 4-1. One of the highest-resolution, fully cosmological hydrodynamical disk galaxy simulations (showing only the gas distribution) to date, and the first generated with a grid-based code (a complementary approach to particle-based codes, like that shown in Figure 4-7). This model uses the RAMSES Adaptive Mesh Refinement code to reach a spatial resolution better than 100 pc at the present day. (Model image from B. Gibson.)
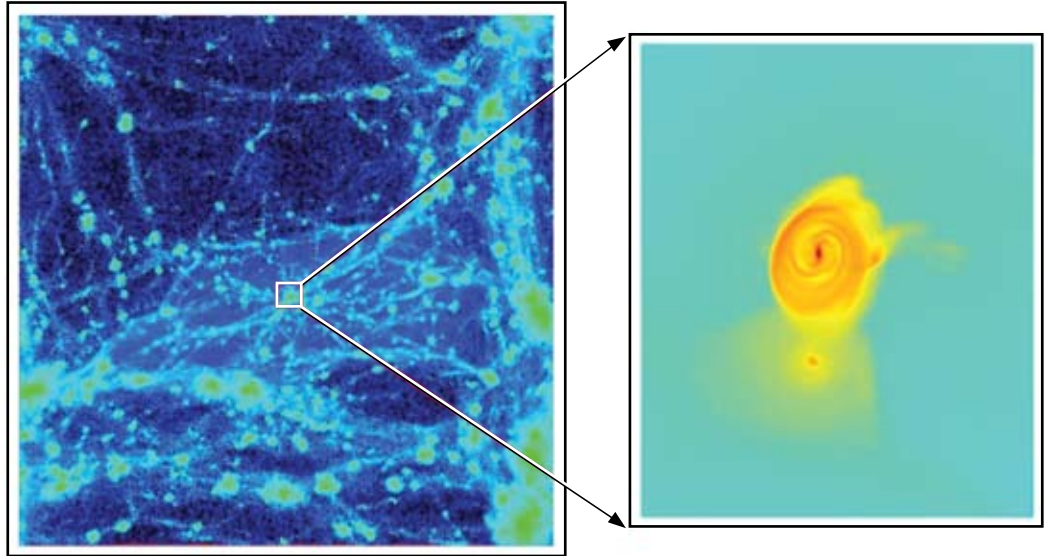
The active merging history on all size scales demonstrated by high-resolution numerical simulations has had remarkable success in matching the observed properties of the largest structures in the Universe. However, the specific paradigm including cold dark matter (CDM) is still a challenge to reconcile with the observed properties of nearby (i.e., present-day) structures on galactic scales, and this discrepancy remains one of the primary challenges to be resolved by near-field cosmology.

While Galactic halo stars, globular clusters, and satellite galaxies represent a small fraction of the baryonic mass of the Milky Way, these stellar systems are "Rosetta Stones" to understanding the origin of our galaxy and the nature of its DM halo. Recorded in the orbital dynamics of halo stars and globular clusters are unique signatures of early galactic formation processes, while the bulk motions of satellite galaxies hold information about the infall processes of more recent galaxy assembly. The kinematics of these systems also provide sensitive probes of the current DM distribution throughout the galaxy.

In this context, aspects of various well-known discrepancies between CDM theory and observations, such as the "missing satellites problem" (§4.2.1, §4.4.1), the "central cusps problem" (§4.5.1), and problems with the angular momentum distributions in galaxies (§4.4.1) are ripe for exploration in our local universe. The Local Group — and in particular the Milky Way and its satellite system — have become particularly important laboratories for testing specific predictions of the CDM models and their alternatives. Most especially, high-accuracy µas astrometric observations enabled by SIM Lite will allow definitive tests of dynamical effects specifically predicted by these models and allow a means to determine the present spatial distribution and primordial phase space distribution of DM in the Local Group. While some tests of local DM do fall within the "Gaia-sphere" — that region of the Milky Way accessible to the European Space Agency's Gaia mission — several key experiments can only be carried out definitively within a part of the (apparent magnitude)-(astrometric precision) parameter space that is out of reach of Gaia and uniquely accessible to SIM Lite's interferometric capability.

While current cosmological simulations have not yet succeeded in spawning structures that truly resemble real galaxies (e.g., Abadi et al. 2003), the present brisk pace of development of these models (e.g., as shown in Figure 4-1) can be expected to continue with eventual convergence in the coming decade to significantly improved and detailed predictions for the formation of the Local Group, the Galaxy, and its stellar components and satellites. These predictions will undoubtedly bring new empirical challenges beyond those envisioned here. An operational SIM Lite in the coming decade will be poised as a primary tool for testing these predictions.

4.2 Probing the Shape, Profiles, and Lumpiness of Dark Matter Halos

4.2.1 Background and Current Problems

Over the last decade, cosmological observations have determined conclusively that normal matter (e.g., protons, neutrons, atoms, etc.) constitutes just one-fifth of the matter in the Universe, with the remaining 80 percent of the cosmic matter budget in the form of DM. Despite the fact that candidate particles for DM have been suggested, the identity of this DM is a complete mystery, but its properties affect how galaxies form and how the Universe evolves. Its existence also is among the strongest pieces of evidence that the Standard Model of particle physics is fundamentally incomplete. In this sense, the nature of DM remains one of the deepest problems in both astronomy and particle physics.

The microscopic nature of DM affects the way it clusters around galaxies, and therefore can be probed by astronomical observations. Dynamical measurements with SIM Lite will provide crucial and unique insights into the properties of the DM in and around our Milky Way, with particular sensitivity to how the DM is distributed on galaxy scales. In the leading model of structure formation, the DM today is mostly "cold," and consists of particles that are much more massive than the proton and that can cluster strongly on small scales. CDM models of structure formation predict that the Milky Way should be surrounded by a diffuse extended "DM halo," which itself should be teeming with smaller, self-bound DM clusters called "sub-halos" (Figure 4-2). These sub-halos orbit the Galaxy like satellites and the mass function of the satellite halos is predicted to rise as the mass decreases (as $1/M$, Diemand et al. 2008). The minimum mass and overall count of dark satellites is linked closely to the particle nature of DM itself. For example, if the DM is cold and consists, e.g., of weakly interacting massive particles (WIMPs), then the mass function may rise steadily to a minimum mass that is close to an Earth-mass (Diemand,

Figure 4-2. The density of DM within the virial radius of a galaxy mass CDM halo simulated with over a billion particles. Over 100,000 substructure halos are present, some orbiting within the inner kpc of the halo. (From Stadel et al. 2008)

Moore, and Stadel 2005), with a total Milky Way count of N_{sat} ~ 10^{13} sub-halos (e.g., Figure 4-2). If, on the other hand, the DM is warm and consists of, e.g., sterile neutrinos, then the mass function may truncate at a mass-scale of ~ 10^8 $M_\odot$, with ≤100 self-bound satellite systems in the Milky Way.

SIM Lite observations will provide key insights towards interpreting the so-called "missing satellites problem," which describes the fact that many fewer satellite galaxies are observed around systems like the Milky Way and M31 than the number of CDM sub-halos predicted (Kauffmann, White, and Guideroni 1993; Klypin et al. 1999; Moore et al. 1999; Strigari et al. 2007b). One popular idea is that these dark satellites exist around the Milky Way, but that they are not lit up by stars because star formation is suppressed in the smallest halos (Bullock, Kravtsov, and Weinberg 2000; Benson et al. 2002; Hayashi et al. 2003; Kravtsov, Gnedin, and Klypin 2004). If the majority of sub-halos are dark, then they may be detectable today through their influence on cold Galactic tidal streams (§4.2.2). Moreover, DM particle properties may be determined by SIM Lite measurements of the properties of the satellites that are visible (§4.5).

Our understanding of the satellite galaxy population has been revolutionized in recent years thanks to an increasingly deep census of satellite galaxies around the Milky Way and M31 (e.g., Willman et al. 2005; Martin et al. 2006; Zucker et al. 2006; Belokurov et al. 2007; Majewski et al. 2007). Indeed, the number of known Local Group satellite galaxies has more than doubled since 2005. It remains to be determined how these new galaxies are to be interpreted in the context of the missing satellites problem, and the origin of galaxies as extreme as the ultrafaint dwarfs (e.g., Boo II with L ~ 1000 $L_\odot$; Walsh et al. 2008) represents a fundamental challenge to galaxy formation models. It is tempting to evoke tidal interactions to explain their extreme nature; however, these objects are so small that, at their current distance from the Milky Way, they should be relatively unaffected by the Milky Way's tidal force. Only by obtaining proper motion determinations of their orbits with SIM Lite observations (§4.3) can we understand the degree to which these extreme objects were shaped by past central encounters with the Milky Way.

SIM Lite observations will also provide unprecedented constraints on the total mass, mass profile, and shape of the DM distribution around the Milky Way all the way out to its virial radius. Such a detailed, accurate, and extensive assessment of DM distribution is unfeasible for any external galaxy. These constraints are essential in the general goal to use the Milky Way as a "Rosetta Stone" in understanding galaxy formation on a cosmic scale. Mass models based on line-of-sight velocities to distant stars and other tracer objects are fundamentally limited by our ignorance of the orbital eccentricities (i.e., anisotropies, see §4.3–4.4). By determining proper motion measurements to distant halo objects, SIM Lite will provide a definitive measure of the mass profile of the Milky Way. This measurement (with proper, calculated error assessments) will allow us confidently to compare our galaxy to other distant galaxies where mass measurements are more straightforward, but where detailed information on stellar populations and other observables are more poorly determined. Moreover, the mass determination may be compared directly with mass profile predictions for DM halos in the concordance CDM model. Once determined, a globally self-consistent Milky Way dark halo model (with proper error bars) will provide information on the mass range and microphysical properties of the DM particle, and thereby be essential for experiments like Cryogenic Dark Matter Search (CDMS13)*, XENON14†, and Large Underground Xenon (LUX15)‡ that aim to detect the DM particle directly in laboratories on Earth.

In addition to mass profiles, CDM predicts that Milky Way–sized DM halos are typically triaxial, becoming rounder at larger radii (Allgood et al. 2006; Macciò, Dutton, and van den Bosch 2008). Current constraints on the shape of the Milky Way DM halo from modeling the debris of the Sagittarius dwarf

---

spheroidal galaxy are hampered by incomplete phase space information (i.e., we have radial velocities but no proper motions) and vary depending on how the extant data are analyzed, yielding shapes from prolate (Helmi 2004), to near-spherical (Fellhauer et al. 2006), to oblate (Law, Johnston, and Majewski 2005; Martínez-Delgado et al. 2004). SIM Lite proper motions of stars throughout the entire Sagittarius stream, stars in other (more distant) tidal streams (§4.2.2), and hypervelocity stars (§4.2.3) will provide a definitive measurement of the halo shape, orientation, and mass profile with radius. This measurement will not only test model predictions, but will determine how the shape of the inner Galactic halo is influenced by dissipation and the formation of the Galactic disk (Kazantzidis et al. 2004; Zentner et al. 2005, §4.3).

4.2.2   Solution with SIM Lite: Probing the Galactic Potential with Tidal Streams

It is now well known that, as predicted by models of structure formation (e.g., Figure 4-3), the luminous Galactic halo is inhomogeneous and coursed by streams of debris tidally pulled out of accreted satellites. SIM Lite will give us the first opportunity to measure the proper motions of stars in entire streams with very high accuracy (Gaia can measure only portions of the very closest streams accurately). This will allow us to probe two different aspects of the Milky Way's potential: (1) its global shape, which drives the overall phase space distribution of extended tidal streams, and (2) the lumpiness of the potential, which imprints its signal in the degree of small-scale incoherence among member stars at each point in the stream.

Figure 4-3. Surface brightness map of a simulated stellar halo formed within a ΛCDM context (Bullock and Johnston 2005). The image is 300 kpc on each side, and shows just the stellar halo component (total luminosity ~10^9 $L_\odot$). Note that (compared to Figures 4-2 and 4-7), the phase space distribution of stars around the Galaxy is predicted to contain more clear streams than the DM distribution in part because stars form deeply embedded within DM halos. The outer parts of these halos are stripped to form a smooth background component, while the inner parts are able to maintain their coherence longer. In addition, only a small subset of sub-halos are expected to contain any stars at all. (Image credit: Sanjib Sharma, Columbia University)
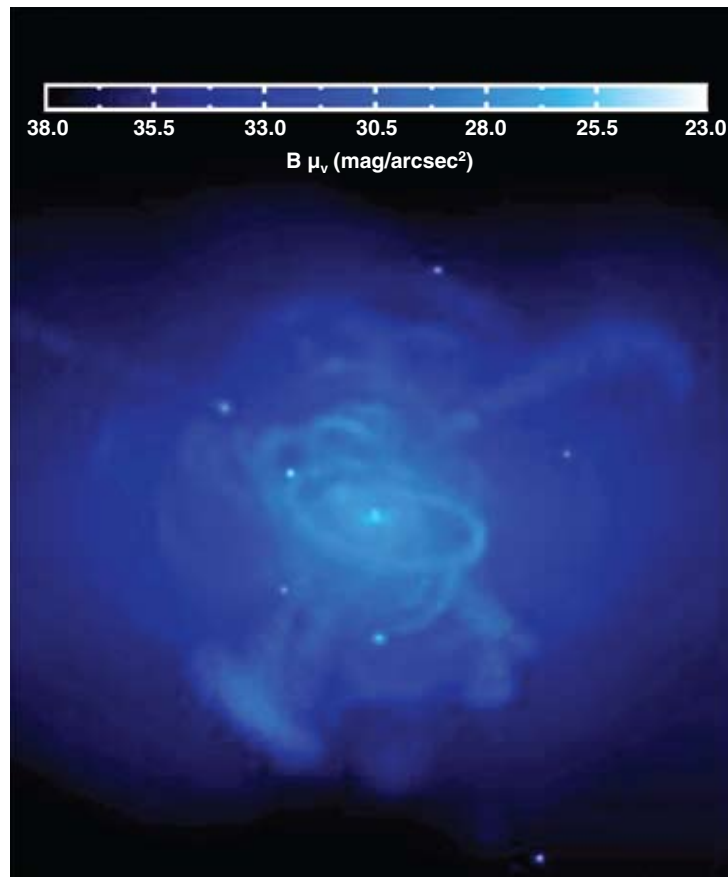
Once precision proper motion measurements from SIM Lite are combined with the stars' observed angular positions, radial velocities, and estimated distances (accurately calibrated by SIM Lite), stream stars provide a uniquely sensitive probe of the global distribution of mass in the Milky Way. Starting from its full phase space position, each star's orbit can be integrated backwards in some assumed Galactic potential. Only in the correct potential will the stream stars ever coincide in position and velocity with the parent satellite and each other (see Figure 4-4). Tests of this idea with simulated data observed with the µas/yr precision proper motions possible with SIM Lite and km/s radial velocities suggest that 1 percent accuracies on Galactic parameters (such as the flattening of the gravitational potential and the circular speed at the Solar Circle) can be achieved with tidal tail samples as small as 100 stars (Johnston et al. 1999).

Applying this method to several streams at a variety of Galactocentric distances and orientations with respect to the Galactic disk would allow us to build a comprehensive map of the distribution of DM in the halo — its shape, density profile, and orientation. In the last few years evidence for dSph galaxy tidal tails has been discovered around Milky Way satellites at very large Galactic radii (Muñoz et al. 2006; Muñoz, Majewski, and Johnston 2008; Sohn et al. 2007), and other distant streams are known (e.g., Newberg et al. 2003; Pakzad et al. 2004; Clewley et al. 2005). With SIM Lite, such distant streams can be used to trace the Galactic mass distribution as far out as the virial radius with an unprecedented level of detail and accuracy. This would provide the very first, accurate three-dimensional observational assessment of the shape and extent of a galactic-scale DM halo.

Stars in tidal tails also promise to place limits on the possible existence of a significant fraction of the halo in the form of dark satellites (Figure 4-2; Moore et al. 1999; Klypin et al. 1999). Large, dark lumps in the Milky Way's potential should scatter stream stars and lessen their local coherence (Ibata et al. 2002; Johnston, Spergel, and Haydn 2002; Mayer et al. 2002). For this experiment, the coldest streams (e.g., from globular clusters like Palomar 5: Grillmair and Dionatos 2006) would be most sensitive. Early tests of such scattering using only radial velocities of the Sagittarius stream suggest a Milky Way halo smoother than predicted (Majewski et al. 2004), but this result is based on debris from a satellite with an already sizable intrinsic velocity dispersion and incomplete knowledge of the full space motions of the stars, so the constraint is not strong.

Gaia will allow the various tests described here to be attempted for some nearby portions of streams, but only with SIM Lite will it be possible to probe the three-dimensional shape, density profile, extent of, and substructure within our entire galaxy's DM halo.

4.2.3   SIM Lite Solution: Probing Galaxy Potentials with Hypervelocity Stars

A complementary method for sensing the shape of the Galactic potential can come from SIM Lite observations of hypervelocity stars (HVSs; Gnedin et al. 2005). Hills (1988) postulated that such stars would be ejected at speeds exceeding 1000 km/s after the disruption of a close binary star system deep in the potential well of a massive black hole, but HVSs can also be produced by the interaction of a single star with a binary black hole (Yu and Tremaine 2003). Recently, Brown et al. (2006) report on five stars with Galactocentric velocities of 550 to 720 km/s. They argued persuasively that these extreme-velocity stars can only be explained by dynamical ejection associated with a massive black hole, and they make similar arguments for three additional stars in Brown et al. (2007). After the success of these initial surveys to find HVSs, it is likely that many more will be discovered in the next few years. If these stars indeed come from the Galactic center (Figure 4-5), the orbits are tightly constrained by knowing their point of origin. In this case the nonspherical shape of the Galactic potential — due in part to the flattened disk and in part to the triaxial dark halo — will induce nonradial inflections (which will be primarily in the transverse direction at large radii) in the velocities of the HVSs of order 5 to 10 km/s, which corre-

Figure 4-4. A demonstration of the use of tidal streams to measure the shape and strength of the Galactic potential when precise six-dimensional information is available for stream stars. First, a Sgr-like tidal stream was created by the disruption of a dwarf satellite in a rigid Galactic potential through an *N*-body simulation (e.g., as in Law et al. 2005), shown at the top of each strip. In reality, the potential is unknown, but guesses of the strength and shape of the Galactic potential can be tested against the complete, six-dimensional phase space information in hand for the stream stars (including, crucially, SIM Lite proper motion measures). The orbits of the individual stars in the tidal streams can be run backwards under these assumed potentials. The left-hand strip demonstrates what happens if the strength of the Galactic potential is overestimated: when the orbit is run backwards, the tidal stream stars orbit at too large a radius and do not converge (in the bottom panel) to a common phase space position. The right-hand strip shows the result when a Galactic potential of the correct strength is guessed: when the stream star orbits are run backwards, the tidal stream stars collect back into the core of the parent satellite (in the bottom panel).
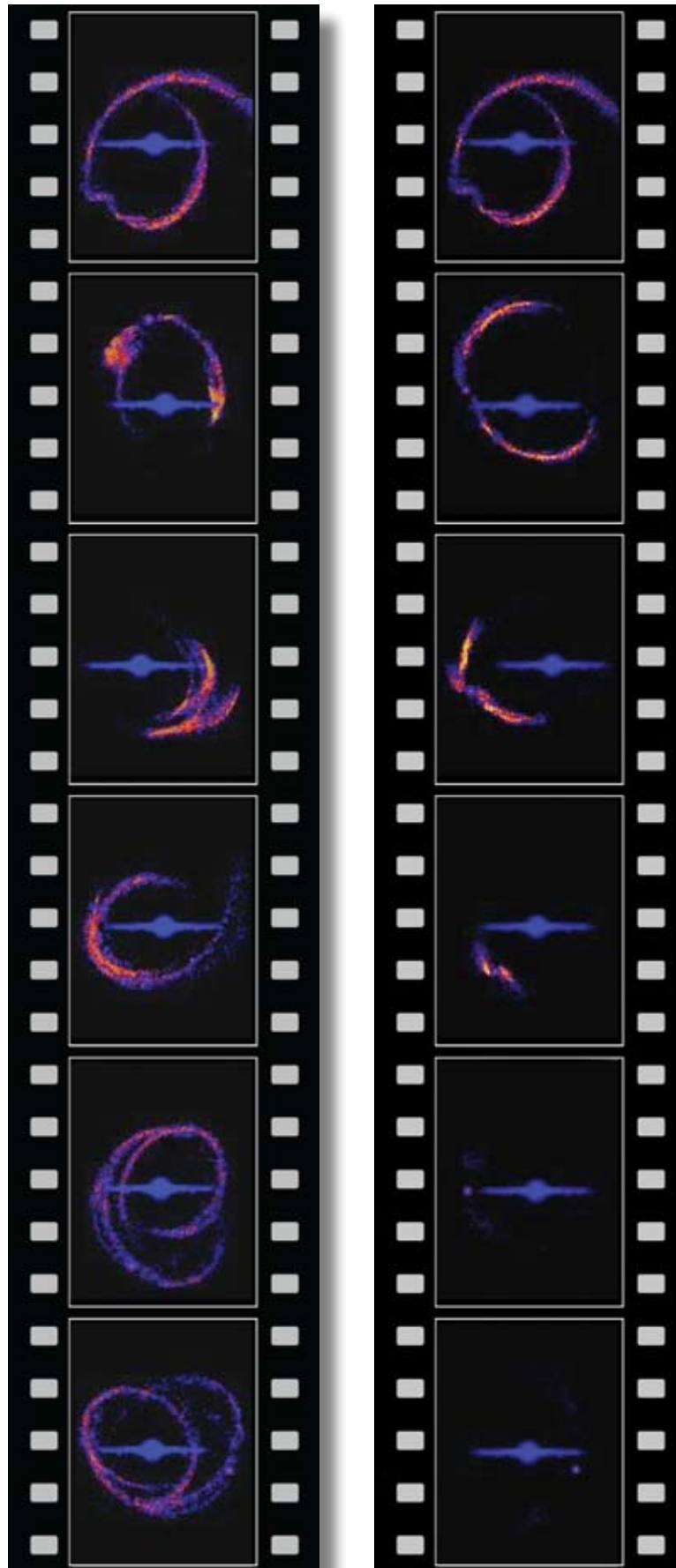
Figure 4-5. Schematic representation of the trajectories of hypervelocity stars in a spherical (red) and non-spherical, flattened (brown) potential. The three-dimensional positions and velocities of hypervelocity stars will, with the inclusion of precise proper motions measured by SIM Lite, have great sensitivity to the global shape of the Galactic potential (see Figure 4-6).
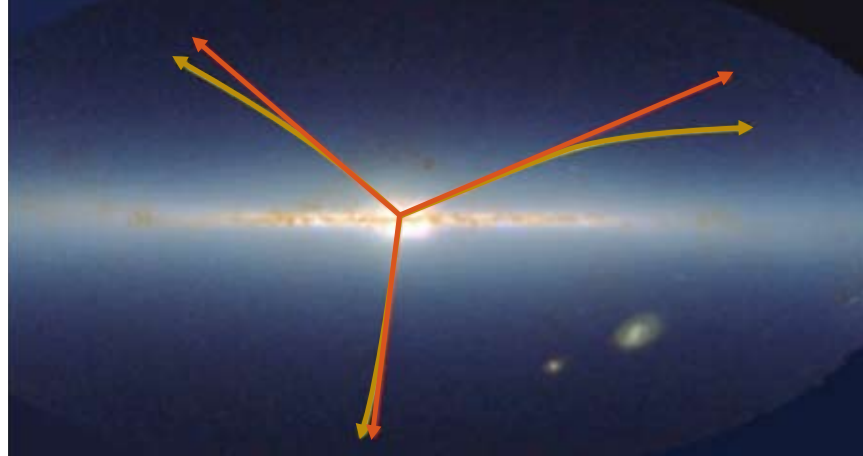
Figure 4-6. Expected proper motions of two known hypervelocity stars, HVS1 (left) and HVS2 (right), under a range of different assumptions (shown as the different symbols) about the triaxial shape and orientation of the Galactic potential, and for one of a range of possible HVS distances (represented by the red lines; see Gnedin et al. 2005). SIM Lite measurements of proper motions can readily select from the families of models shown here.
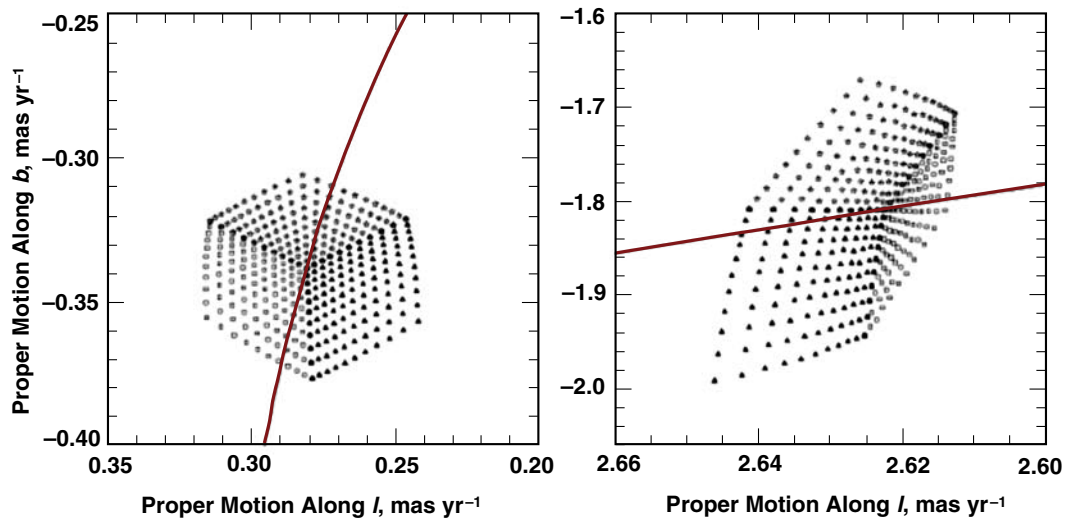
sponds to of order 10 to 100 µas/yr depending on the HVS distance (Gnedin et al. 2005). Each HVS thus provides an independent constraint on the potential, as well as on the solar circular speed and distance from the Galactic center (Figure 4-6). The magnitudes of the known HVSs range from 16 to 20, so their proper motions will be measurable by SIM Lite with an accuracy of a few µas/yr, which should define the orientation of their velocity vectors to better than 1 percent. With a precision of 20 µas/yr, the orientation of the triaxial halo could be well-constrained and at 10 µas/yr the axial ratios will be well-constrained (Gnedin et al. 2005).

More recently the existence of an HVS from the LMC has been reported (Gualandris and Portegies Zwart 2007; Bonanos et al. 2008), and the existence of numerous HVSs from M31, including thousands within the virialized halo of the Milky Way, has been suggested (Sherwin, Loeb, and O'Leary 2008). Thus, the next decade will probably bring the identification of many more HVSs of Galactic and extragalactic origin. For the LMC, establishing the three-dimensional trajectory of its HVSs will allow identification of the location of any massive black hole(s) in this galaxy, either in the galaxy center or in the centers of its star clusters. An accurate understanding of the velocities of hypervelocity stars may also lead to an improved understanding of the black hole content of galactic nuclei — e.g., theoretical models show that HVSs will have a different spectrum of ejection velocities and ejection rates from a binary black hole versus a single massive black hole.

4.3 Testing Hierarchical Formation and Late Infall

4.3.1 Background and Current Problems

With the latest high-resolution *N*-body CDM simulations, it has been possible to make rather detailed predictions for how hierarchical formation of the DM halos should proceed on galaxy scales (Figure 4-7). The infall of DM onto the Milky Way has left a fingerprint of its accretion history that allows for specific tests of CDM if one associates the satellite galaxies (which typically have high mass-to-light ratios) with CDM sub-halos. In the models, sub-halos preferentially align with and are accreted along the intermediate scale filamentary structure (Knebe et al. 2004).

The satellite galaxies of the Milky Way show a clear spatial anisotropy that has often been interpreted as a signature of the specific infall history of the Milky Way's own DM substructures, but this interpretation also strongly depends on the adopted galaxy evolution models applied within the CDM framework (e.g., Hartwick 2000; Libeskind et al. 2005). Moreover, the currently best-available proper motions of the satellite galaxies hint at a strong correlation between their orbits. This might point to (1) the observed satellites not only having fallen in along filaments, but perhaps having fallen into the Milky Way in a few groups of DM sub-halos (Li and Helmi 2008; D'Onghia and Lake 2008) — much as has long been debated for the Magellanic Clouds — or (2) perhaps very different explanations not driven by CDM considerations where alignments are the result of the break-up of formerly larger satellites or the formation of "tidal dwarf" galaxies (Kunkel 1979; Lynden-Bell 1983; Metz, Kroupa, and Libeskind 2008).

Clearly, to understand and test either of these competing theories of the origin of the satellite galaxies, a good understanding of the orbital properties of galaxies in and near the Milky Way is needed. We can establish from their orbits whether and how these satellites correspond to the predicted hierarchically infalling dark sub-halos and what particular infall scenario dominated the formation of the Milky Way's DM halo, or establish whether the dSph galaxies were formed through some other mechanism, e.g., in an early tidal interaction with another galaxy. Orbits for systems at several 100 kpc can also define a complete census of those systems bound to the Milky Way, which places limits on the mass and mass profile of the Galaxy and may be able to probe the hypothesis that there is a third large galaxy in the Local Group hidden behind the bulge of the Milky Way (Loeb and Narayan 2008).

The notion that halo globular clusters were formed in separate environments and were then accreted by the Milky Way over an extended period of time has been a central thesis of Galactic structure studies since the work by Searle and Zinn (1978). More recently, at least some clusters have been identified as part of the Sagittarius stream and the Monoceros structure — which are apparently relatively recent mergers having readily identifiable debris streams — but presumably such mergers have been ongoing and were even more common in the early Galaxy. At present, ≤ 25 percent of Galactic globular clusters have had any attempt at a measured proper motion, and reliable data generally exist only for those clusters closest to the Sun (see, e.g., Palma, Majewski, and Johnston 2002). With full orbital information for the globular clusters, we can learn not only about their origin, but about the earliest stages of the formation of our own galaxy as well.

While orbit determinations will be useful for ascertaining the origins of globular clusters and dwarf satellites, they are also crucial for understanding the fate of such systems. The dynamical evolution of small stellar systems is largely determined by external influences such as tides and dynamical shocks from the disk and bulge (e.g., Gnedin, Lee, and Ostriker 1999), so determining orbits of these satellites will dramatically improve our understanding of their evolution and address the long-standing issue of whether the present population of these systems is the surviving remnant of a much larger initial population. By finally obtaining definitive orbital data for the entire Milky Way globular cluster and dwarf

Figure 4-7. The hierarchical formation of a binary galaxy system (showing only the DM) chosen to have similar separation, masses, and infall velocities as the Milky Way and Andromeda galaxies (Moore et al. 2001). The assembly of structures begins at a redshift $z \sim 100$ with, at first, tiny Earth-mass halos, and proceeds until a redshift $z \sim 1$ with the final formation of the main galactic mass halos that are 15 orders of magnitude more massive.
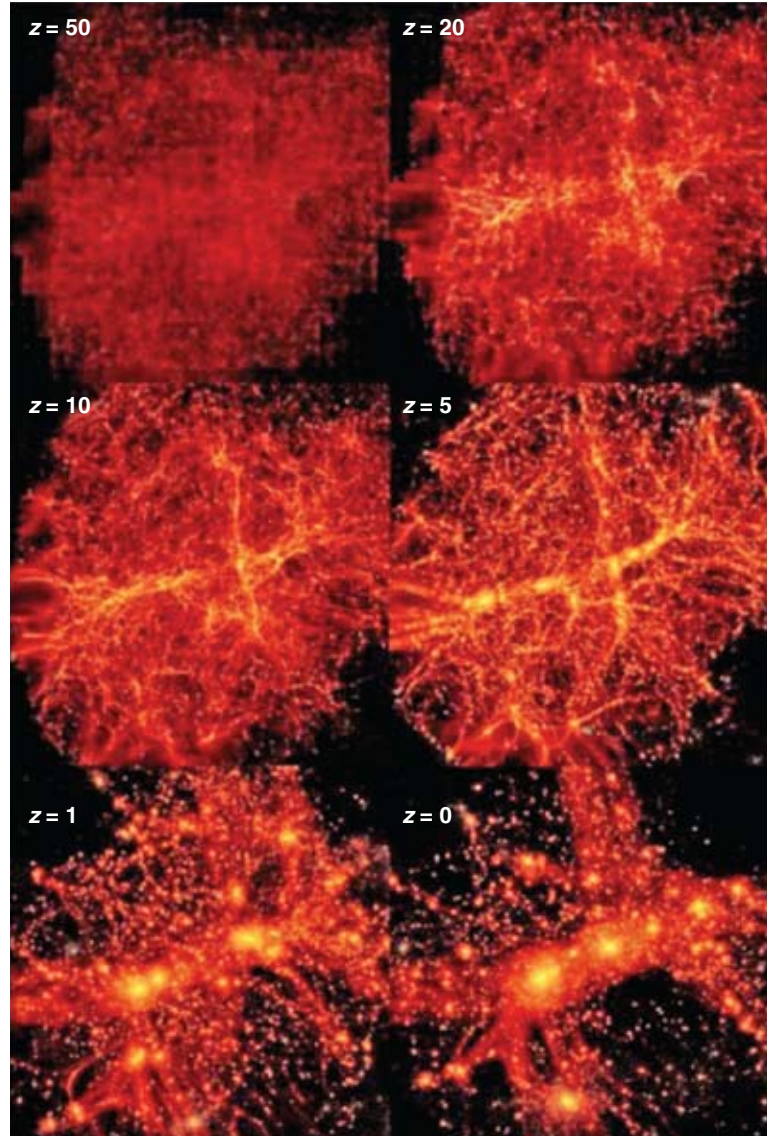
galaxy sample, SIM Lite will make an important contribution to our understanding of the full range of cluster/satellite dynamical histories on the evolution of the Galactic ensemble. Of course, all of these satellite systems can also serve as valuable test particles for constraining the properties of the Galactic gravitational potential (§4.2).

4.3.2   Potential Solutions with SIM Lite: Legacy Measurements of Satellite Orbits

The proper motions of the more distant satellites of the Milky Way are expected to be on the order of ~100 μas/yr. To derive transverse velocities good to ~10 km/s (~10 percent) requires a bulk proper motion accuracy of ~10 μas/yr for the most distant satellites at several hundred kpc distances (e.g., Leo I, Leo II, Canes Venatici, Leo T), in which the brightest giant stars have V ~ 19.5. These are systems that require SIM Lite for an accurate proper motion measurement. The constraints are more relaxed for satellites at roughly 100 kpc distances, ~20 μas/yr, with brightest stars at V ~ 17.5. Such measurements are well within the capabilities of SIM Lite, which could derive the desired bulk motions for Galactic satellites with only a handful of stars per system, and, with more stars, be sensitive to systemic rota-

tion and other internal motions (§4.4). With its μas-level extragalactic astrometric reference tie-in, and the ability to derive proper motions at the level desired for Galactic satellites with each star measured, SIM Lite will make definitive measures of the proper motions of the Galactic satellites that will overcome complications faced by previous satellite proper motion studies. Moreover, most of the outer halo globular clusters, the numerous recently detected lower surface brightness dSph satellite galaxies (e.g., the Boötes and Hercules dwarfs), and some of the "transitional" type systems (which may be globular clusters or dwarf galaxies — e.g., Willman 1, Coma Berenices) have very sparse giant branches, which prohibits the opportunity to obtain reliable bulk motions by averaging the motions of numerous members (e.g., with Gaia). Only an instrument like SIM Lite, which delivers extremely precise per star proper motions to V ~ 20, can take on this challenge.

4.4   Testing the Distribution of Angular Momentum and Anisotropy in Galaxies

4.4.1   Background and Current Problems

A series of papers over the past decade by many different theoretical groups has now led to a converging scenario for understanding the origin and substructure of galactic halos within the context of our hierarchical Universe (e.g., Moore et al. 2006, and references within). This understanding is the result of coupling high-resolution numerical simulations with semi-analytical models for star formation within the first massive DM halos capable of hosting global star and cluster formation and dwarf galaxies. Using this technique we can make predictions for the kinematical and spatial distribution of the stellar remnants of these early star-forming structures in galaxy halos today.

We can begin to understand their spatial distribution and kinematics in a hierarchical formation scenario by associating the protogalactic fragments envisaged by Searle and Zinn (1978) with the rare peaks able to cool gas in the CDM clumps collapsing at redshift $z > 10$. The global effects of reionization at this epoch have been suggested to strongly affect the future evolution of the baryons, preventing them from cooling within subsequent generations of dark halos until a much larger mass scale is attained, equivalent to that of the Magellanic Clouds. As a result, the stellar components and globular clusters of our protogalaxy are distributed amongst the ~100 protogalaxies that inhabit these rare peaks of the density field. The thousands of similar mass halos that collapse after this time remain completely dark since the baryonic fluid is too hot to cool efficiently. This scenario could explain the missing satellites problem, i.e., why the bulk of the many thousands of DM substructures visible in Figure 4-2 are not observed.

Most of the rare, luminous protogalaxies rapidly merge together, their stellar contents and DM becoming smoothly distributed and forming the Galactic stellar and dark halo (Figure 4-8). The metal-poor globular clusters and old halo stars formed in these early Milky Way structures become tracers of this early evolutionary phase, centrally concentrated and naturally reproducing the observed steep number density fall off with radius. The most outlying substructures fall in late and survive to the present day as our familiar satellite galaxies. The observed radial velocity dispersion profile and the local radial velocity anisotropy of Milky Way halo stars are successfully reproduced in this model, but only with full three-dimensional orbits can we be assured that the orbital shapes are truly consistent with predictions.
If this epoch of structure formation coincides with the suppression of gas cooling into halos that collapse after reionization, then we can reproduce the rarity, kinematics, and spatial distribution of satellite galaxies, as suggested by Bullock et al. (2000). Reionization, therefore, provides a natural solution to the missing satellites problem and the origin of the stellar halo and its old globular cluster population.

The angular momentum distribution of the merging and infalling substructures also plays an important role in determining the structure and sizes of galactic disks and by this, in turn, galaxy morphology. Cur-

Figure 4-8. The evolution of dark and luminous sub-halos in a Milky Way–like galaxy. The halos shaded in green in the left panel are those that could have cooled gas and formed stars before reionization at $z = 10$. The right panel shows the location of the particles in those halos at $z = 0$ — most of them have merged together, but the boxes show the luminous satellites that survive the merging process. They were all the most distant from the forming halo at $z = 10$ and survive simply because they fell in late, after virialization. The ~100 other protogalaxies at $z = 10$ shaded in green merged together, with their debris (globular clusters and stars) spread out to form the $\sim r^{-3}$ density law halo (most visible in the right panel by its highest-density central region). Each panel is 250 kpc on a side. (From Moore et al. 2006)
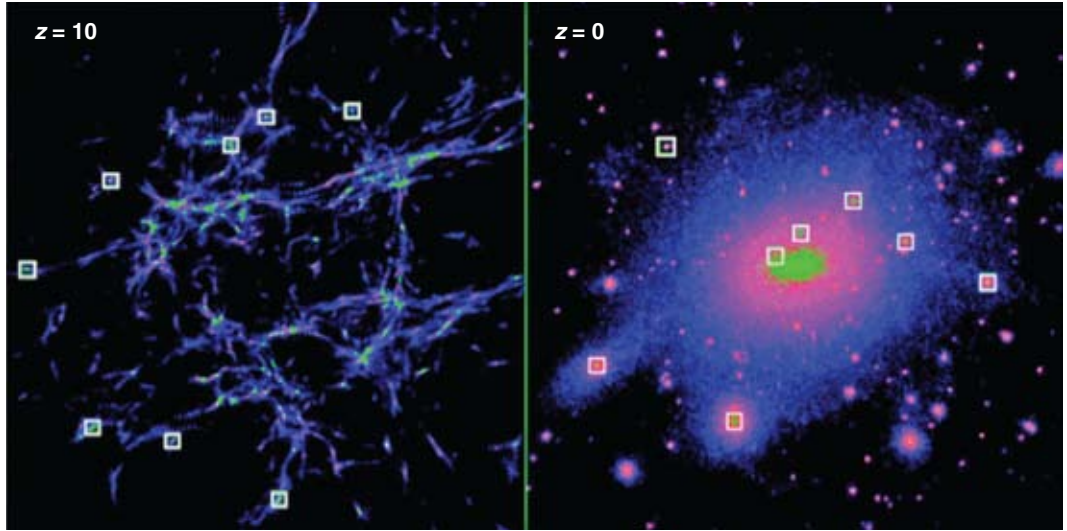
rently, numerical cosmological simulations of disk galaxy formation encounter a serious problem with too much angular momentum being transferred from the visible to the dark component during infall, leading at the end to galactic disks that are too compact and not in agreement with observations (e.g., Abadi et al. 2003). In order to find a solution for this problem it is crucial to determine the average specific angular momentum and the mass distribution of angular momentum in galactic halos.

4.4.2 Potential Solutions with SIM Lite: The Angular Momentum Profile of the Milky Way

Not only can SIM Lite test the predictions of the model for early galaxy formation described above, but it can also disentangle the stellar orbits in phase space in order to reconstruct the accretion history and properties of these protogalaxies. The expected properties of the spatial distribution and kinematics of material within today's Galactic halo that originated within these first CDM protogalaxies that formed before reionization are precisely predicted from high-resolution numerical simulations such as Diemand et al. (2005). According to these models, the outermost Galactic halo stars and globular clusters are on radially biased orbits, while the inner regions contain more isotropic orbits. The kinematics of the predicted surviving satellite dwarf galaxies that fell in late is different, with small anisotropies even in the outer parts. In addition, the net angular momentum of these components is expected to be small and simply reflect that of the dominant DM component at this epoch. These orbital differences between the early and late infalling structures are a simple test for SIM Lite.

A relatively small sample of proper motions for halo stars and the halo globular clusters would check and constrain further these theoretical models. The angular momentum and anisotropy measured within a sample of a few hundred proper motions to a precision of 5 km/s (compared to the radial dispersion of ~100 km/s) in different regions of the sky and at different Galactic radii would allow us to model accurate orbits, obtain orbital angular momenta and eccentricities, and provide a detailed statistical accounting of the initial specific angular momentum of sub-halos. SIM Lite can provide these critical data on the angular momentum and anisotropy at large radii, well beyond the Gaia-sphere. Moreover, SIM Lite may be able to provide a similar assessment of the independent angular momentum profile of the Magellanic Clouds, providing insight into the structure and formation of intermediate mass halos.

4.5   Measuring the Physical Nature of Dark Matter

4.5.1   Background and Current Problems

Determining the nature of the DM that surrounds galaxies and overwhelms the gravitational force from visible matter constitutes a fundamental task of modern astrophysics. CDM particles are characterized by low initial velocity dispersion and high phase space density, resulting from a relatively heavy particle mass. After collapsing, they thermalize into distributions with steep density cusps at their centers (Navarro et al. 2004; Diemand et al. 2005). In cosmologies with a somewhat lighter DM particle there are reduced phase space densities and higher velocity dispersions. These alternative models, broadly classified as warm DM, produce more constant density cores in galactic halos (Tremaine and Gunn 1979).

In this sense, by precisely measuring the shape of the central DM density profile (characterized by the logarithm of the slope there), one places important constraints on the primordial phase space density of DM, which in turn bears on such microphysical properties of the DM particle as its mass and details of its formation mechanism. For example, in the case where the DM was in thermal equilibrium with the plasma in the early Universe (this would be the case with "thermal warm DM"), then the limit comes down to a constraint on the particle mass. If the DM particle is born in a decay, then the phase space constraint limits a combination of the decay lifetime and the particle mass difference between the daughter and the primary (as in the case of SuperWIMPS, where the gravitino is the DM and it emerges as a daughter particle from the late decay of a heavier particle).

Based on measured mass-to-light ratios, dwarf spheroidal (dSph) galaxies occupy the least massive known DM halos in the Universe. Dwarf spheroidals are also unique among all classes of galaxies in their ability to probe the particle nature of DM, because phase space cores resulting from the properties of the DM particle are expected to be most prominent in these small halos (Tremaine and Gunn 1979; Hogan and Dalcanton 2000). In recent years, the measurement of line-of-sight velocities for upwards of a thousand stars in several dSphs has allowed for a precise determination of their masses (e.g., Strigari, Bullock, and Kaplinghat 2007a; Walker et al. 2007). However, despite the great progress made in estimating masses of these systems, determining the logarithmic slope of their central density profile, and thus the nature of the DM contained within, remains elusive.

Modeling of the mass distribution of the dSphs requires a solution of the equilibrium Jeans equation, which gives a relation between the components of the intrinsic velocity dispersion and the mass density profile of the DM halo. When projecting along the line of sight, the observed velocity dispersion is a combination of two orthogonal components, and thus a degeneracy arises between the ratio of the radial and tangential components of the velocity dispersion and the logarithmic slope of the DM density profile (Figures 4-9, 4-10, 4-11). Even with 1000 line-of-sight velocities, the relative error on the log-slope at the King core radius is of order ≈ 1, which cannot distinguish between a cusp model, which has typical log-slope of ≈ 1 at this radius, and a core model, which has a typical log-slope of ≈ 0.3 at this radius (Figure 4-10, upper panels; Strigari et al. 2007a).

4.5.2   Potential Solutions with SIM Lite: Dark Matter Within Dwarf Galaxies

The only way to break this degeneracy is to sample the tangential velocity components in addition to the line-of-sight components. Even were the numbers of stellar radial velocities available in individual dSphs eventually to reach of order 10^5, there would be insufficient numbers at and within the critical radius (about 100 pc) that must be probed to discriminate reliably a central core from a central cusp. The only way to break the degeneracy between the log-slope of the density profile and the velocity

Figure 4-9. The projected error on the log-slope of the DM density profile of Draco at the King core radius as a function of the number of proper motions. From top to bottom, the curves assumed that the errors on the transverse velocities are 10, 7, 5, 3 km/s.
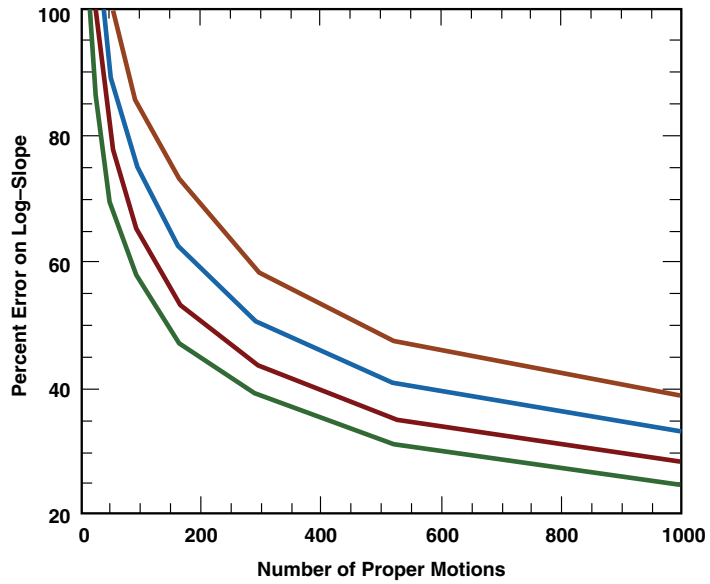
Figure 4-10. A demonstration of the ability to recover information on the nature of DM using observations of dSph stars, from analytical modeling by Strigari et al. (2007a). Ellipses indicate the 68 percent and 95 percent confidence regions for the errors in the measured dark halo density profile slope (measured at twice the King core radius) and velocity anisotropy parameter β in the case where only radial velocities are available for 1000 stars in a particular dSph (top panels). A significant improvement is derived from the addition of 200 SIM Lite proper motions providing 5 km/s precision transverse velocities (bottom panels). The left (right) panels correspond to a cusp (core) halo model for dSphs and the small ×'s indicate the fiducially input model values.
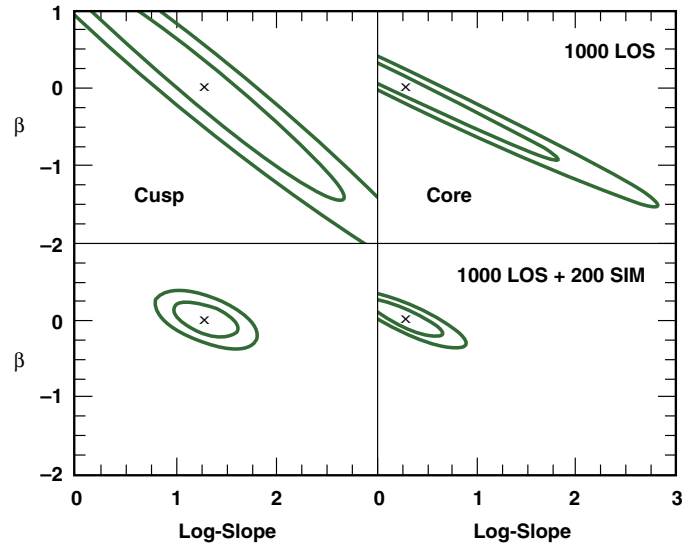
Figure 4-11. Potential SIM Lite exploration of the Draco dSph would need to probe to V ~ M = 19 to derive a sample of 200 red giants as seen by its Washington M-band luminosity function (black line and left axis). The colored lines represent the number of days (right axis) necessary to observe all the stars to a given magnitude limit with SIM Lite and for a given transverse velocity uncertainty: 3 km/s (green line), 5 km/s (red line), 7 km/s (blue line) and 10 km/s (magenta line). (From Strigari et al., in preparation.)
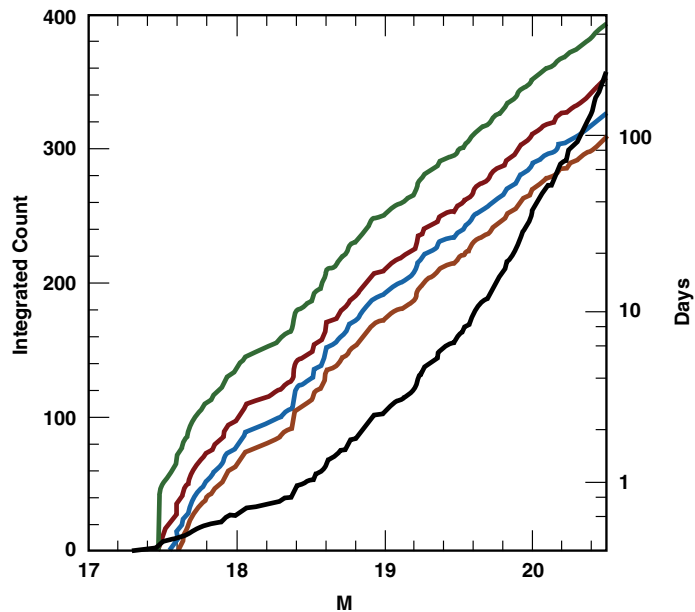
anisotropy of dSph stars is to sample the tangential velocity components in addition to the line-of-sight components. A measurement along these lines requires the proper motion of individual stars to a precision of at least 10 km/s, which is the intrinsic velocity dispersion of the highest luminosity dSphs.

Several dSphs within 100 kpc, in particular Draco (Figure 4-11), Sculptor, Carina, and Ursa Minor, have hundreds of stars with V < 20, and thus proper motions of these stars may be obtained with SIM Lite. SIM Lite will be able to measure the proper motions of hundreds of stars in several of these dSphs to a precision of ~5 km/s. In Figure 4-9, we show the projected error on the log-slope of the DM density profile at the King core radius as a function of the number of measured proper motions for a typical dSph. The number of proper motions is in addition to 1000 line-of-sight velocities. As may be seen, with several hundred proper motions from one dSph it will be possible to measure the log-slope to a precision of ~30 percent, which is several times better than a measurement of the log-slope with line-of-sight velocities alone (Strigari et al. 2007a). Thus, with the investment of 1500 hours (Figure 4-11), SIM Lite should be able to discriminate cusped from cored density profiles in the Draco dSph halo (Figure 4-10). Obtaining the required transverse velocities, while well beyond the capabilities of Gaia, is well-matched to the projected performance of SIM Lite.

4.6   Dark Matter and Dynamics on the Galaxy Group Scale

4.6.1   Background and Current Problems

Within the emitting parts of galaxies, rotation curves are generally flat rather than falling according to Kepler's law, which implies that mass grows roughly linearly with radius. The total mass-to-light ratio depends critically on where this mass growth ends, but this is generally not observable. Just beyond the outermost measured 21 cm isophotes of galaxies, the DM distribution simply becomes unknown. As a result, critical questions about DM on scales from galaxy to galaxy-group sizes remain unanswered. Do dwarf galaxies have lower or higher mass-to-light ratios than regular galaxies? Do the DM halos of galaxies in groups merge into a common envelope? How do these mass components compare with the warmer DM particles smoothly distributed across super-clusters or larger scales?

At present, we can only detect DM through its gravitational effects; therefore, a careful study of the dynamics of nearby galaxies is one of the few ways to resolve these issues. It is reasonable to anticipate that numerical simulations (e.g., constrained *N*-body and least-action method calculations) will find the initial density distribution that transforms into a best fit to present-day redshifts and proper motions, once they are known, for nearby individual galaxies and groups of galaxies. This fit will yield masses for the galaxies and galaxy groups, and will also give the density of uniformly distributed warm/hot DM at Mpc scales. Although the hot DM density is thought to be quite small today, its gravitational signature from early times may be significant because the density of relativistic material grows as $(1 + z)^4$, and, in a high Ω_Λ universe, the cross-over from energy-dominated to matter-dominated occurs at a later time.

Most analyses of peculiar velocity flows have applied linear perturbation theory appropriate for scales large enough that over-densities are << 1 (Peebles 1980). Peculiar velocity analyses (Shaya, Tully, and Pierce 1992; Dekel et al. 1993; Pike and Hudson 2005) have proven the general concept that the observed velocity fields of galaxies result from the summed gravitational accelerations of over-densities over the age of the Universe. Peculiar velocity analyses agree with virial analyses of clusters and Wilkinson Microwave Anisotropy Probe (WMAP) observations that indicate the existence of a substantial DM component strewn roughly where the galaxies are. But these studies apply only to scales of >10 Mpc, the scales of superclusters and large voids. Spherical infall (including "timing analysis" and "turnaround radius") studies do not presume low over-densities and have been applied to the smaller

scale of the Local Group (Lynden-Bell and Lin 1977). These studies indicate mass-to-light ratios for the Local Group of roughly $M/L \sim 100\ M_\odot/L_\odot$ in blue light, but this model is crude; nonradial motions and additional accelerations from tidal fields and subclumping are expected to be non-negligible and would substantially alter the deduced mass (Li and Helmi 2008). A more complete treatment of solving for self-consistent orbits is required, but to properly constrain such models observations of nonradial motions is a prerequisite.

4.6.2   Potential Solutions with SIM Lite: Measuring Galaxy Motions Within the Local Group

If one measured the proper motions of nearby Local Group galaxies with global accuracies of a few μas/yr, one would have another pair of high-quality phase space components with which to construct flow models and determine histories and masses for galaxies and galaxy groups. For a galaxy 1 Mpc away, 4 μas/yr corresponds to 19 km/s transverse motion, which is small compared to the expected transverse motions in the field, ~100 km/s. Therefore, SIM Lite will be able to measure accurate proper motions of any galaxy in the Local Group that has stars brighter than V < 20. The low-velocity dispersion of stars in a typical dwarf galaxy ensure that after averaging just a few random stars, the contribution to the error from the internal motions would be only a few km/s. For larger galaxies, simple rotation models adjusted to the observed velocity profiles, or direct measurements of the rotation with SIM Lite (§6.4), can be removed from the motions to deliver <20 km/s accuracy. There are 27 galaxies beyond the Milky Way satellites (all within 5 Mpc) that have sufficiently bright stars.

SIM Lite measurements of the three-dimensional galaxy flows will be of lasting importance in the modeling of the formation of the Local Group, several nearby groups, and of the plane of the Local Supercluster. Gaia will probably be able to obtain proper motion vectors for satellite galaxies of the Milky Way, M31, M33, and WLM by averaging a sufficient number of stars in these systems that are bright enough. For other galaxies, we would expect Gaia to obtain upper limits based on a few dozen stars near its detection limit. The proper motion measurement of M31 by either SIM or Gaia would be limited essentially by errors in the referenced coordinate grid. It is expected that the SIM frame would be a factor of >2 more accurate than Gaia's. The Gaia measurement should prove to be a significant improvement over the VLBI study of two water masers in M33 (Brunthaler et al. 2005).SIM Lite's ability to point for long periods at targets will allow it to obtain high-accuracy proper motions for the other galaxies, which have just a few stars with V < 20.

The application of the least-action method (LA, Peebles 1989) allows one to solve for the trajectories that result in the present distribution of galaxies (or more correctly, the centers of mass of the material that is presently in galaxies). By making use of the constraint that early-time peculiar velocities were small, the problem becomes a mixed boundary value problem with constraints at both early and late times. Figure 4-12 shows the output of a recent LA calculation for the orbits of nearby galaxies and groups going out to the distance of the Virgo Cluster. The orbits are in co-moving coordinates. This is just a single example of a set of several solutions using present three-dimensional positions as inputs. The masses of four massive objects (Virgo Cluster, Coma Group, CenA Group, and M31) have been adjusted to provide a best fit to observed redshifts. The good news is that complex orbits are rare. With the addition of proper motions of 27 galaxies, the problem becomes fully constrained, and one can solve for the actual masses of all of the dominant galaxies. Experiments have shown that, with 5 percent distance accuracy, errors in mass are below 50 percent for the dominant galaxies. In other words, we will finally learn where the DM ends on each major galaxy. Also, the two components of proper motion will be useful for determining the mass associated with groups aside from that in the individual galaxies, as well as the amount of matter distributed on scales larger than 5 Mpc.

Figure 4-12. The trajectories of nearby galaxies and groups going out to the distance of the Virgo Cluster from a Least Action calculation with parameters $M/L = 90$ for spirals, 155 for ellipticals, $\Omega_m = 0.24$, and $\Omega_\Lambda = 0.76$. The axes are in the supergalactic plane (SGX-SGY) in co-moving coordinates. There are 21 time steps going from $z = 40$ to the present. The large circle is placed at the present position and the radius is proportional to the square root of the mass. The present estimated distances were fixed and the present redshifts were unconstrained.
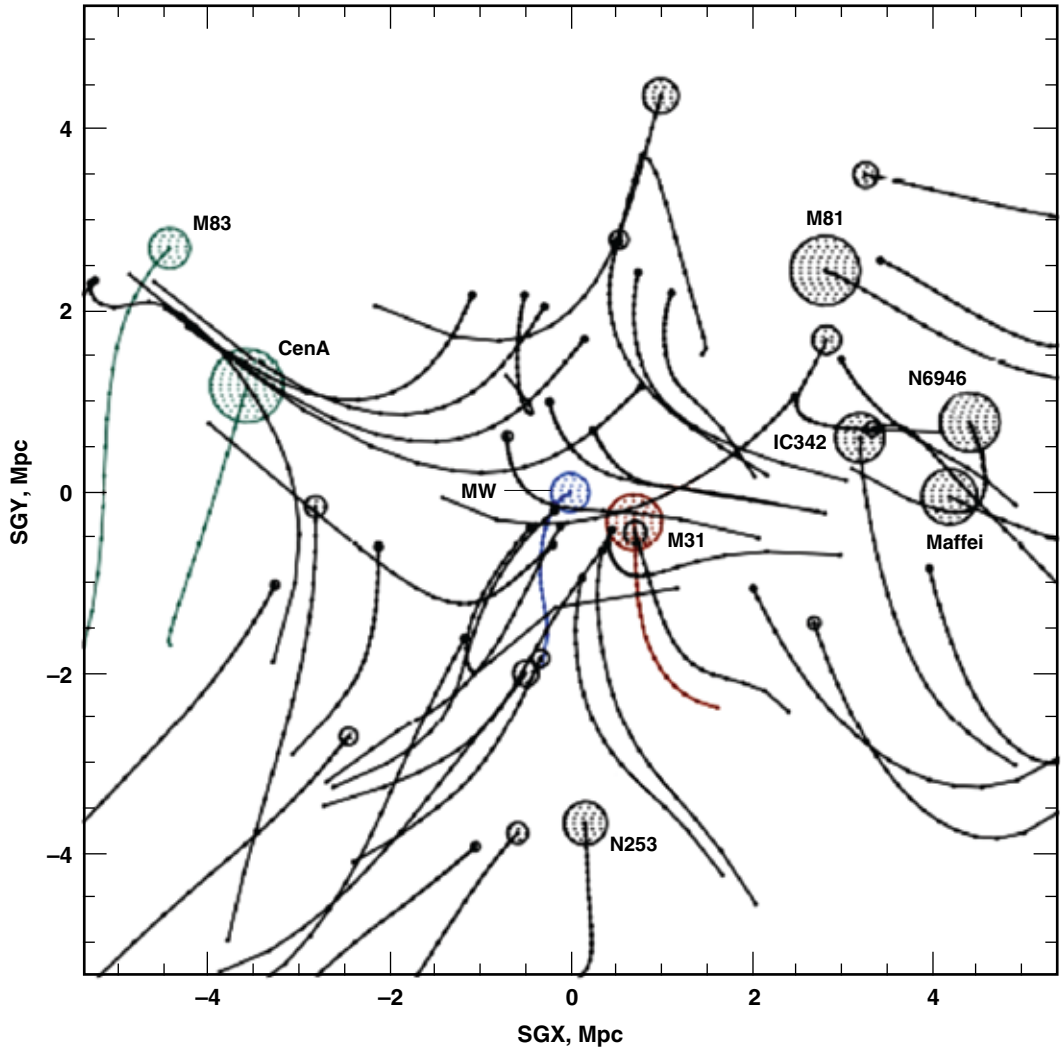
4.7   Summary of Proposed SIM Lite Possibilities and Priorities

While the discussion above has outlined a number of important problems within the study of Local Group dynamics and DM, it may not be possible to address them all with a fixed mission time. Table 4-1 summarizes the experiments discussed in this chapter and the estimated SIM Lite mission times required to approach each problem in a definitive and legacy-creating way. It must be kept in mind that as this active field evolves, the relative priorities of these different experiments — and indeed the consideration and priority of additional experiments as yet uncontemplated — cannot be anticipated for a decade hence. Thus, we do not attempt to prioritize these proposed tests here, but only tabulate the expected mission requirements for each. Whatever sub-suite of these will be selected at final mission definition, SIM Lite will make unique, lasting, and significant contributions to the study of local DM and galaxy formation.

As Table 4-1 summarizes, the ability of SIM Lite to make μas measurements of the positions of faint stars is unmatched among all planned missions. SIM Lite alone will be able to probe accurately the six-dimensional stellar phase space distribution around the outskirts of our own Galaxy, within a nearby sample of dwarf galaxies, and in other Local Group systems — and these are the only galaxies in the Universe for which such data will be available. These measurements provide unique windows on some key astrophysical problems, from galaxy formation and the structure of DM halos, to the nature of DM itself.

Table 4-1. Estimated SIM Lite observing time for galactic dynamics and local DM experiments.

Experiment	No. of Stars	Magnitude Range, V	PM Accuracy, μas/yr	Mission Time, hrs
Tidal Streams (§4.2.2)	400	11–19	4–20	700
Milky Way High-Velocity Stars (§4.2.3)	20	18–20	10–60	300
Extragalactic High-Velocity Stars (§4.2.3)	20	18–20	10–60	300
Satellite Orbits (§4.3.2)	350	14–20	7–40	600
Angular Momentum Profile (§4.4.2)	100	16–20	50–75	100
Dark Matter in Dwarf Galaxies (§4.5.2)	200	17–19	11	1500
Local Group Galaxy Motions (§4.6.2)	600	17–20	2–10	1000

References

Abadi, M. G., Navarro, J. F., Steinmetz, M., and Eke, V. R., 2003, ApJ, 591, 499.

Allgood, B., Flores, R. A., Primack, J. R., Kravtsov, A. V., Wechsler, R. H., Faltenbacher, A., and Bullock, J. S., 2006, MNRAS, 367, 1781.

Belokurov, B. et al. 2007 ApJ, 658, 337.

Benson, A. J., Lacey, C. G., Baugh, C. M., Cole, S., and Frenk, C. S., 2002, MNRAS, 333, 156.

Bonanos, A. Z., López-Morales, M., Hunter, I., and Ryans, R. S. I., 2008, ApJ, 675, L77.

Brown, W. R., Geller, M. J., Kenyon, S. J., and Kurtz, M., 2006, ApJ, 640, L35.

Brown, W. R., Geller, M. J., Kenyon, S. J., and Kurtz, M. 2007, ApJ, 671, 1708.

Brunthaler, A., Reid, M. J., Falcke, H., Greenhill, L. J., and Henkel, C., 2005, Science, 307, 1440.

Bullock, J. S. and Johnston, K. V., 2005, ApJ, 635, 931.

Bullock, J. S., Kravtsov, A. V., and Weinberg, D. H., 2000, ApJ, 539, 517.

Clewley, L., Warren, S. J., Hewett, P. C., Norris, J. E., Wilkinson, M. I., and Evans, N. W., 2005, MNRAS, 362, 349.

Dekel, A., Bertschinger, E., Yahil, A., Strauss, M. A., Davis, M., and Huchra, J. P., 1993, ApJ, 412, 1.

Diemand, J., Moore, B. and Stadel, J., 2005, Nature, 433, 389.

Diemand, J., Zemp, M., Moore, B., Stadel, J., and Carollo, C. M., 2005, MNRAS, 364, 665.

Diemand, J., Kuhlen, M., Madau, P., Zemp, M., Moore, B., Potter, D., and Stadel, J., 2008, Nature, 454, 735.

D'Onghia, E. and Lake, G., 2008, ApJ, 686, L61.

Fellhauer, M. et al., 2006, ApJ, 651, 167.

Gnedin, O. Y., Lee, H.-M., and Ostriker, J. P., 1999, ApJ, 522, 935.

Gnedin, O. Y., Gould, A., Miralda-Escudé, J., and Zentner, A. R., 2005, ApJ, 634, 344.

Grillmair, C. J. and Dionatos, O., 2006, ApJ, 641, L37.

Gualandris, A. and Portegies Zwart, S,. 2007, MNRAS, 376, L29.

Hartwick, F. D. A., 2000, AJ, 119, 2248.

Hayashi, E., Navarro, J. F., Taylor, J. E., Stadel, J. and Quinn, T., 2003, ApJ, 584, 541.

Helmi, A., 2004, ApJ, 610, L97.

Hills, J. G., 1988, Nature, 331 687.

Hogan, C. J. and Dalcanton, J. J., 2000, Phys. Rev. D, 62, 063511.

Ibata, R. A., Lewis, G. F., Irwin, M. J., and Quinn, T., 2002, MNRAS, 332, 915.

Johnston, K. V., Spergel, D. N., and Haydn, C., 2002, ApJ, 570, 656.

Johnston, K. V., Zhao, H., Spergel, D. N., and Hernquist, L., 1999, ApJ, 512, L109.

Kauffmann, G., White, S. D. M., and Guiderdoni, B., 1993, MNRAS, 261, 201.

Kazantzidis, S., Kravtsov, A. V., Zentner, A. R., Allgood, B., Nagai, D., and Moore, B., 2004, ApJ, 611, L73.

Klypin, A., Kravtsov, A. V., Valenzuela, O., and Prada, F., 1999, ApJ, 522, 82.

Knebe, A., Gill, S. P. D., Gibson, B. K., Lewis, G. F., Ibata, R. A., and Dopita, M. A., 2004, ApJ, 603, 7.

Kravtsov, A. V., Gnedin, O. Y., and Klypin, A. A., 2004, ApJ, 609, 482.

Kunkel, W. E., 1979, ApJ, 228, 718.

Law, D. R., Johnston, K. V., and Majewski, S. R., 2005, ApJ, 619, 807.

Li, Y.-S. and Helmi, A., 2008, MNRAS, 385, 1365.

Libeskind, N. I., Frenk, C. S., Cole, S., Helly, J. C., Jenkins, A., Navarro, J. F., and Power, C., 2005, MNRAS, 363, 146.

Loeb, A. and Narayan, R., 2008, MNRAS, 386, 2221.

Lynden-Bell, D. and Lin, D. N. C., 1977, MNRAS, 181, 37.

Lynden-Bell, D., 1983, in IAU Symp. 100: Internal Kinematics and Dynamics of Galaxies, 89.

Macciò, A. V., Dutton, A. A., and van den Bosch, F. C., 2008, MNRAS, 391, 1940.

Majewski, S. R. et al., 2007, ApJ, 670, L9.

Majewski, S. R. et al., 2004, AJ, 128, 245.

Martínez-Delgado, D., Gómez-Flechoso, M. Á., Aparicio, A., and Carrera, R., 2004, ApJ, 601, 242.

Martin, N. F., Ibata, R. A., Irwin, M. J., Chapman, S., Lewis, G. F., Ferguson, A. M. N., Tanvir, N., and McConnachie, A. W., 2006, MNRAS, 371, 1983.

Mayer L., Moore B., Quinn T., Governato F., and Stadel J., 2002, MNRAS, 336, 119.

Metz, M., Kroupa, P., and Libeskind, N. I., 2008, ApJ, 680, 287.

Moore, B., Ghigna, S., Governato, F., Lake, G., Quinn, T., Stadel, J., and Tozzi, P., 1999, ApJ, 524, L19.

Moore, B., Calcáneo-Roldán, C., Stadel, J., Quinn, T., Lake, G., Ghigna, S., and Governato, F., 2001, Phys. Rev. D, 64, 063508.

Moore, B., Diemand, J., Madau, P., Zemp, M., and Stadel, J., 2006, MNRAS, 368, 563.

Muñoz, R. R. et al., 2006, ApJ, 649, 201.

Muñoz, R. R., Majewski, S. R., and Johnston, K. V., 2008, ApJ, 679, 346.

Navarro, J. F. et al., 2004, MNRAS, 349, 1039.

Newberg, H. J. et al., 2003, ApJ, 596, L191.

Pakzad, S. L. et al., 2004, BAAS, 36, 1582.

Palma, C., Majewski, S. R., and Johnston, K. V., 2002, ApJ, 564, 736.

Peebles, P. J. E., 1980, The Large-Scale Structure of the Universe (Princeton, N.J.: Princeton University Press).

Peebles, P. J. E., 1989, ApJ, 344, L53.

Pike, R. W. and Hudson, M. J., 2005, ApJ, 635, 11.

Searle, L. and Zinn, R., 1978, ApJ, 225, 357.

Shaya, E. J., Tully, R. B., and Pierce, M. J., 1992, ApJ, 391, 16.

Sherwin, B. D., Loeb, A., and O'Leary, R. M., 2008, MNRAS, 386, 1179.

Sohn, S. T. et al., 2007, ApJ, 663, 960.

Stadel, J. et al., 2008, ArXiv e-prints, 808, arXiv:0808.2981.

Strigari, L. E., Bullock, J. S., and Kaplinghat, M., 2007a, ApJ, 657, L1.

Strigari, L. E., Bullock, J. S., Kaplinghat, M., Diemand, J., Kuhlen, M., and Madau, P., 2007b, ApJ, 669, 676.

Tremaine, S. and Gunn, J. E., 1979, Physical Review Letters, 42, 407.

Walker, M. G., Mateo, M., Olszewski, E. W., Gnedin, O. Y., Wang, X., Sen, B., and Woodroofe, M., 2007, ApJ, 667, L53.

Walsh, S. M., Willman, B., Sand, D., Harris, J., Seth, A., Zaritsky, D., and Jerjen, H., 2008, ApJ, 688, 245.

Willman, B. et al., 2005, ApJ, 626, L85.

Yu, Q. and Tremaine, S., 2003, ApJ, 599, 1129.

Zentner, A. R., Kravtsov, A. V., Gnedin, O. Y., and Klypin, A. A., 2005, ApJ, 629, 219.

Zucker, D. B. et al., 2006, ApJ, 650, L41.

Masses of Compact Galactic Objects with Microlensing

5

Andrew Gould (Ohio State University) and **B. Scott Gaudi** (Ohio State University)

ABSTRACT

Using the technique of gravitational microlensing, SIM Lite will conduct a representative census of all compact Galactic objects from brown dwarfs to black holes, including white dwarfs, neutron stars, and main sequence stars. The masses of these objects will be derived from a combination of precise measurement of the tiny astrometric deflections that are generated by all microlensing events with a photometric "microlens parallax" measurement. The latter is possible because SIM Lite will be in solar orbit, which means that it measures a "different" photometric event compared to what is seen from the ground. No other known technique can undertake such a systematic survey, although Gaia and ground-based interferometers might succeed in measuring the masses of some black holes.

5.1   Census of Dark and Luminous Objects

What would an unbiased census of Galactic objects — dark and luminous — reveal? At a minimum, it would yield the frequency of black holes, neutron stars, white dwarfs, and old brown dwarfs, which are either completely dark or so dim that they defy detection by normal methods. It might also find a significant component of the dark matter, although the majority of dark matter cannot be in the form of compact objects (Alcock et al. 2000; Tisserand and Milsztajn 2005). The only known way to conduct such a census is to put a high-precision astrometry telescope in solar orbit.

Masses of astronomical bodies can be measured only by the motions they induce on other objects, typically planets and moons that orbit Solar System bodies and binary companions that orbit other stars. Masses of luminous isolated field stars can be estimated from their photometric and spectroscopic properties by calibrating these against similar objects in bound systems. Hence, photometric surveys yield a reasonably good mass census of luminous objects in the Galaxy.

Dark objects like black holes are another matter. Mass measurements of isolated field black holes can be obtained only by their deflection of light from more distant luminous objects. Indeed, it is difficult to even detect isolated black holes by any other effect. However, to go from detection to mass measurement (and therefore positive identification) of a black hole is quite challenging.

5.2   Mass Measurement from the Gravitational Deflection of Light

Gravitational microlensing experiments currently detect about 700 microlensing "events" per year. The vast majority of the "lenses" are ordinary stars, whose gravity deflects (and so magnifies) the light of a more distant "source star." As the source gets closer to and farther from the projected position of the lens, its magnification A waxes and wanes according to the Einstein formula (Einstein 1936):

$$A(u) = \frac{u^2 + 2}{u\sqrt{u^2 + 4}} \quad \text{where} \quad u(t) = \sqrt{u_0^2 + \left(\frac{t - t_0}{t_E}\right)^2} \qquad (1)$$

where u is the source-lens angular separation (normalized to the so-called Einstein radius θ_E), t_0 is the time of maximum magnification (when the separation is u_0), and t_E is the Einstein radius crossing time, i.e., $t_E = \theta_E / \mu$, where μ is the lens-source relative proper motion. The mass M cannot be directly inferred from most events because the only measurable parameter that it enters is t_E, and this is a degenerate combination of M, μ, and the source-lens relative parallax π_{rel}:

$$t_E = \frac{\theta_E}{\mu} \quad \text{where} \quad \theta_E = \sqrt{\kappa M \pi_{rel}} \qquad (2)$$

and $\kappa = 4G/(c^2 \, AU) \sim 8$ mas $/ M_\odot$.

It follows immediately that to determine M, one must measure three parameters, of which only one, t_E, is routinely derived from microlensing events. Another such parameter is θ_E, which could be routinely measured from the image positions, if it were possible to resolve their separation, which is of order 1 mas. A third is the "microlens parallax," π_E,

$$\pi_E = \pi_{rel} / \theta_E \qquad (3)$$

Combining equations (2) and (3),

$$M = \frac{\theta_E}{\kappa \pi_E} \tag{4}$$

implying that the mass can be extracted from θ_E and π_E alone. (See, e.g., Gould 2000.)

Just as θ_E is the Einstein radius projected onto the plane of the sky, $\tilde{r}_E$ is the Einstein radius projected onto the observer plane and is related to the microlens parallax π_E by $\tilde{r}_E \equiv AU/\pi_E$. Just as θ_E could in principle be measured by resolving the two images on the sky, π_E could be routinely measured by simultaneously observing the event from two locations separated by a distance on the order of $\tilde{r}_E$ (Refsdal 1996; Gould 1995). "Routine" measurement of both π_E and θ_E is essential. As of today, there have been a few dozen measurements of these parameters separately (e.g., Poindexter 2005), but only one very exceptional microlensing event for which both were measured together with sufficient precision to obtain an accurate mass (Gould, Bennett, and Alves 2005).

In fact, such routine measurement is possible by placing an accurate astrometric and photometric telescope in solar orbit. For current microlensing experiments carried out against the dense star fields of the Galactic bulge, $\pi_{rel} \sim 40$ µas, so for stellar masses, $\theta_E \sim 500$ µas and $r_E \sim 10$ AU. Hence, a spacecraft in solar orbit would be an appreciable fraction of an Einstein radius from Earth, so the photometric event described by Equation (1) would look substantially different than it would from the ground. From this difference, one could infer r_E (and so π_E).

Determining θ_E is more difficult. As mentioned above, this would be straightforward if one could resolve the separate images, but to carry this out routinely (i.e., for small as well as large values of θ_E) would require larger baselines than are likely to be available in next-generation instruments. Rather, one must appeal to a more subtle effect, the deflection of the centroid of the two lensed images. This deflection is given by (Miyamoto and Yoshii 1995; Hog, Novikov, and Polanarev 1995; Walker 1995):

$$\Delta\theta = \frac{u}{u^2 + 2} \theta_E \tag{5}$$

Simple differentiation shows that this achieves a maximum at $u = \sqrt{2}$, for which $\Delta\theta = \theta_E / \sqrt{8}$, roughly 1/3 of an Einstein radius. Hence, if the interferometer can achieve an accuracy on the order of 10 µas at the time when this deflection is the greatest, then θ_E can be measured to a few percent.

There are some subtleties as well as some challenges. Satellite measurements of $\tilde{r}_E$ are subject to a four-fold discrete degeneracy, which can only be resolved by appealing to higher-order effects (Gould 1995). It is not enough to measure the centroid location to determine the astrometric deflection: one must also know the undeflected position to which the measured position is to be compared, and this can only be found by extrapolating back from late-time astrometry. And the precision of the mass measurement depends directly on the signal-to-noise ratio of the underlying photometric and astrometric measurements. This is important because space-based astrometric telescopes are likely to be photon challenged and so to require relatively bright (and hence rare) microlensing events to provide accurate mass measurements. Gould and Salim (1999) carried out detailed simulations based on the characteristics of SIM Lite and concluded that with about 1200 hours of mission time, it would be possible to make 5 percent mass measurements for about 200 microlenses. Most of these lenses will be stars, but at least a few percent are likely to be black holes, and several times more are likely to be other dark or dim objects like neutron stars, old white dwarfs, and old brown dwarfs. Since such a census is completely new, it may also turn up unexpected objects. (The measurement of masses from microlensing is illustrated in Figures 5-1 and 5-2.)

Figure 5-1. How SIM Lite measures the mass of a dark object. (a) Side view of the geometry of a microlensing event, across the line of sight. The lens passes near the line of sight between an observer and a distant source and produces two images. (b) High-magnification sky view, along the line of sight. Starting from the left, the gravitational lens (red star) passes the background source (green circle), splitting its light into two magnified images (cyan) that trace separate paths above and below the lens. Their combined light (blue circle), measured astrometrically by SIM Lite and photometrically [depicted schematically in (c)] by SIM Lite and on the ground, is displaced from the source (green circle) by an amount that varies according to Equation (5), reaching a maximum deviation of $\theta_E/\sqrt{8}$, where θ_E is the angular Einstein radius. Hence, by measuring this deflection, SIM Lite determines θ_E. (c) The light curve as observed by SIM Lite or from the ground (scaled for their different lines of sight).

The marks on the curve correspond to the positions of the lensing object (red stars). (d) Photometric microlensing events seen from Earth and SIM Lite differ, with different maximum magnifications (and intensities [(c)]) and different times of maximum. (e) From these differences, one infers that the event as seen from Earth has a smaller impact parameter (since it was more highly magnified) and passed the lens later (since it peaked later). Hence, one can infer the offset $\Delta \mathbf{u}$ between the two trajectories in units of the Einstein ring. (f) The scalar separation Δu is equal to the ratio of the SIM Lite–Earth distance to the "projected Einstein radius," $\tilde{r}_E$, i.e., the radius of the Einstein ring projected onto the observer plane. Hence, photometric measurements from SIM Lite and Earth yield $\tilde{r}_E\,\theta_E$. Mass is then given by $M = (c^2/4G)\tilde{r}_E$, while source–lens relative parallax is $\pi_{rel} = (AU/\tilde{r}_E)\theta_E$. (Adapted from Gould and Salim 1999.)
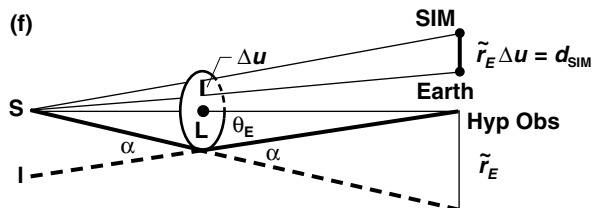

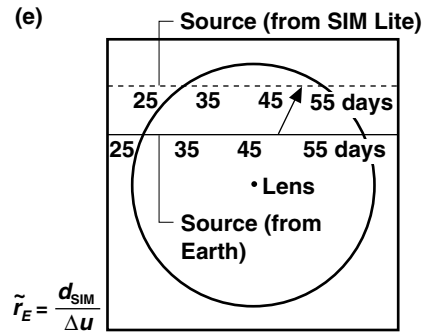$$\tilde{r}_E = \frac{d_{SIM}}{\Delta u}$$
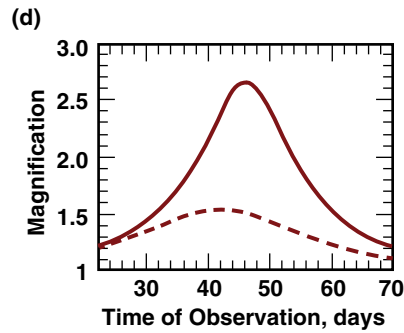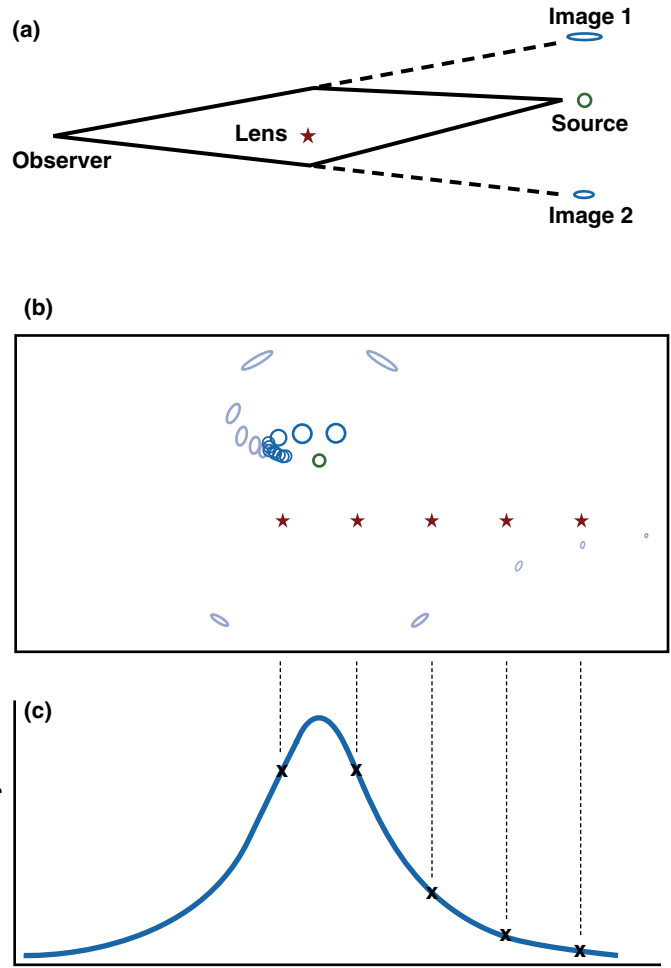
$$\tilde{r}_E \Delta u = d_{SIM}$$

Figure 5-2. Rate of micro-lensing events as function of lens mass as predicted by the model of Gould (2000), including those due to brown dwarfs, white dwarfs, neutron stars, and black holes, as well as main sequence stars. The last are reasonably well-constrained from optical/IR surveys, but distribution functions of the dim/dark objects are un-known. Only SIM Lite in solar orbit can measure them.
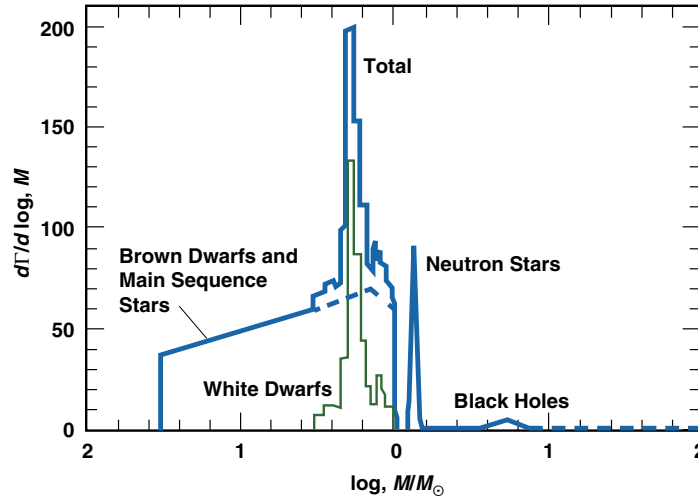
5.3   Performance of Gaia and Ground-Based Instruments

Since Gaia is scheduled to be launched before SIM Lite, it is appropriate to ask whether these measure-ments could be carried out by Gaia, or whether Gaia could somehow leverage its vastly larger number of targets to compensate for its inferior astrometric precision. And, of course, one should also ask how much of this program could be carried out from the ground.

Neither Gaia nor ground-based interferometers can address the integrated problem of measuring the en-tire mass spectrum of compact objects from brown dwarfs to black holes. However, both could make some progress on the more limited (but very interesting) problem of measuring the frequency of black holes.

With regard to the full mass spectrum, Gaia has two problems. First, Gaia will be in an L2 rather than a solar orbit, and it therefore cannot be used as one of two platforms (the other being Earth) from which to measure the microlens parallax. Of course, this applies still more strongly to ground-based observations of any type.

Second, the astrometric precision required for reliable identification of "typical" lenses is substantially higher than will be achieved by Gaia. From equation (2), one finds that for $M = 1M_\odot$ and $\pi_{rel} = 20$ μas (typical of bulge lenses), $\theta_E = 400$ μas. The maximum deflection of the centroid of light from the true source position is therefore $\Delta\theta_{max} \sim 140$ μas, so that a 3σ detection requires a precision of $\sigma \sim 45$ μas. Of course, Gaia is expected to achieve this precision for many stars, but this is the *mission accuracy*. What is required here is to measure the $\theta_E / \sqrt{8}$ "excursion" while it is actually happening, i.e., over rough-ly four Einstein crossing times, $4t_E$ ($2t_E$ while approaching and $2t_E$ while receding), typically 120 days. For these short intervals, Gaia precision will be degraded by a factor $\sim \sqrt{5\ years/120\ days} \sim 4$. Since even the brightest sources (indeed the ones that SIM Lite would observe) will be V ~ 17, the required precision is a factor of several beyond Gaia's capability.

Given its small field of regard (and so shortage of stable reference stars), ground-based interferometry would most likely tackle the θ_E measurement by a different route: detection of the two images, which are separated by 2 θ_E ~ 800 μas. By comparison, at $\lambda = 2$ μm, a 100 m baseline implies a diffraction limit of 4 μas. Hence, for example, the Keck interferometer could not be used. Of course, longer-baseline inter-ferometers are already in use. But here we have to remember that the brighter "typical" sources will be K = 13. While there will be (and already are) a few highly magnified events per season that are amenable to interferometric measurement, their frequency is far too small to permit a systematic survey of compact matter. And, again, even if these measurements were possible, they would yield only θ_E and not π_E (and so the mass and distance).

However, among the dark objects, black holes are probably the most interesting, and because black holes are substantially more massive than typical stellar lenses, black hole events are longer and so are more susceptible to microlens parallax measurements from the ground (Bennett, Anderson, Bond, Udalski, and Gould 2006; Poindexter 2005). This obviates (or partially obviates, see below) the need for a satellite in solar orbit.

Moreover, since they are more massive than typical objects, black holes have larger Einstein rings, which dramatically improves the prospects for measuring them using either Gaia or ground-based interferometers. At the same $\pi_{rel} = 20$ µas, a "typical" black hole of mass $M \sim 6\ M_\odot$ would have $\theta_E \sim 1$ mas and so $\Delta\theta_{max} \sim 350$ µas, so that a 3σ detection would only require a precision of σ = 120 µas. And, the larger θ_E implies a longer t_E, typically 75 days, which reduces the degradation factor on Gaia astrometry from a factor 4 to a factor 2.5. That is, a "typical" black hole would only require a "mission precision" of σ ~ 120 µas / 2.5 = 50 µas. If Gaia meets its design goals, this will be achievable for the brighter sources.

An important collateral point is that such Gaia measurements would break a common (and usually crippling) degeneracy in the ground-based microlens parallax measurements. Unlike trigonometric parallax, microlens parallax is a vector, $\boldsymbol{\pi_E}$, whose direction is that of the lens source relative proper motion and whose amplitude is, of course, π_E. For typical events, $\boldsymbol{\pi_E}$ is not measurable at all because these events are too short. For very long events, it is completely measurable (e.g., Poindexter 2005), but for intermediate-length events, such as those expected for typical black holes, one component of $\boldsymbol{\pi_E}$ (the one parallel to the projected position of the Sun–Earth axis) can be tightly constrained, while the orthogonal component is almost completely unconstrained (Gould, Miralda-Escud'e, and Bahcall 1994). See, e.g., Jiang et al. 2003; Ghosh et al. 2003. By measuring the *direction* of the centroid displacement (which can be determined with roughly the same fractional precision as the amplitude of displacement) one can determine the *direction* of π_E and so break the degeneracy.

The extra factor of 2.5 in θ_E for black holes comes close to reaching the diffraction limit of ground-based interferometers, so that it may be possible for them to partially resolve the two images. However, this assumes that they will reach flux thresholds that are substantially more than an order of magnitude fainter than current limits.

Neither Gaia nor ground-based interferometers have any hope of a complete census of compact objects (stars, black holes, neutron stars, white dwarfs, and brown dwarfs). However, Gaia probably could do a reasonable black hole census, and ground-based interferometry could make some inroads in this direction, although it could not do a black hole census.

References

Alcock C. et al., 2000, ApJ , 542, 281.

Bennett, D., Anderson, J., Bond, I., Udalski, A., and Gould, A., 2006, ApJ , 647, L171.

Einstein, A., 1936, Science, 84, 506.

Ghosh, H. et al., 2003, ApJ , 615, 450.

Gould, A., 1995, ApJ , 441, L21.

Gould, A., 2000, ApJ , 542, 785.

Gould, A. and Salim, S., 1999, ApJ, 524, 794.

Gould, A., Bennett, D., and Alves, D., 2005, ApJ, 614, 404.

Gould, A., Miralda-Escud'e, J., and Bahcall, J., 1994, ApJ, 423, L105.

Gwinn, C. et al., 1997, ApJ, 485, 87.

Hog, E., Novikov, I. and Polanarev, A., 1995, A&A , 294, 287.

Jiang, G. et al., 2003, ApJ, 617, 1307.

Kopeikin, S. M., 2006, AJ, 131, 1471.

Makarov, V. M., 2005, PASP, 117, 757.

Miyamoto, M. and Yoshii, Y., 1995, AJ, 110, 1427.

Poindexter, S., 2005, ApJ, 914, 633.

Refsdal, S., 1996, MNRAS, 134, 315.

Tisserand, P. and Milsztajn, A., 2005, New Views on the Universe, Proceedings of the 5th Rencontres Du Vietnam. Hanoi: In Press (Astro-PH/0501584).

Walker, M., 1995, ApJ, 453, 37.

Will, C., 2006, Living Rev. Relativ., 9, 3.

6 Luminosity-Independent Extragalactic Distances
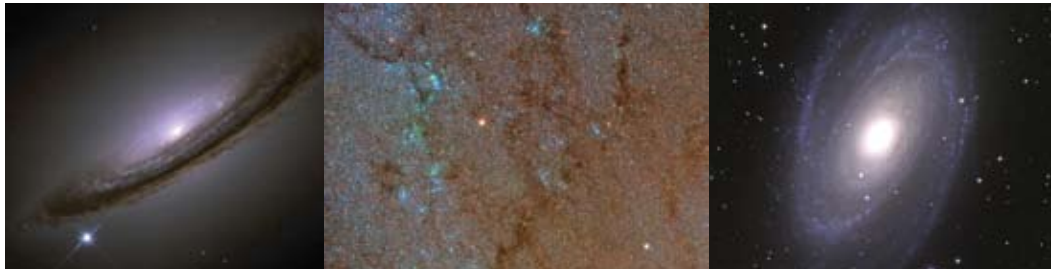
Robert P. Olling (University of Maryland)

ABSTRACT

SIM Lite can provide astrometric data of such high quality that it will be possible to determine geometric (luminosity-independent) distances to the nearest spiral galaxies, even though these systems are too far away for direct trigonometric parallax determination. Instead, the method to use is that of rotational parallax (RP). Percent-level distances to M31 and M33 are within reach of a SIM Lite observing program. Such accurate geometric distances will be required for many projects, such as: (1) to establish a small external error on the Hubble constant, H_0, (2) double-check on the "determination" of H_0 from cosmological data sets, (3) obtain six-dimensional phase-space coordinates for galaxy-dynamics studies with unprecedented accuracies, and 4) establish a uniform comparison between the many stellar populations (and their formation histories) among Local Group galaxies. The RP method extends the 1 percent distance limit of SIM Lite by a factor of over 300, from 2.5 kpc to about 770 kpc.

6.1 An Independent Yardstick

Why are SIM Lite–based extragalactic distances needed if Gaia will calibrate almost every conceivable standard candle, and if the Joint Dark Energy Mission (JDEM) determines the redshift dependence of the Hubble constant? The answer is that an independent determination of the extragalactic distance scale gives us confidence in the external errors. Since small external errors (<1 percent) are required for future applications, it is unwise to rely on a single calibrator (e.g., the LMC or NGC4258) or even a single method. SIM Lite–based rotational parallax (RP) distances can provide such checks. SIM Lite's RP distances will be essentially bias free, so that SIM Lite's RP galaxies provide independent, absolute anchors for most distance indicators, including Cepheids.

Some areas of astrophysical research that would benefit from accurate extragalactic distances are:
- Cosmology and dark energy
- The internal dynamics of disk galaxies
- Star-formation histories of nearby galaxies
- Any other field that requires absolute distances

The aim of this chapter is to illustrate the power of SIM Lite in the area of extragalactic distances. More details can be found elsewhere (Olling and Peterson 2000, hereafter OP2000; Olling 2007, hereafter O2007; Olling 2008, hereafter O2008; and OPO for the combined works).

6.2 H_0, Cosmology, and Dark Energy

There is a growing realization that a 1 percent level determination of the Hubble constant (H_0) is important for cosmology, dark energy (Hu 2005, hereafter H2005; O2007; Macri et al. 2006; Braatz et al. 2007; Ichikawa and Takahashi 2008), and the determination of the critical density,

$$\rho_{CRIT} = 3H_0^2 / (8\pi G)$$

H_0 is important for cosmology because the cosmic microwave background (CMB) data are the most accurate of the various methods (SNe, baryon acoustic oscillations, weak lensing, galaxy clustering, and so on) that probe cosmological evolution and that the CMB data really measure the physical matter densities (H2005). To figure out whether the Universe is open, closed, or flat, one works with relative densities: $\Omega = \rho / \rho_{CRIT}$, which introduces the dependence on H_0.

Measuring the equation of state (w) of dark energy is one of the biggest efforts in observational cosmology today. The accuracy to which w can be determined depends strongly on the uncertainty in the Hubble constant (Figure 6-1). In fact, Hu (2005) states that "…the Hubble constant is the single most useful complement to CMB parameters for dark energy studies ... (if H_0 is) ... accurate to the percent level." A simple analysis (O2007) indicates that the CMB data and H_0 currently contribute in about equal proportion to the error of the equation of state (EOS) and how this proportionality changes for the various stages considered by the Dark Energy Task Force (DETF). Planck's CMB errors will be 8 times smaller than those of WMAP, so it is imperative to reduce the H_0 errors commensurately, to ~1 percent. For DETF-Stage-I data and with the current uncertainties of H_0, the EOS is known to about 9 percent. Decreasing the error on H_0 by a factor of 10 will decrease the error on the EOS by a factor 3.9 to 2.3 percent. Likewise, with DETF-Stage-IV data, a 1 percent error on H_0 would decrease the error on the EOS by the square root of two to 0.9 percent. DETF-stage-I data roughly correspond to the state of the art in DE research, while DETF-Stage-IV represents the *expected* state of the art attainable *after* completion of the JWST *and* LSST *and* the Square Kilometer Array.

Figure 6-1. Measuring the equation of state (*w*) of dark energy is one of the biggest efforts in observational cosmology today. The accuracy with which *w* can be determined depends on the uncertainties in the CMB parameters and the Hubble constant, H_0. SIM Lite will be capable of reducing the uncertainty in H_0 by almost an order of magnitude. This result, when combined with improved CMB parameters from WMAP and Planck, will result in a significant improvement in our determination of *w*. This figure shows how the uncertainty in *w* depends on the uncertainties in the CMB and in H_0. Four curves are shown corresponding to four different uncertainties in H_0, ranging from the current value (10.8 percent) down to the value expected from SIM Lite (1.1 percent). With Planck-like CMB parameters (right-most vertical line) and the current uncertainty in H_0, *w* can be determined with an accuracy of 8.9 percent. Including SIM Lite's result for H_0, the accuracy in *w* will improve to 2.3 percent.
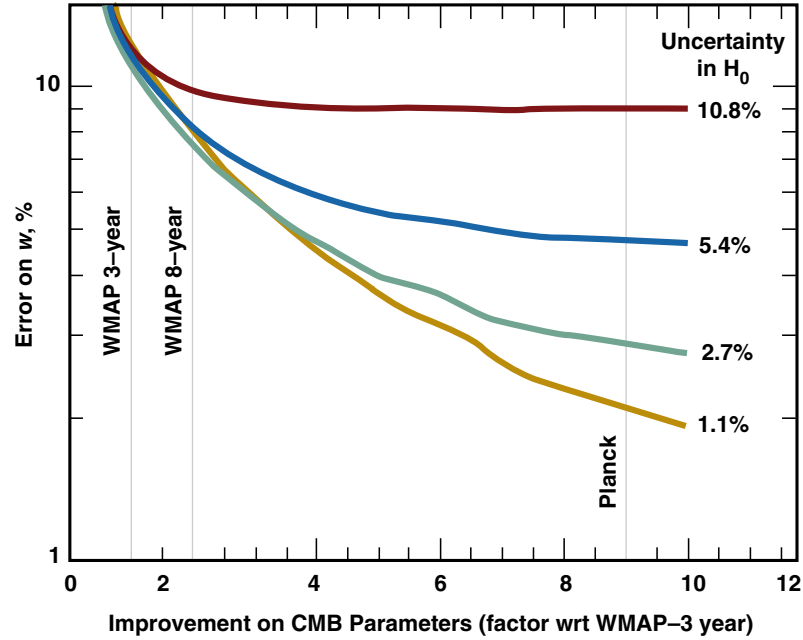
6.3 A Luminosity-Independent Zero-Point for the Distance Scale

6.3.1 Background and Current Problems

Significant progress has been made on the calibration of the extragalactic distance scale, and the determination of H_0 with methods such as Type Ia SNe, the Tully-Fisher relation, surface brightness fluctuations, the Tip of the Red-Giant Branch, and the Fundamental Plane. The primary calibration usually relies on the period-luminosity relation for Cepheids.

While the zero-point of the Cepheid distance scale in the LMC and in the Milky Way is still debated, steady progress is being made in the calibration of Galactic Cepheids' distances (e.g., HST parallaxes and the interferometric calibration of the Baade-Wesselink method).

There is currently a shift to use NGC4258 as a zero-point rather than the LMC, because NGC4258 is much more similar to galaxies that are used to determine H_0 than is the LMC. Currently, the nuclear water-maser distance of NGC4258 (Humphreys et al. 2005) provides a Cepheid zero-point calibration to 3 percent (Macri et al. 2006; Riess and Macri 2007). The search is "on" to find more distant water-maser sources for direct H_0 determination (Braatz et al. 2007, 2008). Also, the Cepheid period-luminosity relation in the near/mid-infrared is much more reliable than the ones based on optical photometry (Freedman et al. 2008).

With standard candle methods, many problems exist that are basically due to the fact that the physical properties of stars are determined only at the 1 to 10 percent level for a small number of stars. Even the metallicity of the Sun is defined rather than measured (Kurucz 2002). Gaia and SIM Lite will provide a large number of high-accuracy calibrators to determine mass, luminosity, radius, temperature, and metallicity, although not necessarily all for the same objects.

6.3.2 Potential Problems with Existing Measurements

The history of the luminosity calibration of standard candles indicates that "ultimate answers" are hard to obtain. Furthermore, even "geometric" methods may be subject to significant uncertainty. See O2007 for an extended discussion.

The Case of the Pleiades: The distance to the Pleiades cluster has been derived by a number of methods. Pinsonneault et al. (1998), Pan, Shao, and Kulkarni (2004), and Soderblom et al. (2005) (see Section 7.2) indicate that the geometric Hipparcos distance is "wrong." Similar discrepancies are found for four other clusters (Kaltcheva and Makarov 2007).

The Case of SN1987A: The "light echo" of SN1987A has been analyzed by several groups to determine the distance to the LMC. However, there is a systematic difference between the groups at the 10 percent level. It appears that this gap cannot be bridged (Gould 2000).

Interferometric Baade-Wesselink Method: Recently, the interferometric Baade-Wesselink calibration of the Cepheid PL relation changed significantly due to a cross-check with independent data (Gieren et al. 2005). However, this result is also disputed (Groenewegen 2007).

Extragalactic Water Masers: There is a renewed effort to improve Cepheid distances based on the VLBI-based water maser zero-point. However, the water maser method samples only parts of the major and minor axes, so that "more complicated models" are difficult to rule out. For example, the derived distances will be systematically off by twice the intrinsic eccentricity (e = 0.01 yields a 2 percent distance error [O2007]). Such small eccentricities might well exist in AGN accretion disks (Armitage 2008), but are not satisfactorily included in the distance determinations.

6.3.3 Potential Solutions with SIM Lite

As discussed earlier, the most important reason to undertake the SIM Lite RP project is to obtain independent data to corroborate the existing, ongoing, and future distance-scale projects. Because the proposed RP method samples large areas of the galaxy disks, the method is not sensitive to sampling effects as is the case for the water maser method. The distance determination will be very robust because four of the six phase space coordinates are measured (per star), while the remaining two can be adequately modeled (OPO). Any "standard candle" present in the RP galaxies will thus have a zero-point determined, also allowing for many essential cross-checks with their counterparts in the Milky Way.

6.4 The Rotational Parallax Method

The rotational parallax method employs the fact that velocity (V), distance (D), and proper motion (μ) are related via $\mu = V / (\kappa D)$, where κ is a constant related to the choice of units. We illustrate (Figure 6-2) the RP method for a toy galaxy model with only circular motion and the rotation speed (V_c) and inclination known (from the HI). Then, a star on the minor axis directly yields the distance $D = V_c / (\kappa \mu)$. The distance can also be recovered from a star at an arbitrary location since there are three unknowns (D, V_c, and inclination) and three observables (the radial velocity and the two proper motions).

For a realistic galaxy, we split the total observed velocity (V_{TOT}) into components that are intrinsic to the galaxy and ones that may vary from star to star: $V_{TOT} = V_{SYS} + V_C + V_P + V_\sigma$, where V_{SYS} is the systemic

Figure 6-2. This figure illustrates the rotational parallax method for a model galaxy with no systemic motion and with only circular internal motion. (The application of this method to a realistic galaxy is given in the text.) When applied to nearby galaxies, RP will provide a luminosity-independent estimate of the extragalactic distance scale, with an absolute accuracy of <1 percent. At the same time, it will serve as a check on estimates using the standard candle indicators, such as Cepheids. Here is a DSS image of M31 showing the relationships between distance (D), inclination (i), velocity from rotation (V_c), radial velocity (V_{radial}) and proper motion (μ_{Major}) for stars on the major axis; it also shows the relationship between D, V_c, and proper motion (μ_{minor}) for stars on the minor axes. The constant κ is related to the choice of units. The colored dots denote bright AB supergiants already identified in M31 (courtesy D. Peterson). Their distances from and rotation about the galactic center cause them to move toward (green) or recede from (red) Earth; stars near the galactic center (yellow) may have relatively little radial velocity from rotation. SIM Lite will make measurements of μ_{Major} and μ_{minor}. When these are combined with ground-based measurements of V_{radial}, distance D can be estimated.
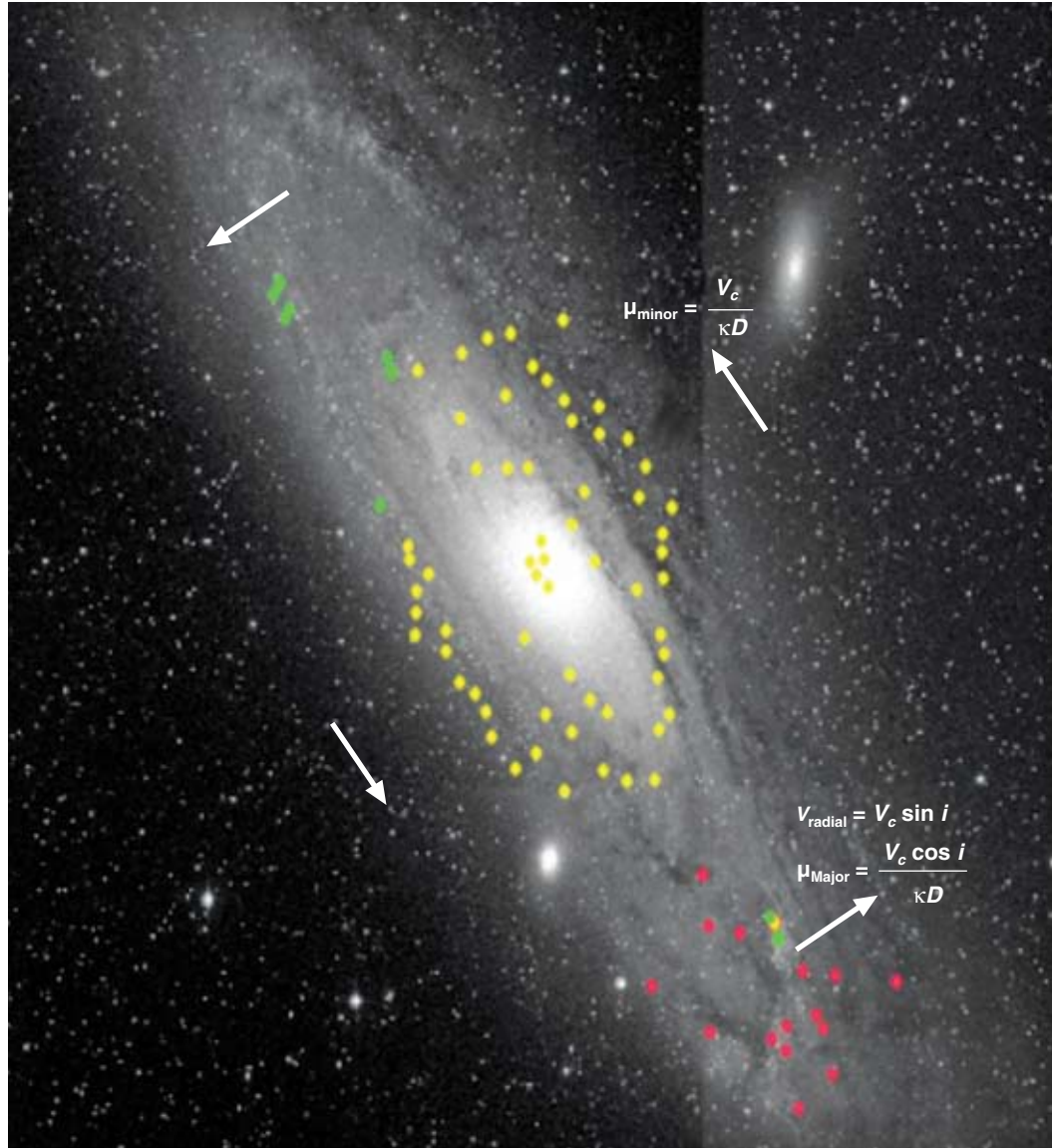
motion of the galaxy, V_σ is the random motion, and V_P is the peculiar velocity due to spiral-arm perturbations, tidal interactions, bar-induced elliptical motions, and so forth, or a combination thereof.

The equation above involves 18 unknowns: three components for V_{SYS}, V_P, and V_σ, the (x,y,z) position of the star, the center of the coordinate system and position angle of the major axis (+3), the circular velocity, distance, and inclination. Only five measurements are taken per star: the three components of the stars' space velocity and two positions. Thus, there appears to be no solution as we have 18 unknowns and five observables, per star.

However, when considering ensembles of several stars, a robust solution can be found. First, the velocity-dispersion values are only required for the group as a whole: 15 unknowns remain and three unknowns shared by all objects. Similarly, the systemic motion, coordinate system parameters, rotation speed, inclination, and distance are shared between stars (at the same galactocentric radius). Thus, the number of shared variables equals 12 ($N_{SV} = 12$). This leaves six star-dependent unknowns (V_P, [x,y,z])

and five observables per star. To solve this problem, OP2000 assumed co-planarity — that $z = 0$ and $V_P(z) = 0$ — so that only four star-dependent unknowns remain and a solution is possible.

This solution can be generalized (O2007) because the peculiar motions are due to some large-scale perturbation (see above). If this were not the case, V_P would be a random velocity instead. Thus, because gravity is a long-range force, the peculiar velocities are correlated from star to star, and V_P can be expressed as a Fourier series that adds ($N_{FS} \geq 0$) shared variables to N_{SV}, but, crucially, eliminates star-based unknowns. Likewise, disk-warping or a radially varying rotation curve will add shared variable ($N_{WRC} \geq 0$). Thus, from first principles, we know that the number of stars (N_{STR}) that needs to be observed must exceed the number of shared variables: $N_{STR} > 12 + N_{FS} + N_{WRC}$.

Our error estimates do not fully include the effects of non-circular motions, and we estimate that a safety margin of about a factor of two is required with respect to OP2000's distance-error relation [their equation (25)]. However, this margin is not included in any of the quoted accuracies below.

With rotational velocities of 270, 97, and 55 km/s, the rotation-induced proper motions for M31, M33, and the LMC are 74, 24, and 192 µas/year, respectively; all easily detectable by SIM Lite. In fact, the achievable distance errors are dominated by the internal velocity dispersions of the stellar population and increase linearly with the per-star proper motion accuracy. We adjust integration time with apparent magnitude to achieve about 8 µas/yr across our magnitude range. We find that, with 300 stars per galaxy (down to V = 16.5), the distance errors will be 0.56 percent for M31. M33 has 300 stars down to V = 17.1 and yields a distance accuracy of 1 percent. Our target stars will be among the most luminous stars with masses over 20 $M_\odot$. For M31, we computed the expected errors based on the true magnitude distribution of M31 stars (Massey et al. 2006) as well as the guide-star catalog (Lasker et al., 2008), both corrected for foreground stars. We find enough bright stars in M31 to achieve the goal of subpercent distance errors in a reasonable time: 0.36 percent (0.52 percent) errors in 32 (16) days of SIM Lite time. M33 is expected to have roughly three times fewer stars, with a commensurate reduction in achievable accuracies.

A similar analysis indicates that Gaia's best-possible accuracy would be as good as for a 32-day SIM Lite program for M31. However, the Gaia-based project would employ 10,000 stars as faint as V = 20. An RP project also needs ground-based radial velocities (RVs) with accuracies of 1–2 km/s for all program stars.* The SIM Lite program needs fewer than than 300 stars (V ≤ 17), requiring several 100 times less observing time than the Gaia-based project. A more realistic Gaia project could read 0.5 percent distance error and would use five times fewer stars (2,000 at V ≤ 18.6) and 30 times more RV observing time than for SIM Lite. Such a Gaia program would be comparable to a modest 16-day SIM Lite project.

Both SIM Lite and Gaia can in principle achieve the goal of subpercent distance errors for M31 based on the rotational parallax method. This result is predicated on the assumption that the data allow for $1 / \sqrt{N}$ accuracy improvements. This may in fact be the case; an absolute reference frame is not required, as the physics of the RP method allow one to measure (and take out) linear and rotation motions of the local astrometric grid. Since it is of paramount importance to have confidence in the derived distances, and their errors, the Gaia/SIM Lite comparison provides a crucial cross-check of procedures.

The LMC stars are relatively bright and have large internal (random) motions, so the LMC requires many thousands of stars: Gaia can probably get a rotational parallax to this system.

Note that one might consider using radial velocities from other sources such as the HI, or from averaging a number of nearby stars at lower RV accuracy. However, that would decrease the robustness of the method.

6.5   Internal Dynamics of Nearby Galaxies

To date, the understanding of the dynamics of the Milky Way has been hampered strongly by the absence of a large sample of stars for which six-dimensional phase space information is available. For example, the vertical force law can only be studied in the immediate solar neighborhood, and is derived from the vertical density and vertical velocity distribution functions. Gaia is designed to solve these kinds of problems for the Milky Way.

Since the peculiar motions of individual stars can be determined with the RP technique, SIM Lite RP studies enable the same kind of dynamical studies of M31 and M33 that Gaia enables for the Milky Way. Such six-dimensional information will only be available for the Milky Way and the RP targets, and can be used to study in great detail the dynamics of bars, warps, spiral-arm streaming motions, tidal encounters, and so forth. These systems will be the laboratories for galactic dynamic studies of spirals for many decades.

The proper motion accuracy (~8.0 μas/yr at V = 16.5) is an *absolute* measure. Important for the internal dynamics are the *relative* motions, which are determined at the 6.7 μas/yr level (25 km/s). At this magnitude, Gaia's accuracy is about four times worse. However, the SIM Lite error has the potential for further reduction: for a 10-year data set, the errors reduce by about a factor of three to 8.2 km/s (2.2 μas/yr), which is below the expected velocity dispersion of the target population.

Finally, it might even be possible to unravel the time dependency of the perturbing force. Some SIM Lite RP targets have well-defined ages, such as Cepheids. By choosing targets with a suitable range of ages, it may be possible to determine their "birth velocities" and whether the perturbing forces have changed over time.

6.6   Stellar Content, Star Formation, and Assembly Histories of Nearby Galaxies

A 1 percent distance for the rotational parallax galaxies would also allow for an accurate age determination (from accurate luminosities) of all stars in those galaxies (10^{11} stellar ages per distance measurement). Although current estimates for stellar ages are not limited by distance uncertainties, the Gaia data are expected to change this situation dramatically. It will determine masses for over 17,000 astrometric binaries to better than 1 percent (Lebreton 2008). Furthermore, distances of about 21 million stars will be measured to ~1 percent. Since about 0.85 percent of stars are detached eclipsing binaries (DEBs), radii can be determined for ~357,000 stars in DEB systems with distance uncertainties ≤1 percent. Masses for these systems will be determined employing Gaia's radial-velocity data supplemented with ground-based spectroscopy and/or SIM Lite astrometry to provide proper sampling of these short-period systems. SIM Lite should contribute significantly to this calibration by getting subpercent distances for the slowly evolving (low-mass) systems that are crucial for the determination of the star-formation history of the Milky Way.

Already, star-formation histories (and, hence, galaxy assembly histories) are inferred from deep star-counts in Local Group galaxies. SIM Lite rotational parallax distances would allow for the direct transfer of these new Gaia-based age calibrations from the Milky Way to the RP galaxies.

While Gaia might get a good rotational parallax for M31, SIM Lite will excel at it. By using all stars down to V = 20, Gaia can just about attain 1 percent distance error for M31, while SIM Lite can easily reach 1 percent distance error for a five-year mission.

References

Armitage, P. J., 2008, astro-ph, 0802.1524.

Braatz, J. A. and Gugliucci, N. E., 2008, ApJ, 678, 9.

Braatz, J. et al., 2007, IAU Symposium, 242, 399.

Freedman, W. L. et al., 2008, ApJ, 679, 71.

Gieren, W. et al., 2005, ApJ, 627, 224.

Gould, A., 2000, ApJ, 528, 156.

Groenewegen, M. A. T., 2007, AandA, 474, 975.

Hu, W., 2005, Observing Dark Energy, ASPC, 339, 215.

Humphreys, E. M. L. et al., 2005, ASP Conf. Ser. 340, 466.

Ichikawa, K. and Takahashi, T., 2008, JCAP, 4, 27.

Kaltcheva, N. and Makarov, V., 2007, ApJ, 667, L155.

Kurucz, R. L., 2002, Baltic Astronomy, 11, 101.

Lasker, B. M. et al., 2008, AJ, 136, 735.

Lebreton, Y., 2008, IAUS, 248, 119, astro-ph/0801.2022.

Lindegren, L. et al., 2008, IAU Symposium, 248, 217.

Massey, P. et al., 2006, 2006, AJ, 131, 2478.

Macri, L. M. et al., 2006, ApJ, 652, 1133.

Olling R. P., 2008 (O2008) http://www.astro.umd.edu/~olling/Papers/SIM_H0_WP_Long_RPO.pdf.

Olling R. P., 2007, MNRAS, 378, 1385, and astro-ph/0607607 = O2007.

Olling R. P. and Peterson D. M., 2000, astro-ph/0005484 (OP2000).

Peterson, D. and Shao, M., 1997, ESA SP-402: Hipparcos — Venice 1997, 402, 749.

Pan, X., Shao, M., and Kulkarni, S. R., 2004, Nature, 427, 326.

Pinsonneault, M. H. et al., 1998, ApJ, 504, 170.

Riess, A. G. and Macri, L., 2007, BAAS, 211, #55.07.

Soderblom, D. R., et al., 2005, AJ, 129, 1616.

Formation History of the Milky Way

7

I. Neill Reid (STScI) and **Brian Chaboyer** (Dartmouth College)

ABSTRACT

Globular clusters and Population II stars are fossil remnants of the first major epoch of star formation in the Milky Way. SIM Lite will determine precise distances to selected Pop II objects to define a reliable distance scale, and establish reliable absolute and relative ages. Those ages set a minimum age for the Universe and map the early formation history of the Milky Way. The resultant ages will be accurate to better than 1.0 Gyr, resolving the detailed chronology of the first epoch of star formation in the Milky Way Galaxy.

7.1   RR Lyrae Stars As Population II Distance Indicators

RR Lyrae stars are solar-mass stars that have exhausted core hydrogen burning on the main sequence (MS); they have evolved through the hydrogen shell-burning phase and, after experiencing the helium flash at the tip of the red giant branch (RGB), have settled onto the helium core-burning phase at ~ $10 \times L_\odot$. Metal-rich stars show little evolution in color over the few $\times$ 10^8 year lifetime of this phase of evolution, and form the "red clump" close to the RGB, but metal-poor stars evolve blueward, forming the horizontal branch (HB). At a certain point, when the surface temperature is ~5,700 K, the star becomes unstable and pulsates; this behavior persists until the surface temperature reaches ~7,000 K, and recurs during the (faster) redward evolution back across the instability strip. The pulsations have periods from 0.3 to 1.5 days and produce luminosity variations with amplitudes up to a factor of 3, rendering these stars easily recognizable not only in the field, but also in globular clusters (Pickering and Bailey 1895) and nearby galaxies such as the Large Magellanic Cloud (LMC) (Thackeray and Wesselin 1953) and M31 (Pritchett and van den Bergh 1987).

These characteristic photometric variations, coupled with their ubiquity, have led to RR Lyrae stars playing a key role as secondary indicators to Local Group systems in the extragalactic distance ladder. However, different calibration techniques lead to different absolute zero points for RR Lyrae luminosities (Figure 7-1). As a result, there remain significant uncertainties in both the absolute magnitudes of RR Lyrae stars and the extent to which those luminosities depend on metallicity (Figure 7-2). There are also (metallicity-based?) inconsistencies between the RR Lyrae results and other distance indicators: for example, RR Lyrae stars give a relative distance modulus δm ~ 6.2 magnitudes between the LMC and M31 (Reid 1999), while Cepheids give δm ~ 5.9 magnitudes (Freedman and Madore 1990), and red clump stars give δm ~ 6.4 magnitudes (Reid 1999).

The first step towards reconciling those differences is to establish the absolute-magnitude calibration, and its dependence on metallicity, of RR Lyrae stars in the Galactic field. The nearest variables, including RR Lyrae itself, lie at distances of 100 to 200 pc, barely within reach of the Hipparcos astrometric satellite. The Hubble Space Telescope has measured submilliarcsecond accuracy parallaxes for a handful of nearby variables (Benedict et al. 2002 and 2007), but the formal uncertainties in the distances remain in excess of 15 percent and therefore do not break the degeneracies evident in Figures 7-1 and 7-2.

Figure 7-1. The absolute magnitude of metal-poor RR Lyrae stars as determined through a variety of techniques; averaging all techniques gives a formal uncertainty of ±0.12 mag or ±6 percent in distance. SIM Lite will make high-accuracy distance measurements for a small sample of field RR Lyrae stars.
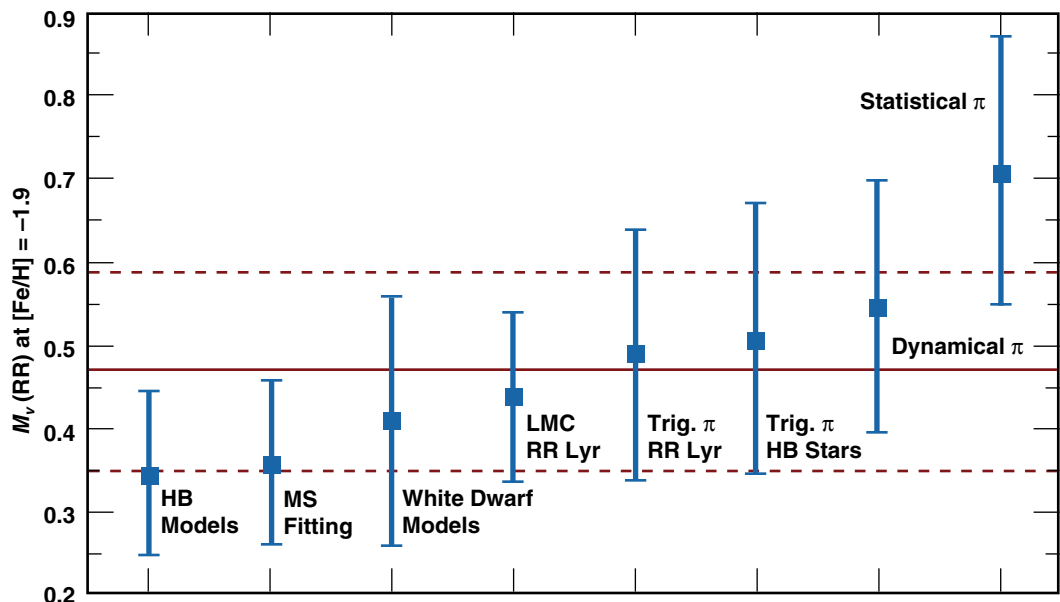
Figure 7-2. A summary of the various RR Lyrae (M_V, [Fe/H]) relations from six different reports. In addition, five solid points mark $\langle M_V \rangle$ for M5, M13, M15, M68, and M92 variables, using Hipparcos-based distance moduli. The upper histogram plots the abundance distribution of the field (from Reid 1999). SIM Lite will target about 20 field RR Lyrae stars, chosen to span a range in distance and metallicity. This will establish the slope and brightness zero point, providing an independent check on Gaia.
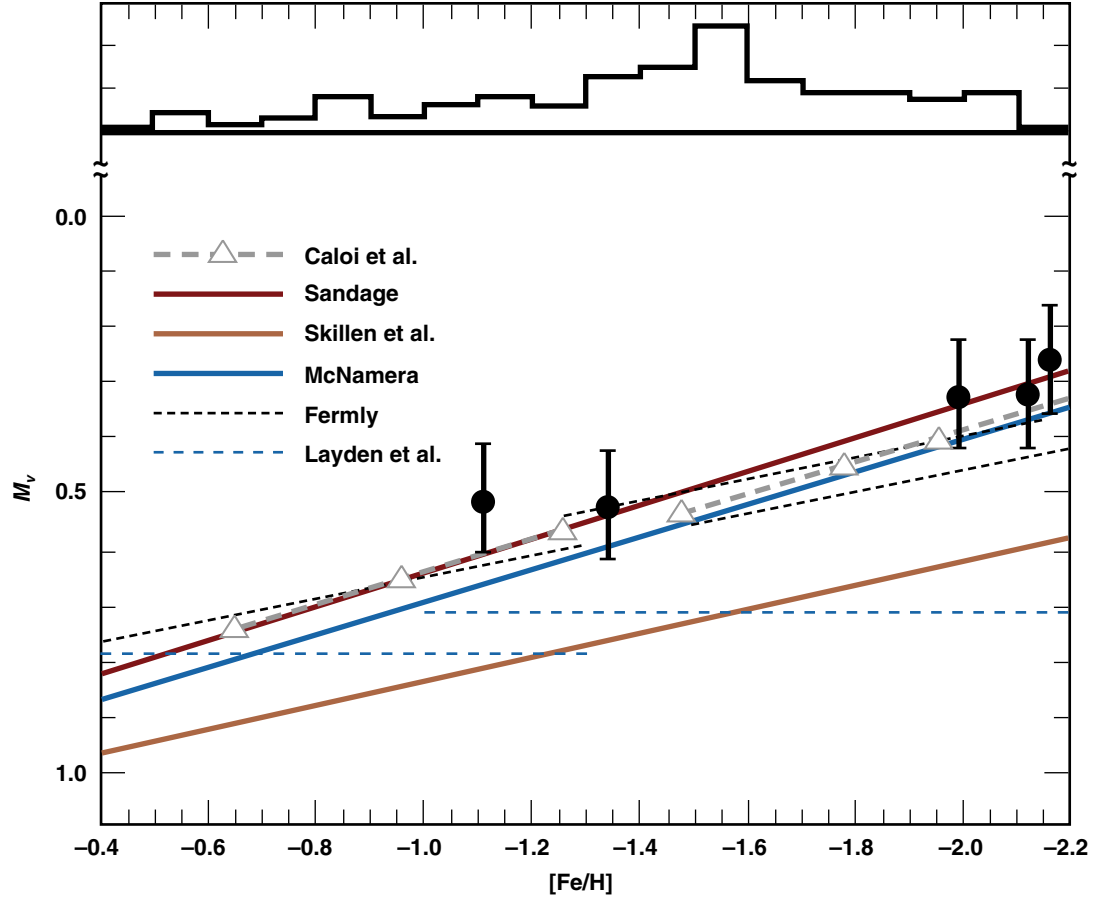
Gaia is expected to have a major impact in this area. At $M_V \approx 0.5$, RR Lyrae stars within 5 kpc have apparent magnitudes V < 14, and, over its mission, Gaia should achieve trigonometric parallaxes accurate to ~10 to 20 µas for those stars (Lindegren et al. 2007), corresponding to uncertainties of 1 to 2 percent at 1 kpc ($\sigma(M_V) \approx 0.05$ magnitudes) and 5 to 10 percent at 5 kpc. With a space density of 5/kpc³, several hundred RR Lyrae stars fall within Gaia's reach, and the resultant data will map the (M_V, [Fe/H]) relation and define the absolute magnitude zero point to a potential accuracy of a few percent.

SIM Lite, with a mission accuracy of 3 to 5 µas — three to four times better than Gaia — can play a crucial role by providing an independent check of the calibration for key stars. We anticipate targeting ~20 field RR Lyrae stars, chosen to span an appropriate range in distance and metallicity. Acquiring those observations will require only 14 to 15 SIM Lite mission hours.

7.2   Ages of Globular Clusters

Globular clusters are the archetypical Population II systems. These metal-poor systems, with total masses between 10^5 and 10^6 $M_\odot$, are generally held to date back to the earliest stages of the formation of the Milky Way. Consequently, an absolute determination of cluster ages sets a lower limit for both the age of the Milky Way and the Universe. Moreover, the distribution of globular cluster ages can probe the overall modus operandi: Did the oldest stars in spiral galaxies form in a rapid burst, or was there a more protracted process, perhaps involving accretion of satellite systems (as in the Searle and Zinn model discussed in Chapter 4)? SIM Lite can illuminate this question by setting cluster distances on a more reliable foundation.

Traditionally, globular clusters are characterized as mini-starbursts, with a single-age stellar population. Recent observations indicate that a handful of the most massive systems (e.g., NGC2808, Piotto et al. 2007) have more complex star formation histories, possibly indicative of their origin as cores of stripped dwarf galaxies. Even those systems, however, have relatively simple color-magnitude diagrams (CMD), with a well-defined main sequence turnoff (MSTO) at $M_V \approx 4$ or ~ 0.85 $M_\odot$. Relative ages for globular clusters can be derived using a variety of techniques, including measuring the (vertical) offset between the MSTO and the HB or the (horizontal) offset between the MSTO and the base of the RGB. Those analyses show that most clusters are coeval, within the uncertainties (~±1.5 Gyr), with a handful of clusters that are a few Gyr younger (De Angeli et al. 2005).

Absolute age estimates, however, require matching the observed color-magnitude diagram against theoretical models (Figure 7-3), and therefore demand reliable distance estimates. Specifically, a change of $\delta m \approx 0.1$ magnitude in the absolute magnitude of the MSTO corresponds to $\delta\tau \approx 1.5$ Gyr.

Figure 7-3. Theoretical isochrones matched against ground-based photometry of the inner halo globular cluster NGC6652. (From Chaboyer et al. 2000). Cluster age is estimated by adjusting distance and reddening to attain a best fit. However, the near-degeneracy of these complicates this method. SIM Lite will circumvent this problem by directly measuring distance via trigonometric parallax.
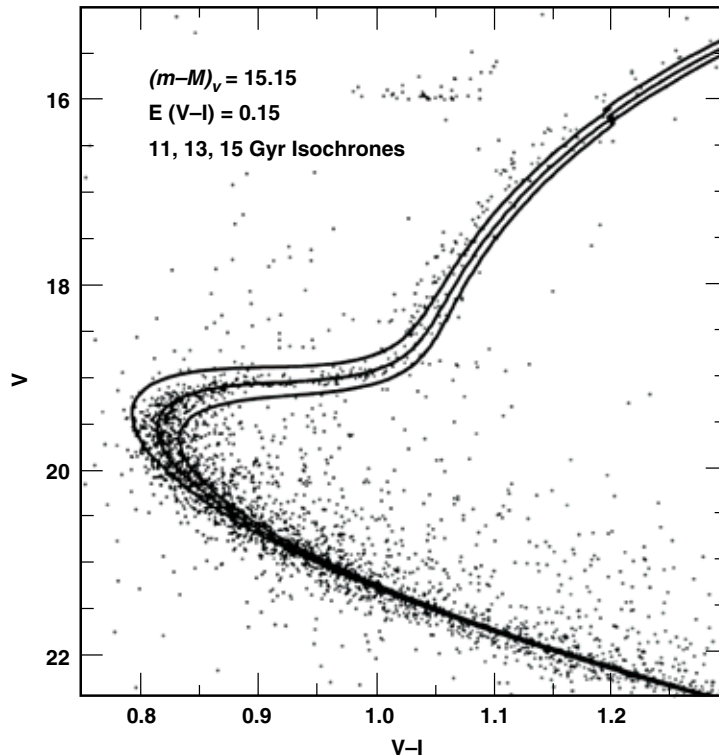
Expressed generally, if ε_τ is the fractional uncertainty in age, σ_τ/τ, and ε_d is the fractional uncertainty in distance, σ_d/d, then $\varepsilon_\tau \sim 2\varepsilon_d$.

It is clear that we will need to resolve age differences of 1 Gyr ($\varepsilon_\tau \approx 7$ percent) to obtain a better understanding of the early star-formation history of the Milky Way. That requirement in age resolution demands that we determine cluster distances to an accuracy of ~4 percent or better.

In the past, cluster distances have been estimated based on (M_V, [Fe/H]) relations derived for HB stars or RR Lyrae stars. Figures 7-1 and 7-2 show that those methods have formal random uncertainties of ~6 percent in distance, with potential systematic errors at comparable levels. Current estimates of cluster distances are therefore based primarily on the main sequence fitting technique, matching the observed

CMD either against local subdwarfs with known trigonometric parallax or directly against theoretical isochrones. Each variant has its own particular set of drawbacks.

Theoretical models offer a precise definition of the CMD from the RGB through the MSTO to the lower main sequence. However, the luminosities and effective temperatures generated in the computations need to be transformed to the observational plane via stellar atmosphere models, and inconsistencies in opacities or temperature distributions can lead to mismatches. Moreover, the exact treatment adopted for processes such as convective overshoot and heavy-element diffusion, as well as the adopted nuclear reaction rates, can lead to systematic errors in the isochrone predictions. As an example, theoretical isochrone fitting consistently predicted globular cluster ages of 14 to 17 Gyr in the mid-1990s (e.g., Vandenberg, Stetson, and Bolte 1996). In more recent years, following Hipparcos and the Wilkinson Microwave Anisotropy Probe (WMAP) estimate of 13.7 Gyr for the age of the Universe (Spergel et al. 2007), the models have been equally consistent in converging on an average age of ~12 Gyr (11.7 ±1.5 Gyr, Chaboyer 2001). In part, this change reflects improvements in our understanding of the physics of stellar interiors, yet these results also strongly suggest that this is one field where observations can drive the theory.

Empirical main sequence fitting has its own problems. Hipparcos provided improved parallaxes for the nearest subdwarfs, and laid the foundation for an extensive reexamination of cluster ages and distances (Reid 1997, 1998; Gratton et al. 1997, 2003). Those analyses provided much of the basis for the recent downward revision in mean age for the cluster system. However, the Hipparcos sample includes fewer than 20 subdwarfs with parallaxes measured to better than 10 percent. Those stars provide sparse coverage in (M_V, color, [Fe/H]), with the result that many clusters are calibrated against only three or four local subdwarfs. This leads to uncertainties of ±0.1 to 0.15 magnitudes in the distance modulus and ±1.5 to 2 Gyr in the age.

Both Gaia and SIM Lite offer means of addressing this problem. Gaia is well suited to supplementing and refining the sample of local subdwarf calibrators. With a formal mission accuracy of 8 to 21 μas for 6 < V < 15, Gaia can determine parallaxes accurate to better than 1 percent for K-type subdwarfs within 300 pc of the Sun, potentially increasing the census to include 1,000+ stars. As with RR Lyrae stars, SIM Lite has the capability to obtain higher accuracy parallaxes for a small subset of this sample, verifying the Gaia calibration. While these observations will lead to a much improved sample of local calibrators, a number of issues will remain. For example, local subdwarfs show a range of detailed elemental abundances, notably [α/Fe] ratios, and this could lead to a mismatch between calibrators and cluster. Moreover, any main sequence fitting technique requires that the cluster photometry be corrected for foreground reddening; this is a significant correction for many globular clusters, including M4 and NGC6397, the two nearest systems.

The best method of circumventing these complications would be to directly measure the trigonometric parallax of a star (or stars) in the globular cluster. The brightest stars in the nearer globular clusters, RGB stars and HB stars, have visual magnitudes in the range 12 < V < 14, and are therefore readily accessible to SIM Lite and even Gaia. Both missions plan to capitalize on this, measuring multiple stars in the accessible systems, and averaging the individual parallax measurements to derive higher-accuracy measurements for the parent clusters. Gaia expects to achieve parallax accuracies of 10 to 20 μas for the individual (mainly RGB) stars, corresponding to uncertainties of 10 to 20 percent in distance for a globular cluster at 10 kpc. In principle, one can combine observations of 5 to10 stars to derive cluster distances with improved accuracy, and Gaia aims to achieve ~8 μas accuracy, corresponding to 8 percent at 10 kpc. In practice, Hipparcos offers some vital lessons in this type of analysis: specifically, the parallax of 8.45 ±0.25 mas derived for the Pleiades (van Leeuwen 1999) is based on combining 1 to 2 mas accuracy Hipparcos astrometry of 55 cluster members; that result is at odds with other measurements (see also Section 6.3), and poses severe problems for stellar evolution theory. Soderblom et al.

(2005) have demonstrated that astrometry of three cluster members with the fine-guidance sensors on the Hubble Space Telescope yields a mean parallax of 7.43 ±0.17 mas, consistent with the distances derived from orbital parallaxes (of Pleiades binaries [Pan, Shao, and Kulkarni 2004]) and from conventional main sequence fitting (Pinsonneault et al. 1998).

This Hipparcos Pleiades problem emphasizes the vital importance of understanding and controlling systematic errors before attempting to achieve gains in accuracy by combining separate measurements. SIM Lite has a clear advantage over Gaia in this respect. Not only are the measurements of individual stars more accurate, but those measurements are tied to the reference grid, providing a stringent test for hidden systematic errors.

SIM Lite will be used to measure parallaxes for six 14th-magnitude stars in each of the 35 globular clusters that lie within 12 kpc of the Sun. These observations, which require ~6.6 mission hours per cluster, will yield parallaxes accurate to 5 to 6 μas over the mission lifetime. The individual parallaxes can be combined to yield a mean cluster parallax matching the projected accuracy of the SIM Lite grid, ≈3.6 μas, or ~4 percent accuracy at 12 kpc. Thus, with an investment of ~230 hours over the course of its mission, SIM Lite can significantly tighten the constraints on the age distribution of the cluster system and set a new, improved benchmark for the oldest stars in the Milky Way.

7.3   Summary

A strong synergy exists between Gaia and SIM Lite for investigations of key characteristics of Population II and the early star-formation history of the Milky Way. Gaia will conduct an exhaustive census of local halo stars, specifically RR Lyrae stars and field subdwarfs, providing parallaxes accurate to 1 to 2 percent for stars within 1 kpc. Gaia also has the potential to measure distances to ~5 percent, and ages to ~10 percent, for the nearest globular clusters, given that the systematic errors can be well controlled. SIM Lite, in contrast, will enable high-accuracy measurements for a small, but representative, sample of field RR Lyrae stars and subdwarfs, verifying and refining the Gaia-based (M_V, [Fe/H]) calibration for those stars. SIM Lite offers the most reliable route to direct distance measurements for 30 to 40 globular clusters within ~12 kpc. The resultant ages will be accurate to better than 1.0 Gyr, resolving the detailed chronology of the first epoch of star formation in the Milky Way Galaxy.

References

Benedict, G. F. et al., 2002, AJ, 124, 1695.

Benedict, G. F. et al., 2007, AJ, 133, 1810.

Chaboyer, B., Sarajedini, A., Armandroff, T. E., 2001, AJ, 120, 3102.

Chaboyer, B., 2001, ASPC, 245, 162.

De Angeli, F. et al., 2005, AJ, 130, 116.

Freedman, W. F. and Madore, B. F., 1990, ApJ, 365, 186.

Gratton, R. G. et al., 1997, ApJ, 491, 749.

Gratton, R. G. et al., 2003, AandA, 408, 529.

Layden, A. C. et al., 1996, arXiv:astro-ph/9608108 v1.

Lindegren, L. et al., 2007, IAU Symposium 248, 217.

Pan, X., Shao, M., and Kulkarni, S. R., 2004, Nature, 427, 326.

Pinsonneault, M. H. et al., 1998, ApJ, 504, 170.

Piotto, G. S., 2007, ApJ, 661, L53.

Pickering, E. C., Bailey, S. I., 1895, ApJ, 2, 321.

Pritchet, C. and van den Bergh, S., 1987, ApJ, 316, 517.

Reid, I. N., 1997, AJ, 114, 161.

Reid, I. N., 1998, AJ, 115, 204.

Reid, I. N., 1999, ARAA, 37, 191.

Searle, L. and Zinn, R., 1978, ApJ, 225, 357.

Soderblom, D. et al., 2005, AJ, 129, 1616.

Spergel, D. N. et al., 2007, ApJS, 170, 377.

Thackeray, A. D. and Wesselink, A. J., 1953, MNASSA, 12, 33.

Vandenberg, D. A., Stetson, P. B., Bolte, M., 1996, ARAA, 34, 461.

Van Leeuwen, F., 1999, AandA, 341, L71.

Precision Stellar Astrophysics

What is the most massive star?

What is the stellar mass content of the Galaxy and how does it evolve?

How do stellar properties vary with metallicity and age?

What are the total luminosities and jet velocities of X-ray binary microquasars?

What are the masses of black holes and neutron stars and the neutron star equation of state?

Where are the sources in various radio-emitting stars?

What is the nature of the mass-loss process in asymptotic giant branch stars?

How will parallax distances improve applications of main-sequence fitting of star clusters?

What are the ages of metal-poor stars in the Milky Way halo and globular clusters?

Stellar Maps with SIM Lite

8

Todd J. Henry (GSU), **Douglas R. Gies** (GSU), **Wei-Chun Jao** (GSU), **Adric R. Riedel** (GSU), **John P. Subasavage** (GSU), **G. Fritz Benedict** (U Texas), **Hugh C. Harris** (USNO), **Philip A. Ianna** (U Virginia), **John R. Thorstensen** (Dartmouth College), **Charles Beichman** (NExScI), **Lisa Prato** (Lowell Observatory), and **Michal Simon** (SUNY Stony Brook)

ABSTRACT

Stellar astronomy is largely based on two maps, the Hertzsprung-Russell diagram and the mass-luminosity relation. Because of its reach into the Galaxy and its flexible observing modes, SIM Lite can make substantial contributions to both of these fundamental stellar maps for relatively rare objects, for which large populations are not found until the observing horizon reaches hundreds or thousands of pc. SIM Lite also effectively has no bright limit for stellar targets, so it can pinpoint the locations of every star seen by the naked eye in the night sky. Among these stars are the nearest massive O stars and bright supergiants that SIM Lite can place on the Hertzsprung-Russell diagram with unprecedented precision. Precise distances to the rare central stars of planetary nebulae can also be determined by SIM Lite, allowing them to be placed on the Hertzsprung-Russell diagram and permit the physics of their surrounding nebulae to be understood in more detail than ever before. For the mass-luminosity relation, SIM Lite will determine exquisitely accurate masses for stars in fundamental clusters, young stars, massive O stars, subdwarfs, and white dwarfs. With an extensive collection of high-accuracy masses from SIM Lite, astronomers will be able to "stress test" theoretical models of stars as never before.

8.1   SIM Lite and Gaia

Both the Gaia and SIM Lite efforts will revolutionize our understanding of stellar astrophysics via the Hertzsprung-Russell diagram (HRD) and the mass-luminosity relation (MLR), albeit in different ways. Gaia's high-precision astrometry of one billion sources will provide superb measurements of luminosities, temperatures, and masses of most of the stellar main sequence, giants, subdwarfs, and white dwarfs. More specifically, Gaia will determine distances to 1 percent for 10^7 stars having V = 6 to 13 within ~1 kpc (Lindegren et al. 2008).

SIM Lite provides complementary depth to Gaia's astrometry in specific regimes of both magnitude and distance. SIM Lite can effectively observe stars with V = −1.5 to 20, adding complementary phase space at bright magnitudes to Gaia's bright cutoff at V ~ 6 and making more accurate astrometric measurements at the faint end. Thus, only SIM Lite can pinpoint the locations of many of famous naked-eye stars in the night sky while opening up new territory for intrinsically faint stars at tens or hundreds of pc. For magnitudes 6 to 13, SIM Lite's wide-angle mode parallax precision of 4 µas is modestly better than Gaia's 8 µas, which will observe a far larger stellar sample. For magnitudes 14 to 20, SIM Lite's precision is 3 to 70 times better than Gaia's (Lindegren et al. 2008). By combining SIM Lite's somewhat better precision at moderate magnitudes with its increasingly better precision at faint magnitudes, accurate masses for suites of pre-main-sequence to solar-aged stars in specific clusters can be measured to reveal how the MLR changes over time. In addition, samples of intrinsically faint subdwarfs and white dwarfs can be targeted by SIM Lite for accurate mass measurements.

The combination of the ability to observe bright objects at all, and faint objects with superior precision, provides several niches important to stellar astronomy that only SIM Lite can explore. In what follows, we provide details of several astrophysical locations on the HRD and MLR stellar maps that are ideally suited for SIM Lite's attention. Table 8-1 lists representative parameters for the observational programs discussed below that could be carried out to define the HRD and MLR stellar maps. Ultimately, the goal

Table 8-1. Example SIM Lite observing programs for stellar maps.

Object	Mag Range	No. Objects	No. Visits per Object	Integration Time, s	Parallax Error, µas	Distance Reached	Error	Time, hrs
HRD Map								
O Stars	2–12	259	100	10	4–5	2.5 kpc	<1.3%	287
Supergiants	<6	219	80	10	4	2.5 kpc	<1.0%	195
PNe	<17	170	20–50	15–800	4–14	8.5 kpc	<10%	170
MLR Map								
M34 Cluster*	11–16	12	100	30	4–10	400 pc	<0.2%	10*
Young Stars	9–18	20	100	30–120	4–20	1.0 kpc	<2%	46
O Stars	2–12	20	100	10	4–5	1.0 kpc	<0.4%	22
Subdwarfs	8–14	15	100	30	4–5	100 pc	<0.1%	25
White Dwarfs	15–18	20	100	30–120	5–20	200 pc	<0.4%	66

* Representative cluster for the MLR work. Many clusters could be studied with SIM Lite with somewhat more or less observing time devoted to each depending on the number of binaries targeted and their brightnesses.

is to pinpoint each type of star's location on the HRD so that the effects of age, metallicity, rotation, magnetic fields, spots, convective overshoot, and meridional circulation can be disentangled. Then, matching stellar luminosities to masses via the MLR would permit us to fundamentally understand stellar astrophysics. A 1 percent threshold in luminosity and mass measurements is adopted for the discussion that follows because evolution within the main sequence causes the observed ranges in luminosity and mass to be at least 15 percent for a given stellar color or temperature (see Andersen 1991; Henry et al.

2006, Figure 2; and Figures 8-1 and 8-2 in this chapter). Given an understanding of the effects of age — which result in changing stellar radii, luminosities, and temperatures for stars of a given mass — it may be possible to reduce the scatter to 5 percent (Andersen 1991), at which point metallicity and other effects come into play. Thus, if we can determine both luminosities and masses to 1 percent, we have some hope of unravelling the many causes of the variations seen in stars.

8.2   The Hertzsprung-Russell Diagram

The HRD is generally the first figure a stellar astronomer considers to understand any given star in context. All different classes of stars appear on the HR diagram, including supergiants, asymptotic giant branch (AGB) stars, giants, subgiants, dwarfs, subdwarfs, and white dwarfs, as well as other exotic stars. The HRD maps a star's temperature and luminosity, which together determine the star's radius. However, placing a star on the HRD requires knowledge of its luminosity, and, hence, an accurate distance measurement. Trigonometric parallax is the most reliable and straightforward method of measuring stellar distances, and is usually the most accurate method as well. Ground-based parallax efforts have continued for 170 years (van Altena et al. 1995) with continuing efforts collected in the RECONS Parallax Database (Research Consortium on Nearby Stars, www.recons.org). In the past 20 years, space-based efforts have made great headway, both in sheer numbers (Hipparcos, ESA 1997; van Leeuwen 2008) and precision (Hubble Space Telescope, Benedict et al. 2007).

In the coming era, astrometric efforts like the Panoramic Survey Telescope and Rapid Response System (Pan-STARRS), the Large Synoptic Survey Telescope (LSST), and Gaia will measure parallaxes of millions of stars to unprecedented precision. Even so, SIM Lite has much to offer to the HRD because it can reach further into the Galaxy than any other instrument and will, therefore, measure accurate distances to rare, astrophysically compelling objects.

8.2.1   Massive Stars

The massive O* stars are among the brightest objects observed in galaxies and they play a central role in sculpting the interstellar medium (ISM) through their radiative and mechanical energy input, while driving the chemical enrichment of galaxies. With lives of only a few million years, they quickly burn through their fuel and explode catastrophically in supernovae. However, the fundamental parameters of these extraordinarily rare stars are still poorly known because they are generally found at large distances. Some O stars are found in clusters, but roughly 20 percent are runaways or field O stars, while many others are found in loose associations with poorly defined boundaries and distances; e.g., the Cep OB6 association has a 3 degree extent and a consequent 5 percent dispersion (1σ) in distance (Benedict et al. 2002).

The placement of massive stars in the HRD relies heavily at present on model atmosphere results that need thorough verification. Hot stars all have essentially the same colors in the optical/IR spectral range (after correcting for interstellar reddening), so estimates of their effective temperatures are made by comparing spectral line profiles with those calculated from sophisticated models (Repolust et al. 2004); the resulting temperature estimates are typically accurate to 5 percent. Their luminosities are determined from their absolute magnitudes and bolometric corrections (again derived from models for the estimated temperature), but reliable absolute magnitudes are only available for O stars in clusters where distances are known from other techniques. For the majority of O stars, the absolute magnitudes are

_____

For much of this discussion, B stars and Wolf-Rayet stars are also eligible. We concentrate here on the O stars for clarity.

estimated from spectral classification calibrations (based upon those stars in clusters) that typically result in 25 percent distance errors, consequently resulting in luminosity errors approaching 50 percent. Thus, the observational HRD only loosely constrains modern evolutionary models for massive stars (Herrero et al. 2007).

Progress will clearly require better distance measurements from accurate trigonometric parallaxes. Most O stars are very distant, and the Hipparcos mission produced reliable distance measurements for just one or two cases (Schröder et al. 2004). In fact, of the 265 stars of spectral type O listed in the Hipparcos catalog (ESA 1997; van Leeuwen 2007), 75 have zero or negative parallaxes. None of the remaining 190 stars have parallax errors better than 10 percent, and only six have errors better than 20 percent (several of those are not dwarfs). Both Gaia and SIM Lite will dramatically change the situation, but in quite different ways (Figure 8-1).

Gaia can measure 1 percent parallaxes to only 33 of 378 stars in the Galactic O star Catalog (Maíz-Apellániz et al. 2004) because the majority of O stars are either brighter than V = 6 or too far away. On the other hand, SIM Lite will determine distances accurate to 1 percent for 259 of the 378 catalog stars,

Figure 8-1. Characteristic regions of the HRD to be explored effectively by SIM Lite (blue) and Gaia (yellow), with error bars representative of current knowledge in the SIM Lite regions. Supergiants have been plotted using Hipparcos data for stars brighter than V = 6 with luminosity classes I or I/II. The mean parallax error is 37 percent for these stars. A representative sample of O stars is shown, although only six parallaxes are currently available with errors less than 20 percent; most errors are much larger. The 16 PNe central stars with parallaxes from Harris et al. (2007) are also shown, for which the average parallax error is 19 percent. Note that the representative error bars shown for O stars and PNe central stars are for the few stars for which any trigonometric parallax is known. Main sequence and giant branch data points represent stars from Hipparcos (van Leeuwen 2007 with updated 2008 data used) with distances less than 50 pc and errors less than 5 percent. Data for white dwarfs have been taken from Bergeron et al. (2001). Typically, objects extreme in the HRD are either very distant, very faint, or very bright. The precision and magnitude dynamic range of SIM Lite will reduce the error bars on those objects by factors of 10 to 20.
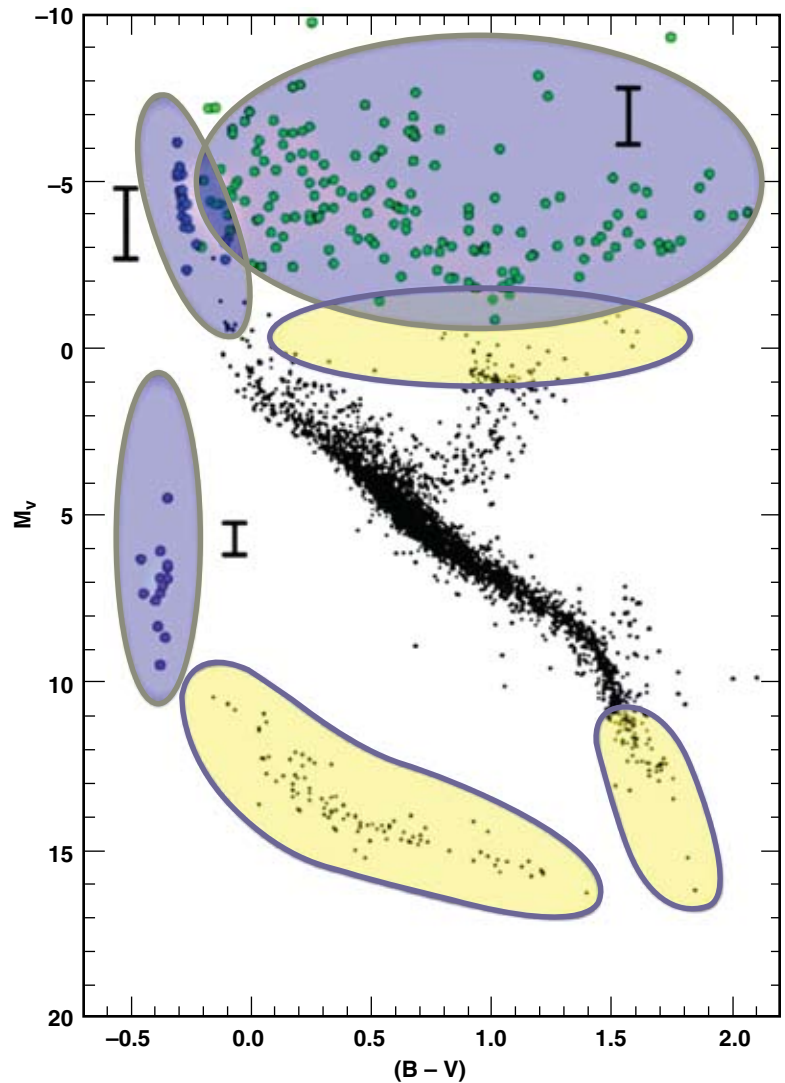
allowing us to select a larger and more astrophysically interesting group of massive stars that will allow us to test the predictions of evolutionary models. With 1 percent distances, we can accurately estimate ages of individual stars in young clusters and test models of star and cluster formation, find evidence of very faint, unresolved binary companions, and determine the ionizing flux from these stars that illuminates the surrounding ISM. Furthermore, accurate luminosities are crucial to testing the assumptions about interior structure, in particular the roles of rotation and meridional circulation (Ekström et al. 2008) that are important for the kinds of supernovae and compact remnants produced by massive stars. As a by-product, the distances to massive stars will reveal the spiral structure patterns in our quadrant of the Milky Way Galaxy.

8.2.2   Supergiants

SIM Lite can observe stars visible to the naked eye better than any other current or planned astrometric technique, including Gaia, which is not designed to measure stars brighter than V = 6. Found among the naked-eye stars are many famous supergiants, many of which are not in clusters, so fainter stars cannot be used as proxies for determining distances. With parallaxes accurate to 4 µas in wide-angle mode, SIM Lite will enable astronomers to (1) pinpoint supergiants' luminosities on the HRD, (2) understand how metallicities affect their positions, and (3) improve the wind-momentum luminosity relation (WLR) and flux-weighted gravity luminosity relation (FGLR) used to derive extragalactic distances. In addition, a bright-star parallax program with SIM Lite offers a fantastic public outreach opportunity not available to other efforts — astronomers will be able to tell anyone who might ask where the stars they can see are in our Galaxy.

Although Hipparcos did observe the brightest stars, many of the more distant supergiants have poorly determined distances. For example, among the 219 supergiants (luminosity classes I or I/II) brighter than V = 6 in the Hipparcos catalog, 167 have parallax errors greater than 10 percent and most are less than 1 kpc away (if the sizes of the Hipparcos parallaxes are correct). Some of these targets are among the famous stars seen in backyard skies the world over, including Alnitak (O9.5 Ia, π = 4.43 ±0.64 mas), Antares (M1.5 Iab, π = 5.89 ±1.00 mas), Betelgeuse (M2 Iab, π = 6.55 ±0.83 mas), Deneb (A2 Ia, π = 2.31 ±0.32 mas), and Rigel (B8 Iab, π = 3.78 ±0.34 mas), to name a few.* Improving the distance uncertainties from more than 10 percent to less than 1 percent would allow astronomers to understand the total flux contribution made by supergiants at various wavelengths, which has cascading effects on star-formation regions, dust creation, and the possible use of supergiants as standard candles for Galactic arm structure analyses. More specifically, knowing the distance to supergiants like Betelgeuse to 1 percent permits definitive checks on stellar radii in the late states of stellar evolution and what effects expanding layers have on binary star orbital migration and planetary habitable zone destruction.

Some supergiants have recently been used to determine distances to nearby galaxies through the WLR (Kudritzki et al. 1999) and the FGLR. These methodologies offer additional ways to determine extragalactic distances, at least to nearby galaxies. Kudritzki et al. (1999) selected 14 O/B-type supergiants to build the WLR, but only one of those stars has parallax determined to better than 10 percent. Therefore, the distances to these targets must be determined from their associations and presumed cluster memberships. On the other hand, the FGLR technique has been constructed using supergiants in the nearby galaxies NGC300 and NGC3621, which have distances determined using Cepheids (Freedman et al. 2001). In effect, no parallaxes have been used to develop these two relations, but this can be remedied

---

Parallax data are from the new Hipparcos reduction by van Leeuwen (2007). Betelgeuse has been recently observed by the Very Large Array at radio wavelengths, resulting in a trigonometric parallax of 5.07 ±1.10 mas (Harper et al. 2008).

with SIM Lite. For example, a V = 6 supergiant observed for 10 s 100 times will yield a parallax accurate to 4 µas, which is a factor of 50 to 100 better than currently possible. Although it is unclear whether or not either methodology will ultimately prove viable as a distance ladder rung, what SIM Lite may reveal by measuring accurate distances to a large sample of supergiants is not entirely known — perhaps an entirely new type of standard candle will appear, once hundreds of supergiants are examined with SIM Lite's exquisite capabilities.

8.2.3 Planetary Nebulae Central Stars

Distances to planetary nebulae (PNe) are important for understanding the physics of the nebulae, the evolutionary state of the central stars (e.g., time since the ejection of material), and the space density and formation rate of PNe. At present, however, distances are notoriously uncertain, both in terms of systematic effects and for individual nebulae. Only 16 have measured trigonometric parallaxes (Benedict et al. 2003; Harris et al. 2007), and distances are large enough for most PNe that ground-based parallax errors (~300 µas) and HST errors (~200 µas) will preclude many more being measured until Gaia or SIM Lite. There are roughly 2000 PNe known in the Galaxy, many in and around the Galactic bulge that are particularly good targets for SIM Lite. They include a large variety of types, and understanding these different types adds scientific importance to getting accurate distances to many PNe. A goal might be to have distances with 10 percent errors or better to 300 PNe by the time Gaia and SIM Lite complete their observations.

Error estimates vs. magnitude from Lindegren et al. (2008) indicate that Gaia might be used to acquire parallaxes with 10 percent errors to about 190 PNe, using the Acker et al. (1992) catalog for central star magnitudes and estimated distances. SIM Lite can reach 10 percent error at a distance of 8 kpc at V = 16 in ~48 min total mission time (20 visits, 110 s integrations), which expands the target sample considerably. There are 170 PNe with 16 < V < 18, for which Gaia is expected to have distance errors of 20 to 30 percent — these are potentially excellent targets for SIM Lite that would double the available sample of PNe with distance measurements accurate to 10 percent or better.

One additional product of SIM Lite astrometric data will be the identification of binary motion for PNe central stars. One theory of the origin of bipolar symmetry seen in many PNe argues that binary central stars are common. The accuracy of SIM Lite data and a planned cadence for SIM Lite visits will offer an advantage over Gaia for identifying (or placing upper limits on) binary motion for a sample of PNe central stars. A selected sample of bright (V ~ 15) central stars in bipolar PNe with an increased number of SIM Lite visits will provide constraints on the frequency of binaries: observing 140 bright PNe central stars 50 times each with SIM Lite can be accomplished in 140 hours of observing time. As a bonus, accurate proper motions for very faint PNe stars would permit the identification of halo objects and provide bench-marks for historical enrichment due to evolution of the oldest Galactic stars.

8.3   The Mass-Luminosity Relation

Mass is arguably the single most important characteristic of a star, as it determines a star's size and color, as well as how long it will live and what fuels it will burn. Knowing the masses of main sequence stars answers basic astrophysical questions such as: What is the biggest star? What is the smallest star? How is the mass of a stellar nursery partitioned into various types of stars? What is the mass content of the Galaxy and how does it evolve? To answer these and other fundamental questions, the ultimate goal is to determine masses to 1 percent accuracy, which allows us to challenge stellar models more severely than ever before.

The MLR's broad appeal is its applicability to many areas of astronomy. A reliable MLR lets us use a star's luminosity as a proxy for its mass, which is a valuable commodity in radial velocity, astrometric, cataclysmic binary, and extrasolar planet work. In the broader Galactic context, an accurate MLR provides benchmarks for comparisons to objects in stellar clusters, and allows us to estimate just how much of the "missing" mass is made up of the smallest stars. At the faint end of the stellar main sequence, the MLR is crucial for brown dwarf studies because measurement of a sufficiently small mass can demonstrate that a star is a bona fide brown dwarf. High-accuracy masses are needed because, as shown in Figure 8-2, the width of the main sequence on the MLR is 20 percent or more at a given luminosity. This is because, even though the individual stellar masses calculated to date are determined to 5 percent or better, they are of mixed pedigree in age and metallicity. SIM Lite will be a breakthrough mission for stellar mass determinations because it will be able to measure masses accurate to 1 percent in myriad environments and for a suite of different kinds of stars, as discussed below.

Figure 8-2. The mass-luminosity relation in 2008, using eclipsing binary data (open red points) from Andersen (1991) and others, supplemented with visual binary data (open blue points) from the SIM Science Team project, MASSIF, and others. Model curves for the MLR at the indicated ages and solar metallicity are shown, from Schaller et al. (1992) at high masses and Baraffe et al. (1998) at low masses. Note the spread in empirical mass determinations at a given luminosity throughout the main sequence, caused primarily by different ages and metallicities. SIM Lite's magnitude range from V = −1.5 to 20 enables binary star astrometry at the extremes of the MLR, including bright O dwarf and faint M dwarf binaries. In addition, most O binaries lie at great distances, requiring the high-fidelity parallaxes and resolving capability of SIM Lite's long baseline for accurate mass and luminosity measurements.
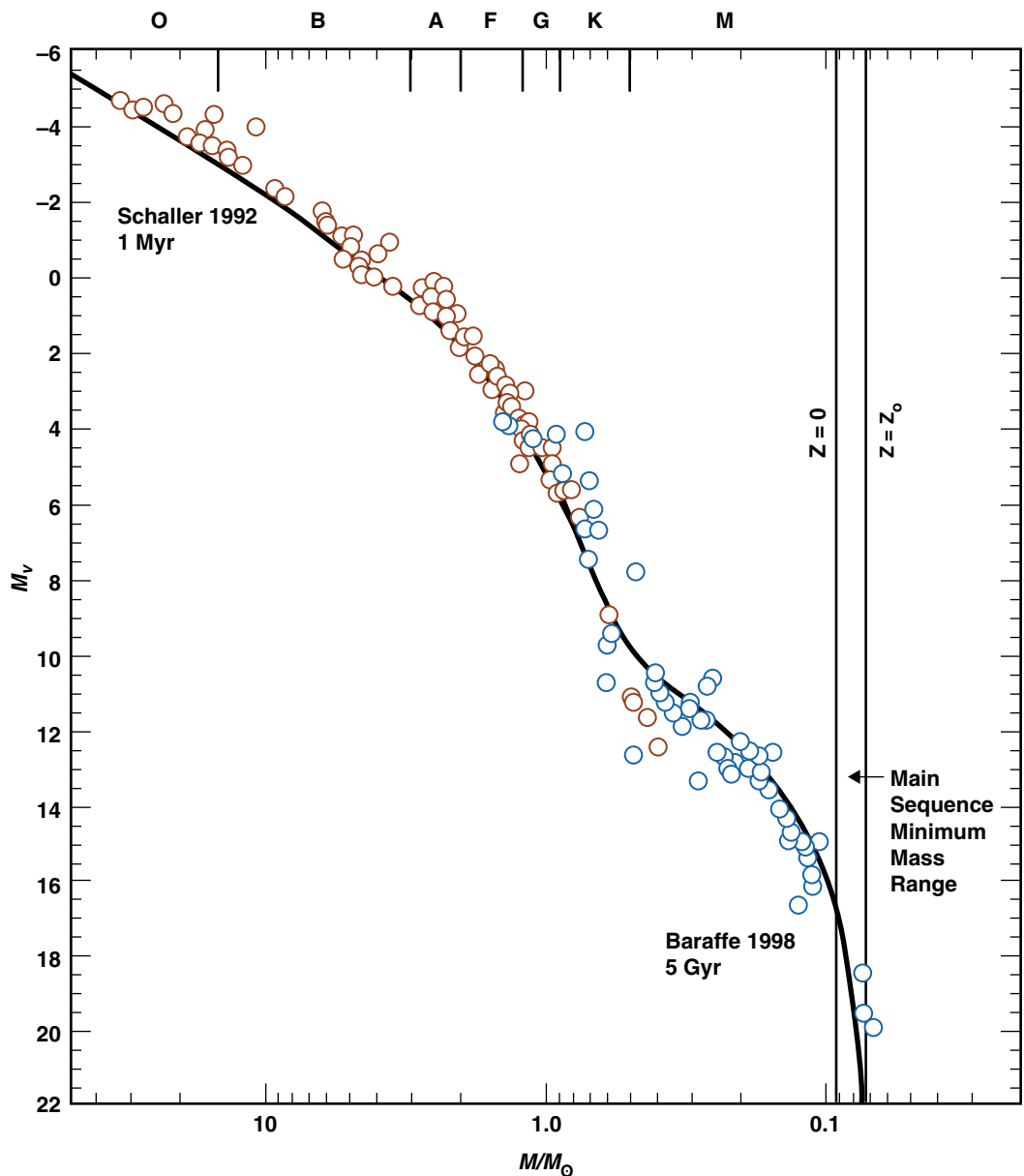
8.3.1 How SIM Lite Measures Masses

Typically, stellar mass estimates come from measurements of the orbital motions of binary stars. In particular, most accurate stellar masses have been inferred from studies of eclipsing spectroscopic binaries (Andersen 1991), but this method is severely limited for several important types of stars. At the highest masses, only a few known eclipsing systems contain O stars (Gies 2003), and many of these are interacting systems whose members may not be representative of single stars. At the lowest masses, stars are small, so few binaries eclipse and visual binaries must be used (Henry et al. 1999). Other rare but important types of evolved stars remain almost completely unmeasured.

To measure stellar masses, various combinations of imaging, interferometric, and radial velocity techniques are often used. Individual masses are typically computed via two paths: (1) by determining astrometrically the orbital inclination of the photocentric orbit of a double-lined spectroscopic binary (SB2), e.g., with SIM Lite, or (2) in the absence of high-quality radial velocities, resolving the system and measuring the relative orbit referenced to a grid of reference stars, also possible with SIM Lite. Resolution is particularly important for the MLR because the component luminosities must be measured to place the stars on the MLR (and on the HRD). To reach 1 percent mass accuracy for SB2s, an inclination precision of 0.2 percent is required for an orbit with $i = 45$ deg, assuming uncertainties in other orbital parameters do not dominate. For resolvable binaries, the minimum requirement for a 1 percent mass determination is a 0.33 percent distance measurement, which corresponds to 833 pc for SIM Lite's 4 µas wide-angle precision. Ideally, SB2s found in various target samples will be observed with SIM Lite to develop a well-stocked "toolbox" of MLRs determined for clusters of known age and metallicity; these MLRs will become the standards to which all stars can be compared.

The extraordinary abilities of SIM Lite allow us to both measure accurate distances to binary systems and resolve the systems into two stars. This allows us to pinpoint the locations of each component in the grid of reference stars and thereby determine individual masses. The diffraction limit of the SIM Lite 6-m interferometer operating at 0.55 µm is 10 mas. Given 80 spectral channels that can be used to compute fringe visibilities, we might expect to do somewhat better than the traditional diffraction limit, and simulations indicate that SIM Lite will be able to super-resolve systems with separations as small as 2 to 3 mas. SB2s that are resolved by SIM Lite will provide a wealth of redundancy in orbital elements, providing opportunities for increased mass precision and crosschecks.

For unresolved binaries, we can map the photocentric orbit to determine the all-important orbital inclination. For those that are not resolved, the SB2 orbits provide $M \sin^3(i)$, where i is the inclination angle (i.e., the angle between our line of sight and the normal to the orbital plane). The size of the photocentric orbit's semi-major axis is given by

$$\alpha = 19571 M_1^{1/3}(1+q)^{-2/3} \; p^{2/3} \frac{q-f}{1+f} d^{-1} \; \mu\text{as}$$

where M_1 is the mass of the primary star (in units of $M_\odot$), $q = M_2 / M_1$ is the mass ratio, p is the orbital period (days), $f = F_2 / F_1$ is the monochromatic flux ratio (related to the magnitude difference by $\log f = -0.4 \Delta V$), and d is the distance to the binary (pc). For SB2s measured astrometrically, the shape of the photocentric orbit yields the inclination, and the measured photocentric orbit semi-major axis potentially provides redundant information on the flux ratio f and distance d. Single-lined systems (SB1s) can also be targeted, but components' locations on the MLR will be less precise because assumptions must be made about the flux and mass ratios, which are not determined explicitly for the components. Overall, with its combination of exquisitely accurate astrometry, faint-magnitude limit, and flexible scheduling, SIM Lite will allow us to measure masses for classes of objects for which accurate masses are

scarce, such as pre-main-sequence stars, O stars, subdwarfs, and white dwarfs. These are representative examples of mass determinations that can be made with SIM Lite. Other classes of objects that might be targeted include stars with peculiar abundances, blue stragglers, subdwarf O and B (sdO/B) stars, X-ray binaries, cataclysmic binaries, and microquasars.

8.3.2 Star Clusters: MLRs for the Toolbox

Open-star clusters are excellent laboratories for the study of stellar astrophysics because they provide large numbers of stars with the same age and chemical composition. Mapping an ensemble of clusters to a grid of compositions, ages, and kinematics would lead to a greater understanding of star formation, chemical evolution, and abundance gradients in the Galaxy. To date, the only cluster for which an MLR has been determined is the Hyades (Torres et al. 1997). However, the Hyades MLR extends only from 2.4 to 0.8 $M_\odot$ with mass errors of 5 to 10 percent. This MLR is insufficient for critical tests of the models and does not include the smallest stars, for which the age and metallicity effects are most pronounced. SIM Lite's great accuracy is needed to reduce these errors to the 1 percent level needed for meaningful analyses.

The Hyades is a local, relatively old cluster. At the other age extreme is the Trapezium association in Orion. The Trapezium has been beyond the reach of precise trigonometric parallax measurements from the ground or with Hipparcos, with errors of 10 percent (translating to 20 percent luminosity errors and 30 percent mass errors, at best). Recently, VLBI work has provided a distance of 414 ± 7 pc (Menten et al. 2007), or an error of only 1.7 percent, at least for the four stars targeted in the Trapezium region. At roughly 10 times the distance of the Hyades, SIM Lite can measure hundreds of parallaxes for stars in the Orion Complex, while allowing accurate masses to be determined for selected binaries. The Hyades and Orion are but two of several fundamental clusters within the reach of SIM Lite, some of which are listed in Table 8-2 in order of their estimated distances.

Table 8-2. Binary systems, observable by SIM Lite, in fundamental stellar clusters containing binaries with orbital periods of 2.5 years. Binary systems in which component masses can be measured accurately (~1 percent) by Gaia are shaded in yellow. Those that are only reachable by SIM Lite for 1 percent masses are shaded in blue. SIM's high accuracy, especially at faint magnitudes, brings a wealth of clusters into reach for accurate masses. Particularly noteworthy are the Orion and M67 clusters, which span a factor of 1000 in age.

Mass, $M_\odot$ M_v			A Star Primary 1.5 3.0	G Star Secondary 1.0 5.0	K Star Primary 0.7 7.5	M Star Secondary 0.4 11.0
Cluster	**Est Dist, pc**	**Est Age, Myr**	**V mag Pri+Sec**	**Semi-Major Axes Rel/Phot, mas**	**V mag Pri+Sec**	**Semi-Major Axes Rel/Phot, mas**
Hyades	45	630	6.3 + 8.3	55.6 / 14.6	10.8 + 14.3	42.3 / 13.7
TW Hydrae	55	10	6.7 + 8.7	45.5 / 12.0	11.2 + 14.7	34.6 / 11.2
Pleiades	135	80	8.7 + 10.7	18.5 / 4.9	13.2 + 16.7	14.1 / 4..6
IC2602	160	20	9.0 + 11.0	15.6 / 4.1	13.5 + 17.0	11.9 / 3.9
IC2391	160	40	9.0 + 11.0	15.6 / 4.1	13.5 + 17.0	11.9 / 3.9
NGC6774	200	2000	9.5 + 11.5	12.5 / 3.3	14.0 + 17.5	9.5 / 3.1
M7	240	220	9.9 + 11.9	10.4 / 2.7	14.4 + 17.9	7.9 / 2.6
NGC0752	360	2700	10.8 + 12.8	6.9 / 1.8	15.3 + 18.8	5.3 / 1.7
M34	400	250	11.0 + 13.0	6.3 / 1.6	15.5 + 19.0	4.8 / 1.5
Orion	450	5	11.3 + 13.3	5.6 / 1.5	15.8 + 19.3	4.2 / 1.4
NGC3532	500	300	11.5 + 13.5	5.0 / 1.3	16.0 + 19.5	3.8 / 1.2
M35	700	150	12.2 + 14.2	3.6 / 0.9	16.7 + 20.2	2.7 / 0.9
M67	800	5000	—	—	17.0 + 20.5	2.4 / 0.8

The Hyades cluster, several stars in the Pleiades, and a few stars in TW Hydrae currently have reliable parallaxes. Gaia will provide parallaxes good to 1 percent out to 1.2 kpc. Assuming a large enough number of observations and sufficient orbital coverage, Gaia should also determine photocentric (unresolved) binary orbits to similar precision. To reach 1 percent precision in the masses, however, both the parallax and orbital semi-major axis must be known to 0.33 percent because the semi-major axis in AU enters as the cube when determining masses using Kepler's Law.*

In Table 8-2, we outline the characteristics of two hypothetical binary pairs in several clusters of interest, including an A/G pair and a K/M pair (no A stars remain in M67). In each case, we assume orbital periods of 2.5 years to allow both Gaia and SIM Lite to map each system through two complete orbits. We assume identical parallax and semi-major axis errors for a binary observed with a given mission, with Gaia errors of 8 to 55 μas for V = 6 to 17 and 4 μas uniformly for SIM Lite. For SIM Lite, fainter targets require longer observing times, but 4 μas can be reached on a V = 17 target with 32 hours of mission time. As a baseline, we assume no errors in orbital period and fractional mass, as well as no error in translation from a photocentric orbit to a relative orbit.

In the Hyades, Gaia can measure masses to 0.1 percent for both the A/G and K/M pairs, while SIM Lite produces errors half as large. In the old cluster NGC6774 at 200 pc, Gaia's mass errors for the A/G binary are 0.5 percent and for the K/M binary 0.9 percent, again assuming no errors other than those in parallax and photocentric semi-major axis. SIM Lite measures masses with errors of 0.3 percent for both pairs. Gaia's mass precision deteriorates beyond 200 pc because the parallax and photocentric orbit errors become significant, and the K/M binaries become faint. In the crucial Orion complex at 450 pc, mass errors for the pairs are 1.2 percent and 5.2 percent for Gaia, but only 0.6 percent in both cases for SIM Lite.

An important binary in Orion illustrates SIM Lite's broad power clearly: θ^1 Ori C is an O7V + B2V pair with an orbital period of 26 ±13 years and semi-major axis of 41 ±14 mas (Patience et al. 2008). With V = 5.1, Gaia cannot observe this important system because it is too bright, while SIM Lite can determine the parallax to 0.2 percent (and luminosity to 0.4 percent), resolve the pair easily, and map a portion of the orbit during its five-year mission.

Thus, beyond about 200 pc, SIM Lite can maintain the high-precision mass determinations necessary to challenge theoretical models throughout the main sequence, while Gaia cannot. Of special significance is that SIM Lite can resolve binaries with separations of a few mas and to differences in component fluxes of at least three magnitudes, so it can provide both the separations and luminosities of the components for all of the A/G pairs listed in Table 8-2 as well as most of the K/M pairs, none of which can be resolved with Gaia. Because of SIM Lite's flexible schedule, observations can also be timed to provide coverage near crucial periastron passages to provide the most accurate masses possible. Of special interest is SIM Lite's ability to produce a reliable MLR for ancient M67, whose constituent stars are all the same age and metallicity as the Sun. Overall, what is particularly compelling about this work is that the clusters span a range of 1000 in age, thereby providing a beautiful framework within which to study many aspects of stellar evolution once accurate distances and masses are available from SIM Lite.

For the numbers presented in Table 8-2, we provide the most straightforward example, assuming a dynamical orbit determined entirely by SIM Lite and resolution of the binary by SIM Lite or another technique. Of course, by combining astrometric and radial velocity data, some of the astrometric constraints can be relaxed. In practice, there is a complicated interplay between orbital elements (inclination, for example) determined using a combination of techniques to derive orbital period, relative semi-major axis on the sky, parallax, proper motion, and fractional mass necessary for individual component mass determinations. A complete discussion of these factors is beyond the scope of this chapter.

8.3.3 Pre-Main Sequence Stars

With the exception of solar-mass objects, evolution models of stars from birth to the zero-age main sequence are poorly calibrated (Schaefer et al. 2008 and references therein). Binaries in star formation regions provide an opportunity to determine precise dynamical masses in low-mass, young star systems (e.g., Prato et al. 2002; Hillenbrand and White 2004). Fewer than 100 pre-main-sequence (PMS) spectroscopic binaries (SBs) are currently known (Melo et al. 2001), and even fewer eclipsing PMS SBs have been identified (Stassun et al. 2007). Models of young star evolution would be revolutionized by mass determinations of a few dozen binaries among the youngest T Tauri star populations that are accurate to a few percent, via SIM Lite.

Unfortunately, only a small handful of young stars are at once close enough to determine precise radial velocities of the components and yet widely separated and bright enough to be accessible to ground-based interferometry (Boden et al. 2007; Schaefer et al. 2008). SIM Lite is the only facility that has the capacity to accurately determine the orbit of the photocenter of the shortest period (<100 days) T Tauri star SBs, providing the system inclinations and, hence, absolute component masses to the required few percent precision for meaningful calibration of evolutionary tracks.

About three dozen PMS SB1 and SB2 systems are currently known with P <100 days, including many in the Taurus, Ophiuchus, and TW Hya regions within 150 pc. Gaia will do well on the brighter systems, but only SIM Lite can provide the masses for PMS systems of low mass, where young star models show the greatest variations. Finally, a significant advantage of SIM Lite over other techniques for PMS binaries, many of which do not provide accurate radial velocity measurements, is its ability to resolve binaries with separations of a few mas, thereby placing both components in a grid of reference stars so that individual masses can be measured.

8.3.4 Massive Stars

Although O stars are rare, as a group they are known to contain many binaries, with a multiplicity fraction of 75 percent for those found in clusters or associations (Mason et al. 1998). Many of those that are found to be SB2s also eclipse, which would be ideal for mass determinations except that such binaries are usually so close that they may have physically interacted in the past. Thus, mass estimates for such systems may tell us more about the evolutionary mass exchange histories of binaries rather than providing fundamental data to calibrate the properties of stars in general. For non-interacting, non-eclipsing O star binaries, masses are determined by supplementing an SB2 orbit with a precisely determined orbital inclination, or by resolving the binary and finding the shape of the orbit. Because O stars are rare and consequently distant, such measurements will require the precise astrometric and interferometric measurements of SIM Lite.

There are many spectroscopic binaries containing massive stars where observations of the photocentric orbit would lead directly to masses. One example is the system CygOB2 #8A, which consists of O5.5 I and O6 stars in a 22-day orbit (De Becker et al. 2004). The system resides in the Cyg OB2 association at a distance of 1.5 kpc, and the expected photocenter semi-major axis is predicted to be 59 μas, much larger than the typical single observation position error of ≈16 μas for wide-angle measurements with SIM Lite. A more challenging object is HD93205 in the Carina Nebula region at a distance of 2.6 kpc. This is a 6 d binary consisting of O3 V and O8 V stars (Antokhina et al. 2000), and the maximum photocenter motion will be in the range of 9 to16 μas (depending on the adopted flux ratio). SIM Lite will be uniquely suited to obtain the orbital inclination and distance of this system and to peg the mass of a star at the top of the main sequence (~45 $M_\odot$ for an O3 V star).

SIM Lite will also provide insight into the evolutionary descendants of massive stars. The most massive stars develop strong stellar winds early in life that can remove their outer hydrogen layers and create a helium-rich Wolf-Rayet (WR) star. SIM Lite positional measurements of the binary WR 22 (WN7 + O9 III; Schweickhardt et al. 1999) will show a maximum positional displacement of 45 μas over its 80-day orbit and will lead to secure mass estimates for both stars (the mass of the WR star is ~55 ±7 $M_\odot$).

SIM Lite will also play a key role in determining masses of low-luminosity companions of massive stars. Many interacting binaries experience mass and angular momentum transfer that lead to the spin up of the mass-gainer and the loss of the donor star's envelope. Eventually, the donor may appear as a stripped-down helium star or white dwarf. The nearby B7 V star Regulus is one example of a rapid rotator that was recently found to have a faint binary companion (probably a low-mass white dwarf; Gies et al. 2008). SIM Lite observations of the photocenter motion of Regulus may reveal orbital excursions as large as 1200 μas, and these would lead directly to the mass of the faint companion (note that Gaia cannot observe Regulus at V = 1.4).

Finally, we know that many massive binaries are also members of triple or higher multiplicity systems, and with its resolving capabilities, SIM Lite can give us the complete picture of both wide (mas) and close (μas) members of hierarchical systems. Ultimately, SIM Lite will finally be able to tell astronomers what the upper mass limit is for a star.

8.3.5   Subdwarfs

Subdwarfs are Galactic fossils that presumably comprise the bulk of the halo, and are crucial touchstones of the star-formation and metal-enrichment histories of the Milky Way. The local dearth of subdwarfs and their intrinsic faintness make them difficult to characterize, unlike their disk counterparts. Because of these challenges, their masses are barely measured, but would be of great use in studies of the Galactic halo, globular clusters, and low-metallicity stars in general.

The MLR for main-sequence stars has been studied in detail for decades, but constructing the MLR for the neglected metal-poor stars has barely begun. There are currently only three subdwarf systems (defined here to have [Fe/H] ≤ –0.5) with mass measurements: μ Cas AB (Drummond et al. 1995) with [Fe/H] = –0.71 (Karaali et al. 2003); HD157948 AB with [Fe/H] = –0.5 (Horch et al. 2005); and HD195987 AB with [Fe/H] = –0.5 (Torres et al. 2002). Clearly, there remains much work to do in calibrating the empirical MLR of metal-poor subdwarfs.

Utilizing the unique combination of precise astrometry and high-resolution capability of SIM Lite, we can expect to map many more subdwarf orbits. Prime examples are 15 F- and G-type low-metallicity (–2.5 ≤ [Fe/H] < –0.5) SB2 systems from Goldberg et al. (2002) that have $a \sin(i) > 1.0$ mas and orbital periods less than four years. Roughly 100 additional SB1 systems from Latham et al. (2002) with period less than three years could also be targeted by SIM Lite to increase the total number of resolved binaries. Because of the combination of faint magnitudes and small separations, no other current astrometric technique can resolve either set of binaries, but SIM Lite can. A typical F/G binary pair with orbital period 2.5 years and semi-major axis 22 mas would yield masses with errors less than 1 percent, assuming SIM Lite can measure the semi-major axis to 0.1 mas. To expand dynamical mass measurements to lower masses, we need to survey the ~120 nearby K- and M-type subdwarfs within 60 pc. Optical speckle surveys (Jao et al. 2008, submitted) fail to detect binaries with appropriate separations for mass determinations because at the comparatively large distances of the subdwarfs, optical speckle cannot reach to the mas separations needed for short (less than a decade) orbits. Gaia should reveal which subdwarfs have photocentric orbits appropriate for mass determinations, but only SIM Lite can resolve the systems and provide the high-fidelity mass measurements needed to test theoretical models for low-metallicity stars.

8.3.6   White Dwarfs

White dwarf (WD) research has far-reaching implications in diverse astronomical fields, from cosmology to Galactic halo populations to nearby star studies. Gaia will undoubtedly reveal many systems containing WDs that are appropriate for mass determinations, but SIM Lite's ability to measure masses with exquisite precision reveals a niche that is unique to SIM Lite — understanding the theoretical mass-radius relation for WDs. From the youngest WDs found as central stars in PNe to the oldest WDs from the halo, SIM Lite's reach brings unusual objects into reach for mass determinations of this class of objects with various compositions and ages.

Nearly every aspect of WD research relies on the theoretical mass-radius relation for WDs. This relationship depends on the internal composition of the WD, whether it is a pure or mixed combination of He, C, N, Ne, or Mg. Ideally, WD masses need to be known to 1 percent (or better) to stress test the mass-radius relation to reveal the true chemical makeup of WDs, and permit us to discriminate, for example, between different hydrogen envelope masses (Jordan 2007).

To date, empirical masses to support the theoretical mass-radius relationship are severely limited — only three WDs have dynamical mass measurements known to better than 5 percent: Sirius B, Procyon B, and 40 Eri B (Provencal et al. 2002). Other WDs with masses, such as the remaining 18 WDs that populate the mass-radius relation in Figure 13 of Provencal et al. (2002), have masses gleaned from gravitational redshift studies of common proper motion systems (in which a companion is used to determine systemic parameters) or have spectroscopically inferred masses. In general, such mass determinations are rather poorly constrained, with errors of 10 percent or more.

It is important to obtain precise dynamical masses for a much larger number of WDs to better test and validate the theoretical mass-radius relation that is vital to WD modeling. Empirical determinations of dynamical masses in visual, spectroscopic, or interferometric binaries for WDs will better constrain the relative proportions of internal compositions of WDs found in the solar neighborhood. This information may then be applied to pulsating ZZ Ceti stars, whose pulsation modes are used to determine details of the internal structure.

A combined Gaia (for detection) and SIM Lite (for resolution and high precision) effort will likely provide a wealth of additional WD masses that could be used to map out the mass-radius relation for WDs. Through ongoing studies of double-degenerate systems with Hubble Space Telescope's fine-guidance sensors, eight systems have already been identified that might provide masses accurate to 1 percent when examined with SIM Lite. At separations of a few to tens of mas, these systems, as well as many more detected by Gaia, can be resolved by SIM Lite. Hence, SIM Lite's measurements will play a crucial role in populating the mass-radius diagram with multiple empirical checks of the theoretical mass-radius relation. These checks will reveal new insights into the internal structures of WDs and answer questions about WD compositions that have long eluded astronomers.

8.4 Summary

SIM Lite and Gaia are clearly complementary observatories for studies of stellar astrophysics. As shown in Figure 8-1, with its breadth of coverage Gaia will effectively complete our understanding of the HRD for common stars, while SIM Lite will target the rare supergiants, O stars, and PNe central stars. Other truly rare stellar phenomena, such as X-ray binaries and their precursors, will require the laser accuracy of SIM Lite simply because they are not common enough to have nearby representatives. SIM Lite's exquisite accuracy is also crucial to mapping the MLR in fundamental stellar clusters such as Orion and M67, where individual masses can be measured to 1 percent only by SIM Lite. Binaries containing pre-main sequence stars, O stars, subdwarfs, and white dwarfs are superb targets for SIM

Lite, which can not only measure their distances and orbits but resolve the systems into components to provide individual masses — there is much to be said for mapping a binary's orbit and resolving the system with the same instrument to minimize systematic translation errors between observing techniques. Finally, there is little doubt that Gaia will be a pathfinder mission for SIM Lite, much like the Palomar Schmidt was for the 200-inch telescope. New and extraordinary objects will be revealed by Gaia, and breakthroughs in stellar astrophysics will be made when SIM Lite's µas astrometry capabilities are applied.

References

Acker, A., Ochsenbein, F., Stenholm, B., Tylenda, R., Marcout, J., and Schohn, C., 1992, Strasbourg-ESO Catalogue of Galactic Planetary Nebulae.

Andersen, J., 1991, A&A Reviews, 3, 91.

Antokhina, E. A., Moffat, A. F. J., Antokhin, I. I., Bertrand, J.-F., and Lamontagne, R., 2000, ApJ, 529, 463.

Baraffe, I., Chabrier, G., Allard, F., and Hauschildt, P. H., 1998, A&A, 337, 403.

Benedict, G. F. et al., 2002, AJ, 124, 1695.

Benedict, G. F. et al., 2003, AJ, 126, 2549.

Benedict, G. F. et al., 2007, AJ, 133, 1810.

Bergeron, P., Leggett, S. K., and Ruiz, M. T., 2001, ApJS, 133, 413.

Boden, A. F. et al., 2007, ApJ, 670, 1214.

De Becker, M., Rauw, G., and Manfroid, J., 2004, A&A, 424, L39.

Drummond, J. D. et al., 1995, ApJ, 450, 380.

ESA, 1997, VizieR Online Data Catalog, 1239, 0.

Ekström, S., Meynet, G., Maeder, A., and Barblan, F., 2008, A&A, 478, 467.

Gies, D. R., 2003, in A Massive Star Odyssey: From Main Sequence to Supernova (Proc. IAU Symp. 212), ed. van der Hucht, K., Herrero, A., and Esteban, C. (San Francisco: ASP), 91.

Gies, D. R. et al., 2008, ApJ, 682, L117.

Goldberg, D. et al., 2002, AJ, 124, 1132.

Harper, G. M., Brown, A., and Guinan, E. F., 2008, AJ, 135, 1430.

Harris, H. C. et al., 2007, AJ, 133, 631.

Henry, T. J. et al., 2006, AJ, 132, 2360.

Henry, T. J. et al., 1999, ApJ, 512, 864.

Herrero, A., Simon-Díaz, S., Najarro, F., and Ribas, I., 2007, in Massive Stars in Interacting Binaries (ASP Conf. Ser. 367), ed. St-Louis, N. and Moffat, A. F. J. (San Francisco: ASP), 67.

Hillenbrand, L. A. and White, R. J., 2004, ApJ, 604, 741.

Horch, E. P. et al., 2005, Astrometry in the Age of the Next Generation of Large Telescopes, ASP Conference Series, vol. 338, Proceedings of a meeting held 18–20 October 2004 at Lowell Observatory, Flagstaff, Arizona, USA. Ed. Seidelmann, P. K. and Monet, A. K. B., San Francisco: Astronomical Society of the Pacific, p. 90.

Jordan, S., 2007, 15th European Workshop on White Dwarfs, 372, 169.

Karaali, S. et al., 2003, MNRAS, 343, Issue 3, 1013.

Kudritzki, R. P. et al., 1999, A&A, 350, 970.

Latham, D. W. et al., 2002, AJ, 124, 1144.

Lindegren, L. et al. 2008, IAU Symposium 248, 217.

Mason, B. D., Gies, D. R., Hartkopf, W. I., Bagnuolo, W. G., Jr., ten Brummelaar, T., and McAlister, H. A., 1998, AJ, 115, 821.

Maz-Apellaniz, J., Walborn, N. R., Galue, H. A., and Wei, L. H., 2004, ApJS, 151, 103.

Melo, C. H. F., Covino, E., Alcala, J. M., and Torres, G., 2001, A&A, 378, 898.

Menten, K. M., Reid, M. J., Forbrich, J., and Brunthaler, A., 2007, A&A, 474, 515.

Patience, J. et al., 2008, ApJ, 674, L97.

Prato, L., Simon, M., Mazeh, T., McLean, I. S., Norman, D., and Zucker, S., 2002, ApJ, 569, 863.

Provencal, J. L., Shipman, H. L., Koester, D., Wesemael, F., and Bergeron, P. 2002, ApJ, 568, 324.

Repolust, T., Puls, J., and Herrero, A., 2004, A&A, 415, 349.

Schaefer, G. H., Simon, M., Prato, L., and Barman, T., 2008, AJ, 135, 1659.

Schaller, G., Schaerer, D., Meynet, G., and Maeder, A., 1992, A&AS, 96, 269.

Schröder, S. E., Kaper, L., Lamers, H. J. G. L. M., and Brown, A. G. A., 2004, A&A, 428, 149.

Schweickhardt, J., Schmutz, W., Stahl, O., Szeifert, Th., and Wolf, B., 1999, A&A, 347, 127.

Stassun, K. G., Mathieu, R. D., and Valenti, J. A., 2007, ApJ, 664, 1154.

Torres, G., Boden, A. F., Latham, D. W., Pan, M., and Stefanik, R. P., 2002, AJ, 124, 1716.

Torres, G., Stefanik, R. P., and Latham, D. W., 1997, ApJ, 485, 167.

van Altena, W. F., Lee, J. T. and Hoffeit, E. D., 1995, Catalogue of Trigonometric Parallaxes.

van Leeuwen, F., 2007, Hipparcos, the New Reduction of the Raw Data, Astrophysics and Space Sciences Library, 350, Springer, and updated data via Vizier in 2008.

9 Black Holes and Neutron Stars
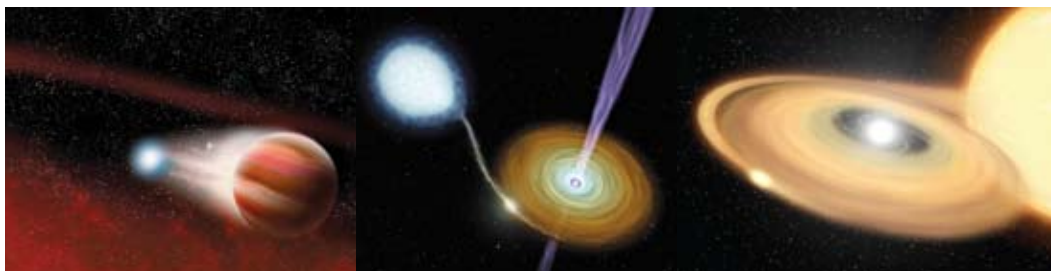
John A. Tomsick (UC Berkeley/SSL), **Stuart B. Shaklan** (JPL), and **Xiaopei Pan** (JPL)

ABSTRACT

Black holes and neutron stars are fascinating objects with great potential for testing physical theories in extreme conditions. The gravitational fields near these objects provide an opportunity for tests of General Relativity in the strong-field limit and the properties of matter at the remarkably high densities that exist within neutron stars are unknown. While many of these objects are in binary systems where accreting matter from the stellar companion provides a probe of the compact object, a main difficulty in making measurements that lead to definitive tests has been uncertainty about basic information such as distances to the sources, orientation of their binary orbits, and masses of the compact objects. Through astrometry, SIM Lite will, for the first time, be able to obtain precise distances and proper motions for dozens of these systems and will also be capable of mapping out orbital motion, leading to direct compact object mass measurements. Obtaining such information is critical for a wide variety of investigations that range from probing the space-time around the compact object to constraining the origin and evolution of the systems themselves.

9.1   Matter Under Extreme Conditions

The capability of SIM Lite for precise stellar astrometry will move the field of compact object astrophysics forward by providing measurements of quantities such as black hole and neutron star masses as well as distances to the systems that harbor compact objects. We expect that some of the most exciting results in this area will come from SIM Lite observations of X-ray binaries, which consist of a black hole or neutron star accreting matter from a stellar companion. Hundreds of these systems have been found in our Galaxy by X-ray satellites since the first one was discovered in the early 1960s (Giacconi et al. 1962), and a significant fraction of them are bright enough in the optical for SIM Lite to provide new constraints on these remarkable systems.

When we observe Galactic compact objects, we are probing the most extreme physical conditions in the Universe, providing the most rigorous tests of physical models as well as the opportunity to find new physical phenomena. For example, in discussing possible tests of General Relativity (GR) in the regime of strong gravity, it is often stated that the strongest gravitational potentials are found around black holes, and this is true whether one is talking about stellar mass or supermassive black holes. However, Psaltis (2008) points out that the relevant parameter for determining the "strength" of a gravitational field is the space-time curvature, and this quantity is a trillion times larger in the vicinity of a 10 $M_\odot$ black hole than it is for a 10^7 $M_\odot$ supermassive black hole. Thus, it is near the smaller compact objects (both black holes and neutron stars) where any deviations from GR due to strong gravity will be largest.

In addition to the great interest that these objects hold for gravitational studies, determining the properties of neutron star interiors is important for nuclear and particle physics. Although current measurement techniques still do not strongly constrain these properties, it is thought that the densities in neutron star cores may be as much as an order of magnitude above nuclear densities (Lattimer and Prakash 2007), making this the location of the densest material in the Universe and making it critical to determine what form matter takes at these densities. Extreme aspects of X-ray binaries include the interaction of accreting matter with very high neutron star magnetic fields (Coburn et al. 2002) as well as the relativistic jets that are very commonly seen streaming away from neutron stars and black holes (Fender 2006), though the details of their production are yet to be fully understood.

Through precision measurements of these systems, SIM Lite has the potential to address many of the questions that are currently the most difficult to answer. Determinations of the source luminosities, mass accretion rates, radii of neutron stars, sizes of accretion disks, and jet size-scales and velocities all depend on knowing the distances to these systems. While reliable distances to most X-ray binaries have been very difficult to obtain, SIM Lite will provide parallax distance measurements for any system in the Galaxy that is sufficiently bright in the optical. Through orbital measurements, SIM Lite can directly address the question of the properties of matter inside neutron stars by measuring their masses, and both neutron star and black hole studies will benefit from SIM Lite's determination of binary inclinations, which is typically the largest contributor to the error on the compact object's mass.

While distances and masses will be a major step forward, SIM Lite will also measure the proper motions of these systems, which will help to determine their birthplaces as well as answer the question of whether a supernova is required for the formation of a black hole. For systems with radio jets or other sources of radio emission, SIM Lite will provide an absolute reference frame that will constrain where in the system the radio emission originates. For this application and also for the study of other variable phenomena in these systems, it is notable that the flexible scheduling (e.g., the possibility of "target of opportunity" observations) that SIM Lite allows is critical. In the following material, we discuss in more detail several of the investigations that SIM Lite will enable.

9.2 Overview of SIM Lite Targets

Most of the currently planned SIM Lite targets we discuss in this chapter are X-ray binaries. These types of systems are usually divided into low-mass X-ray binaries (LMXBs), which have K- or M-type companions and masses below 1 $M_\odot$, and high-mass X-ray binaries (HMXBs), which have massive O- or B-type companions. Systems that do not fall into these categories (e.g., those with A- or F-type companions) are often called intermediate-mass X-ray binaries (IMXBs), and LMXBs may descend from IMXBs through a phase of thermal mass transfer (Tauris and van den Heuvel 2006). Selecting the best targets for SIM Lite to observe depends on several considerations, including the optical brightness of the targets, their distances, the sizes of their binary orbits, and the level of scientific interest.

Generally, the HMXBs are the best for orbital measurements due to their optical brightness and large orbits. HMXB orbital periods are typically several days to months compared to hours to a couple of days for LMXBs. In Unwin et al. (2008), we list 16 neutron star HMXBs with orbital astrometric signatures (i.e., the angular size of the semi-major axis of the optical companion's orbit) between 4 μas and 1 mas. Half of these have signatures >40 μas. Such signatures are large enough to allow for a precise determination of the binary orbit with SIM Lite (see Figure 9-1). In addition to the neutron star sources, there are black hole HMXBs, such as Cygnus X-1 (see Section 9.6), SS433, and V4641 Sgr, for which we expect SIM Lite to determine their orbits.

Figure 9-1. Expected astrometric signature from orbital motion vs. V-band magnitude for neutron star (white circles) and black hole (black circles) X-ray binaries. The dashed blue line shows the threshold for detection of orbital motion in 40 hours of SIM Lite mission time. The threshold is defined as the level at which the system's semi-major axis is 10 times larger than the astrometric noise per observation (i.e., the single-measurement accuracy) divided by the square root of the number of observations.
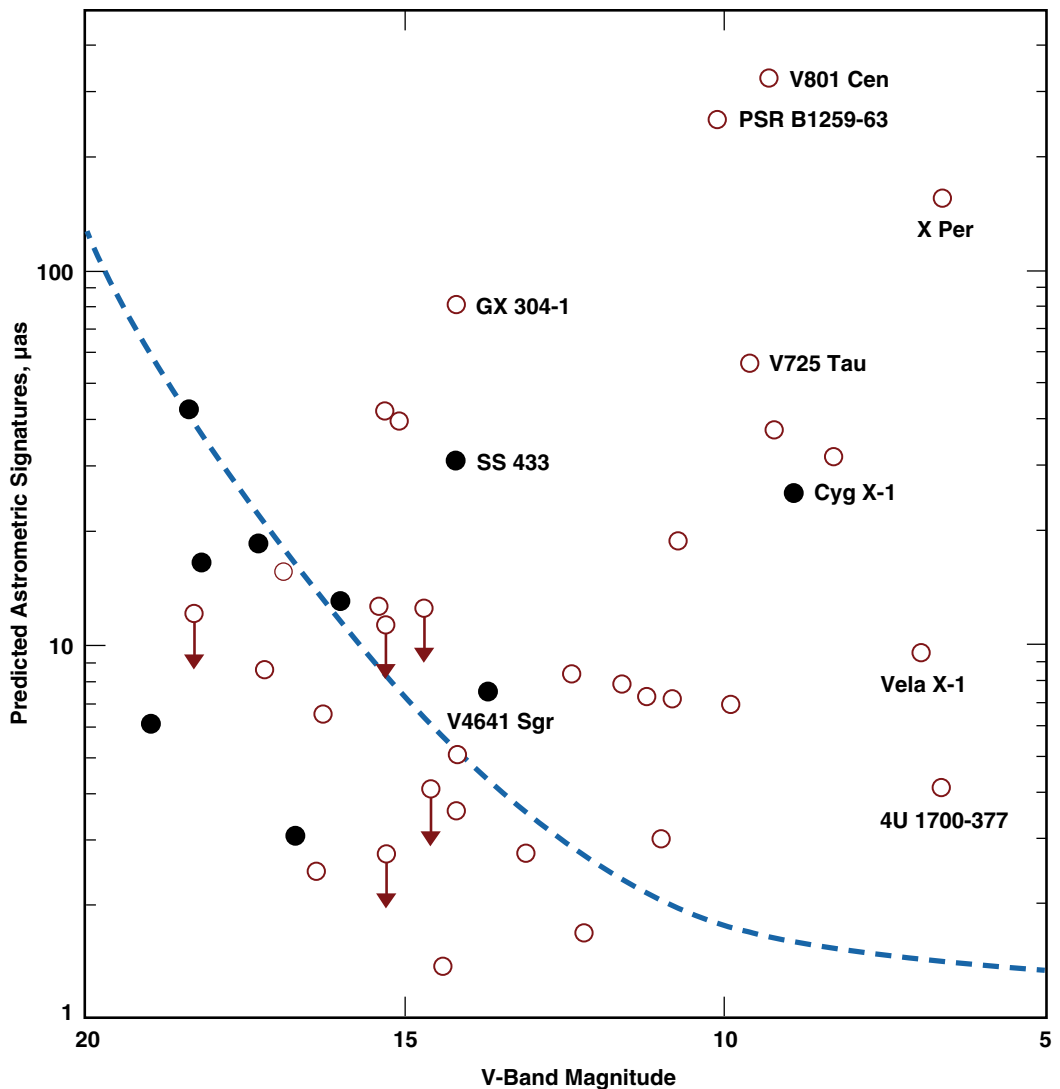
Distance and proper motion determinations with SIM Lite are feasible for any Galactic system that is optically bright enough, and targets will include all types of X-ray binaries. However, it is probably the LMXBs that will benefit most from improved distance measurements since the current estimates of their distances can be uncertain by a factor of two or more. SIM Lite will be capable of distance and proper motion measurements for at least the 27 LMXBs with V-band magnitudes brighter than 20 (Unwin et al. 2008), providing distances to 1 to 6 percent accuracy in most cases. Some of these LMXBs are radio jet sources, and there are also plans to observe RS CVn and Algol-type binaries with radio emission.

Gaia will only be able to do a small subset of the black hole and neutron star science described here. While Gaia may obtain orbital measurements for a few of the brightest HMXB systems with the largest astrometric signatures, the μas measurement capabilities of SIM Lite are absolutely essential for the vast majority of our planned targets, including the interesting neutron star source Vela X-1 (see Section 9.3). The situation is similar for LMXB distances in that obtaining accurate distances for the brightest and closest LMXBs is expected to be feasible for Gaia. However, of our 27 LMXB targets, 19 have magnitudes fainter than V = 17 and most of these are estimated to have distances of 5 to 10 kpc. Of these 19 fainter LMXBs, there are only five for which Gaia is expected to obtain distance measurements to better than 40 percent accuracy (Lindegren et al. 2008). For these five LMXBs, Gaia will obtain distances to 15 to 33 percent while the SIM Lite distances are expected to be 10 times more accurate (1.6 to 3.3 percent). Finally, as mentioned above, the planned observations make use of the SIM Lite capability to perform target of opportunity observations, which will not be possible with Gaia.

9.3   Inside Neutron Stars

Although the inside of a neutron star is certainly hidden from direct viewing, significant constraints on the composition can be obtained by measuring masses and radii of neutron stars. This is because the pressure-density relationship (i.e., equation of state, EOS) that is theoretically calculated for various neutron star compositions directly predicts the star's mass-radius relation. Lattimer and Prakash (2001) discuss the different types of matter that may be inside neutron stars, including normal matter (neutrons and protons) as well as exotic matter such as hyperons, kaon condensates, and quark matter. Constraining the composition of neutron star interiors has important implications for fundamental physics, including understanding the nature of strong force interactions at high densities and determining if strange-quark matter is the ultimate ground state of matter.

Observations of neutron star HMXBs with SIM Lite have the potential to place significant constraints on the EOS. Each EOS predicts a maximum neutron star mass, so an accurate mass measurement for even a single neutron star above the maximum value predicted by an EOS would rule out that EOS. Although Thorsett and Chakrabarty (1999) found that many neutron stars have masses that are close to the canonical value of 1.4 solar masses, which allows essentially all EOSs, more recent observations have shown evidence for more massive neutron stars with median mass measurements in the 1.8 to 2.8 $M_\odot$ range (Barziv et al. 2001; Clark et al. 2002; Freire et al. 2008). Confirming these high neutron star masses by reducing the uncertainties would lead immediately to ruling out a large fraction of the proposed EOSs.

As mentioned above, SIM Lite will be able to detect orbital motion for at least 16 neutron star HMXBs and the best mass constraints will be obtained for the accreting X-ray pulsars. For five SIM Lite HMXB targets, the neutron star orbit has already been very accurately mapped (Bildsten et al. 1997; Unwin et al. 2008), and when this is combined with a SIM Lite measurement of the companion's orbit, a direct neutron star mass measurement will be obtained. One of the most tantalizing of these targets is Vela X-1, which has a current neutron star mass measurement of 1.86 ± 0.16 $M_\odot$ (68 percent confidence errors, Barziv et al. 2001). Simulations have shown that when SIM Lite measurements are combined with

the X-ray measurements, it will be possible to measure the neutron star mass to 3.9 percent accuracy (Tomsick et al. 2005; Unwin et al. 2008). This is a major improvement over the current mass measurement and will be sufficient to determine if Vela X-1 harbors an over-massive neutron star. As our estimate of the astrometric signature for Vela X-1 is 9.5 μas, the SIM Lite capabilities are critical.

SIM Lite will also contribute to constraining the neutron star EOS by improving constraints on the neutron star radius by accurately determining the distance to neutron star X-ray binaries. There are at least two radius determination techniques that use X-ray measurements for which uncertain distances are a primary source of radius uncertainty. First, when X-ray transient systems are at their lowest flux levels, the X-ray emission is dominated by blackbody emission from the neutron star surface (Rutledge et al. 2002, Lattimer and Prakash 2007). Knowing the distances to sources like Cen X-4 and Aql X-1 will remove a major uncertainty in the radius measurement. Thermal X-ray emission is also seen from the entire surface of the neutron star when actively accreting neutron star systems undergo X-ray bursts. While this is a promising technique for measuring neutron star radii, source distances are the primary uncertainty (Galloway et al. 2008).

9.4　Probing Strong Gravity

Both distance and orbital measurements of X-ray binaries by SIM Lite are important for probing the strong gravitational fields near black holes and neutron stars, potentially allowing for tests of GR. One GR prediction that SIM Lite can contribute to testing is that black holes should, by definition, have an event horizon, i.e., a geometrical boundary from which not even light can escape. Observational evidence for this comes from a comparison of the X-ray luminosities of black hole and neutron star transients when they are at their lowest flux levels, presumably with a very low level of mass accretion. The most up-to-date results show good evidence that the black hole systems are, in fact, less luminous than neutron star systems (Narayan and McClintock 2008), and a very likely interpretation to this difference is that the accreted mass is advected through the black hole event horizon (Narayan et al. 1997). Still, it is notable that although this result rests on luminosity measurements, not one of the systems used to obtain the result has a direct distance measurement. Several of the systems are bright enough to have their distances measured with SIM Lite, which would be a major improvement to the study.

A second GR prediction that is being tested is that black holes and neutron stars should have an innermost stable circular orbit (ISCO). The implication of an ISCO is that since there are no stable orbits within some radial distance from the compact object, the accretion disk should be truncated at that radius. There are at least two techniques that are being applied to X-ray observations of actively accreting black holes with the goal of finding the location of the ISCO. One of these relies on measuring the shape of the iron Kα emission line, which is produced when X-rays incident on the accretion disk cause the iron in the disk to fluoresce. At the inner edge of the accretion disk, the motion of the accretion disk material produces red and blue Doppler shifts and the gravitational field produces a redshift, causing the emission line to be extremely distorted (Tanaka et al. 2005; Miller 2007). The measurement of the inner radius comes from modeling the shape of the line, but in addition to the location of the inner radius, the shape of the line also depends on the inclination of the accretion disk. Thus, one major contribution that SIM Lite can make to this study is to measure the binary inclination, which should be the same as the disk inclination. Two black hole systems with iron line measurements for which SIM Lite will be able to constrain the binary inclination are Cyg X-1 and GRO J1655-40. In the case of Cyg X-1, the best estimate for the orbital astrometric signature is in the range of 27 to 34 μas (also see Section 9.6), making it an easy target for orbital studies that will measure the binary inclination precisely (Pan and Shaklan 2005; Unwin et al. 2008).

Another ISCO measurement technique that would greatly benefit from precision measurements with SIM Lite is the effort to use the thermal continuum emission from black hole accretion disks to determine the location of the inner edge of the disk. There are times when this component dominates the X-ray emission from black hole systems, and its shape is well described by thermal spectral models. Using fully relativistic models, McClintock et al. (2006) have carried out detailed analyses for several sources to find the location of the inner radius of the disk. While the work has been successful, both distance and accretion disk inclination are uncertain parameters in the interpretation of the results (Psaltis 2008) and these are parameters that are accessible to SIM Lite.

9.5   Birth and Evolution of Black Holes and Neutron Stars

In order to place black holes and neutron stars in the larger context of stellar life cycles, including questions related to stellar and binary evolution as well as connections to phenomena such as supernovae (or "hypernovae") and gamma-ray bursts, it is of great importance to investigate how and where these compact objects are born. By measuring the proper motions and distances to X-ray binaries, SIM Lite can help to answer this question for a large number of sources. When combined with systemic radial velocities that can be obtained using spectroscopy, proper motions and distances provide a three-dimensional space velocity that can be used to determine the object's runaway kinematics (e.g., "kick" velocity) as well as its Galactocentric orbit (Mirabel et al. 2001; Mirabel and Rodrigues 2003a). In many cases, this information can be used to test relationships between specific sources and nearby clusters of stars (e.g., Cyg X-1 and its nearby OB association) or to constrain whether a source was born in the plane of the Galaxy or out of the plane in a globular cluster.

To date, the radio and Hubble Space Telescope (HST) proper motion measurements that have been made for a few black hole systems have provided very interesting results. While results for two black hole LMXBs (GRO J1655-40 and XTE J1118+480) show space velocities consistent with the systems having received a supernova kick at the time of the birth of the black hole (Mirabel et al. 2001; Mirabel et al. 2002), the very low space velocity for Cyg X-1 indicates that less than 1 solar mass of material could have been ejected when the black hole was formed, suggesting that the Cyg X-1 black hole came from the collapse of a massive star without a supernova (Mirabel and Rodrigues 2003b). Unfortunately, the current measurement precision for proper motions is only sufficient for the most nearby systems. SIM Lite will provide at least two orders of magnitude improvement for proper motion measurements over HST, which will greatly increase the number of systems for which accurate proper motion measurements are possible.

9.6   Black Hole Masses and the Case of Cyg X-1

Mass is one of the fundamental properties of a black hole, and it has important implications for the strong gravity studies discussed in Section 9.4 as well for understanding the birth of black holes and the evolution of the X-ray binaries in which they are found (Section 9.5). Theoretical predictions for the mass distribution of black holes that result from the deaths of massive stars rely on a wide range of physics, including the maximum mass of a neutron star (see Section 9.3), the strength of the stellar winds of the progenitor stars, and the details of supernova explosions as well as the necessary conditions for supernovae to occur. From theory and simulations, Fryer and Kalogera (2001) predict a continuous distribution of black hole masses with the largest number of black holes being just above the maximum neutron star mass (between 1.5 and 3 $M_\odot$) and a gradual drop in the numbers of black holes with higher masses.

Currently, black hole mass estimates have been obtained for 20 black hole systems, and when the relatively large uncertainties in the estimates are taken into account, the possible masses range from 3 to 18 $M_\odot$ (Remillard and McClintock 2006). While comparisons between these measurements and the theoretical predictions are still difficult due to the relatively small numbers of black holes and the large uncertainties in the mass estimates, the range of measured masses is very similar to the predictions. To go beyond such rough comparisons requires the largest number of black hole masses to be measured as accurately as possible. Both uncertain binary inclinations and distances make large contributions to the current errors in the mass measurements and SIM Lite can make an important contribution to this study by measuring these parameters to provide accurate mass determinations.

The first discovered stellar black hole, Cyg X-1, is a good example of the need for SIM Lite's capabilities. The estimates of mass and distance for Cyg X-1 are still controversial even though the source has been suspected of harboring a black hole since the early 1970s. One controversy has been the mass of the O9.7 Iab stellar companion. Although an isolated star with this spectral type would have a mass near 33 $M_\odot$, in a binary, mass transfer and binary evolution can cause the mass to be considerably less. Herrero et al. (1995) give a best estimate for the companion mass of 17.8 $M_\odot$, which would indicate a black hole mass of 10.1 $M_\odot$ using the best estimate for the binary inclination of 35 degrees. A plausible lower limit on the companion mass of 10 $M_\odot$, combined with an upper limit to the binary inclination of 65 degrees (based on the absence of X-ray eclipses), leads to a black hole mass of 4 $M_\odot$. For possible ranges of the black hole and companion masses, we present the astrometric signatures in Table 9-1. We have assumed the largest likely distance for Cyg X-1 of 2.5 kpc, but it should be noted that parallax measurements put the distance at 1.7±1.0 kpc (Hipparcos) or 1.4±0.9 kpc (VLBI), which would make the astrometric signatures even larger. Even at the larger distance, the wobbles of Cyg X-1 are in the range of 20 to 30 µas for the most likely combinations of component masses, providing an excellent opportunity for SIM Lite to provide a long-awaited definitive measurement of the compact object mass in this system.

Table 9-1. Astrometric signatures (in µas) due to binary motion in Cyg X-1 for different combinations of companion star and black hole masses (a distance of 2.5 kpc is assumed). The full range is measurable by SIM Lite.

Companion Mass, $M_\odot$	Black Hole Mass, $M_\odot$				
	17.5	15	10	7	3.5
10	—	—	33.5	26.1	15.2
20	38.6	34.6	25.6	19.2	10.5
30	32.9	29.3	21.1	15.6	8.3
40	29.0	25.6	18.2	13.3	7.0
50	26.1	22.9	16.1	11.7	6.1

References

Barziv, O., Kaper, L., van Kerkwijk, M. H., Telting, J. H., and van Paradijs, J., 2001, A&A, 377, 925.

Bildsten, L. et al., 1997, ApJS, 113, 367.

Clark, J. S., Goodwin, S. P., Crowther, P. A., Kaper, L., Fairbairn, M., Langer, N., and Brocksopp, C., 2002, A&A, 392, 909.

Coburn, W., Heindl, W. A., Rothschild, R. E., Gruber, D. E., Kreykenbohm, I., Wilms, J., Kretschmar, P., and Staubert, R., 2002, ApJ, 580, 394.

Fender, R. P., 2006, in Compact Stellar X-ray Sources (Cambridge: Cambridge Univ. Press), 381.

Fryer, C. L. and Kalogera, V., 2001, ApJ, 554, 548.

Freire, P. C. C., Ransom, S. M., Begin, S., Stairs, I. H., Hessels, J. W. T., Frey, L. H., and Camilo, F., 2008, ApJ, 675, 670.

Galloway, D. K., Ozel, F., and Psaltis, D., 2008, MNRAS, 387, 268.

Giacconi, R., Gursky, H., Paolini, F. R., and Rossi, B. B., 1962, Phys. Rev. Lett., 9, 439.

Herrero, A., Kudritzki, R. P., Gabler, R., Vilchez, J. M., and Gabler, A., 1995, A&A, 297, 556.

Lattimer, J. M. and Prakash, M., 2007, Physics Reports, 442, 109.

Lattimer, J. M. and Prakash, M., 2001, ApJ, 550, 426.

Lindegren, L., Babusiaux, C., Bailer-Jones, C., Bastian, U., Brown, A. G. A., Cropper, M., Hog, E., Jordi, C., Katz, D., van Leeuwen, F., Luri, X., Mignard, F., de Bruijne, J. H. J., and Prusti, T., 2008, in Proceedings IAU Symposium, 248, 217.

McClintock, J. E., Shafee, R., Narayan, R., Remillard, R. A., Davis, S. W., and Li, L.-X., 2006, ApJ, 652, 518.

Miller, J. M., 2007, ARA&A, 45, 441.

Mirabel, I. F . and Rodrigues, I., 2003a, A&A, 398, L25.

Mirabel, I. F . and Rodrigues, I., 2003b, Science, 300, 1119.

Mirabel, I. F., Mignani, R. P., Rodrigues, I., Combi, J. A., Rodriguez, L. F., and Guglielmetti, F., 2002, A&A, 395, 595.

Mirabel, I. F., Dhawan, V., Mignani, R. P., Rodrigues, I., and Guglielmetti, F., 2001, Nature, 413, 139.

Narayan, R., Garcia, M. R., and McClintock, J. E., 1997, ApJ, 478, L79.

Narayan, R. and McClintock, J. E., 2008, New Astronomy Reviews, 51, 733.

Pan, X. and Shaklan, S., 2005, BAAS, 37, 454.

Psaltis, D., 2008, review article for Living Reviews in Relativity, arXiv:0806.1531.

Remillard, R. A. and McClintock, J. E., 2006, ARA&A, 44, 49.

Rutledge, R. E., Bildsten, L., Brown, E. F., Pavlov, G. G., Zavlin, V. E., and Ushomirsky, G., 2002, ApJ, 580, 412.

Tanaka, Y., Nandra, K., Fabian, A. C., Inoue, H., Otani, C., Dotani, T., Hayashida, K., Iwasawa, K., Kii, T., Kunieda, H., Makino, F., and Matsuoka, M., 1995, Nature, 375, 659.

Tauris, T. M. and van den Heuvel, E. P. J., 2006, in Compact Stellar X-ray Sources (Cambridge: Cambridge Univ. Press), 623.

Thorsett, S. E. and Chakrabarty, D., 1999, ApJ, 512, 288.

Tomsick, J. A., Quirrenbach, A., and Reffert, S., 2005, BAAS, 2007, 117.02.

Unwin, S. C. et al. 2008, PASP, 120, 38.

10 Milky Way Stars and Stellar Populations

Guy Worthey (Washington State University)

ABSTRACT

SIM Lite will revolutionize the study of almost every category of star (Chapter 7). However, a few stellar types are especially applicable to the study of galaxies. These include classical Cepheid variable stars and Population II stars. The former are reliable standard candles, which, given improved calibration, will help establish distance scales, both to external galaxies and within our own. Cepheids are also interesting because of their (poorly understood) pulsation mechanism and what it may reveal about the physics of stars in general. Population II stars — older, less luminous, and in general metal-poor — comprise a fossil record, the preserved remains of the Milky Way's remote past. Their study will help establish a Galactic time scale and the evolutionary path leading from formation to the present day.

In the study of extragalactic stellar populations, a plethora of questions remain: field versus cluster environment, chemical evolution, morphological evolution, emergence from the dark ages, and the overall scheme of galaxy assembly. The isochrone-based ages of these populations are currently uncertain at the level of 30 percent. The Galactic clusters studied by SIM Lite, rich in Population II stars, will help reduce this to about 5 percent, leading to increased precision and better understanding of galaxy evolution at all redshifts. By targeting the distance scale, we will complement the more direct studies of dynamics and the role of dark matter in galaxy assembly and evolution (Chapter 4). Better distances, filtered through stellar evolution models and models for the integrated light of stellar populations, translate to better understanding of the chemical and age structure of the various stellar populations that make up the Milky Way and external galaxies. The age-measurement tools can also be applied to data from the James Webb Space Telescope and from the new generation of adaptive-optics ground-based telescopes. They will play a vital role in their studies of galaxy formation.

10.1 Galactic Distances and Age Scales

Cepheid variable stars are reliable standard candles, which, given improved calibration, will help establish the distance scale to external galaxies. SIM Lite will dramatically improve calibration of the period-luminosity relationship. At the same time, it will yield a wealth of Cepheid science. An accurate distance calibration will allow for an accurate determination of extinction and (currently mysterious) metallicity effects on the inferred absolute luminosity. The physics of the pulsation mechanism (including the mysterious amplitude decline of Polaris) can be studied in great detail for those nearby Cepheids where the extinction is small or well measured (such as in clusters), as well as for Cepheids that are members of binary systems where accurate mass measurements can be made. In addition, SIM Lite will use star clusters to determine accurate ages for metal-poor (Population II) stars by identifying the various evolutionary sequences in a stellar color-magnitude diagram. This will provide a firm lower limit on the age of the Universe and probe the early formation history of the Milky Way, including the interplay between age, abundance pattern, and dynamics.

10.1.1 Classical Cepheid Variable Stars

A SIM Lite program will yield a plethora of Cepheid science, even with a successful all the distances Gaia determines, since SIM Lite maintains the same high astrometric precision for stars that are brighter than Gaia's magnitude range and for fainter stars for which Gaia's precision decreases:

(1) Variable stars identified as Cepheids would be useful for inertial frame Galactic rotation dynamical studies if sufficiently precise proper motions are available.
(2) An accurate distance calibration allows for an accurate determination of extinction and (currently mysterious) metallicity effects on the inferred absolute luminosity.
(3) The physics of the pulsation mechanism (including the mysterious amplitude decline of Polaris) can be studied in great detail for those nearby Cepheids where the extinction is small and/or well measured (such as in clusters), and for Cepheids that are members of binary systems where accurate mass measurements can be made.

The second and third points are essential for our understanding and usage of Cepheids as tools. From the deeper physics comes the deeper understanding. Currently, our lack of detailed understanding of the physics of the pulsation mechanism (i.e., the calibration of the period-luminosity-color relation) yields galaxy distances that carry systematic uncertainties of order plus or minus 5 percent (Pietrzynski et al. 2006; Macri et al. 2006). A better understanding of the physics would likely result in smaller sys-

tematic errors, and hence, in an easier method for determining accurate distances to a large number of galaxies. For example, it has been claimed that "bump Cepheids" can be used to determine distances below the 2 percent level. This method is based on a detailed analysis of the light-profile and nonlinear pulsation models (e.g., Keller and Wood 2006).

On the subject of disk dynamics, the Milky Way is the only galaxy for which we can perform detailed three-dimensional dynamical studies because all six phase-space parameters can be determined for a number of tracers of the gravitational potential. Young stars like Cepheids (age ~50 Myr) are very sensitive to small- and large-scale perturbations of the potential (Mayor 1974), and are thus very useful to study the dynamical effects of the bar, spiral structure, the Gould Belt, and the warp. For such studies, the apparent magnitude is not important, just the distance and space velocity. Cepheids are useful for these kinds of studies because they can be identified based on their light curve (Metzger, Caldwell, and Schechter 1998). A total of about 900 Galactic Cepheids are currently known (Welch 1998), while only the 200-odd nearest of these stars are typically used in studies of Galactic dynamics (Zhu 2000; Metzger, Caldwell, and Schechter 1998; Feast and Whitelock 1997; Pont et al. 1997; Pont, Mayor, and Burki 1994; Caldwell and Coulson 1987). The Cepheid sample provides a unique opportunity to perform very detailed studies of the dynamics of disk galaxies. Many of these Cepheids will have Gaia data, and these could have refined distances and much better proper motions with SIM Lite. Because the binarity rate amongst Cepheids is large (≈80 percent; Szabados 2003), it is crucial to monitor the Cepheids astrometrically throughout the SIM Lite mission.

Cepheids in the Milky Way typically suffer a significant amount of dust extinction. For example, the nearest 180 stars in the sample of Pont and collaborators (Pont, Mayor, and Burki 1994; Pont et al. 1997) have $A_V = 1.7\pm1$ mag. In general, it is hard to determine extinction better than about 0.05 mag for stars with Cepheid colors, even with the Gaia instrument suite (Jordi et al. 2006). Currently, the extinction is estimated from an intrinsic period-color relation (e.g., Laney and Stobie 1994; Caldwell and Coulson 1986) that is calibrated on Cepheids in open clusters. Future work to measure extinction promises to nail the currently fuzzy relations between period, luminosity, color, and abundance for bright, local stars.

Independent measurements of the period-distance-metallicity-extinction calibration would be available via the Cepheids in galaxies with rotational-parallax distances (see Chapter 6): M31 and M33 (employing SIM Lite) and the LMC (employing Gaia).

A final point is that Cepheids are pulsating variable stars and it is through this dynamic that we can learn much more about the internal structure and atmospheric physics than for normal stars. The ultimate goal is to usher in the age of precision stellar physics and hence stellar population studies.

10.1.2 Population II Ages and Chemistries

Age determinations for metal-poor (Population II) stars allow us to set a firm lower limit to the age of the Universe and to probe the early formation history of the Milky Way with the interplay between age, abundance pattern, and dynamics. Star clusters provide the best opportunity to determine ages of Population II stars, as it is easy to identify the various evolutionary sequences in a stellar color-magnitude diagram. The main sequence turnoff (MSTO) luminosity is the best stellar "clock" that can be used to determine the absolute ages of globular clusters (e.g., Demarque 1980; Rood 1990; VandenBerg 1990; Renzini 1991; Chaboyer et al. 1996). However, the main sequence turnoff becomes redder as well as fainter as a cluster of stars gets older. Thus, ages can be derived from the color of the turnoff, independent of distance, and this fact is exploited in the application of integrated-light models to extragalactic stellar populations.

To briefly recap Chapter 7 material, the largest uncertainty in the determination of globular cluster ages based upon the MSTO luminosity is the distance scale for Pop II objects. A 1 percent error in the distance leads to a ≈2 percent error in the derived age (e.g., Chaboyer et al. 1996). SIM Lite will be able to determine distances to the bulk of the Milky Way globular cluster system and other distant stars in the halo. To illustrate the expected accuracy of our relative age determinations for the field halo stars and the globular clusters in our SIM program, Unwin et al. (2008) ran a Monte Carlo simulation that allowed for the true distance to the object to vary within its current estimated uncertainties, and which took into account the uncertainties in the SIM distance determination, reddening determinations, and in the chemical composition of the stars. They found that the field stars will have a typical age uncertainty of about 0.6 Gyr, while the globular cluster ages will have an error of about 0.9 Gyr (column 8 in Table 5 of Unwin et al.).

Only SIM Lite can get parallax distances to the bulk of the Milky Way globular cluster population.

10.1.3 Local Group Rotational Parallax Calibrators

In Chapter 6 we saw that local galaxies will have 1 percent rotational parallax distances from SIM Lite. Thus, with additional photometry, most of which is already available, stellar groups such as Cepheid variables, Miras, post-planetary nebula objects, red giants, and hot main sequence stars can all be compared with Milky Way equivalents with essentially zero error due to luminosity uncertainty.

10.2 All-Redshift Galaxy Evolution

10.2.1 Galactic Evolution at All Redshifts

In the study of extragalactic stellar populations, many questions remain. These regard field versus cluster environment, chemical evolution, morphological evolution, emergence from the dark ages, and the overall scheme of galaxy assembly. The error in the isochrone-based ages of these populations — currently 30 percent — is the principal limitation on our ability to address these questions. Improved age determination, combined with an improved distance scale, will complement the direct studies of dynamics and the role of dark matter in galaxy assembly and evolution (Chapter 4). Better ages and distances, filtered through stellar evolution models and models for the integrated light of stellar populations, translate to better understanding of the chemical and age structure of the various stellar populations that make up the Milky Way and external galaxies. The age measurement tools can also be applied to data from the James Webb Space Telescope and from the new generation of adaptive-optics ground-based telescopes and play a vital role in their studies of galaxy formation.

10.2.2 Extragalactic Stellar Populations

The study of normal galaxy evolution will be greatly enhanced by SIM projects that target dynamics and dark matter, naturally. But those that target the distance scale provide a crucial, complementary strategy that mushrooms into much more than just distance knowledge. Better distances, filtered through stellar evolution models and models for the integrated light of stellar populations, translate to much more precise information on the chemical and age structure of the various stellar populations that make up the Galaxy and external galaxies.

With odd irony, the key for deriving ages throughout the universe is the humble and ubiquitous main sequence turnoff star. In the integrated light of galaxies, the game is to use spectroscopy to measure the

chemical makeup of a galaxy and then uncover the temperature of the main sequence turnoff stars. Advanced phases of evolution (e.g., asymptotic giant branch stars) and the effects of binarism (e.g., blue straggler stars) and other physical effects (initial mass function [IMF], dust, rotation) serve, at this point, as complications, although they may turn into opportunities as our knowledge increases.

In the study of extragalactic stellar populations, a plethora of questions regarding field versus cluster environment, chemical evolution, morphological evolution, emergence from the dark ages, and the overall scheme of galaxy assembly remain, and are likely to remain for many years. Present age errors intrinsic to isochrone-based models are of order 30 percent (Charlot et al. 1996), but the clusters studied by SIM Lite should allow for increased precision for better understanding of galaxy evolution at all redshifts. A reasonable goal in this regard is 5 percent age precision for favorable, well-observed extragalactic stellar populations from the next generation of large, ground-based spectroscopic telescopes.

Morphological look-back studies (e.g., Galaxy Evolution from Morphology and Spectra, [GEMS], Rix et al. 2004) and spectroscopic surveys (e.g., Classifying Objects by Medium-Band Observations — a spectrophotometric 17-filter survey [COMBO-17], Wolf et al. 2004) dovetail nicely with stellar populations studies that earlier predicted in a broad way what the direct observations are finding. That is, spiral galaxies look as if they have had quasi-continuous star formation for long epochs, as expected, but elliptical galaxies, while largely quiescent today, have also had much more complex star formation histories than one would suppose, not too drastically different from spirals (Worthey 1998). The charting of galaxy assembly is a major scientific thrust of the James Webb Space Telescope and much of extragalactic astrophysics today.

SIM Lite will contribute toward this push by providing the foundation of age measurement tools that will be applied to JWST data. It can be used to obtain parallax distances to Galactic (disk; Population I) clusters. This will complement SIM Lite's Population II (halo and thick-disk) distance scale investigations described in Section 7.1. A critical step in studying ages and chemical compositions of stellar populations is to establish a collection of standard clusters, mostly Galactic clusters, for which distances, reddenings, abundances, and ages will be derived with unprecedented accuracy. SIM Lite is critical to this task by providing accurate parallax distances. These standard clusters can then be used to tightly constrain theoretical isochrone sets more stringently than ever before. The isochrones, in turn, give ages for clusters and also for galaxies via integrated-light models. Precision studies of galaxy evolution are the ultimate aims enabled by this SIM study.

Figure 10-1 illustrates this concept by parceling the universe of galaxies and clusters into age and metallicity bins. Galaxies that are not actively forming stars — leaving aside extreme post-starburst objects — will have ages of order 100 Myr, rather like the Pleiades star cluster, or older. Upper limits are imposed by the redshift of the galaxy, being younger at high redshift and, by the age of Milky Way globular clusters, at zero redshift. This age range is marked on the figure as "Red Envelope" Galaxies: those galaxies that are ready for the highest-quality spectral analysis, that is, their starlight is not too severely affected by internal dust and gaseous nebular emission.

The second dimension of Figure 10-1 is abundance. It is already crystal clear that metal-poor populations are a very minor component of the mass and the light output of any chemically mature galaxy (less than 5 percent contribution from stars less than a tenth of the solar abundance: Worthey, Dorman, and Jones 1996), so the parameter range of most interest is from somewhat subsolar to the supersolar regime of the most massive elliptical galaxies. Finally, a sprinkling of target clusters in the Milky Way has been overlaid on the figure, showing how Milky Way calibrators can indeed unlock the high-redshift Universe. The goal is to be able to age-date any stellar population at any redshift to 5 percent precision, given high-quality data.
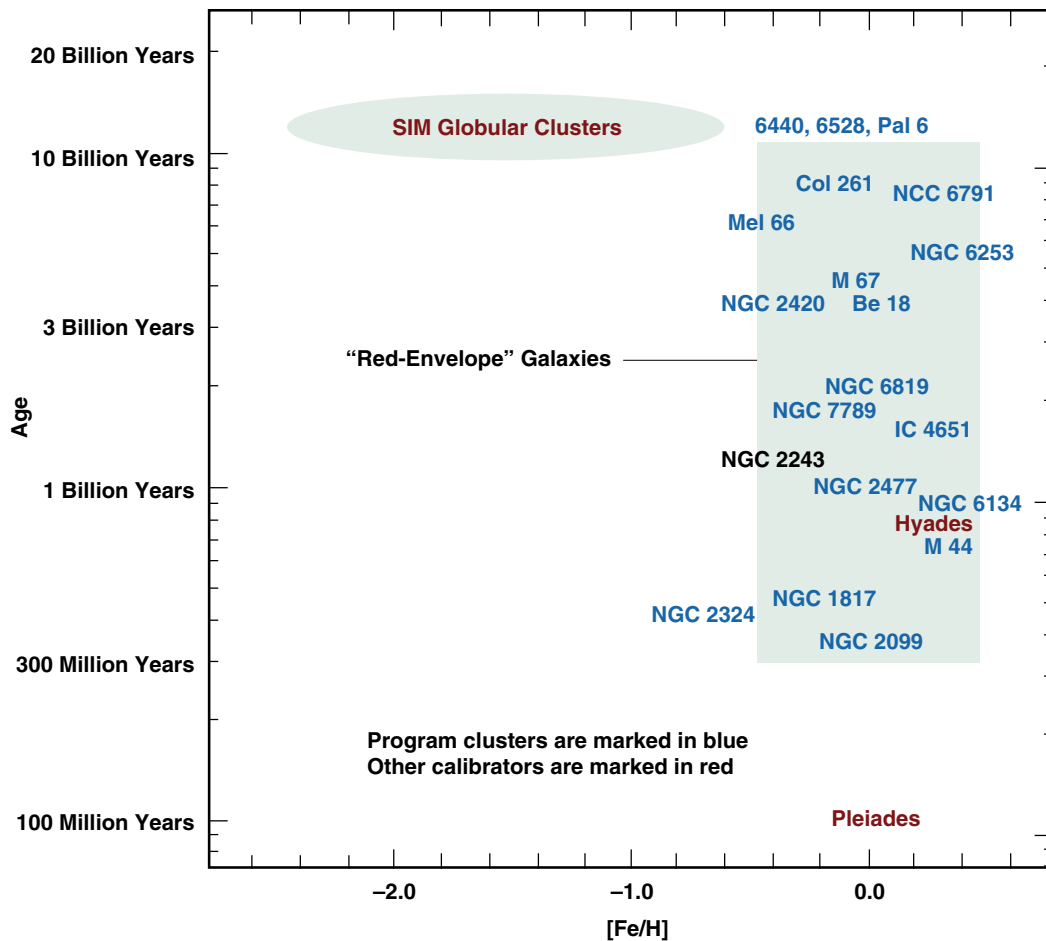
10.2.3 Understanding the Systematics of Stellar Populations

An absolute 5 percent age precision requires a better grip on the systematics of stellar populations than presently exists. With precise distances from SIM Lite, distance will no longer contribute significantly to the uncertainties and, instead, other effects will dominate. For example, the uncertainty in heavy element abundance (Z) propagates approximately as $\delta \log (age) = -3/2 \, \delta \log (Z)$ (Worthey 1994) using stellar temperatures as age indicators, as one is forced to do for integrated-light applications. This implies that overall heavy element abundance uncertainty be less than 0.02 dex, a goal reached only rarely at present, but which should be very common in the near future.

The detailed, element-by-element composition also matters. Worthey (1998) estimates that abundance ratio effects need to be tracked and calibrated if they induce more than a 7 K shift in stellar temperature. Progress on such detailed effects is underway (Dotter et al. 2007) and should be available in a few years. Progress on bolometric corrections, absolute flux scale, and stellar color-T_{eff} relations can also be expected over time.

A standard cluster set ties down points for stellar modelers, which relate intimately to the interpretation of high-redshift stellar population studies. SIM Lite will measure parallax distances to distant Galactic and globular clusters unreachable by Gaia, including the crucial old, metal-rich NGC6791 (see Figure 10-1 and the target list in Unwin et al. 2008). The luminosity of the main sequence turnoff in the color-magnitude diagram is the best age indicator: the one with the smallest errors (Chaboyer 1995) and the one that ties most directly to the "fusion clock" of the hydrogen-burning star.

Distance uncertainty is currently the dominant uncertainty, and that will be removed by SIM Lite (to less than 1 percent for most individual Galactic clusters, and perhaps 1 percent for the globular clusters in aggregate). After abundance effects, the remaining uncertainties are those of interstellar extinction, which may prove to be the dominant uncertainty in the end, along with the practical difficulty of extracting the main sequence turnoff temperatures amid the light of less well-understood phases of stellar evolution, notably the asymptotic giant branch that becomes quite important in the near infrared.

References

Caldwell, J. A. R. and Coulson, I. M., 1986, MNRAS, 218, 223.

Caldwell, J. A. R. and Coulson, I. M., 1987, AJ, 93, 1090.

Chaboyer, B., 1995, ApJ, 444, 9.

Chaboyer, B., Demarque, P., Kernan, P., Krauss, L., and Sarajedini, A., 1996, MNRAS, 283, 683.

Charlot, S., Worthey, G., and Bressan, A., 1996, ApJ, 457, 625.

Demarque, P., 1980, in Star Clusters, IAU Symp. 85, ed. J. E. Hesser (Dordrecht: Reidel), 281.

Dotter, A., Chaboyer, B., Ferguson, J. W., Lee, H.-c., Worthey, G., Jevremovic, D., and Baron, E., 2007, ApJ, 666, 403.

Feast, M. and Whitelock, P., 1997, MNRAS, 291, 683.

Jordi, C. et al., 2006, MNRAS, 367, 290.

Keller, S. C. and Wood, P. R., 2006, ApJ, 642, 834.

Laney, C. D. and Stobie, R. S., 1994, MNRAS, 266, 441.

Macri, L. M., Stanek, K. Z., Bersier, D., Greenhill, L. J., and Reid, M. J., 2006, ApJ, 652, 1133.

Mayor, M., 1974, A&A, 32, 321.

Metzger, M. R., Caldwell, J. A. R., and Schechter, P. L., 1998, AJ, 115, 635.

Pietrzynski, G. et al., 2006, AJ, 132, 2556.

Pont, F., Queloz, D., Bratschi, P., and Mayor, M., 1997, A&A, 318, 416.

Pont, F., Mayor, M., and Burki, G., 1994, A&A, 285, 415.

Renzini, A., 1991, in Observational Tests of Cosmological Inflation, eds. T. Shanks et al. (Dordrecht: Kluwer), 131.

Rix, H. W. et al., 2004, ApJS, 152, 163.

Rood, R. T., 1990, in Astrophysical Ages and Dating Methods, eds. E. Vangioni-Flan et al. (Gif sur Yvette: Ed. Frontières), 313.

Szabados, L., 2003, Informational Bulletin on Variable Stars, 5394, 1.

Unwin, S. et al., 2008, PASP, 120, 38.

VandenBerg, D. A., 1990, in Astrophysical Ages and Dating Methods, eds. E. Vangioni-Flan et al. (Gif sur Yvette: Ed. Frontières), 241.

Welch, D., 1998, "McMaster Cepheid Photometry and Radial Velocity Data Archive," crocus.physics.mcmaster.ca/Cepheid/.

Wolf, C. et al., 2004, A&A, 421, 913.

Worthey, G., Dorman, B., and Jones, L. A., 1996, AJ, 112, 948.

Worthey, G., 1994, ApJS, 95, 107.

Worthey, G., 1998, PASP, 110, 888.

Zhu, Z., 2000, Ap&SS, 271, 353.

Supermassive Black Holes and Quasars

Does the most compact optical emission from an AGN come from an accretion disk or from a relativistic jet?

Are there binary black holes? What are their orbits?

Does the separation of the radio core and the optical photocenter of the quasars used for the reference frame tie change on the time scale of the photometric variability, or is the separation stable?

BLACK HOLES ARE PERHAPS THE MOST EXOTIC OBJECTS TO IMPINGE ON THE COSMIC CONSCIOUSNESS.

Christopher Reynolds

11 Quasar Astrophysics

Ann E. Wehrle (Space Science Institute), **Norbert Zacharias** (USNO), **Kenneth Johnston** (USNO), **David Boboltz** (USNO), **Alan L. Fey** (USNO), **Ralph Gaume** (USNO), **David L. Meier** (JPL), **David W. Murphy** (JPL), **Dayton L. Jones** (JPL), **Roopesh Ohja** (USNO), **B. Glenn Piner** (Whittier College), and **Stephen C. Unwin** (JPL)

ABSTRACT

Active galactic nuclei (AGN) can be studied by SIM Lite at unprecedented µas scales. This capability opens up direct study of areas within light-days of the central supermassive black hole. Topics to be addressed include the triggering of relativistic jets, the search for binary black holes, and the cause of the radio-loud/radio-quiet dichotomy.

11.1 Introduction

The resolution needed to directly measure motions in the inner tenth of a parsec in quasars is beyond the reach of current optical and near-infrared ground- and space-based telescopes (Hubble 100 mas, Keck and Very Large Telescope Interferometers ~10 mas). The region contains the central billion-solar-mass black hole and its accretion disk, including the starting location of relativistic jets and their initial collimation into narrow cones. SIM Lite's single-measurement precision for 16th to 17th magnitude quasars will exceed Gaia's by a factor of 10 to 20, and its end-of-mission precision will be 6 to 10 times better than Gaia's end-of-mission precision (Table 11-1).

Table 11-1. Estimated errors for SIM Lite and Gaia quasar observations.

Spacecraft	End-of-Mission Accuracy, μas	Single-Measurement Error, μas	V mag	No. of AGN and Quasars Observed	No. of Obs.	Radio-Loud Fraction
SIM Lite: Science	4	11	13–18	50	150[b]	80%
SIM Lite: Grid	4	16	16	50	150[a]	40%
Gaia	25	150	<16	200	80–100[c]	10%
	70	400	<18	20,000	80–100[c]	10%
	200	1200	<20	500,000	80–100[c]	10%

[a] Measurement cadence matches grid star measurement cadence   [b] Measurement cadence determined by science
[c] Measurement cadence determined by mission design

The ability of SIM Lite to measure motions and position differences on μas scales means that we can study AGN on scales of tens to hundreds of Schwarzschild radii, which previously has been achieved only at radio wavelengths with very long baseline interferometry. Some of the most exciting theoretical questions in quasar research today are:

1. Where are relativistic jets triggered?
2. Do the cores of galaxies harbor binary supermassive black holes remaining from galaxy mergers?
3. What makes some quasars highly variable and radio-loud but most quasars radio-quiet?

Specific observational questions that SIM Lite can address include:

1. Does the compact optical emission from an AGN come from an accretion disk, a corona, or a relativistic jet?
2. On what physical scales does collimation into a narrow jet occur?
3. Are different regions visible when a quasar flares or fades? How stable is the separation of the radio core and the optical photocenter of the quasars used for the reference frame tie?
4. Is there direct evidence of orbital motion in the cores of quasars and other active galactic nuclei?
5. How are the Broad-Line-Region clouds stratified at distinct distances from the continuum-emitting nucleus: in cones, filaments, or "smoke rings" across the nuclear region?

A supermassive black hole with mass scaling as 0.1 percent of its host galaxy's spheroidal bulge is surrounded by an accretion disk and corona, and in some cases, a pair of relativistic jets, according to current AGN models. Unifying schemes seek to relate a few underlying physical parameters (mass, accretion rate, spin, magnetic field, viewing geometry) to the observed properties. Observationally, in radio-quiet quasars (RQQs, which make up 90 percent of all known quasars), the optical emission has continuum power laws, emission lines, and a thermal Big Blue Bump (BBB). Radio-loud quasars have an additional nonthermal power-law continuum attributed to strong relativistic jets. To understand how SIM Lite observations can provide insights into the physical processes in AGN, we depict the canonical quasar model in Figures 11-1a and 1b. Table 11-2 lists candidate targets for SIM Lite.

Figure 11-1a. Schematic diagram (logarithmic scaling) of the structure of a typical quasar on scales from 0.002 to 100 pc, after Elvis (2000) and Niall Smith (private communication, Cork Institute of Technology). Differential astrometry with SIM Lite allows us to study the central regions (the Broad-Line Region and the base of the jet) on a scale of µas far below the resolution of any imaging telescope.
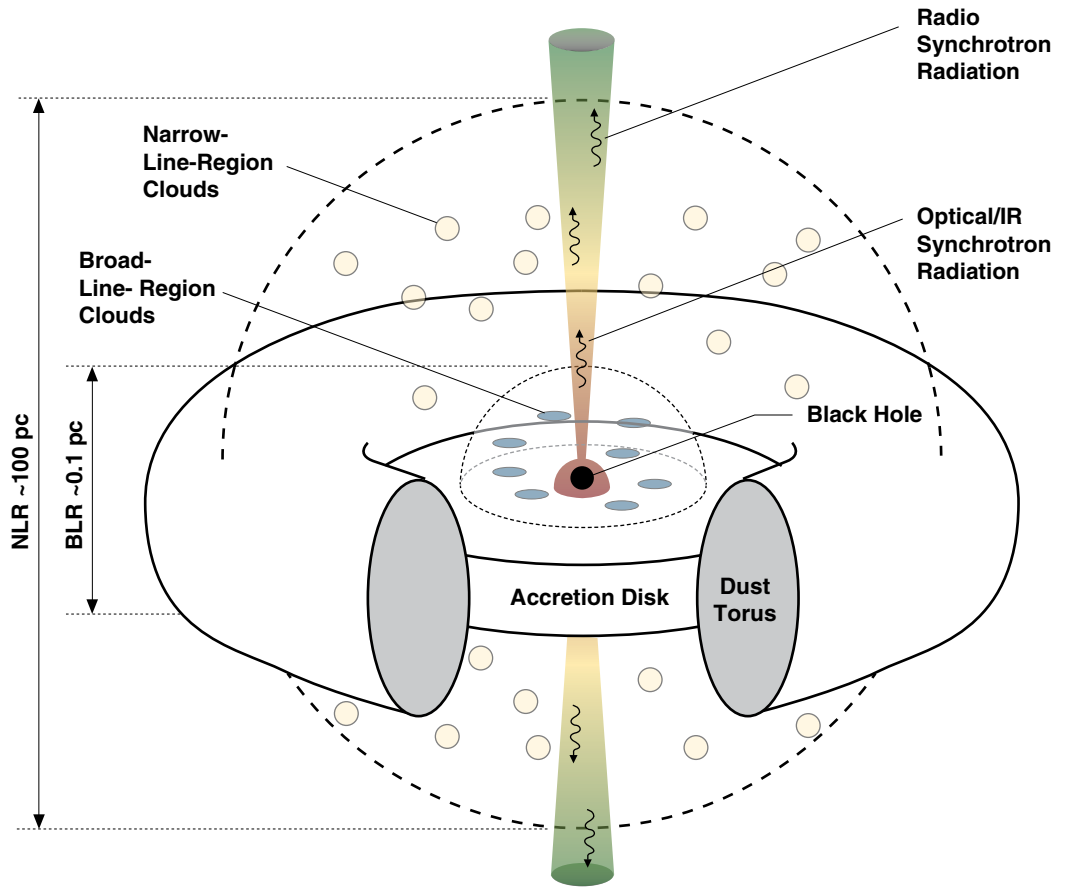
Figure 11-1b. The origin of optical emission from a quasar nucleus (shown schematically, with logarithmic scaling) on scales that are not resolved by any imaging telescope. SIM Lite astrometry can directly probe the emission on the scale of the corona, the thin disk, and the base of the relativistic jet. The astrometric signal, its spatial alignment, and its variability depend on the relative strength of these components.
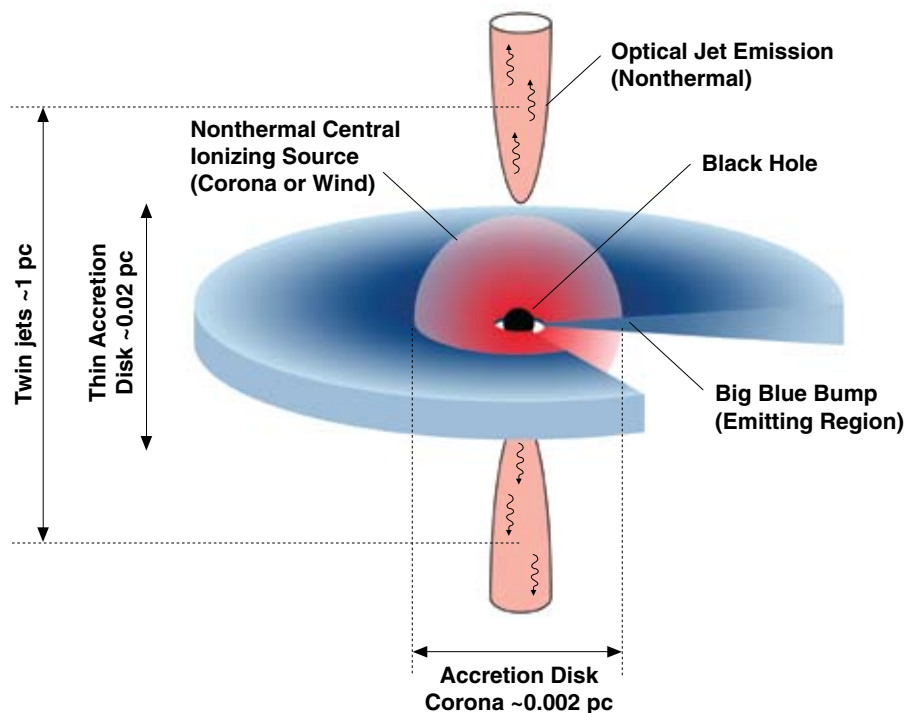
Table 11-2. Characteristics of candidate quasar and AGN targets.

Sample Targets	Redshift or Distance	Distance Subtended by 10 μas, Light-Days	Optical Magnitude Range, V	Black Hole Mass, $M_\odot$	Class
M87	17 Mpc	1.3	17 (nucleus)	3.2×10^9	Nearby AGN
3C273	0.158	32	12–13	1.7×10^7	Nearest Quasar
OJ287	0.306	52	14–17	2.0×10^9	Blazar, binary candidate
3C279	0.536	73	14–18	2.8×10^8	Blazar
3C454.3	0.859	84	13–17	1.5×10^9	Blazar

References for mass estimates: M87: Macchetto et al. 1997; 3C273, 3C279, 3C454.3: compilation by Woo and Urry 2002; OJ287: Valtonen et al. 2008a.

11.2 Accretion Disk, Corona, or Jet: Distinguishing AGN Models Using Color-Dependent Astrometry

SIM Lite can directly test the currently suggested AGN models by measuring a color-dependent positional shift in radio-loud quasars (RLQs) and radio-quiet quasars (RQQs). A relative positional displacement in optical photocenter between the red and blue ends of the SIM Lite passband can be readily measured on the μas level and is very insensitive to systematic errors. SIM Lite measurements will be primarily limited by photon noise, not instrument errors. This color-dependent displacement, its time-derivative in variable sources, and its direction on the sky can be compared to the orientation of a radio jet imaged by VLBI or the VLA. We do not expect to see such a shift in RQQs because of the absence of any contribution of a relativistic jet whose optical emission might introduce an astrometric asymmetry. The red emission from the corona and the blue emission from the disk both should be coincident with the central black hole within ~1 μas. Any color-dependent astrometric shift seen in RQQs would challenge the current models of accreting systems in AGN. By contrast, the astrometric position may be strongly color-dependent in any object with strong optical jet emission. So while the blue end of the spectrum should be dominated by the thermal disk, the red region may be dominated by the beamed relativistic jet. Furthermore, we would expect any variable position shift to be aligned on the sky with the direction of the shift itself (Figure 11-2).

An example of a moderate-redshift jet-dominated quasar is 3C345 ($z = 0.6$), for which the red optical jet emission should be roughly coincident offset by ≈10 μas with the 22 GHz radio emission, at about 80 μas from the black hole. For 3C273 ($z = 0.16$), the separation may be as large as 300 μas. Not only is such a large shift readily detectable, but SIM Lite could also detect variations in the offset with time.

In the nearby radio galaxy M87 we expect the red optical emission to be dominated by the accretion disk corona because its jets are not pointing within a few degrees of our line of sight. Therefore, SIM Lite should not see a significant shift of the optical photocenter as a function of color in this source. However, M87 is so close that we might see an absolute position offset between the measured radio center and the optical photocenter because the location of the last scattering surface is farther from the black hole for radio photons than for optical photons. This radio-optical position offset should be even larger for this low-redshift radio galaxy than for 3C345 — perhaps in the 1000 μas range.
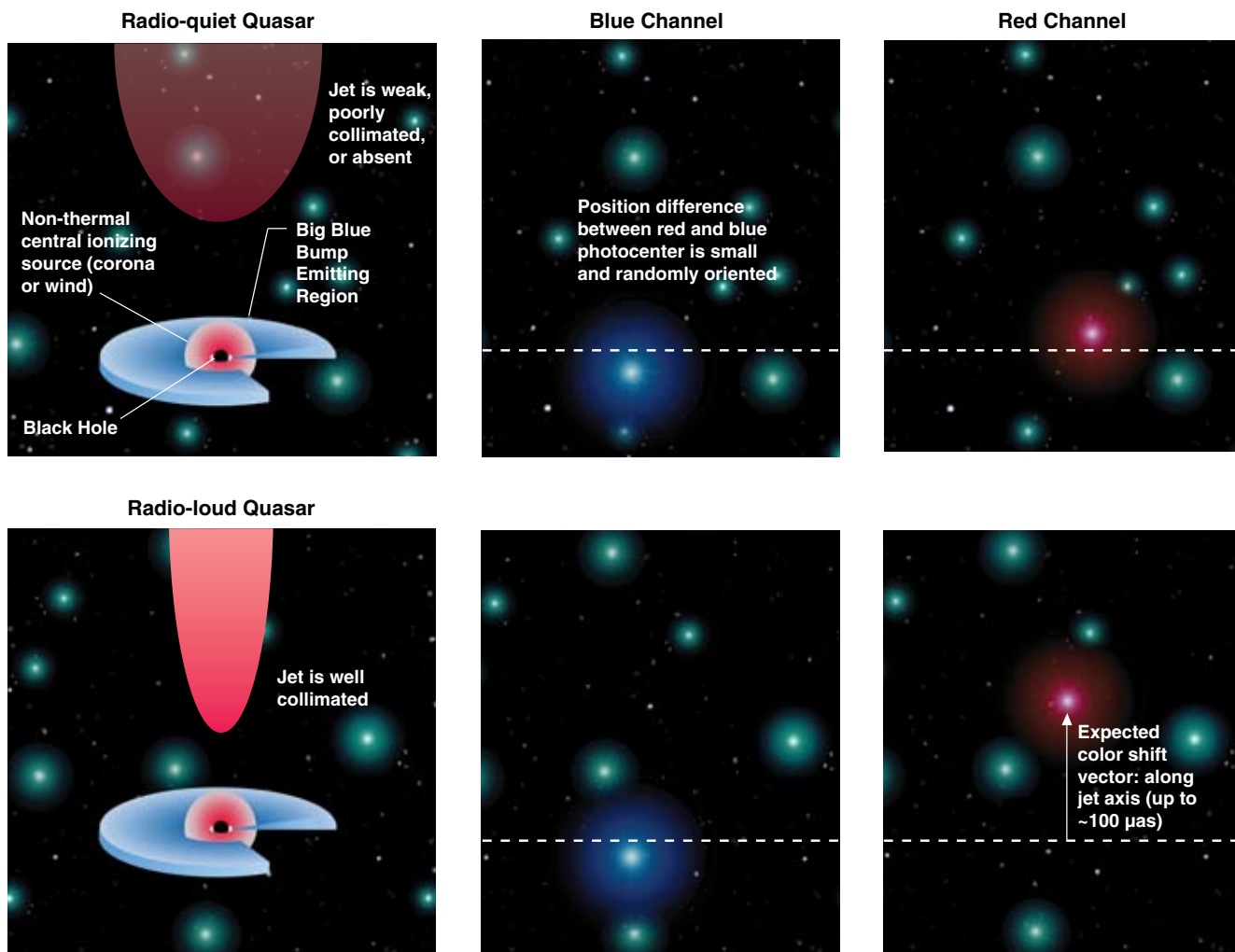
Radio-quiet Quasar

Jet is weak, poorly collimated, or absent

Non-thermal central ionizing source (corona or wind)

Big Blue Bump Emitting Region

Black Hole

Blue Channel

Position difference between red and blue photocenter is small and randomly oriented

Red Channel

Radio-loud Quasar

Jet is well collimated

Expected color shift vector: along jet axis (up to ~100 μas)

Figure 11-2. SIM Lite can use color-dependent astrometry to directly probe the collimation region at the base of a quasar's relativistic jet. Upper panel: in a radio-quiet quasar, any color shift is expected to be small and random. Lower panel: in a radio-loud quasar, a strong asymmetry is expected in the astrometric position between red and blue light; this shift should be aligned with the jet axis. If the quasar is variable, the astrometric variability should be along the same axis.

11.3 Physical Scales on Which Jet Collimation Occurs

In the high-accretion case, the accretion disk produces a thermal peak in the near-ultraviolet region. For a typical 10^9 $M_\odot$ black hole system, accreting at 10 percent of the Eddington rate, the diameter of the portion of the disk that is radiating at a temperature of 10^4 K or above is ~ 3.6×10^{16} cm, or 0.012 pc (Shakura 1973). At a nearby distance of 15 Mpc, this region would subtend an angular size of ~160 μas, while at moderate redshift ($z = 0.6$), the angular size would be only ~2 μas.

Coronal emission is probably nonthermal — either optical synchrotron or inverse-Compton-scattered emission from a radio synchrotron source. For most quasars, this is not beamed optical radiation from a relativistic jet, because there is no evidence that the geometry is that of a narrow cone, so the corona is expected to emit fairly isotropically. Models of this ionizing source (e.g., Band and Malkan 1989) indicate a size of only ~70 Schwarzschild radii (R_S). At moderate redshift ($z = 0.5$), this subtends an angular size of only ~1 μas, centered on the black hole and comparable in size to the Big Blue Bump.

The physical process by which jets are accelerated is an active area of research. For example, a powerful jet may not be produced unless the central black hole is spinning rapidly (Wilson and Colbert 1995; Blandford 1999; Meier et al. 2001). The Konigl (1981) model for relativistic jets predicts that

the majority of the optical emission comes not from synchrotron emission from the base of the jet but from synchrotron-self-Compton emission in the region of the jet where the synchrotron emission peaks in the radio or millimeter (Hutter and Mufson 1986). An alternative model developed by Marscher et al. (2008), based on simultaneous VLBI and optical polarization monitoring, suggests that knots of optical emission move outward through an acceleration and collimation zone toward a standing conical shock region thought to be the "core" at millimeter wavelengths.

Absolute position offsets between SIM Lite optical observations and radio positions can be measured on the ~10 μas level (limited by the definition of the radio frame) because the SIM Lite inertial coordinate frame will be aligned to the radio International Celestial Reference Frame (ICRF) (see Section 11.4).

11.4 Quasar Flaring and Fading and the Effect on the SIM Lite Reference Frame

About 10 percent of RLQs (i.e., about 1 percent of all quasars) are blazars — strong and variable compact radio sources that also emit in the optical (mainly red and near-infrared) and in x-rays and gamma rays and viewed by us nearly end-on to the jet. Looking down the jet allows us to "stick our heads in the beam" of the most energetic particle accelerators in the Universe. In many cases, their radio jets flow at relativistic speeds (Lorentz factors of 10 or more; 99 percent of the speed of light). Relativistic beaming toward the observer produces an order of magnitude or more increase in apparent radio luminosity as well as apparent "superluminal" proper motions of jet components of up to 1000 μas yr^{-1}. Tiny changes in the intrinsic brightness of the jet or in its direction with respect to the line of sight alter the observed brightness significantly. The jet components are identified with moving and stationary shocks in the plasma flow (see, for example, Marscher et al. 2008). If they display similar internal proper motions in their optical jets, these would be readily detectable with SIM Lite. We expect that when a quasar is in a faint state, the optical emission from the BBB and corona are revealed, and when the quasar brightens by 30 to 100 times during a flare, the synchrotron jet emission completely swamps the other components.

SIM Lite can measure absolute proper motions to the level of its global reference frame. Observations of grid stars and quasars will provide this inertial reference frame on the ~4 μas per year level, exceeding the accuracy of the current ICRF (see Chapter 12).

Nearly 100 percent of the ICRF sources are known or assumed to be blazars because they are the most compact radio sources. However, ICRF sources are optically faint (~15 to 25 mag in V), polarized, and variable by up to 5 magnitudes on time scales of months. A sample of non-ICRF RQQs will be defined and observed that will have a typical optical magnitude of V ~15 to 16. SIM Lite will observe 30 ICRF sources in order to tie the SIM Lite optical and ICRF radio reference frames together. An additional 25 non-ICRF RQQ sources will be observed for the SIM quasar reference frame itself and for astrophysical research.

11.5 Finding Binary Black Holes

Do the cores of galaxies harbor binary supermassive black holes remaining from galaxy mergers? If massive binary black holes are found, we will have a new means of directly measuring their masses and estimating the coalescence lifetimes of the binaries.

SIM Lite can detect binary black holes in a manner analogous to planet detection: by measuring positional changes in the quasar optical photocenters due to orbital motion. If a quasar photocenter traces an elliptical path on the sky, then it could harbor a binary black hole; if the motion is random, or not

detectable, then the quasar shows no evidence of binarity. How is it possible that an entire AGN black hole system could be in orbit about another similar system (Figure 11-3)? Such a situation can occur near the end of a galactic merger, when the two galactic nuclei themselves merge. Time scales for the nuclei themselves to merge, and the black holes to form a binary of approximately one pc in size, are fairly short (on the order of several million years) and significantly shorter than the galaxy merger time (a few hundred million years). Furthermore, once the separation of the binary becomes smaller than 0.01 pc, gravitational radiation also will cause the binary to coalesce in only a few million years (Krolik 1999). However, the duration of the "hard" binary phase (separation of 0.01 to 1 pc) is largely unknown, and depends critically on how much mass the binary can eject from the nucleus as it interacts with ambient gas, stars, and other black holes (Yu 2002; Merritt and Milosavljevic 2005). Depending on what processes are at work, the lifetime in this stage can be longer than the age of the Universe (implying that binary black holes are numerous) or as short as the "Salpeter" time scale

Figure 11-3. Artist's impression of a binary black hole pair in OJ287 (image courtesy Mauri Valtonen, Tuorla Observatory). SIM Lite will be able to track the motion of the suspected black hole pair.
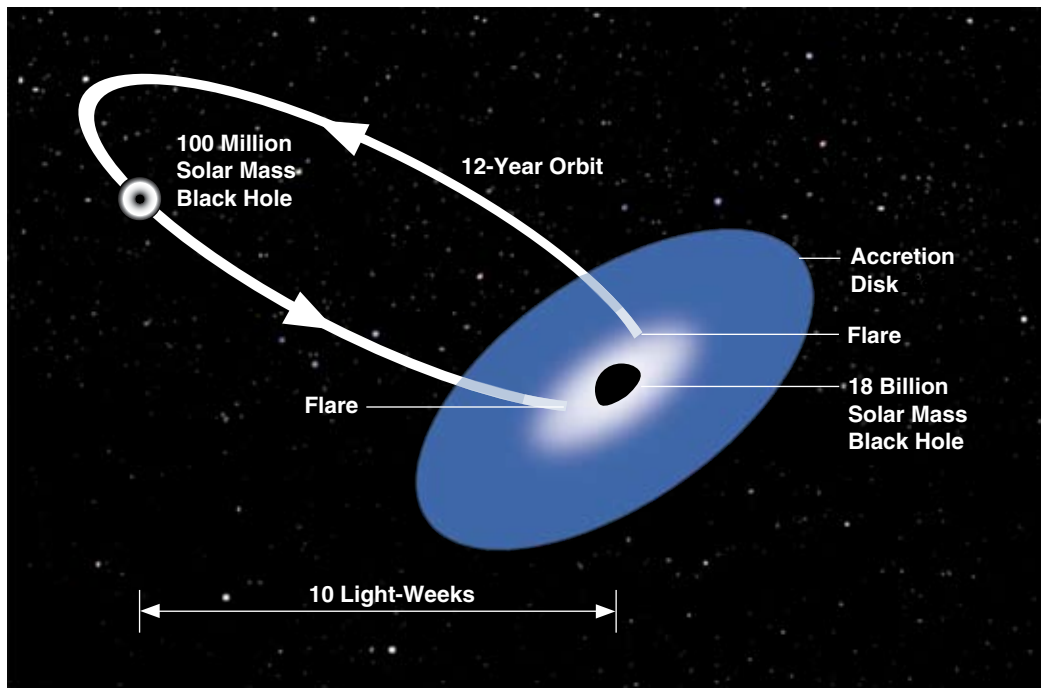
$(M_1 + M_2) / \dot{M}_{Edd} \sim 5 \times 10^7$ years, implying that binaries might be rare). Therefore, the search for binary black holes in the nuclei of galaxies will yield important information on their overall lifetime and on the processes occurring in galaxies that affect black holes and quasars. A promising candidate may be an object that looks like a quasar (with broad lines and optical–UV continuum) but with absolute luminosity being somewhat less than 10 percent of the Eddington limit expected from the central black hole. These might be objects with a large, but dark, primary central black hole that is orbited by a secondary black hole of smaller mass; the secondary would have cleared out the larger hole's accretion disk interior, but still will be accreting prodigiously from the inner edge of the primary's disk (Milosavljevic and Phinney 2005). In this case, the astrometric motion would indicate the full orbit of the secondary about the primary, which could be a few to a few hundred µas, depending on the source distance.

When the optical emission is dominated by the nonthermal jet that is some distance from the black hole, rather than by the thermal accretion disk that is centered on the hole, an unusual time-dependent astrometric signature (such as a corkscrew) might be seen instead of an ellipse.

OJ287 is one of the most promising binary black hole candidates. It shows quasi-periodic brightness variations that come in pairs separated by one or two years, and each pair occurs about 12 years apart (Kidger 2000; Valtonen et al. 2006, 2008a). This behavior is best modeled as a secondary black hole piercing the accretion disk of the primary black hole, producing two impact flashes per period (Lehto and Valtonen 1996). This model is supported by the recent observation of a predicted optical outburst (Valtonen et al. 2008a) and the detection of a predicted soft x-ray excess bump by the Rossi X-Ray Timing Explorer (RXTE) and the X-Ray Multi-Mirror (XMM-Newton) observatory (Valtonen 2008b). For an assumed orbital period of 24 years, a binary black hole system with a mass of at least 10^{10} solar masses has a mean separation of 0.07 pc. For OJ287 ($z = 0.306$), this separation subtends 15 μas, and the orbital motion expected during a five-year span is about 19 μas. For closer systems (e.g., 3C273, M87), SIM Lite will be sensitive to binaries of much lower mass.

About a half dozen of low-redshift quasars and AGN such as 3C273 will be observed with SIM Lite to look for possible binary black holes. These observations require a very high single-epoch positional accuracy and many individual epoch observations over the lifetime of the mission. Thus, only compact, bright, and nearby targets are considered.

11.6 Distribution and Location of the Broad-Emission-Line Clouds

Within the inner pc, clouds of ionized gas that emit lines Doppler-broadened by a few percent of c are observed in the optical spectra of many quasars and Seyfert galaxies (Figure 11-4). Narrow-line (<0.1 percent c) clouds appear tens to hundreds of pc from the nucleus.

The technique of reverberation mapping measures the time delay between changes in the continuum and resulting changes in the broad lines, and so the distance in cm. As the line width gives a size in Schwarzschild radii, the mass of the central black hole can be measured (for a review, see Peterson

Figure 11-4. Broad lines, e.g., Magnesium II and Hydrogen α, β, and γ, are emitted from Seyfert galaxies like NGC4151, radio galaxies, and quasars like 3C273. The structure of the broad-line region can be elucidated with SIM Lite phase offset observations that show the relative positions of high and low ionization line-emitting gas and the continuum source. Image courtesy of William Keel.
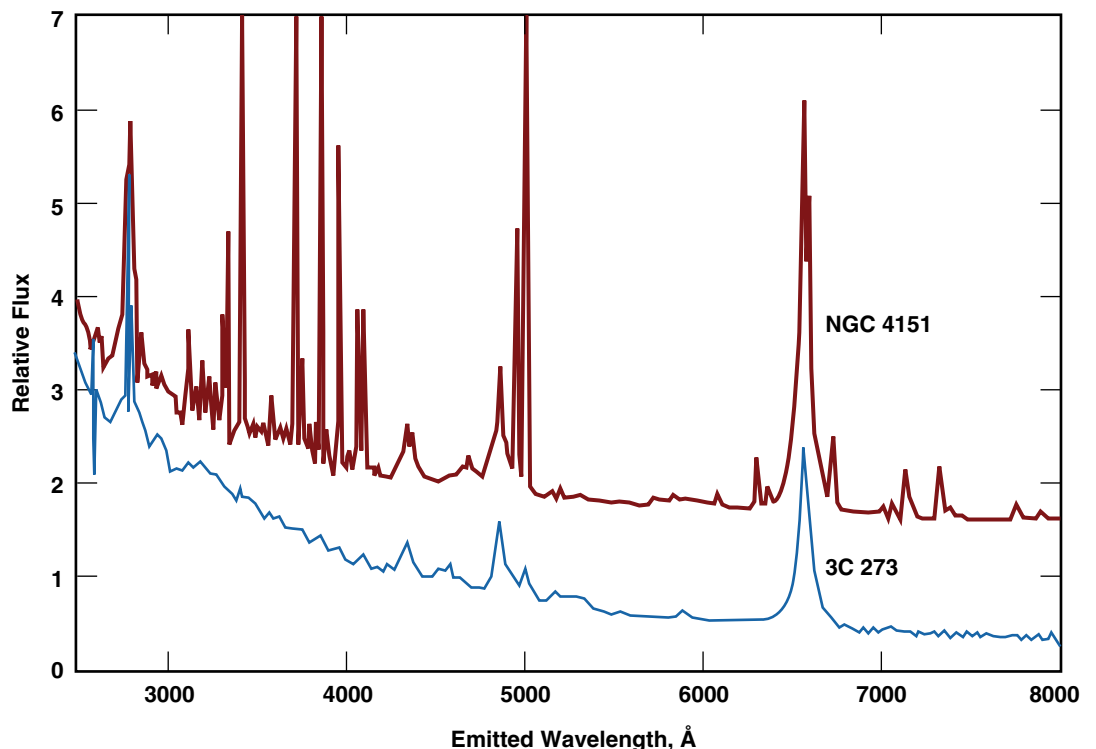
1993, and for analysis and compendium see Peterson et al. 2002). The light detected by the 80 channels of SIM Lite's CCD can be binned to separate the light from emission lines and the intervening continuum emission. Pioneering observations of Be stars made with this technique are underway at the Navy Prototype Optical Interferometer.

Using the same technique as the red/blue color differential measurement described in §11.2, the measured phase offsets from various emission lines may be compared to each other and to the continuum. Lines with different ionization potential are produced at different radii from the central ionizing source, with higher ionization lines nearer to the center than lower ionization lines; i.e., the ionization structure is stratified. For example, distant low-ionization clouds producing Fe II, broad Mg II (2798 Å), and the broad Balmer lines may be an outer extension of the accretion disk. However, some fraction of the Balmer-line-emitting clouds may arise along with higher ionization lines such as He II (4686 Å) and C IV (1549 Å) as part of a wind escaping the disk (Murray and Chiang 1995) in a system of filaments or thin sheets on either side of the nucleus along the cone surfaces (e.g., Elvis 2000), as shown in Figure 11-5. For example, reverberation mapping from ground-based and space-based telescopes has shown the Hβ and Mg II clouds are about seven light-days from the central continuum source in NGC4151 (Bentz et al. 2006; Metzroth, Onken, and Peterson 2006), although there is currently little to constrain the geometry of the line-emitting region (Ulrich and Horne 1996). Understanding the structure and distribution of the broad-line clouds will remove the factor of 2 to 3 geometric uncertainty in reverberation-based

Figure 11-5. The Broad-Line Region (0.1 pc) subtends 25 µas in a quasar at redshift 0.5; the central accretion disk about 1 µas. Spectral lines with different ionization potential are produced at different radii from the central ionizing source, with higher ionization lines nearer to the center than lower ionization lines; i.e., the ionization structure is stratified, as indicated by the change in colors with radial distance from the central region. SIM Lite can illuminate the structures present with red/blue color differential measurements. Artist's concept by David Hinkle, JPL.

masses of the central supermassive black hole, which is of fundamental importance in understanding the physics of AGN, and of the origin of the relationship between black hole mass and velocity dispersion (Ferrarese and Merritt 2000; Gebhardt et al. 2000) that revolutionized our understanding of black hole–Galaxy co-evolution.

Acknowledgments

References

Blandford, R., 1999, in Astrophysical Discs — An EC Summer School, Astronomical Society of the Pacific, Conference series, vol. #160, eds. J. A. Sellwood and Jeremy Goodman, p. 265.

Band, D. L. and Malkan, M. A., 1989, ApJ, 345, 122.

Bentz, M. et al., 2006, ApJ, 651, 775.

Elvis, M., 2000, ApJ, 545, 63.

Ferrarese, L. and Merritt, D., 2000, ApJ, 539, L9.

Gebhardt, K. et al., 2000, ApJ, 539, L13.

Hutter, D. J. and Mufson, S. L., 1986, ApJ, 301, 50.

Jester, S., Meisenheimer, K., Martel, A. R. , Perlman, E. S., and Sparks, W. B. , 2008, MNRAS, 380, 828.

Kidger, M. R., 2000, AJ, 119, 2053.

Konigl, A., 1981, ApJ 243, 700.

Krolik, J., 1999, Active Galactic Nuclei, (Princeton University Press: Princeton).

Lethto, H. J. and Valtonen, M. J., 1996, ApJ, 460, 207.

Macchetto, F. et al., 1997, ApJ, 489, 579.

Marscher, A. et al., 2008, Nature, 452, 966.

Meier, D. L., Koide, S., and Uchida, Y., 2001, Science, 291, 84.

Merritt, D. and Milosavljevic, M., 2005, Living Reviews in Relativity, 8, 8.

Metzroth, K. G,, Onken, C.A., and Peterson, B. M., 2006, ApJ, 647, 901.

Milosavljevic, M. and Phinney, S., 2005, ApJ, 622, L93.

Murray, N. and Chiang, J., 1995, ApJ, 454, L105.

Peterson, B., 1993, PASP, 105, 247.

Peterson, B. et al., 2002, ApJ, 613, 682.

Tsvetvanov, Z. et al., 1998, ApJ, 493, L83.

Ulrich, M.-H. and Horne, K., 1996, MNRAS, 283, 748.

Unwin, S. C., Wehrle, A. E., Urry, C. M., Gilmore, D. M., Barton, E. J., Kjerulf, B. C., Zensus, J. A., and Rabaca, C. R., 1994, ApJ, 432, 103.

Valtonen, M. J. et al., 2006, ApJ, 643, 9.

Valtonen, M. J. et al., 2008a, Nature, 452, 851.

Valtonen, M. J., 2008b, RevMexAA, 32, 22.

Wilson, A. S. and Colbert, E. J. M., 1995, ApJ, 438, 62.

Woo, J-H. and Urry, C. M., 2002, ApJ, 579, 530.

Yu, Q., 2002, MNRAS, 331, 935.

12 Astrometric Reference Frame Science
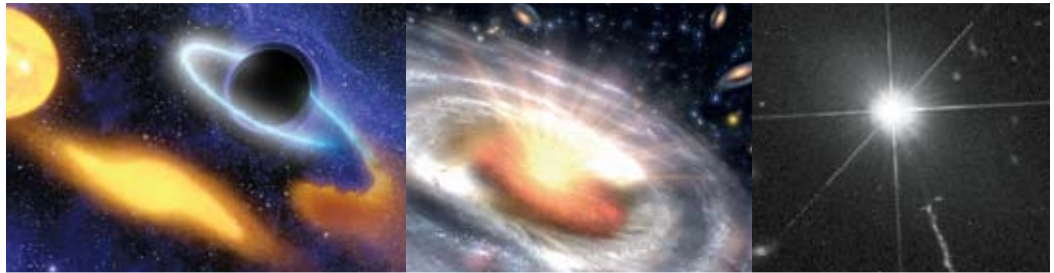
Kenneth J. Johnston (USNO), **Ann E. Wehrle** (Space Science Institute), **Valeri Makarov** (NExScI), **David W. Murphy** (JPL), **Stephen C. Unwin** (JPL), **Norbert Zacharias** (USNO), **Alan L. Fey** (USNO), **Roopesh Ojha** (USNO), and **David A. Boboltz** (USNO)

ABSTRACT

The establishment of an inertial reference frame based on grid stars anchored with extragalactic sources will allow for the first time the direct detection of the motion of the Solar System within the Milky Way as well as the Local Group toward the Virgo cluster at the µas/year level. All of this will be accomplished by observing stellar motions with respect to distant "fixed" quasars, which provide an inertial frame against which absolute proper motions can be measured. At the same time, this inertial frame enables possible detection of the apparent motion of the center of light of some "peculiar" quasar sources. By establishing an accurate link between the optical SIM Lite frame and the radio International Celestial Reference Frame (ICRF), high-resolution imaging data at these different wavelengths can be accurately lined up for absolute positional correlation. This enables a better understanding of the mechanisms giving rise to their spectral energy emission.

12.1 Introduction

SIM Lite is an astrometric mission capable of defining a global grid of stars with positions to 4 μas (Makarov and Milman 2005), along with approximately 50 extragalactic sources to similar precision, will establish a new reference frame that will calibrate all the studies of the SIM Lite mission and be applicable to many other astrophysical studies. Here we discuss the inclusion of quasars into the SIM Lite grid and the resulting improvements in the SIM Lite reference frame. In addition, we discuss the science that can be accomplished on the objects comprising the frame, namely the quasars themselves, and the science enabled by a more precise SIM Lite grid and by an accurate tie to other celestial reference frames.

12.2 Quasars and the SIM Lite Astrometric Grid

Aside from their astrophysical properties, which can be studied with SIM Lite (see Chapter 11), quasars are critical objects for the formation of a robust astrometric grid. This grid frame forms the astrometric bedrock on which all other SIM Lite observations are built. Even the narrow-angle differential astrometry (e.g., planet detection and microlensing) relies on the grid solution in determination of baseline and instrument parameters.

SIM Lite grid simulations using grid stars alone have shown that the resulting astrometric grid has two undesirable properties. First, there is a relatively large offset in the parallax common to all grid stars from mission realization to mission realization, known in astrometry as zero-point error. Second, the entire frame formed by the grid can spin about some arbitrary axis at an arbitrary rate and thus be non-inertial. Quasars, in particular radio-quiet quasars (RQQs) with little or no optical jet emission, are ideal additions to the grid that can correct these defects. Quasars are typically so far away (of order 1 Gpc) that on the μas scale they have no parallax and probably no peculiar proper motion. Our extensive analysis and simulations have shown that quasars are ideal objects to remove both the grid frame parallax bias and other large-scale distortions (zonal errors), and the residual spin. For example, the overall accuracy of parallax with only 23 quasars in the grid improves significantly, as seen in Figure 12-1.

Figure 12-1 displays the probability density distribution of the mission-average absolute parallax error for 13,000 individual SIM Lite mission realizations with grid stars only (blue histogram). Although the median and the mode performance are within the goal requirements, the long sloping tail of the distribution toward larger errors shows that accidentally poor performance cannot be precluded. With only 23 quasars in the grid, the probability distribution (red histogram) becomes narrow and the tail is eliminated. Consequently, a dramatic improvement is observed in confidence intervals on the mission performance; for example, the 99 percent confidence on the parallax accuracy improves by more than a factor of 2. Other studies have been performed that show how the gain in astrometric performance and confidence varies as function of the number of quasars used and the length of time that they are observed. Using vector spherical harmonics to fit quasar proper motions resulting from the residual frame spin allows this spin to be removed from all objects. Figure 12-2 illustrates distribution of potential SIM Lite grid quasar targets on an Aitoff equal-area projection of the celestial sphere.

In summary, quasars are a practical insurance policy for the SIM Lite mission to achieve excellent astrometric performance, for a cost of only a few percent of the total mission observing time. Photometric observations (Ojha et al. 2008) of selected, bright (R ≤ 16; UBVRI system) quasars show that more than 50 suitable candidates are available with a sufficient homogeneous sky distribution. These 50 sources will be observed numerous times each during the mission resulting in single measurement accuracy of 16 μas and mission accuracy of 4 μas.

Figure 12-1. Comparison of the simulated SIM Lite astrometric grid accuracy with and without quasars. Monte Carlo simulations show that without quasars in the grid (blue histogram), the possibility of poor mission performance, while small, cannot be precluded. But when only 23 quasars are included in the grid (red histogram), the probability distribution becomes narrow and the most probable accuracy is greatly improved.
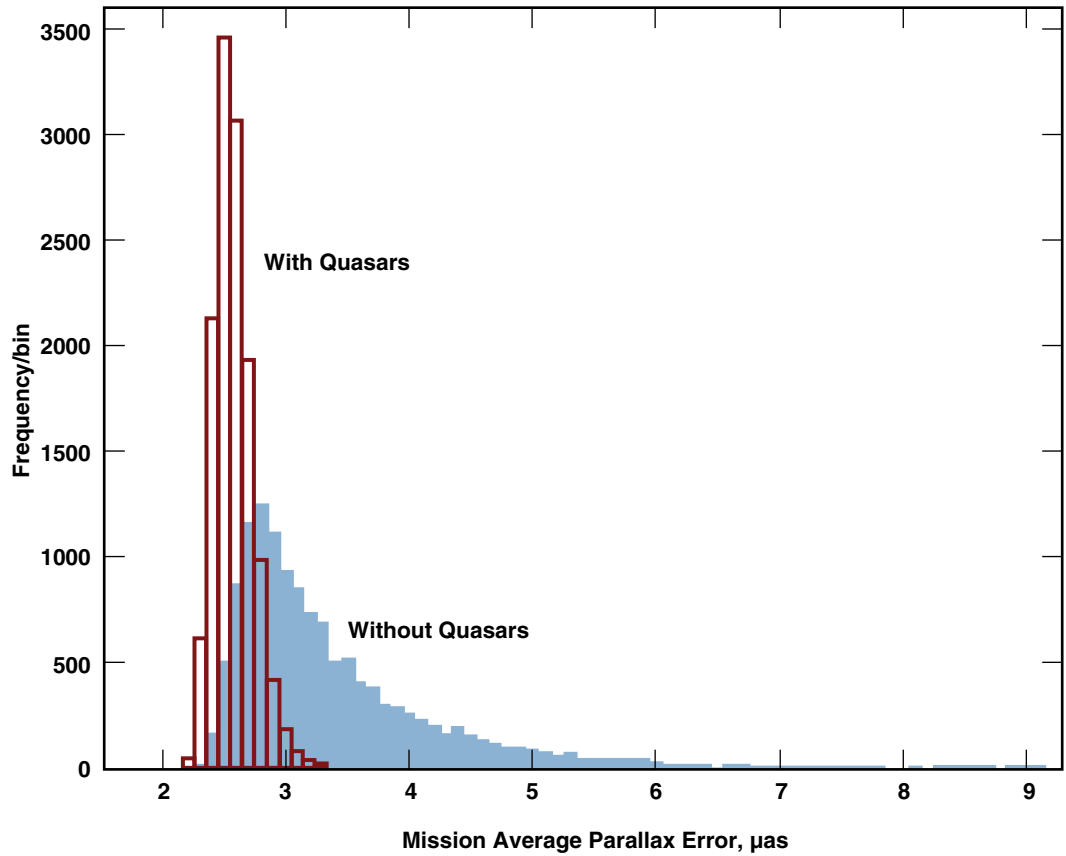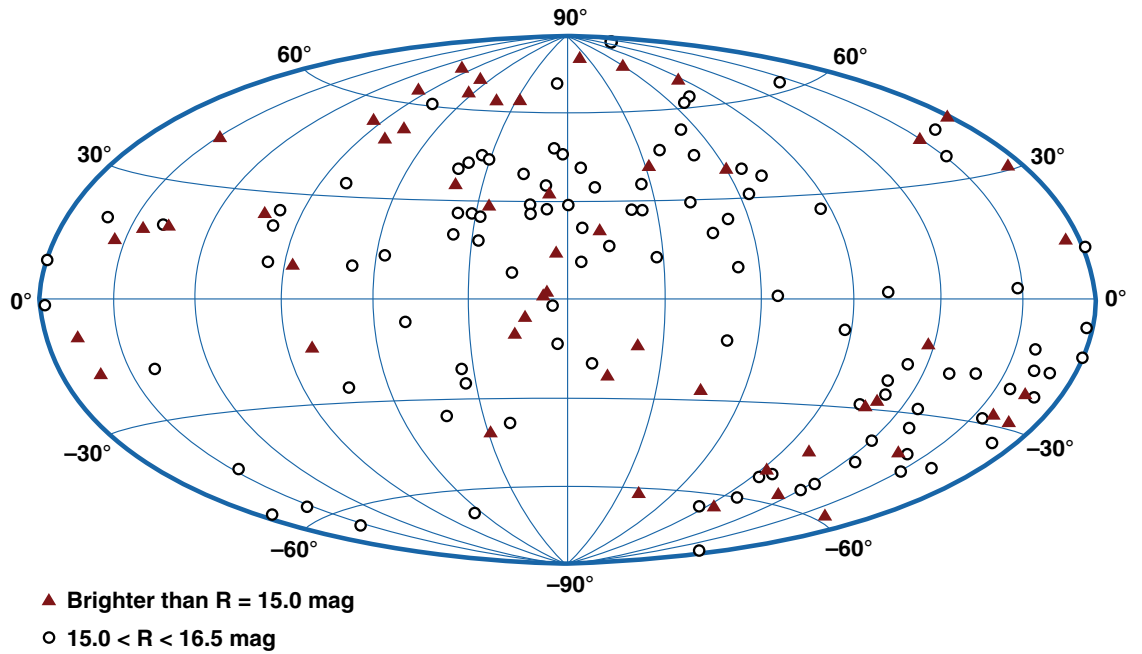

Figure 12-2. Distribution of potential SIM Lite grid quasar targets on an Aitoff equal-area projection of the celestial sphere. USNO photometry for the SIM Lite Project (2005–2007) shows quasars brighter than R = 15.0 mag as red triangles and quasars in the range 15.0 < R < 16.5 mag as open circles.

12.3 SIM Lite–Gaia Complementarity

SIM Lite and Gaia are the next-generation astrometry missions and almost perfectly complement one another, as is well illustrated in Table 12-1. Thus, while SIM Lite will observe fewer objects than Gaia, these objects will have better single-measurement errors (SMEs) and end-of-mission life accuracies, and will be observed more times. In particular, Table 12-1 shows that, for a given magnitude, SIM Lite has a factor of 10 better SMEs, an advantage that will be leveraged to the maximum extent in all the astrophysics it will undertake, and in particular in the quasar and grid astrophysics that are described in Chapter 11. This complementarity is primarily due to the fact that SIM Lite is a pointed instrument where variable integration times are used based on object magnitude, whereas Gaia is a scanning instrument with constant integration time independent of magnitude. SIM Lite, like Gaia, uses quasars as fiducial markers to determine the parallax zero point, the frame spin, and the International Celestial Reference Frame (ICRF) frame tie.

Systematic and zonal errors prove to be the most intractable kind of imperfections in the global astrometry because it is often difficult or impossible to find out their origin and predict their character. At the same time, these imperfections become the main concern for astrophysical research involving large sets of objects, for example, determination of the distance to the Large Magellanic Cloud (LMC) or detection of tidal streams and Galactic merger remnants. We do not know enough about the propagation of zonal errors in Gaia to make a detailed comparison, but one fact is evident: these errors will be very different for Gaia and SIM Lite because of the mission architectures and the astrometric methods that have little in common. SIM Lite will have relatively large imperfections at the largest scales on the sky comparable to 4π, whereas Gaia will probably suffer from zonal errors on the intermediate scale (15 to 50 degrees) where SIM Lite achieves the highest accuracy. Therefore, a comparison of the two reference systems will not only reveal these imperfections, but will probably allow us to correct them by combining the results.

Table 12-1. Estimated errors for SIM Lite and Gaia quasar observations.

Spacecraft	End-of-Mission Accuracy, µas	Single-Measurement Error, µas	V mag	No. of AGN and Quasars Observed	No. of Obs.	Radio-Loud Fraction
SIM Lite: Science	4	11	13–18	50[b]	150	80%
SIM Lite: Grid	4	16	16	50[a]	150	40%
Gaia	25	150	<16	200[c]	80–100	10%
	70	400	<18	20,000[c]	80–100	10%
	200	1200	<20	500,000[c]	80–100	10%

[a] Measurement cadence matches grid star measurement cadence

[b] Measurement cadence determined by science

[c] Measurement cadence determined by mission design

12.4 Grid Science

Establishing the SIM Lite frame is a no-cost benefit to the other SIM Lite science projects, as no additional observing time is required besides the routine grid and extragalactic source observations, nor are changes required in the instrument design or observing schedule. For example, the parameterized post-Newtonian (PPN, Will 2006) prediction for small bending of light in gravitational fields [correction factor, $(1-\gamma)$], can be tested to a few parts in 10^{-5}. SIM Lite will make a significant contribution in the verification of the principles of General Relativity and in testing the causal nature of the gravitational field by making ultraprecise measurements of star positions close to the major planets of the Solar System, in particular,

Jupiter and Saturn. When a planet happens to pass near a background star, the light rays from the latter become deflected by the gravitation of the planet. Utilizing to the full extent the pointing capabilities, the small-field aperture, and the unprecedented precision of small-angle differential observations with SIM Lite, the deflection angles can be measured as functions of time for predicted limb-grazing passages of major planets near brighter stars. Several differential observations with SIM Lite will make it possible to determine not only the main monopole component of this deflection, but also, for the first time, the quadrupole component caused by the oblateness of the planet (Kopeikin and Makarov 2007). Furthermore, the gravitomagnetic term in this deflection, caused by the radial Doppler correction to the planet mass, will amount to a few μas in some instances. Taking several measurements at different relative orbital velocities will enable us to differentiate this exotic effect (not yet observed) from the possible contribution of the scalar gravitational field represented by the γ parameter.

The proper motions of extragalactic sources will display secular aberration drift due to the Sun's orbit around the center of the galaxy. The Sun's own motion in the Galaxy shifts the apparent positions of all stars and quasars in a dipole pattern on the sky (Kopeikin and Makarov 2006). The pattern of secular aberration is in fact not static, but will slowly change with time because of the Sun's galactocentric motion and other components of acceleration. SIM Lite astrometry, at its unprecedented level of precision, will be quite sensitive to this gradual change, which manifests itself as a predictable pattern of apparent angular motions (proper motions) of all objects on the sky. Therefore, quasars will also be involved in this gradual motion on the sky with amplitude of approximately 4.2 μas yr^{-1} (Figure 12-3). Global astrometry of 50 stable grid quasars during five years will allow us to detect and directly determine the solar acceleration in the Galaxy.

Figure 12-3. Simulated secular aberration effect over the celestial sphere showing the effect of the Sun's galactocentric motion, measurable by SIM Lite. This must be fit to the frame quasars used to calibrate the astrometry. Deviations from this pattern will result from changes in the Sun's galactrocentric motion and from gravitational deflections due to massive bodies in our vicinity, including Jupiter and Saturn. This will also probe whether the Sun has a dim companion, long a subject of speculation.
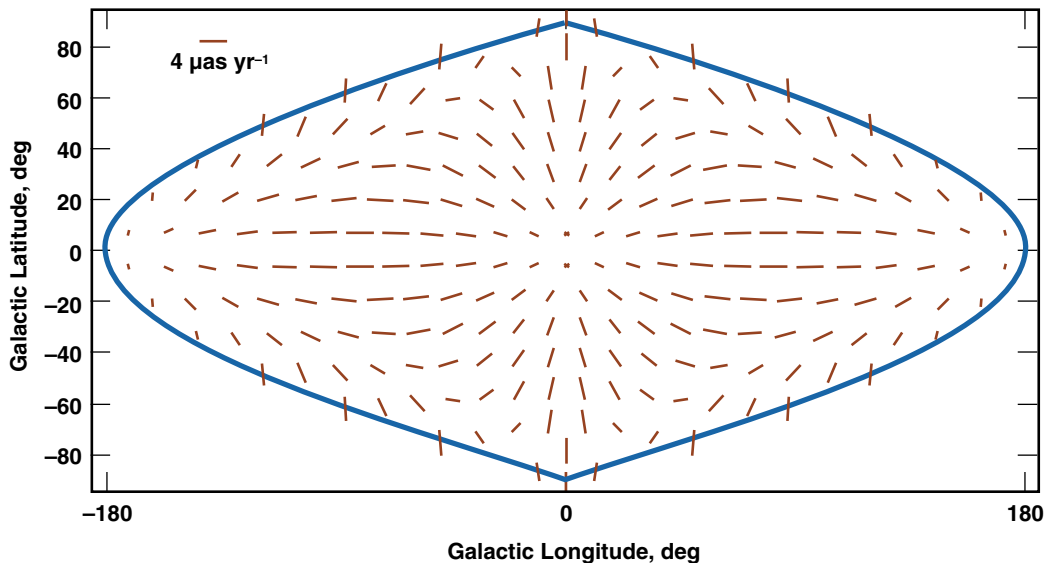
Astronomers have been discussing the intriguing possibility that the Sun has a dim companion (Nemesis) on an eccentric orbit. SIM Lite will be able to detect any invisible gravitating body in our vicinity in an elegant way if this body is close and massive enough. Any acceleration of the Sun (and SIM Lite) caused by the gravitational pull from the companion will be observable as a systematic pattern of apparent proper motions of distant quasars. The axis of this pattern will indicate the direction in which such a companion should be visible. Calculations show that a body more massive than 0.33 M_J (mass of Jupiter) will be safely detected within 100 AU, and anything more massive than 330 M_J within 3160 AU.

Cosmological models of the early Universe imply the existence of relic gravitational waves (GW), including inflation and anisotropic phases. The present-day energy density of these long-period waves is expected to be of order $\Omega_{GW}h^2 \approx 10^{-9}$ and comprise different modes of polarization and power spectrum. A plane monochromatic, linear-polarized GW propagating through the local part of the Universe bends light rays from distant sources in the transverse directions. The latter effect is observable with SIM Lite as apparent motion of quasars on the sky. Because of the quadrupole nature of GW radiation, ~80 percent of power spectrum is carried by second-order vector harmonics of the proper motion field (Gwinn et al. 1997). Most theorists estimate the energy of relic GW to be too small to be actually detected with SIM Lite. However, detection of GW from anisotropic phases in the early Universe may be possible in coherent spectral lines because of the "broadband" nature of astrometric measurements, in that the apparent motion of an object would integrate the wave power over a certain interval of frequency. A nondetection would put upper limits on the energy carried in such coherent spectral lines, with significant implications for cosmology.

12.5   Frame-Tie Science

The current realization of the ICRF is based on very long baseline interferometry (VLBI) positions of sources with accuracies on the order of 300 µas. This accuracy is expected to improve to order 50 to 100 µas with the release of ICRF-2 in the near future. SIM Lite observations of ICRF sources need only to be made to this accuracy to align the SIM Lite frame with the ICRF. There will be an overlap of about 30 sources between the SIM Lite and ICRF frames.

An accurate tie between the SIM Lite frame and the ICRF will provide valuable insights into the physics of quasars and their jets. By directly linking the frames through quasar astrometry, one will be able to investigate the relationship between the radio core and optical photocenter at unprecedented accuracies. Scientific studies related to the linking of the frames will investigate correlations between the variability, separation, motion, and direction of radio/optical jet components close to the point of origin. In addition, an accurate tie between the frames will enable a variety of multi-wavelength scientific studies of both galactic and extragalactic sources. See Chapter 11 by Wehrle et al. for more details on quasar science.

Given the ability of future astrometric satellite missions to directly observe quasars, future ties between the optical and radio frames will naturally be accomplished through observations of such compact extragalactic objects. To enable a high-precision tie between the SIM Lite and ICRF frames, candidate quasars must necessarily exhibit a high degree of astrometric stability at both radio and optical wavelengths. It is well known that the structure of the emission at cm wavelengths has a significant impact on astrometric stability (Fey and Charlot 1997, 2000). This impact is reduced as the observations move toward the mm regime (Charlot et al. 2008). However, the effects of optical source structure and photocenter wander on the µas-level astrometric precision expected for SIM Lite is a completely unexplored region of phase space.

12.5.1   Frame-Tie Quasars

Quasar optical emission may originate from three potential sources: thermal emission from the accretion disk surrounding the black hole, nonthermal coronal disk emission, and for a subset of the extreme radio-loud quasars (i.e., blazars), nonthermal emission from knots in the relativistic jet. Recent results by Marscher et al. (2008), involving simultaneous VLBI and optical polarimetric monitoring, suggest that these knots of optical emission move outward through an acceleration and collimation zone toward a

standing conical shock region thought to be the "core" at millimeter wavelengths. Studies involving the tie between the SIM Lite and radio reference frames have the potential to greatly improve our understanding of this phenomenon by registering and tracking the wander of the optical photocenter relative to the radio core and by correlating changes in the radio and optical flux. Since SIM Lite is a pointed mission rather than a scanning mission, frame-tie investigations will almost certainly take advantage of multi-epoch concurrent SIM Lite/VLBI observations, thus improving both the frame link and the quasar science (see Figure 12-4).
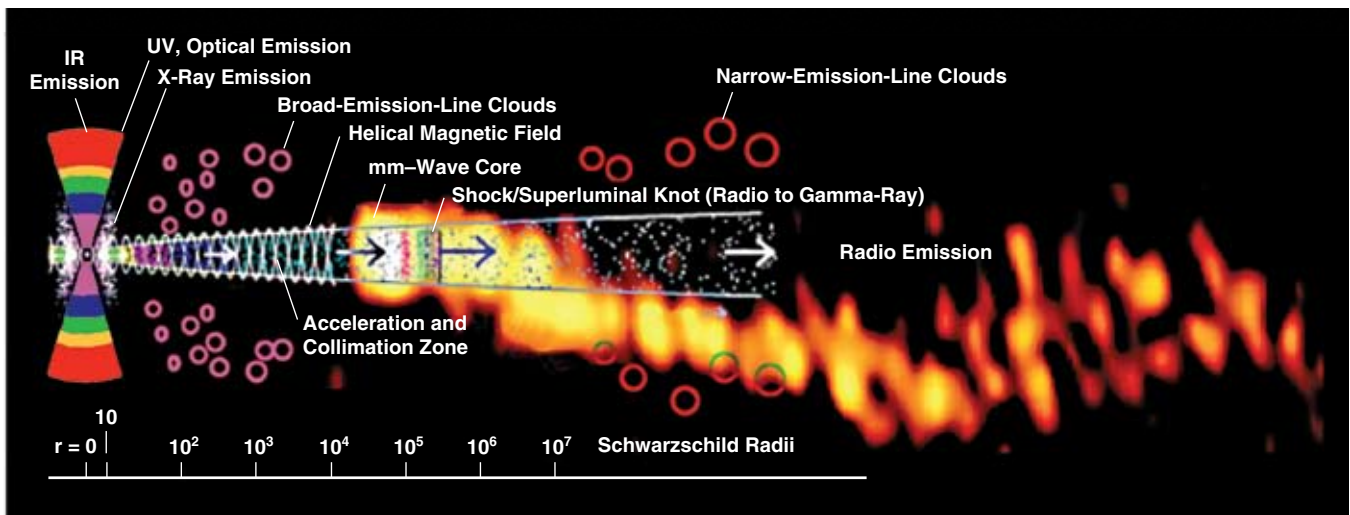
Figure 12-4. Overlay of 3 mm radio image of the blazar 3C454.3 (Krichbaum et al. 1999) on a diagram of a quasar from Marscher et al. (2008), not to scale. The figure shows the potential frame-tie quasar science that could be accomplished with SIM Lite. Knots of optical emission move outward from the black hole's accretion disk (left) through an acceleration zone toward the millimeter and radio "cores" and radio jet (right). Concurrent SIM Lite and VLBI observations will register and track the wander of the optical photocenter relative to the radio core.

12.5.2 Multi-Wavelength Science Enabled by the Frame Tie

There are a variety of galactic sources (e.g., microquasars, RS CVn binaries, Algol binaries, late-type stars, X-ray binaries, etc.) for which an accurate frame tie would enable multi-wavelength science. For SIM Lite, observations will be limited to systems with either a large difference in magnitude between the primary and secondary stars or orbital separations of order of the fringe spacing of the interferometer. Figure 12-5 provides an example of an RS CVn binary system, σ Geminorum, for which the radio emission could be tied to the SIM Lite–determined positions of the stars in the binary. The system consists of a K1 III giant primary with M_V = 4.15 and a companion that is unseen in both photometric and spectroscopic observations. The radio emission as measured with VLBI shows a double-lobed structure with the lobes separated by ~3.4 mas. Interestingly, the major axis of the spectroscopically determined orbit is 2 a sin (i) = 0.13 AU (~3.4 mas at the assumed distance to σ Gem of 37.5 pc). However, without precise astrometric data, it is impossible to determine whether the radio emission is coincident with one or both of the stars at the time of the observations. Possible models for the generation of radio emission in chromospherically active stars include phenomena such as gyro-synchrotron radiation from polar-cap regions of the active K-giant–type star, emission at the tops and/or feet of one or more coronal loops originating on the K-giant, and emission from active regions or hot spots near the surface of both stars in the binary, with possible channeling of energetic electrons from the K-giant to the surface of the smaller companion star along interconnecting magnetic field lines.

For systems such as σ Gem, SIM Lite will provide positional information on the 10 μas level and the three-dimensional orbit for the binary. As a pointed mission, SIM Lite will have the flexibility to coordinate observations with other instruments such as the Very Large Baseline Array (VLBA) to allow the

Figure 12-5. A total intensity contour map of the radio emission from the RS CVn binary system σ Geminorum. The peak flux density is ~55 mJy. The system is composed of a K-giant primary and an unseen companion. The spectroscopically determined major axis of the orbit is 2 a sin (i) = 0.13 AU (~3.4 mas at 37.5 pc). The relative separation between the two radio components is ~3.4 mas. SIM Lite's wide-angle measurement accuracy has to be magnified 50 times to be presented on the scale of this map.
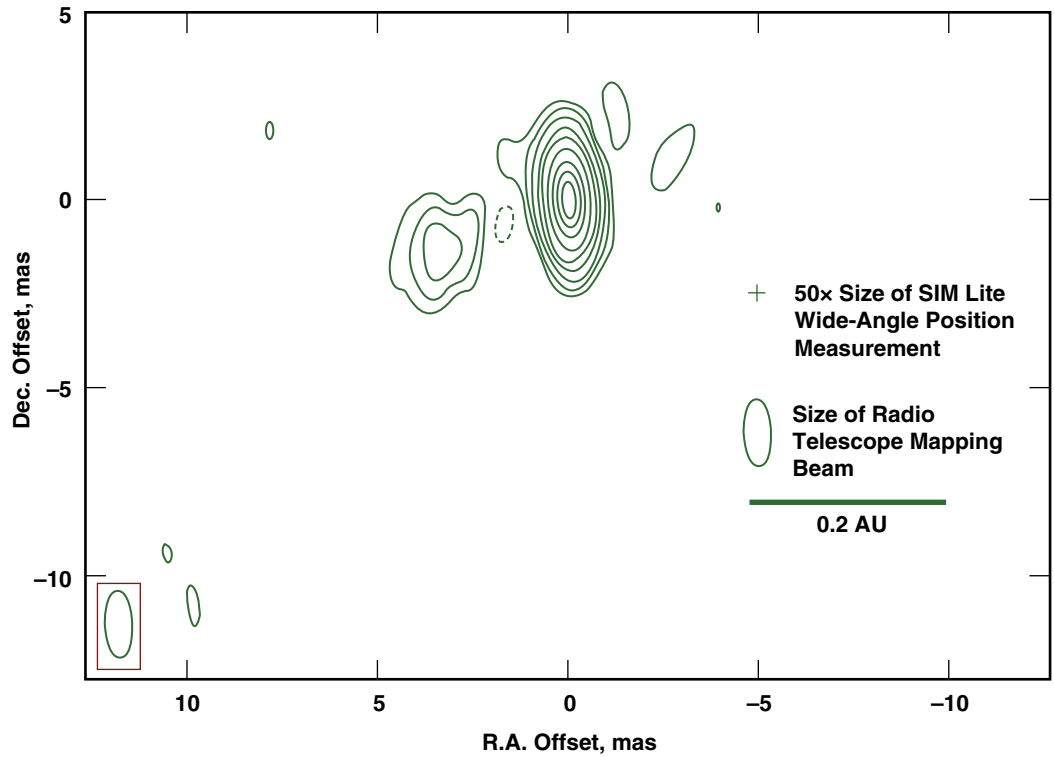
registration of the radio emission relative to the system components for systems with orbital periods on the order of days. This more complete picture of the system will, in turn, help to distinguish between the various mechanisms by which the radio emission is generated.

References

Charlot, P. et al., 2008, AJ (in press).

Fey , A. F. et al., 1997, ApJS, 111, 95.

Fey, A. F. et al., 2000, ApJS, 128, 17.

Gwinn, C. G. et al., 1997, ApJ, 485, 87.

Kopeikin, S. M. and Makarov, V. V., 2006, AJ, 131, 1471.

Kopeikin, S. M. and Makarov, V. V. 2007, Phys. Rev. D, 75, 2002.

Krichbaum, T. P., Witzel, A., Zensus, J. A., 1999, 2nd millimeter-VLBI science workshop: IRAM, Granada, Spain, 27–29 May 1999, ed. A. Greve and T. P. Krichbaum, St. Martin d'Heres, France: IRAM, 5.

Makarov, V. V. and Milman, M., 2005, PASP, 117, 757.

Marscher, A. P. et al., 2008, Nature, 452, 966.

Ojha, R. et al., 2008, in preparation.

Will, C. M., 2006, Living Rev. Relativ., 9, 3.

Charting the Uncharted Waters

Can we understand resonant planetary systems?

Can we determine if white dwarfs have planets?

What can dwarf spheroidal galaxies tell us about dark matter?

What can dynamics tell us about star formation?

13 SIM Lite Science Studies

Rachel Akeson (NExScI)

ABSTRACT

In April 2008, the SIM Project and the Michelson Science Center (MSC, now called the NASA Exoplanet Science Institute, NExScI) released a Request for Proposals (RFP) entitled "SIM Science Studies." The objective of this solicitation was to enhance the science return from SIM Lite by supporting researchers to conduct concept studies that will lead to the most scientifically productive observations using SIM Lite. SIM Lite will offer astronomers a fundamentally new class of astronomical observations. The most effective use of this new capability will require not only careful selection of science targets and observing strategies, but also will require community input of innovative ideas that take full advantage of SIM Lite's precision, sensitivity, and flexibility.

Responses to the RFP were solicited in all areas of astrophysics that are enabled by observations with SIM Lite, including, but not limited to, modeling of dynamical or physical processes to be studied with SIM Lite, the selection of suitable targets, assessment of instrument performance, and the design of observing sequences to take best advantage of SIM Lite's flexible scheduling. Although no SIM Lite observing time was awarded through this call, it is expected that the results of these studies will enable the teams to produce competitive observing proposals in the next general observing call for SIM Lite.

Twenty-five proposals were received in response to the call. Three panels of external reviewers were convened, and, with the overall review committee chair, Frank Shu, made recommendations

to fund all or part of 19 of the proposals. The selected studies cover the full range of SIM Lite astrophysics from objects within our own Solar System to black hole binaries to nearby galaxies. The titles and abstracts of the selected proposals are given below.

Each team will conduct their proposed study over a period of 12 to 18 months and produce a final report detailing their findings. Each team will also present these findings at a meeting of the American Astronomical Society. The final reports and presentations to the entire astronomical community will be published to disseminate the lessons learned during the studies.

13.1 Planets and Planetary Systems

Detection and Characterization of Resonant Planetary Systems
Eric Ford (U. Florida)

The combination of SIM Lite and long-term, high-precision radial velocity (RV) observations will provide a unique tool to precisely measure planet masses and orbital elements, enabling precision dynamical modeling. Since some (but not all) planet formation models predict that many low-mass planets may be found in mean-motion resonances (MMRs), measuring the frequency of such planets will test planet formation models. For technical reasons, detecting and characterizing such planetary systems may be significantly more challenging than in the case of nonresonant planetary systems. We propose to explore the sensitivity of combined SIM Lite and RV data for detecting planets in or near MMRs. We will study how the number and time span of observations affect the detection probability and the precision of orbital elements for resonant planetary systems. We will identify when it is essential to include mutual planetary interactions and pay particular attention to identifying what types of planetary systems and observing strategies would be able to distinguish systems "in resonance" from those "near resonance." Our results will help to inform the design of SIM Lite planet searches and could lay the foundation for a future SIM Lite observing proposal to determine the frequency of resonant planetary systems as a function of mass and orbital period. Ultimately, we aim to improve the capability of SIM Lite observations to test, and perhaps distinguish, between models of planet formation, migration, and eccentricity excitation.

Measuring the Astrometric Signature of Transiting Planets
B. Scott Gaudi (Ohio State U.)

When a planet with radius R_p transits in front of its parent star with radius R_*, the flux of the star decreases by a fractional amount $r^2 = (R_p/R_*)^2$, while the stellar photocenter shifts by $r^2\theta_*$, where θ_* is the angular radius of the star. For the nearest transiting planets, this shift is of order µas and so is within the reach of SIM Lite. Measurement of the astrometric shift during transit yields the angular radius of the star, which, when combined with the stellar density determined from the photometric light curve and the stellar parallax, yields the radius and mass of the star. This astrometric shift also allows one to determine the planet's (three-dimensional) orbit, including the direction of the vector normal to its orbital plane, which is useful for a number of applications. I propose to perform an in-depth study of the astrometric signature of transiting planets as applied to SIM Lite, and in particular fully explore the feasibility of detecting this signature, considering all practical aspects, including mission scheduling and pointing constraints. In addition, I will consider the astrometric signature of eclipsing binaries.

Search for Planets Orbiting White Dwarfs

John Subasavage (Georgia State U.)

Once launched, SIM Lite will be the most precise astrometric instrument ever developed. These capabilities are vital to exoplanetary studies, in particular, for low-mass, Earth-like planets. I propose to use SIM Lite to observe a sample of ~25 nearby white dwarfs in hopes of detecting planetary companions with masses in the 10 $M_\oplus$ range. Because of the nature of white dwarfs' spectral signatures (a few broad, if any, absorption lines), current radial velocity planet hunting techniques are not viable. Astrometry is currently the only technique capable of detecting low-mass planets around white dwarfs, and SIM Lite is the best-suited astrometric instrument to do so. One advantage of white dwarfs is that they have lost a significant amount of mass during their evolution so that an astrometric signature is amplified when compared to an identical system around the more-massive progenitor.

Planetary detections around white dwarfs would better enable us to probe planetary formation theory as well as planetary evolution theory in conjunction with stellar evolution. Because astrometric signatures are inversely related to distance, the closer the system, the larger the signature (all else being equal). Since most stars will eventually end their lives as white dwarfs, these objects are plentiful and on average closer to the Sun than are more-rare objects. Thus, a number of white dwarfs are close enough to the Sun to permit low-mass planetary signature detections. Given that white dwarfs are the remnants of main-sequence dwarfs with spectral classes from B to K (thus far), we could better understand planetary formation over a broader range of objects than those currently investigated using radial velocity techniques (primarily F, G, and K stars).

Detecting Terrestrial Mass Planets Around M-Dwarfs

Angelle Tanner (Santa Barbara Applied Research)

In the past few years, there have been public claims that SIM Lite is unnecessary as a terrestrial planet search tool since radial velocity studies will be able to reach sensitivities of 10 cm/s. This is adequate to detect terrestrial planets in the habitable zones of M and K dwarfs. However, it has not been demonstrated that the RV technique will be sensitive to terrestrial planets at these separations under the different sources of stellar jitter inherent to M dwarfs — granulation, star spots, flares, and p-mode oscillations. Therefore, we have designed a study to investigate the astrophysical jitter inherent to potential SIM Lite M dwarf targets using spacecraft, including Convection, Rotation, and Planetary Transits (CoRot), Hubble Space Telescope, Spitzer Space Telescope, Microvariability and Oscillations of Stars (MOST), and ground-based, ultraprecise photometric data. The goal of the study will be to present a thorough comparison of the sensitivity to terrestrial planets using either SIM Lite or 10 cm/s radial velocity measurements with realistic noise sources. Since the exoplanet taskforce has recently placed M dwarfs as high-priority targets, the results of this study can be used to guide near-term planet search programs as well as promote SIM Lite.

Planets in Binary Systems: A Catalog of Wide, Low-Mass Binaries for SIM
Keivan Stassun (Vanderbilt U.)

A critical piece of SIM Lite exoplanet science will be to determine the frequency and nature of planets in binary star systems. Among the most scientifically interesting of these will be wide, low-mass binaries, in which planetary orbits about one or both stars are stable and where the detection of planets in the habitable zone is most feasible. We are assembling the largest catalog to date of wide (typical orbital separations ~3000 AU), low-mass (typical spectral type ~M0) binaries. The binaries in our sample are in a range of brightness easily amenable to study with SIM Lite. Importantly, our sample includes a broad diversity of stellar subpopulations that is of considerable interest for determining the frequency of planets in different regimes of parameter space: stellar mass ratios, metallicity, age, activity, and dynamical history. Finally, to explore the value-added stellar science made possible with our sample, we will study the extent to which multiple observations of these binaries with SIM Lite's exquisite astrometric precision will permit the determination of orbital parameters and dynamical stellar masses with which to test stellar evolutionary models.

Searching for Solar System Giant Analogs
Robert Olling (U. Maryland)

SIM Lite astrometry, in combination with Hipparcos data and other astrometric observations from the 20th century, can uncover giant extrasolar planets with masses exceeding Jupiter's with orbital periods up to about 200 years. At a mission time of less than 2.5 hr per star, SIM Lite could survey 500 to 1000 nearby stars to determine the frequency of very-long-period, massive extrasolar planets. Detection of planetary companions can be achieved for systems with periods up to about 1000 years. Current theories of planet formation predict that migration moves the outer cutoff of giant planets from the ~200-yr to the ~600-yr regime. Our proposed survey will probe giant planets and light brown dwarfs with these periods and can help constrain planetary migration models. We propose to study how well period and mass estimation will work in the long-period regime, with a major focus on the effects of elliptical orbits. In addition to the Hipparcos data, astrometric catalogs dating back as far as 90 years are expected to significantly constrain the presence of high-mass companions such as brown dwarfs. We will also investigate alternate observing strategies that could reduce the required mission time by a factor up to about four.

13.2 Dark Matter and Galactic Dynamics

Determining the Nature of Dark Matter Using Proper Motions of Stars in the Milky Way Satellites
Manoj Kaplinghat (UC Irvine)

Dwarf spheroidal (dSph) satellite galaxies in the Local Group provide ideal laboratories for deciphering the nature of dark matter and testing theories of hierarchical structure formation on small scales. Theoretically, their status as the most dark-matter-dominated galaxies in the Universe enables the determination of their dark matter density structure without the intrinsic uncertainties usually associated with baryonic mass contributions. Observationally, their proximity allows for detailed studies of their dark matter density structure via proper motion studies with SIM Lite. Moreover, the intrinsically high phase-space densities of these small galaxies make them ideal candidates for constraining the particle properties of dark matter. We propose to develop methods to use proper motion measurements to

constrain fundamental properties of the dark matter particle. In the standard model, the dark matter is a cold thermal relic and is born with a high primordial phase-space density that allows the dark matter to collapse into halos with very steep density cusps in their centers. Observations of dark-matter-dominated galaxies suggest that dark matter halos may have shallow density slopes in their centers, which is more suggestive of "warm" dark matter models. However, there are several potential systematic problems with interpreting these observations associated with uncertain baryon physics. We propose to develop methods to constrain the central densities of dwarf spheroidal galaxies using proper motion observations. While line-of-sight motions alone are unable to place constraints on the log-slope, proper motions will provide a definitive measurement of the log slope and a direct way to connect the dynamic properties of stars in local dwarf galaxies to the microphysical properties of dark matter. We will identify the best Milky Way satellite candidates for this purpose and develop the theoretical machinery necessary to connect measured log-slopes to constraints on the primordial phase-space density of dark matter and to the microphysical properties of the dark matter particle.

Using Rotational Parallax to Estimate 1 Percent Luminosity-Independent Distances to Nearby Galaxies

Robert Olling (U. Maryland)

SIM LIte can provide data with high enough quality to determine luminosity-independent distances to the nearest spiral galaxies by employing the rotational parallax (RP) technique. Since proper motion is defined as velocity over distance, the distance follows from proper motion and radial velocity observations. An accuracy of around 1 percent is possible for M31 and M33 using about 200 stars per galaxy. Due to its large random internal motions, the Large Magellanic Cloud (LMC) is not a SIM Lite target for RP. A 1 percent error is ~8 times better than the systematic error on H_0 attained by the Hubble Space Telescope, the Wilkinson Microwave Anisotropy Probe (WMAP), and extragalactic water masers. In our review of methods that can potentially yield extragalactic distances at the 1 percent level, we find that the RP method is the most accurate distance indicator because: 1) it is a 100 percent geometric method (e.g., eclipsing binaries also rely on astrophysics to derive distances), and 2) it samples a large part of the stellar disk so that non-axisymmetric motions can be determined accurately (e.g., in contrast to nuclear water masers that sample just three lines of sight). It has been shown that knowledge of the Hubble constant to better than 1 percent is crucial for constraining the equation of state of dark energy, in combination with Planck data. Accurate RP distances facilitate detailed comparisons between almost all standard candles between various zero-points (MW, M31, M33, the LMC, and NGC4258). Successful cross-checks are crucial if we are to believe galaxy distances (and H_0) at the 1 percent level. The RP technique may be complicated by noncircular motions that could be due to, for example, spiral structure. However, the initial analyses suggest that these effects can be diagnosed and remedied. Because SIM Lite will provide five-dimensional phase space information, the RP galaxies (along with the Milky Way) will be the galaxy-dynamics laboratories for decades to come. Currently, there is no RP SIM Lite project, while the Key Project on proper motions of nearby galaxies will observe just a few stars per galaxy. We propose extensive theoretical analyses of the RP technique, focused on noncircular motions. In addition, we will investigate observational aspects such as the trades between the number of stars, the accuracy per star, and mission time. We will also specify the requirements of a locally defined astrometric grid.

Project Runaway: Calibrating the Spectroscopic Distance Scale Using Runaway O and Wolf-Rayet Stars
William Hartkopf (USNO)

Massive stars play an essential role in enriching the interstellar medium with material later recycled into stars and planets. However, the most basic information about these stars — their masses — is not well-determined. Major reasons for this include high multiplicity rates, crowded fields, and interstellar extinction, all leading to poorly known distances. Runaway O stars can provide a potential "clean sample" of single O stars that reduces some of these problems, allowing much more accurate calibration of the spectroscopic distance scale. We propose to verify the runaway nature of the current tentative list of these objects and to augment that list from current catalogs of O stars and Wolf-Rayet stars, using new proper motion information from the upcoming *Third USNO CCD Astrograph Catalog* (UCAC3). The new runaway sample will provide an observing list for SIM Lite parallax determinations of these important objects. SIM Lite has distinct advantages over Gaia in its ability to provide these new parallaxes.

13.3   Precision Stellar Astrophysics

Stellar Astrophysics with SIM and Optical Long Baseline Interferometry
Stephen Ridgway (NOAO)

This proposal addresses several interesting and important astrophysical questions concerning stars. SIM Lite astrometry will be used in combination with precision ground-based measurements, particularly optical interferometry, and supporting modeling. We will extend an ongoing study of Cepheid stars, with emphasis on resolution of possible biases in the use of the P-L relation, aiming for a confidence level of better than 1 percent. We will determine the radii, T_{eff}, luminosity, and, in some cases, masses of massive stars with sufficient accuracy to validate models of their structure and evolution with dramatically improved discrimination. We will determine the orbits of post-Algol systems, to test the hypothesis that they are the precursors to cataclysmic variable stars and the wide variety of evolved objects that they produce. We will measure the radii of nearby stars to support asteroseismological studies of the stellar interiors. For all measurements here proposed for SIM Lite, Gaia will not provide a realistic alternative, owing to brightness of the targets, expected errors, and/or required observational cadence.

Dynamical Processes in Massive Star and Star Cluster Formation
Jonathan Tan (U. Florida)

We propose to carry out a detailed study of how high-precision astrometric measurements by SIM Lite of stars involved in dynamical ejection events from star clusters can constrain theories of massive star and star cluster formation. Our study focuses on the Orion Nebula Cluster (ONC) and has two distinct parts. First, we will investigate the rich scientific potential associated with an accurate measurement of the distance and proper motion of Theta 1 Orionis C, which is the most massive star in the cluster and was recently involved (about 4000 years ago) in the ejection of a now embedded B star: the Becklin-Neugebauer (BN) star. The motion of the BN star has taken it close to a massive protostar, known as source I, where it appears to have influenced the accretion and outflow activity, most likely by a tidal interaction with the accretion disk. An accurate proper motion measurement of Theta 1 Orionis C will

constrain BN's initial motion, allowing us to search for deflections caused by the gravitational potential of the massive protostar. Second, we will search the Hipparcos catalog for candidate runaway stars, i.e., that have been dynamically ejected from the cluster over the course of the last several Myr. SIM Lite observations of these stars will be needed to confirm their origin from the ONC. The results of this study will constrain the star cluster formation time scale and the statistics of the population of ejected stars.

Parallax Observations of Local Supergiants
Wei-Chun Jao (Georgia State U.)

We propose to use SIM Lite to measure accurate parallaxes of supergiants in the near spiral arms of the Galaxy. All selected targets have V < 6, so that no other astrometry effort in this era — not the Panoramic Survey Telescope and Rapid Response System (Pan-STARRS), the Large Synoptic Survey Telescope (LSST), nor Gaia — can observe them because of those projects' bright-magnitude cutoffs. SIM Lite offers unique opportunities to measure the first-ever meaningful parallaxes to a few µas precision for a large sample of supergiants. The improved parallaxes will provide accurate supergiant luminosities so the supergiants can be placed on the HR diagram and will permit the eventual derivation of their stellar radii and mass loss rates at dramatic moments in the evolution of massive stars. In addition, hidden among the supergiant sample are luminous representatives of object classes that can potentially be used as reliable extragalactic distance estimators. Because so few supergiant distances are currently known, this work will undoubtedly yield fundamental breakthroughs in stellar astrophysics, and will likely lead to new insights that cannot yet be anticipated.

A Novel Technique for the Precise Determination of Absolute Stellar Fluxes
Jay Holberg (U. Arizona)

We propose a novel use of SIM Lite parallaxes to provide a geometrically based determination of absolute stellar fluxes. Our method relies on the use of accurate model-based fluxes for precisely characterized DA (pure-hydrogen) white dwarfs that are directly normalized to observed SIM Lite parallaxes rather than to a traditional Vega-based photometric flux scale. It has already been demonstrated that parallaxes (and absolute magnitudes) derived from broadband photometry for DA white dwarfs are consistent with currently existing trigonometric parallaxes for these stars at the 1 percent level. This study will investigate the logical extension of our technique: the direct calibration of absolute stellar flux scales below the 1 percent level using precise parallax data.

How Accurately Can SIM Measure Parameters of Neutron Star and Black Hole Binaries?
John Tomsick (UC Berkeley)

The vast improvement that SIM Lite will provide for astrometry will allow for the measurement of orbital motions of many types of binary systems. Some of the most interesting cases are the binaries for which one component is a compact object. This proposal focuses on the advances that SIM Lite will allow in the study of neutron stars and black holes. In particular, we are proposing to perform simulations to determine how accurately SIM Lite will be able to measure the orbital parameters of X-ray binaries, including compact object masses. In the neutron star case, a direct dynamical mass measurement will be possible, and SIM Lite is critical for measuring the parameters, such as binary

inclination and source distance, that are the most difficult to determine with current techniques. We have experience with performing realistic SIM Lite simulations for X-ray binaries and for planetary studies, and we expect that our work will lead to improved computer code for analyzing SIM Lite data, optimizing SIM Lite observing strategies, and choosing the best reference stars as well as targets.

The Dynamical Legacy of Star Formation
Adam Kraus (Caltech)

Star clusters are the primary sites of star formation, and cluster evolution establishes the environment within which star and planet formation occur. The internal kinematics of young clusters directly constrain the initial conditions and early evolution, but the typical proper motion dispersions (<1 to 2 km/s; <1 mas/yr) are impossible to measure from the ground. SIM Lite's unprecedented astrometric capabilities represent a transformative opportunity for studying the primordial kinematics of young clusters, reaching precisions of 5 to 10 m/s for the nearest star-forming populations. We propose to study the requirements and expected results for a kinematic survey of nearby young clusters and associations. The first stage of our study will use existing RV surveys and new statistical methods to estimate the velocity dispersion as a function of angular scale for these target populations. We will then use results from the literature, including our numerous high-resolution imaging surveys, to screen unsuitable candidate targets like binary systems and spatially resolved edge-on disks. Finally, we will estimate the total mission time required to study each association and will recommend a final set of targets that maximize the scientific return from this unprecedented survey.

NGC6791: SIM Plans for Binaries, Colors, and Parallaxes
Ruth C. Peterson (UCO/Lick Observatory)

We propose to investigate how to determine (1) the distance to the open star cluster NGC6791 from SIM Lite–based parallax measurements of stars we have identified as single; (2) the masses of one or two subgiants we have identified in binaries, from SIM Lite–based astrometric determinations of the orbit of the primary and the radial velocity displacement of primary and secondary; and (3) the frequency and mass–ratio distribution of its substantial population of binaries, from existing photometry and future radial velocity measurements. To better constrain membership and binarity of stars in the NGC6791 field, we will take advantage of our ongoing decade-long program that has determined radial velocities good to 0.2 km/s for all 88 red stars with V < 14.7 and monitored their variability. The goal is to ultimately provide from SIM Lite observations an improved parallax distance for NGC6791, and the masses of stars in binary systems consisting of one subgiant or giant and one near-main-sequence star, which will stringently constrain calculations of single-star evolution at high metallicity. Independent of SIM Lite observations, we also propose to establish 4) how to determine reddening, temperature, metallicity, and binarity simultaneously at high metallicity from panchromatic color information. We plan to do this empirically by constructing color–color diagrams from existing photometry in a multitude of bandpasses for the cluster. We will then attempt to model each diagram theoretically, by extending calculations of fluxes and colors for solar-metallicity and metal-rich stars across the range of temperatures from the giant branch to the main sequence. By itself this will yield color conversions from the observational color-magnitude diagram (CMD) colors to the physical stellar parameters of temperature and metallicity, also of critical importance to age and metallicity determinations based on comparing cluster CMDs to theoretical isochrones. Applied directly to NGC6791 photometry, it will yield constraints on the frequency and mass ratio distribution of cluster binaries.

13.4 The Uncharted Waters

Gaia–SIM Lite Legacy Project
Guillem Anglada-Escude (DTM/Carnegie Institution of Washington)

According to current plans, the NASA SIM Lite mission with be launched just after the end of operations of the ESA Gaia mission. This is a new situation that enables long-term astrometric projects that could not be achieved by either mission alone. In some cases, it may increase the science value of SIM Lite targets with a much smaller effort than originally assumed. This SIM science study will be the first to analyze in detail this new situation and try to explore the benefits that can be obtained by both communities (NASA and ESA) by combining both data sets. A few particular science targets will be analyzed in great detail to prove with examples the capabilities of long-term astrometric coverage. Before any attempt at combining both data sets, several issues must be addressed, such as the reference frame used and the precise coordinate definition of the observable quantities in both missions.

Effect of Photocenter Contamination on the Estimation of Reflex Motions and Dynamical Orbits for Interacting Binaries
Dawn Gelino (NExScI)

We propose to investigate how SIM Lite can best be utilized to attain accurate masses for the primary and secondary stars in interacting binary systems. Currently, there are two SIM Lite Key Programs to measure the masses of black holes and neutron stars in binary systems. Accurate and precise orbital solutions are needed across the full mass spectrum of interacting binaries in order to fully understand the secular evolution of binary systems. A more complete picture of stellar evolution requires the inclusion of lower-mass degenerate stars. These interacting binaries are complex, including a degenerate primary star, a main sequence or giant secondary star, and accretion material flowing from the secondary to the primary. We propose to investigate many systems in each interacting binary class spanning the entire range of primary component masses in order to study the effects of multiple luminosity components on the apparent photocenter of the system and its apparent motion. This work will allow us to quantify the effect of photocenter determination, extract true orbital parameters, and determine masses of the interacting binary stellar components. Photocenter contamination is an issue that affects all interacting binaries, including those sources already selected by SIM Lite for study. Our work will benefit the entire SIM Lite community.

Sizes and Shapes of Kuiper Belt Objects and Centaurs with SIM
Marc Kuchner (GSFC)

We propose to study and plan a SIM Lite survey of giant Kuiper Belt objects (KBOs) and Centaurs, their dynamical relatives. This survey will measure precise sizes and shapes of these newly discovered primordial objects, constraining their compositions, material strengths, and other properties in a way no other technique can. We will use Hapke models of rotating bodies combined with light curve data and thermal measurements to model the visibilities of these targets and select an optimal observing strategy. We will investigate non-sidereal tracking and the use of the co-linear guide interferometer baseline to do visibility science.

14 A General Observer Program

Ronald Allen (STScI), **Charles Beichman** (NExScI), **Stephen Unwin** (JPL), and
Todd Henry (GSU)

ABSTRACT

We anticipate the demand for, and the possible parameters of, a General Observer (GO) program for SIM Lite. This program would enable researchers in the astronomy community to share in the promise of precision astronomical science by carrying out their own research projects with SIM Lite. In general, the program would operate in a fashion similar to those put in place for other NASA missions of comparable cost and capability. However, there are several important differences owing to the special nature of SIM Lite's measurement process. In addition, some observing programs may require long lead times in order to carry out lengthy preparatory work.

14.1 Introduction

SIM Lite will provide astrometric data (positions, parallaxes, and proper motions) on stellar targets with unprecedented precision. Accurate parallaxes permit precise determinations of distances to, and hence luminosities of, astronomical objects. Precise proper motions provide vital data on the gravitational forces that govern the movement of astronomical objects, and, hence, provide information on the masses of and the mass distributions within these objects. SIM Lite data will be relevant for precision science on a wide variety of topics in general astrophysics and exoplanet research, and the demand for this capability is bound to grow as researchers become aware of it. SIM Lite is also being built with public funds and therefore ought to be open to the scientific research community for merit-based, peer-reviewed research proposals. NASA has always intended this, so the SIM Project has kept about 30 percent of the five-year mission time as yet unallocated. The precise balance between new "Key Projects" and smaller "General Observer (GO) Projects" has not been addressed in any detail. Here we take the first exploratory steps in defining a more comprehensive framework for a program whereby NASA can provide opportunities for the broader astrophysics research community to participate in the SIM Lite mission and to compete for unassigned SIM Lite observing time.

A variety of observing programs will be carried out with SIM Lite. Already envisaged are 10 Key Projects, five Mission Scientist Projects (http://planetquest.jpl.nasa.gov/SIM/sim_team.cfm), special projects carried out in Director's Discretionary Time, and a necessary allocation for engineering and calibration. The possibility that there could be a GO program for SIM Lite was acknowledged at an early stage of the project, and the first "SIM book" announced such a program in 1999. The goal of this chapter is to update those plans taking into account various advances that have been made in the intervening years and to provide a paradigm for such a program. We have taken a wide view of the topic, and left many important details to a future discussion of the implementation of this plan.

We anticipate that all remaining unallocated observing time on SIM Lite will be treated as GO time, to be assigned through a competitive peer-reviewed process. As we describe, GO projects may vary in size from the determination of distance to a single target to projects as large in size and cost as the current Key Projects.

14.2 Objectives and Examples

14.2.1 Objectives

The objectives of the GO program for SIM Lite are:

1. To enhance the scientific productivity of SIM Lite by enabling the broad participation of the astronomical community.
2. To simplify the processes of observing, reducing, and calibrating high-precision astrometric data so as to make SIM Lite measurements accessible and useful to the broad community.
3. To provide advice and support tools to the members of the community so they can explore and exploit the astrometry relevant to the research projects being carried out.

14.2.2 Examples of Possible GO Programs

By way of illustration, we list here several examples of programs that could fall in the GO category. We emphasize that these are meant only as examples, and that GO programs will not be limited to these categories. Examples might include:

- Measurement of the orbital parameters for a new list of extrasolar planet candidates determined, for example, from planetary transits.
- Measuring the astrometric parameters of a specific (small) set of stellar targets in the Galaxy in order to determine distances, kinematics, and precision spectral energy distributions (SEDs). Examples might include galactic globular clusters, a list of white dwarfs, etc.
- Synthesis imaging of compact stellar groups in order to provide high-dynamic-range structural information. The angular resolution will approximately correspond to that of a telescope with a diameter equal to SIM Lite's baseline.
- A precise distance measurement to a specific faint target star.

14.3 Current Status of SIM Science Observing Time Allocations

Approximately 36 percent of the nominal five-year baseline mission was competitively awarded to a Science Team selected by NASA Headquarters through the first Announcement of Opportunity (AO-1) in 2000. The current flight time allocations are shown schematically in Figure 14-1. The team currently consists of the Principal Investigators (PIs) of 10 Key Projects and their Co-Investigators (Co-Is) and five Mission Scientists and their Co-Is. Key Projects require both significant amounts of time on SIM Lite over the entire nominal mission lifetime and significant preparatory science in order to make effective use of that time. Mission Scientists were selected for their specific expertise in support of SIM Lite and have smaller time allocations for their science. The nature of the preparatory work varies by project and includes candidate target list preparation, observation and characterization of candidate targets, modeling of astronomical phenomena and SIM Lite observations, and theoretical studies.

Figure 14-1. Current observing time allocations.
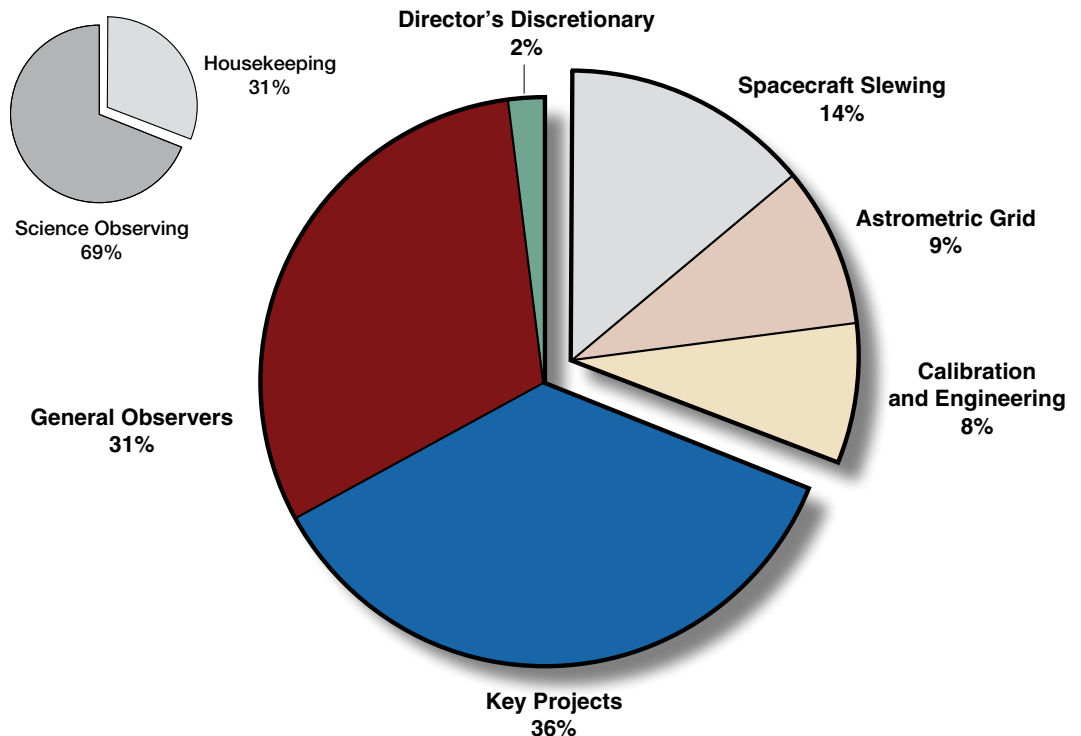
The SIM Lite mission has suffered unanticipated delays owing to a shortage of funds in NASA and is currently "on hold." In the meantime, the ESA mission Gaia has moved from concept studies to implementation. SIM Science Team members are therefore presently re-evaluating their projects in order to optimize the science they will do with SIM Lite. The changes are primarily intended to take account of recent advances in astronomy and to avoid unnecessary overlap with Gaia, while at the same time remaining within the confines of the specific science goals initially approved for each investigation.

Concerning a comparison of SIM Lite's capabilities with those of Gaia, it is important to note the following points:

1. SIM Lite remains superior in its astrometric precision throughout the range of stellar magnitudes accessible to Gaia.
2. Gaia cannot observe bright targets with V < 6 and the mission precision for faint targets (V > 16) is significantly less that what SIM Lite can achieve.
3. SIM Lite is unique in its ability to focus quickly on new targets in order to address new science.
4. SIM Lite is flexibly scheduled, allowing optimal observing of, for instance, binary stars or variable QSOs.

After the addition of mission time for calibrations, measurement of the grid stars, and miscellaneous engineering work, approximately 30 percent of the observing time on SIM Lite remains available for GO programs during the prime mission (first five years). Should an extended mission be approved, an additional GO call would be held toward the end of the prime mission, to re-compete all of the science. As well as continuing those programs that benefit most from the longer time baseline (e.g., proper motions), a second GO call would provide an opportunity for a fresh set of science investigations. The SIM Science Studies proposal call (Chapter 13) provides ample evidence of new ideas awaiting observations with this unique instrument.

14.4   A Framework for a SIM Lite GO Program

The concept of "Proposal Cycles," as used, e.g., by the Hubble Space Telescope, Spitzer Space Telescope, or Chandra X-Ray Observatory, will be different for SIM Lite. In that concept, essentially 100 percent of the available mission time for a limited period (e.g., one or two years) is fully subscribed, and is followed by another cycle to subscribe the next period. Since most SIM Lite observing programs require observations spread over an extended period, with many requiring the entire prime mission of five years, SIM Lite observing time will instead be allocated in mission slices, which are a percentage of the available time but may be spread through a duration of five years. In addition, analogous to the Key Projects, some large GO projects will require extensive preparatory work, whereas others may not. Figure 14-2 sketches time lines for examples of different kinds of GO programs envisaged with SIM Lite. In this figure, typical mission slices are shown as broken horizontal bars extending for various fractions of the nominal mission time. There are no "cycles" in the usual sense.

SIM Lite GO programs will fall into several categories depending on the amount of preparatory work, the required observing time, and the extent of the data processing and analysis required:

1. Large Programs: These are typically of the same scope and size as the existing Key Projects. They require significant preparatory work, observations spread over the entire prime mission time, and major analysis work after the data set is complete. (Example: study of a new set of planetary systems revealed by new transit data.)
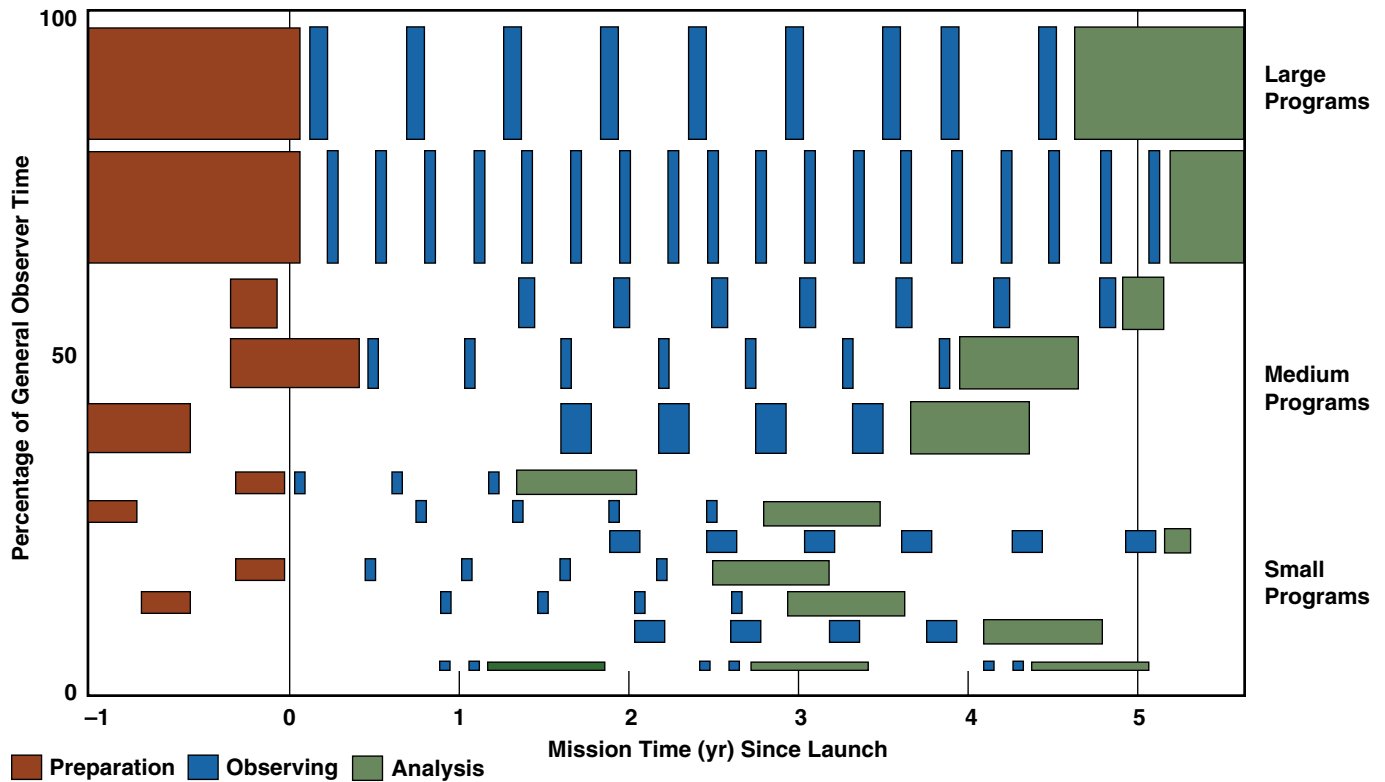
Figure 14-2. Schematic timelines for sample SIM Lite programs.

2. Medium Programs: These require only a modest amount of preparatory work, involve only a modest number of targets, require only a few observations per target over the prime mission, and need modest amounts of analysis work afterwards in order to get the science results. (Example: Proper motions of stars in an open cluster in the Galaxy.)

3. Small Programs: These typically require little or no preparatory work, involve a few targets with a handful of observations per target, and require little analysis to obtain the result. (Example: A distance to a white dwarf.) Certain targets of opportunity (TOO) may fall in this category, such as Galactic novae or cataclysmic variable stars, and certain types of microlensing events. For reasons of cost in the planning and scheduling, TOOs must meet a number of restrictions.

14.4.1 Anticipated Proposal Load Per Cycle

Proposal pressure will be the major factor driving the relative balance among the different categories of proposals listed above; this is difficult to estimate with any accuracy at present. However, some rough guess of the proposal load during a typical cycle is needed in order to estimate the resources required to support it.

We presume here that the best science is achieved with a balanced program of large, medium, and small proposals. A possible distribution could be as follows: 3 to 5 large requests, on the same order as the existing Key Projects, might be received; only 1 to 2 would likely be selected. We might reasonably expect 10 to 15 medium-sized requests, and selection of 5 to 6. Finally, small proposals, perhaps as simple as precision parallaxes of a single object or small group, could well be numerous, and half of the 40 to 60 requests might be selected.

14.4.2 Schedule

A significant complication in planning the schedule for release of announcements of observing opportunities with SIM Lite is the necessity to allow for preparatory work, which in some cases means additional ground-based observations and may require long lead times prior to the start of observations with SIM Lite. The GO Announcement of Opportunity must, therefore, be issued well before the anticipated launch of SIM Lite and proposers must explicitly address the questions of preparatory work and lead time. Judging from experience with the current Key Projects, three to four years before launch sounds reasonable.

The following draft schedule is proposed. This schedule has a symbolic launch date for SIM Lite of "L" and intervals are measured in years:

* L-4.0 — Announcement of the plan to release the GO Proposal Call, at a winter AAS meeting.
* L-4.0 — GO planning resources on line; e.g., web-based SIM Lite exposure time estimator, Reserved Observation Catalog.
* L-3.5 — GO Proposal Call released; procedures and forms online, help desk online, support website online, start posting FAQs on support website.
* L-3.5 — Proposal Workshop (a webcast, linked to a summer AAS meeting).
* L-3.0 — Proposals due. Review Panel provides recommendations.
* L-2.5 — Selection and start of successful GO proposals requiring preparatory work.
* L-2.0 — Update GO planning resources on line; e.g., web-based SIM Lite exposure time estimator, Reserved Observation Catalog.

14.4.3 Proposal Evaluation

Analogous with other NASA astrophysics missions, the evaluation of SIM Lite proposals will have a scientific and a technical component. The initial screening will be made on scientific considerations: overall scientific merit; suitability of SIM Lite for the problem; degree to which the proposal uses the unique capabilities of SIM Lite; feasibility of accomplishing the objectives; suitability of the data reduction methods; competence and experience of the PI and the role of Co-Is; and the availability of other ground, space, simultaneous, and/or contemporaneous data that can contribute to the science. Successful proposals will then be subject to a technical review in order to identify programs that are technically not feasible or that may have nonstandard requirements for the observations and/or the data reduction.

14.5 Implementation Plan

There are many more details of the nature, level, and cost of a GO program than can be discussed in this brief chapter. Such issues include user support, data products and archiving, and funding for U.S. investigators. Many of those details will have some similarities with existing missions (Hubble Space Telescope, Spitzer Space Telescope, etc.), and the body of past experience of what has already worked best can be used to deal with them. However, a few issues are unique to SIM Lite, and these must be addressed at an early stage in the development of the mission in order to make a GO program a success. The SIM Science Studies program initiated in mid-2008 (see Chapter 13) was created with strong support from the Science Team to help extend the potential SIM Lite user community beyond the current group of "black-belt" astrometrists on the Science Team. But that is still not sufficient. Whereas many members of the future SIM Lite GO community will have some familiarity with the principles governing

reflecting telescopes, few of them will have the background in Fourier optics and interferometry needed for an understanding of how SIM Lite works, let alone how it can be used effectively for astrometry. A broad effort needs to be initiated soon to provide tutorials in optical interferometry and in astrometry with interferometers, and to develop SIM Lite observing templates for a representative set of typical SIM Lite GO programs. Examples of such "educational" materials can be found on the websites for existing special-purpose facilities such as the Very Large Telescope Interferometer and the Palomar Testbed Interferometer, and at more general websites such as the NASA Exoplanet Science Institute. Developing, publicizing, and disseminating this kind of information at an early stage will help to ensure the success of a GO program for SIM Lite.

14.6   Conclusion

Creating a GO program for SIM Lite is more than facilitating the observations, opening access to archival data, and supporting the research with funding. It is essential that the future user community be educated if we are to realize the full scientific potential of this mission within its limited lifetime. Many details of such a GO program remain to be addressed. The JPL SIM Project and the SIM Science Team are committed to assisting with all aspects of a GO program for this unique and exciting mission.

Acknowledgments

We are grateful for advice from a number of colleagues, including Bill Blair and Warren Moos (JHU/ FUSE), Matt Mountain and Mike Hauser (STScI), and George Sonneborn (GSFC). We acknowledge past efforts to consider a GO program for SIM, including the first "SIM book" in 1999, and a draft of the present document by S. Unwin in 2006. Neill Reid provided helpful comments on an earlier draft of this chapter.

SIM Lite Science Program

15

Stephen Unwin (JPL)

ABSTRACT

We describe three versions of a notional science program for SIM Lite. With several years to launch, and with scientific advances in the meantime, these versions should be regarded as illustrative of the strength of SIM Lite's expected contributions to astrophysics. Because SIM Lite is a flexibly scheduled instrument with astrometric capabilities far in excess of the current state of the art, there are many science areas to which it can contribute. In this respect, it is an observatory like Spitzer, Hubble, or JWST, for which the scheduling is entirely driven by the peer-reviewed science that can be accomplished. But for an astrometric mission there is a practical difference from other observatories because the majority of observations comprise measurements spread over months or years and must, therefore, be preplanned. This consideration plays into how the observing program will be set up to maximize the scientific return from the mission. The three programs described here result from different assumptions about scientific priority. We fully expect that the actual program several years from now will be selected by peer review.

15.1   Committee Recommendations

SIM Life has an impressive record of endorsements from independent advisory committees. The concept of a "Space Optical Interferometer" dates from the 1981 Field Committee report — the first of three Astronomy and Astrophysics Decadal Surveys to consider precision astrometry using a targeted instrument. The Bahcall Committee report in 1991 laid out the science case for an "Astrometric Interferometer Mission." Ten years later, a carefully crafted technical development plan (including testbeds) was in full swing, and had already showed that the goals of the Bahcall Report could likely be exceeded. This encouraged a third decadal committee (McKee-Taylor 2001) to extend the science objectives to include not just stellar and giant-planet science but also a search for rocky (perhaps habitable) planets. With almost another decade of testbeds and instrument design work since then, it is now clear that SIM Lite should be capable of detecting Earth-like planets in the habitable zones, not just around the closest few stars, but around a substantial sample. Such a database of known nearby rocky planets will be invaluable information in planning and developing next-generation instruments to perform exoplanet spectroscopy.

These three Decadal Survey committees took a very broad view, as is appropriate, of the science enabled by a precision astrometric instrument with high accuracy even on faint targets that can be pointed anywhere in the sky.

A more recent review by the Astronomy and Astrophysics Advisory Committee's (AAAC) Exoplanet Task Force (2008) considered just one science area, albeit one of the key areas for SIM Lite; namely, the identification and characterization of Earth-like planets in the habitable zones around nearby stars — i.e., those planets for which we can reasonably expect to gather the most detailed information on their properties. The ExoPTF considered a wide range of techniques, not just astrometry, using both ground and space observatories. They concluded, in part because of the maturity of the needed technology and in part because of its comprehensiveness, that an astrometric mission should be the next major step and, as noted above, an important step in preparation for the more-challenging spectroscopy missions.

In this chapter we describe three versions of a science program (Design Reference Mission, or DRM), informed by the recommendations of these peer advisory committees. One version takes a broad view of the science of precision astrometry, with a large General Observer (GO) Program; a second program places more emphasis on exoplanets, by reserving most of the GO program for exoplanets. A third program presumes that the quest for Earth-like planets in the habitable zones should extended to a much longer star list, which requires committing the majority of the available science time. All of these use the same instrument, SIM Lite, described earlier in this book; only the observing strategies differ.

15.2   SIM Lite Mission Time

Like any space-based observatory, SIM Lite must perform a variety of functions in support of the science, as well as the actual science observations. Because SIM Lite operates differently from a conventional imager or spectrometer, it is worth outlining how the time is book-kept. In this chapter, we book-keep the time in terms of percentage of mission time, not "available" time, because the numbers are subject to revision as the mission develops (Figure 15-1).

Mission time is divided into the following four categories:

- Calibration and engineering activities, including data downlink, will require about 8 percent, preplanned and integrated with the science observations.
- Spacecraft slewing assumes there are a total of 63,000 tiles during the mission, with a small proportion of large-angle slews; this is representative, but is dependent on the details of how the science observations are scheduled.

- The astrometric grid comprises 1302 tiles, observed repeatedly during the mission (see Chapter 16) to establish a global reference frame. The reference frame is a resource that will be made available to all observers.
- Science observing time comprises the remaining time, about 69 percent. Included in science time is 2 percent assigned to the NExScI Director, as is traditional for space observatories, for urgent or exceptional science needs outside of the normal proposal process. Also included are the overheads associated with acquiring targets and reference stars in each tile (but not grid stars, which are part of the above-mentioned 9 percent). Slews between tile locations are accounted for in the 14 percent portion graphically shown in Figure 15-1.

Figure 15-1. Allocation of major instrument activities on SIM Lite, averaged over the five-year mission, as a percentage of five years of mission time.
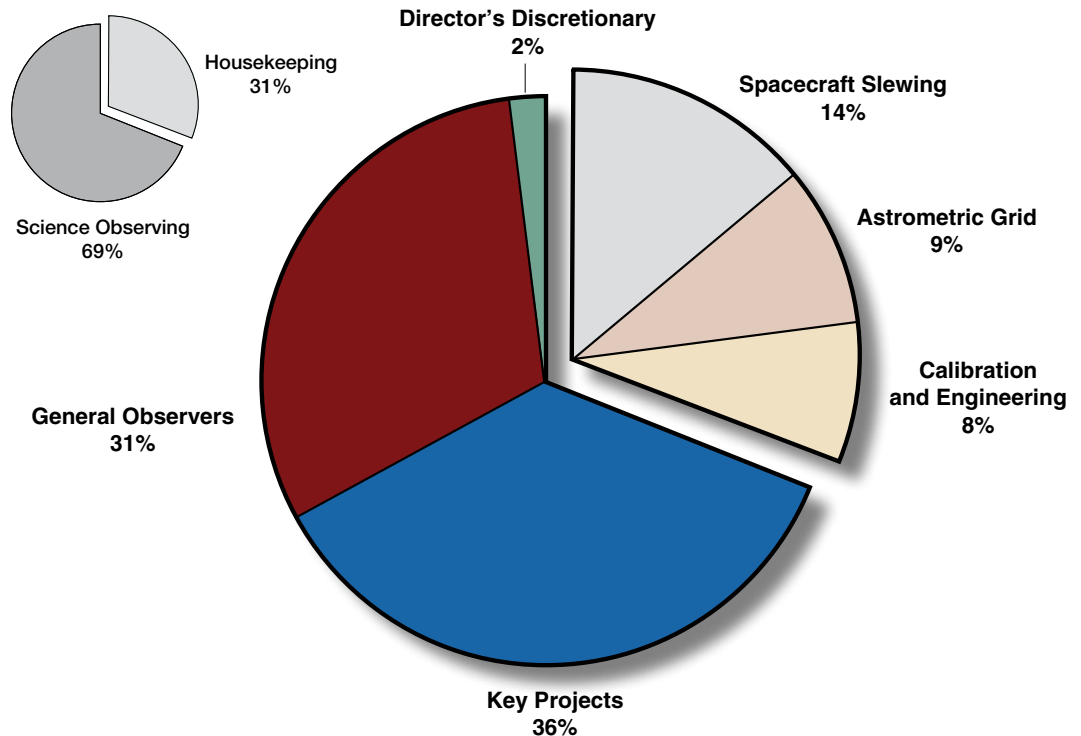
15.3 Design Reference Mission

We now describe three versions of a Design Reference Mission (DRM) for SIM Lite (Figure 15-2). There are many other possibilities, but these cover a range of criteria by which a science program may be defined. The science observations that SIM Lite will actually execute cannot be defined with any certainty at the present time — it is several years until launch, and there will undoubtedly be scientific advances and new instrumental capabilities developed in the intervening period. Stated simply, the task of selecting and executing science programs is to maximize the science return from SIM Lite. We discuss some of the considerations that go into the development of an effective science observing program.

Note that the conventional use of the term DRM is to define an instrument suite for a mission in very early development. For SIM Lite, of course, the instrument is completely defined. Its performance has been specified, and in large part verified through ground testbeds and subsystem brassboards (Chapter 18). So here we use the term DRM to refer only to possible allocations of the mission observing time.

Figure 15-2. Graphical representation of three possible Design Reference Missions for SIM Lite. In DRM Version 1, the General Observer (GO) time is open. In DRM Version 2, a portion of the GO and Key Project time is allocated to (a) search for Earth-like planets, and (b) all other astrophysics. DRM Version 3 devotes almost the entire science allocation to exoplanets, so there are no Science Team Key Projects.

Search for Earth-Like Planets 10%

Director's Discretionary 2%

General Observers 31%

Spacecraft Slewing 14%

Astrometric Grid 9%

Calibration and Engineering 8%

Key Projects 36%

DRM VERSION 1

Search for Earth-Like Planets 34%

Director's Discretionary 2%

General Observers 31%

Spacecraft Slewing 14%

Astrometric Grid 9%

Calibration and Engineering 8%

Key Projects 36%

DRM VERSION 2

Search for Earth-Like Planets 57%

Director's Discretionary 2%

General Observers 10%

Spacecraft Slewing 14%

Astrometric Grid 9%

Calibration and Engineering 8%

Search for Earth-Like Planets 57%

DRM VERSION 3

15.4   Design Reference Mission Version 1

The first version of the Design Reference Mission (Figure 15-3) is based on a large General Observer (GO) Program, along with the SIM Science Team Key projects. In the current science plan for SIM Lite, science observing amounts to 69 percent of the five-year mission and is divided into three categories:

- Guaranteed Time Observers (GTO) — the SIM Science Team (36 percent)
- General Observers (GO) — i.e., through a new NASA Announcement of Opportunity (31 percent)
- Director's Discretionary Time (2 percent)

Figure 15-3. Details of the assignment of science observing time in DRM Version 1 showing the key project's allocations for specific topics.
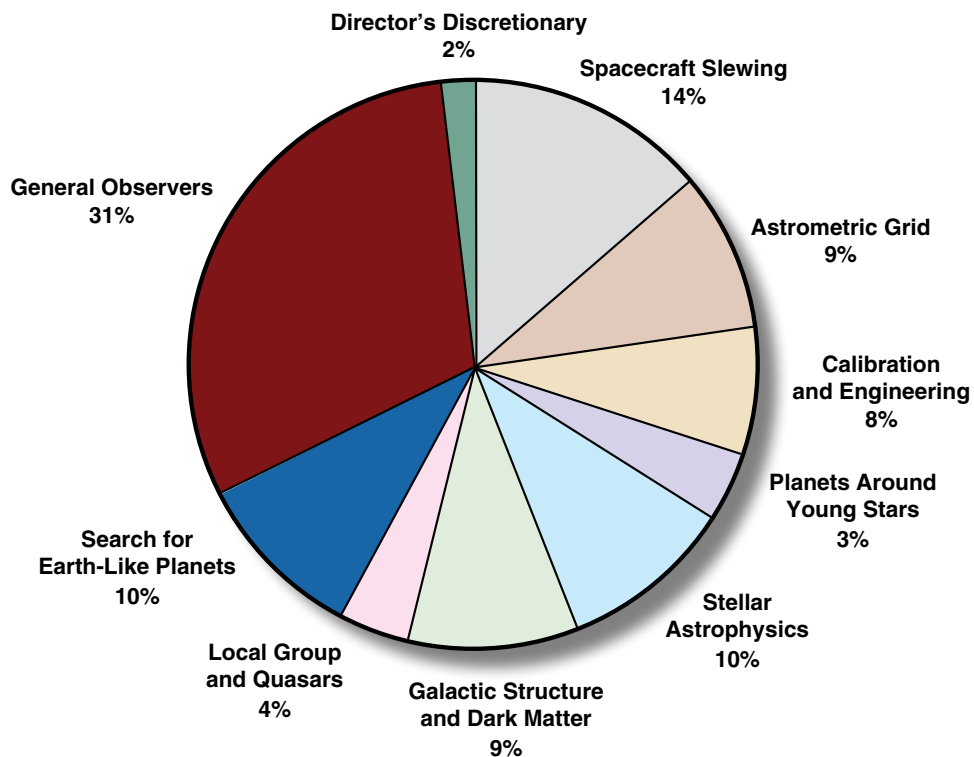
15.4.1   Guaranteed Time Observers — The SIM Science Team

In 1999, when SIM Lite was on track for a launch in 2005, a NASA Announcement of Opportunity was issued to select the SIM Science Team. Through scientific peer review, a team of 15 members was selected, covering a wide range of possible SIM Lite science topics. Approximately half of the available observing time was assigned to large programs called Key Projects, recognizing that the scientific yield required significant up-front investment from the PIs and their teams. Proposal time demands were very high and a number of very good scientific concepts were rejected for lack of observing time.

Ten members serve as the PIs of Key Projects — major investigations requiring up to several percent of the five-year mission time. Five Mission Scientists were selected to conduct smaller programs; these individuals were chosen for their specific technical expertise relevant to the mission. The Science Team, including officially recognized co-investigators, totals 86 individuals.

The Science Team has two main functions. First, it advises the project on the development of the science program and it consults on various technical issues in instrument design, scheduling, data analysis, etc. The team played a central role in developing the formal mission Science Requirements. Since 2000, there have been over 20 formal two-day meetings of the Science Team, and numerous informal gatherings at conferences, workshops, and seminars. Second, the team

The programs of the NASA-selected 15-member SIM Science Team. For each, more details of the planned science program may be found in the chapters noted.

SIM Lite Science Team

Key Science Projects and Principal Investigators

- Discovery of Planetary Systems — *Geoffrey W. Marcy, University of California at Berkeley (Chapters 1 and 3)*
- Extrasolar Planets Interferometric Survey — *Michael Shao, JPL (Project Scientist) (Chapters 1 and 3)*
- The Search for Young Planetary Systems and the Evolution of Young Stars — *Charles A. Beichman, NExScI (Chapter 2)*
- Taking the Measure of the Milky Way — *Steven R. Majewski, University of Virginia (Chapter 4)*
- Dynamical Observations of Galaxies — *Edward J. Shaya, University of Maryland (Chapter 4)*
- Stellar, Remnant, Planetary, and Dark-Object Masses from Astrometric Microlensing — *Andrew P. Gould, Ohio State University (Chapter 5)*
- Anchoring the Population II Distances and Ages of Globular Clusters — *Brian C. Chaboyer, Dartmouth College (Chapter 7)*
- Determining the Mass-Luminosity Relation for Stars of Various Ages, Metallicities, and Evolutionary States — *Todd J. Henry, George State University (Chapter 8)*
- Binary Black Holes, Accretion Disks, and Relativistic Jets: Photocenters of Nearby Active Galactic Nuclei and Quasars — *Ann E. Wehrle, Space Science Institute (Chapter 11)*
- Astrophysics of Reference Frame-Tie Objects — *Kenneth J. Johnston, U. S. Naval Observatory (Chapter 12)*

Mission Science Projects and Principal Investigators

- A New Approach to Microarcsecond Astrometry with SIM Allowing Early Mission Narrow-Angle Measurements of Compelling Astronomical Targets — *Stuart Shaklan, JPL (Chapters 1, 3, and 9)*
- Masses and Luminosities of X-Ray Binaries — *Andreas Quirrenbach, University of Heidelberg and California Institute of Technology (Chapter 9)*
- Exceptional Stars' Origins, Companions, Masses, and Planets — *Shrinivas R. Kulkarni, California Institute of Technology (Chapter 9)*
- Open and Globular Cluster Distances for Extragalactic, Galactic, and Stellar Astrophysics — *Guy Worthey, Washington State University (Chapter 10)*
- Synthesis Imaging at Optical Wavelengths with SIM — *Ronald J. Allen, Space Telescope Science Institute (Chapters 14, 16)*

conducts preparatory work, including target selection, supporting ground-based observations, theory, and modeling on the Key Projects to ensure that the best science would be obtained from the allocated time.

The Key Project and Mission Scientist programs of the Science Team form the core of the science described in earlier chapters of this book, and members of the team wrote much of this material. But there are topics that are not covered by the Key Projects. Some, like the rotational parallaxes described in Chapter 6, might be considered for inclusion as future Key Projects. Many other topics, some requiring very modest amounts of observing time, may be found among the SIM Science Studies in Chapter 13.

15.4.2   General Observer Program

Most of the remaining time (about 31 percent of the five-year mission) is planned for open community participation through a NASA Announcement of Opportunity for General Observers. This proposal call would be issued approximately two years before SIM Lite launch, and would be open to all individuals and organizations, without restriction as to scientific topic (appropriate to the instrument capabilities, of course). See Chapter 14 for details of the planned program. A small amount of time (2 percent) will also be available for later assignment as Director's Discretionary time.

15.5   Design Reference Mission Version 2

In Design Reference Mission (DRM) Version 2, we base the science on the Guaranteed Time Observer (GTO) science of the Science Team, again with a large General Observer (GO) program. Recognizing the unique role that SIM Lite will play in the search for Earth-like planets in the habitable zones (HZ) around nearby stars — those that can be followed up with spectroscopy — we assume that most of the GO time to be awarded is reserved to this search. This contrasts with DRM Version 1, for which the GO time is unrestricted as to science topic.

Two of the Key Projects, those of Marcy and Shao (Chapters 1 and 3), are devoted to searches for terrestrial exoplanets. Combining these with the reserved GO time gives a total of 33 percent of the mission devoted to planets. Figure 15-4 summarizes the observations comprising DRM Version 2. It shows the major categories of science as defined by the Science Team's Key Projects.

As a guide to the exoplanet science that this time would be used for, we start with the recommendations of the Exoplanets Task Force (2008). The ExoPTF proposed a program that searches the closest 60 stars for 1 $M_\oplus$ (orbiting at the inner edge of the Habitable Zone, or HZ, around 0.8 AU for a Sun-like star). This program would require about 57 percent of SIM Lite time — much more than we are allocating here, in Version 2. However, using only the notional 33 percent of SIM Lite time, we can conduct any one of the following searches (Figure 15-5):

* Search 42 stars for planets down to 1 $M_\oplus$ at the inner edge of the HZ.
* Search 55 stars for planets down to 1 $M_\oplus$ at the center of the HZ (1 AU for a Sun-like star) — very close to the ExoPTF recommendation.
* Search 70 stars for planets down to 1.5 $M_\oplus$ at the inner edge of the HZ.
* Search 90 stars for planets down to 1.5 $M_\oplus$ at the center of the HZ.

Which of these scenarios, or some combination, will SIM Lite adopt? They differ only in the "depth" of the search of each target star. There is no "right" answer, of course. Most likely the strategy would be defined by two considerations: (a) the state of knowledge at the time the targets are selected, informed

Figure 15-4. Design Reference Mission Version 2, showing the Science Team's Key Projects, a substantial General Observer program devoted to exoplanet searches, and a General Observer program (8 percent) devoted to openly competed topics in astrophysics. See also Figure 15-2.

Director's Discretionary
2%

General Observers
8%

Spacecraft Slewing
14%

Astrometric Grid
9%

Calibration and Engineering
8%

Planets Around Young Stars
2%

Stellar Astrophysics
10%

Galactic Structure and Dark Matter
9%

Local Group and Quasars
4%

Search for Earth-Like Planets
34%

Search for Earth-Like Planets
34%
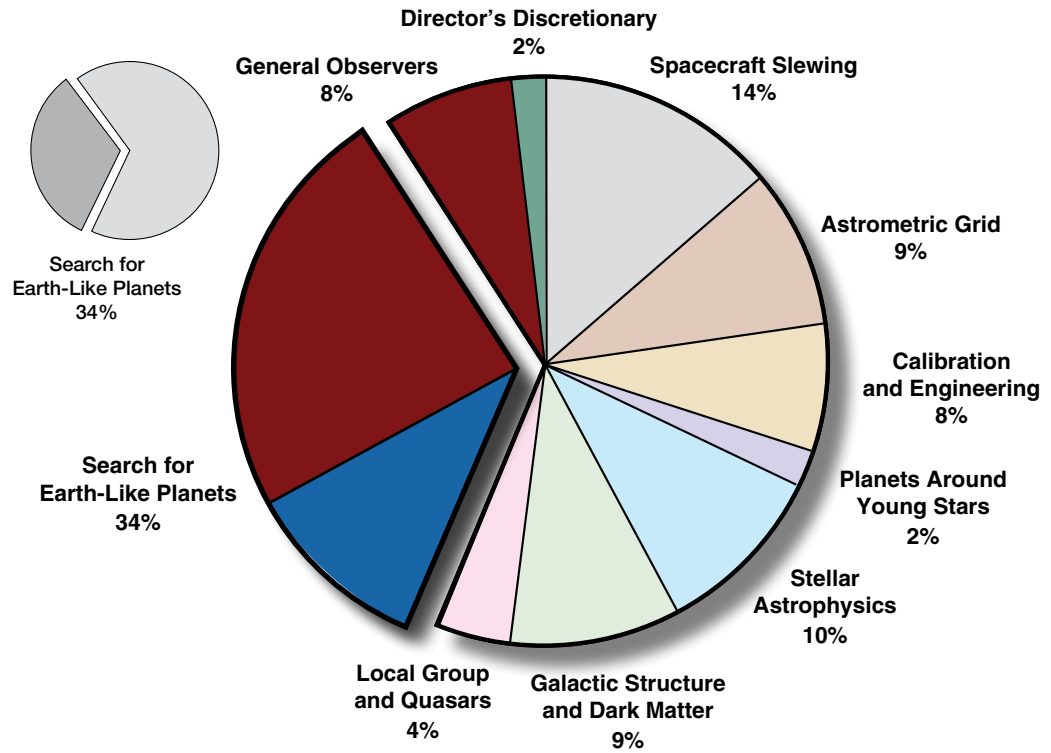
Figure 15-5. Number of nearby Sun-like stars searched by SIM Lite for Earth-like planets, as a function of observing time invested. Curves are drawn based on the mass sensitivity of various searches; for instance 1 $M_\oplus$ at the center of the HZ, for which 55 stars can be searched in 33 percent of the mission. Note that the total time available for science (Figure 15-1) is about 69 percent.

3.0 $M_\oplus$ at Earth HZ

2.5 $M_\oplus$ at Earth HZ

2.0 $M_\oplus$ at Earth HZ

1.5 $M_\oplus$ at Earth HZ

1.0 $M_\oplus$ at Earth HZ

Number of Targets

Percent of Total Mission Time Allocated to Planet Search
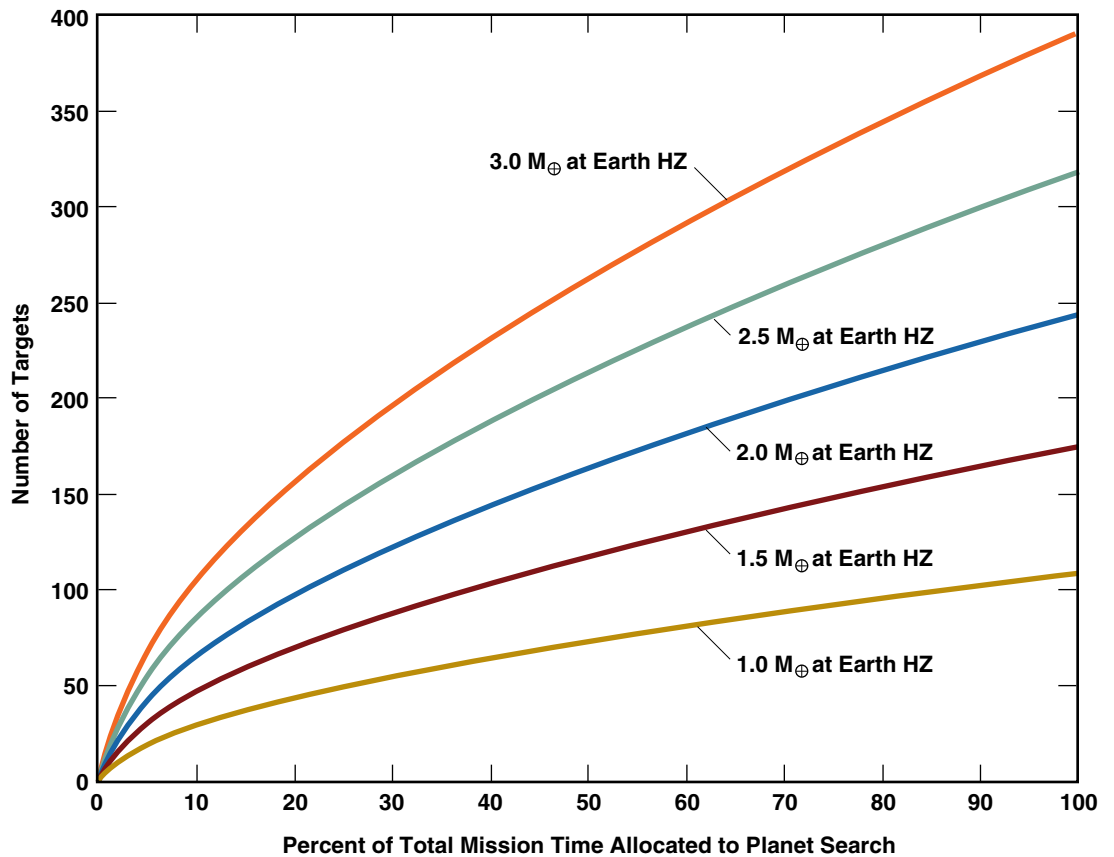
by advances in the field — results from the CoRoT and Kepler missions, better observation and modeling of the process of planet formation through observation of debris disks, and detections by other methods, including transits and microlensing experiments; and (b) peer-reviewed competition, which will take into consideration all of the above factors.

15.6   Design Reference Mission Version 3

An alternate approach to the DRM is to take the ExoPTF recommendations at face value. This can be done, but it requires substantially more observing time assigned to exoplanets than in DRM Version 2 because the more distant stars require proportionately much more time to achieve the desired search accuracy. Also note that specifying a search defined for the inner edge of the HZ is considerably more demanding than the exact same search, but specified for the center.

Taking the search criteria as 1 $M_\oplus$ at the inner edge of the HZ for a list of 60 stars, as recommended by the ExoPTF, requires 57 percent of the total mission time (Figure 15-2). There are several points to note about an assignment of observing time made in this way:

- Planet searching consumes almost all of the available SIM Lite time and it becomes almost a planets-only mission.
- Only 10 percent of the mission, plus 2 percent for Director's time, is available for all of the astro-physics, roughly equivalent to two Key Projects.
- Most of the SIM Lite time assigned to the SIM Science Team would have to be returned to the "pool" to be re-competed in a competition dedicated solely to exoplanet searches.
- Mission time devoted to a search at 1 $M_\oplus$ at the inner edge of the HZ is very "flat" in observing time (Figure 15-5); that is, the number of targets to which this depth is reached grows only slowly with observing time.
- DRM Version 2 achieves qualitatively the same exoplanet science, and provides bigger opportunities for astrophysics research.

15.7   Conclusions

Three versions of a Design Reference Mission for SIM Lite are presented above. The first represents an open approach to the science program: the Science Team programs were selected from an unrestricted proposal call; and the General Observer call would be similarly unrestricted. The second version presumes that some of the GO time will be reserved for proposals in the field of exoplanet searches. A third version assumes that almost the entire mission is devoted to exoplanets.

In Version 1, only 10 percent is assigned to exoplanets initially, with additional time through the GO program. Note that Version 2 and Version 3 differ drastically in the "other" science that they can do, but they differ only modestly in the exoplanet science:

- Version 2: in 33 percent of the mission:
    — 92 stars searched to 1.5 $M_\oplus$ in the middle of the HZ , or
    — 55 stars searched to 1.0 $M_\oplus$ in the middle of the HZ.

- Version 3: in 57 percent of the mission:
    — 60 stars searched to 1.0 $M_\oplus$ at the inner edge of the HZ (the ExoPTF recommendation).

Since the intent of the ExoPTF recommendation can be met using about half of the time devoted to science, rather than most of it, it seems likely that an open AO for science time would likely be assigned closer to DRM Version 2 than to Version 3.

Finally, it is worth noting that observatories always exhaust the available observing time long before all viable targets can be observed. This is inherent in the exploratory nature of astronomical observatories. A five-year SIM Lite science program, as laid out in this book, would be an outstanding achievement for this entirely new class of space observatory. An extended mission beyond five years is obviously attractive. Part I of this book showed the power of astrometry to search for exoplanets; an extended mission allows the target list to be broadened — both to more stars, but also for more comprehensive studies of the constituents of the most interesting multiple-planet systems. Many of the astrophysics topics in this book would benefit from more targets — not just for better statistics, but to understand correlations with physical properties. The precision of proper motion measurements improves rapidly (as $t^{-1.5}$), so many dynamical studies, such as galactic dynamics and dark matter characterization, would benefit strongly from a longer time baseline.

A Design Reference Mission is an exercise in possibility. For a high-precision, flexibly scheduled observatory like SIM Lite, at the forefront of research that uses astrometry as a tool, the actual observing program will be decided close to launch, several years from now. The earlier chapters of this book attempt to provide a comprehensive view of the possible science areas. But it is the opportunities for adapting to newly developing fields, and the opportunities for unexpected discoveries, that make SIM Lite such an exciting mission for the next decade.

References

Bahcall, J. and the Astronomy and Astrophysics Survey Committee, Board on Physics and Astronomy, National Research Council, 1991, The Decade of Discovery in Astronomy and Astrophysics, Washington, DC: NAS.

Field, G. and the Astronomy Survey Committee, Board on Physics and Astronomy, National Research Council, 1982, Astronomy and Astrophysics for the 1980s, Washington, DC: NAS.

Lunine, J. and the ExoPlanet Task Force, Astronomy and Astrophysics Advisory Committee, 2008, Worlds Beyond: A Strategy for the Detection and Characterization of Exoplanets, Washington, DC: NSF.

McKee, C. and Taylor, J. and the Astronomy Survey Committee, Board on Physics and Astronomy, National Research Council, 2001, Astronomy and Astrophysics in the New Millennium, Washington, DC: NAS.

Project Technology Readiness

The MAM testbed showed that microarcsecond astrometric accuracy can be achieved in a stellar interferometer under realistic operational scenarios.

The Kite testbeds demonstrated that we can meaningfully measure the displacements of optical elements to a hundredth of an atom.

SIM Lite's beam launchers have achieved the required picometer accuracy: one to two orders of magnitude better than the best commercially available gauges.

The G2T testbed has demonstrated star tracking precision to 50 microarcseconds.

The STB-3 testbed demonstrated nanometer-level pathlength control in a flightlike environment — even for the dimmest stars, where it takes minutes to collect enough photons to estimate the fringe position.

16 Astrometric Interferometers
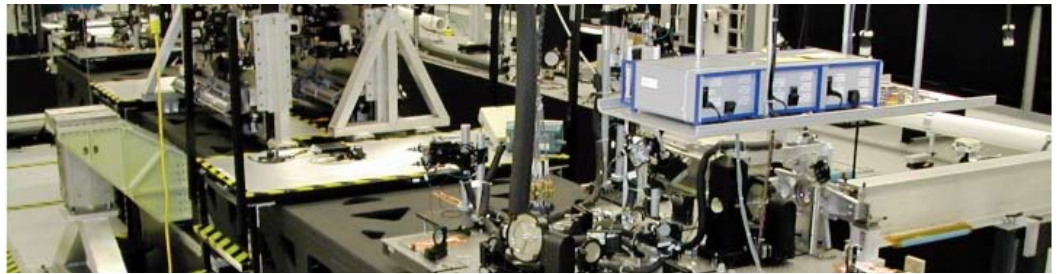
Bijan Nemati (JPL)

ABSTRACT

Across the panoply of modern astronomical instruments, SIM Lite holds a unique position as a space-based long-baseline astrometric interferometer. As such, it represents the most capable astrometric instrument currently ever invented In this chapter, we show that interferometers are the optimal choice for wide-angle astrometric measurements, providing good performance in regimes where telescopes are not feasible. We introduce the key elements of stellar interferometry and conclude with an overview of the SIM Lite instrument architecture.

16.1 Interferometers As Optimal Astrometric Instruments

For imaging, the ideal instrument is a telescope with an unobscured circular aperture. This yields a point-spread function that is minimal in width, resulting in the highest overall definition. It is also possible, as is done in radio astronomy, to synthesize an image using an interferometer whose collectors can be moved to fill a much larger "synthesized" aperture. Doing so would afford finer definition at the expense of artifacts arising from what is usually a sparse sampling of the aperture plane. Thus, for imaging extended scenes, the telescope is the optimal instrument while the interferometer that adequately samples the aperture plane can be an approximation.

In astrometry, on the other hand, we are usually interested in the angle between unresolved objects. Here the ideal instrument is one that samples the wavefront at two spatially separated points and measures the tilt of the wavefront using the samples. The ideal instrument here is the Michelson stellar interferometer and a telescope can at best be an approximation.

We can compare the astrometric performance of the telescope to the interferometer from a signal to noise standpoint. In the absence of systematic errors, the accuracy of an astrometric instrument is approximately given by:

$$\sigma_a = \frac{w}{2\sqrt{N}} \tag{1}$$

where w is the angular width of the signal peak and N is the number of detected photons. For the telescope, w is related to the point-spread function while for the interferometer it is given by the peak fringe width:

$$w_{tel} = 2.44\frac{\lambda}{D} \qquad w_{int} = \frac{\lambda}{B} \tag{2}$$

Thus, from a photon-limited point of view, the astrometric resolution of an interferometer with a 6-m baseline and two 50 cm collectors is roughly equal to that of a 3.2 m telescope. But astrometric resolution is only the beginning of the story.

A critical advantage comes from the fact that an interferometer like SIM Lite is not limited to the field of view of its telescopes, but rather to the field of regard of its siderostats. In relative astrometry over narrow angles, one measures the position of a target star with respect to a set of reference stars. If the target star is bright and the reference stars faint, as is the case in the search for nearby Earths, one is often limited more by the photon statistics of the reference stars than the target star. In this case, the photon-limited precision is dependent on the size of the field of view. A telescope with a small camera, for example with a 3-arcmin-diameter field, would on average have fainter reference stars than a telescope with a wide-field camera, say 30 arcmin field. In general, the photon-limited accuracy is approximately proportional to the diameter of the field being observed, so that, for narrow-angle (exoplanet) astrometry, SIM Lite with a field of regard diameter of 2 degrees would be equal, in terms of photon-limited precision, to a 32 m telescope with a 12 arcmin field of view.

For precision astrometry, systematic errors and their control are at least as important as noise considerations. Here too, interferometers have advantages over telescopes. Chapter 18 will introduce the basic classes of systematic errors affecting astrometric interferometers. The SIM technology program, it will be shown, has demonstrated the mitigation of these errors down to the level of $\lambda/60000$. The technical challenges in achieving the same level of performance with telescopes are at this time formidable.

When telescopes are used for astrometry, there are two common modes of operation. One is called staring, wherein a star field is imaged on a large focal plane array. The second is called scanning, in which a CCD detector is fixed to the telescope but the telescope is scanned across the sky and the CCD is clocked out at the scan rate.

A telescope doing astrometry by staring will face systematic errors arising from sampling issues and optics errors. Astrometry at the 100 µas level has been demonstrated with the Wide-Field and Planetary Camera on the Hubble Space Telescope (HST) with 45 mas pixels and a point-spread function (PSF) size of approximately 50 mas. This is centroiding to nearly 1/500 of a pixel. Astrometry at the 10 µas level requires at least 3 to 4 pixels per PSF. For HST, with a 10 arcmin field of view, this would require a 16 gigapixel detector. If a mosaic focal plane is used to achieve this, there will be position and rotation errors among the devices. Moreover, since a variety of materials with different coefficients of thermal expansion are used to put together the CCDs in the mosaic, there will be thermal errors whose mitigation would have to be demonstrated through testing. One might argue that by placing the stellar image at the same part of the CCD (to a small fraction of a pixel) in every epoch, we can make PSF errors repeatable, and thereby avoid having to improve the sampling of the PSF. Unfortunately, at Earth's orbit, the differential stellar aberration even across the 10 arcmin HST field is approximately 60 mas, or larger than a pixel. As a result, it is impossible to repeat the positioning of the stellar image in the CCD at different epochs.

All existing space telescopes have at least two curved optics. If the pupil of the system is the primary mirror, the secondary is oversized, and the footprint of the starlight on the secondary depends on the position of the star in the field of view. The wavefront errors on the primary add to the wavefront errors on the secondary, but differently for each star in the field because the stellar wavefront's footprint on the secondary varies with the field position. If the wavefronts in different parts of the field of view are different by $\lambda/100$, there could be a field-dependent centroid bias of $\lambda/100$, or about 600 µas for a 2 m telescope. One could in theory do astrometry at the 60 µas level if these wavefront differences were fixed to $\lambda/1000$ between epochs, but this may not be technically feasible.

A number of astrometric telescopes perform astrometric measurements in a totally different way. Instead of staring at a part of the sky and in effect taking a picture, the telescope and focal plane array scan across the sky at a nearly constant rate. The CCD detector is read out in time delay integration (TDI) mode, matched to the rotation rate of the telescope. This approach has several advantages to the staring telescope approach. The first is that the image of a star is detected not with just a few pixels but thousands of pixels, so that small random differences in pixel quantum efficiencies are averaged. Second, many of the field-dependent optical biases are also averaged out. If star 1 scans across the middle of a CCD, and star 2 scans across the same set of pixels but a fraction of a second later, both stars will experience the same set of optical distortions. If the PSF is undersampled, (less than two pixels per λ/D), there will be a color-dependent bias in the centroid, whose value depends on how accurately the color dependent PSF is modeled. The Gaia and Hipparcos missions are the most prominent space astrometric missions that make use of the scanning telescope concept. For Gaia, each star will be scanned on average about 80 times over five years, resulting in end-of-mission accuracy of about 7 µas at magnitude 10, 20 to 25 µas at magnitude 15, and 200 to 300 µas at magnitude 20.

In conclusion, astrometry at the sub-µas level, the regime sensitive to Earth-mass planets around nearby stars, is technically feasible only for space-based stellar interferometers at this time. From both the photon noise and systematic error standpoints, telescopes are limited to tens of µas at best for the staring approach and a few µas for the scanning approach.

Figure 16-1. The minimal astrometric stellar interferometer requires the measurements of the starlight fringe, the internal path difference, and baseline length.
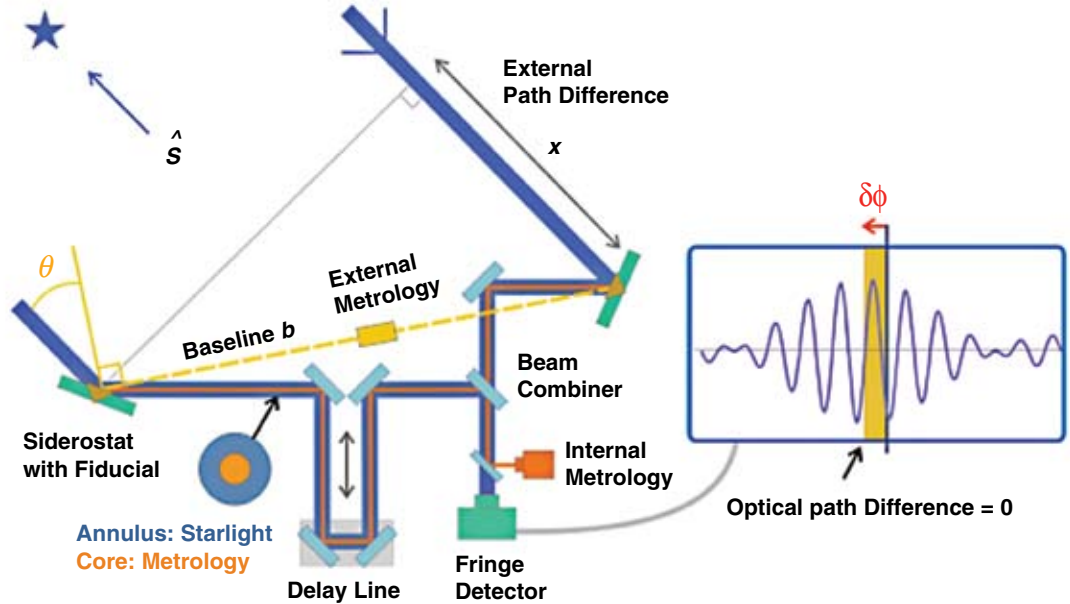
16.2   Astrometric Stellar Interferometry

The stellar interferometer, when used for astrometry, measures the optical pathlength difference (called relative "delay") between two light paths. These two paths originate at the source (a star) and end at the interferometer's two fiducials. The essential components of a minimal stellar interferometer are shown in Figure 16-1.

Two spatially separated samples of the starlight are collected and interfered via a beam combiner (physically, a beam splitter). Visible interference occurs and fringes are detected when the optical pathlength from the star to the beam combiner is equal for the paths through the two arms of the interferometer to within a few mean wavelengths. The fringe pattern envelope has maximum contrast when the total optical pathlength difference (OPD) is zero. Reference points (or "fiducials") for astrometry are created by introducing a pair of retroreflectors centered within the starlight beam on each of the two paths.

The interferometer baseline *b* is a vector that extends from one fiducial to the other. The total starlight path can be divided notionally into an "external" path *E*, originating from the source star to a fiducial, and an "internal" path *I*, starting from the fiducial down to the beam combiner. The difference of the total optical paths, left minus right, is given by:

$$\delta T = \delta E + \delta I \tag{3}$$

where δT, δE, and δI are the left-minus-right differences in the total, external and internal paths, respectively; δT is measured with the fringe detector and is called the white light fringe delay $\delta\phi$, as illustrated in Figure 16-1. The astrometric angle θ is related to the external OPD and the baseline length, *b*, according to:

$$\delta E = \vec{b} \cdot \hat{s} = b \sin \theta \tag{4}$$

The baseline length *b* is determined using both "external" metrology and post-processing of the astrometric measurements. The internal OPD is measured, modulo an overall constant offset, by the internal metrology reading δM:

$$\delta I = \delta M + C \tag{5}$$

C is sometimes called the interferometer "constant term," and is the actual internal OPD when the metrology reading is zero. Since, at the picometer level, this zero-point is initially unknown, it is determined using astrometric calibration measurements. We now define the instrument measured delay *x* as:

$$x \equiv \delta\phi - \delta M \tag{6}$$

Combining these, we arrive at the basic astrometric equation for the interferometer:

$$\begin{aligned} x &= \delta T - (\delta I - C) = \delta E + C \\ &= \vec{b} \cdot \hat{s} + C \end{aligned} \tag{7}$$

Hence, three measurements — the white light fringe delay, internal metrology, and external metrology — form the basic ingredients of the astrometric angle. Errors in each of these areas translate into a delay error. To indicate the level of accuracy needed, consider the planet-finding case, with a desired error level of less than 1 µas per visit. If the baseline is 6 m long and is orthogonal to the star direction, then knowledge of the astrometric angle at the 1 µas (5 picoradians) level necessitates that the delay *x* be measured to less than 30 pm (Figure 16-2).

Figure 16-2. Relationship between astrometric error and delay error.

$$\delta x = \vec{b} \cdot (\hat{s'} - \hat{s}) = \vec{b} \cdot \hat{s'}$$
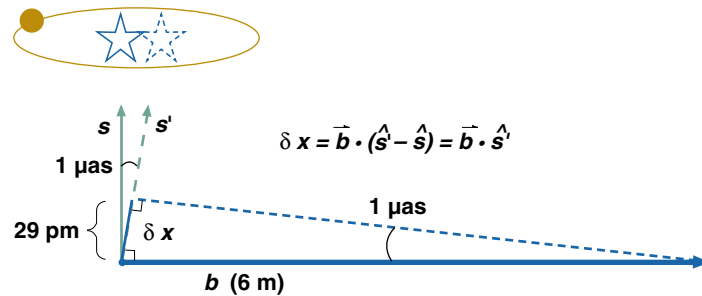
16.3   Accounting for the Motions of the Baseline

Since the astrometric measurement is relative to the baseline, variations of this vector directly affect the measurement. In a realistic space-based instrument, the baseline orientation can change by arcseconds during a measurement and its length can vary by microns. These changes must be monitored accurately to achieve a meaningful measurement.

The SIM Lite approach can be helpfully illustrated using the simplified two-dimensional situation shown in Figure 16-3. The item of interest is the astrometric position angle of the "science" star. One interferometer, designated Science Interferometer, is used to determine the angle between its baseline vector and this star. Since the measurement takes a finite amount of time, any changes in the magnitude or direction of the baseline need to be monitored while the measurement is in process.

Changes in the length of the baseline can be measured by laser metrology gauges interrogating the baseline endpoints. Changes in the direction of the baseline are measured using a combination of a second interferometer (guide interferometer) looking at a "guide" star and an external metrology system that measures the relative changes of the science and guide baselines. The external metrology system consists of a trusswork of laser metrology links interconnecting the nodes (corner cubes) at the ends of the science and guide baselines. The guide interferometer tracks the angle between its baseline and the guide star. As such, it also provides continuous baseline tracking throughout the entire set of science observations made with a common baseline attitude.

In three dimensions, the baseline can rotate in two angles, and the metrology truss can move in three directions. As a result, a second guide instrument is needed, along with a truss "roll sensor." This is reflected in the architecture of SIM Lite.

Figure 16-3. In a two-dimensional world, SIM Lite would consist of two inter-ferometers and an external metrology system.
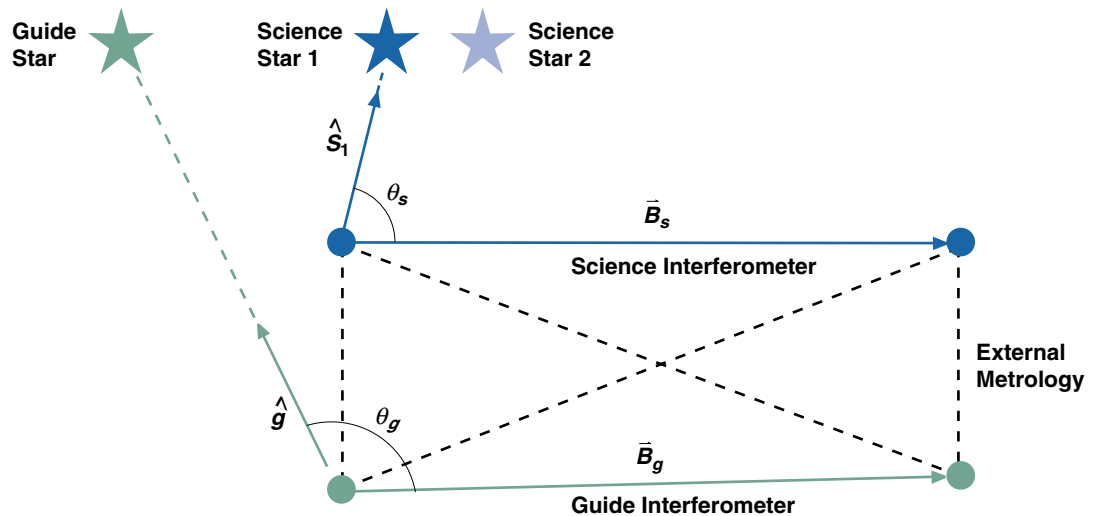
16.4   SIM Lite Architecture

SIM Lite consists of four fundamental sensors (together constituting the "instrument," Figure 16-4) mounted on a precision structure and serviced by a spacecraft. The four sensors together accomplish the measurement of the three fundamental ingredients, viz., the white light fringe delay, the internal delay, and the baseline variations.

The primary sensor is the science interferometer, which provides the external delay associated with each astrometric target by measuring the white light fringe and the internal delay (two of the three fundamental ingredients). To track the variations in the science baseline (the third ingredient), SIM Lite's other three sensors are needed. These are the Guide-1 and Guide-2 instruments and the external metrology system.

SIM Lite's external metrology system tracks the motions of six nodes (fiducials made from corner cubes) situated in a three-dimensional configuration as shown in Figure 16-5. Beam launchers situated between the fiducials send metrology laser beams that probe the distance between the nodes.

Guide-1 is an interferometer that points in the same direction as the center of the science field of regard (FOR). It is similar in performance and design to the science interferometer, except that its FOR is limited to a narrow region at the center of the science FOR, and its baseline is shorter.

Guide-2 is a telescope pointed 90 degrees away from the nominal science line of sight (LOS), and tracks the rotations of the science baseline in the plane orthogonal to the nominal LOS. The sensitivity of the science measurements to Guide-2 errors is comparatively small. SIM Lite takes advantage of this reduced sensitivity by using a simpler instrument to achieve the Guide-2 function. Guide-2 also tracks the "roll" of the external metrology truss about the science baseline (Figure 16-6).

Figure 16-4. SIM Lite can be thought of as four fundamental sensors operating together to make an astrometric observation.
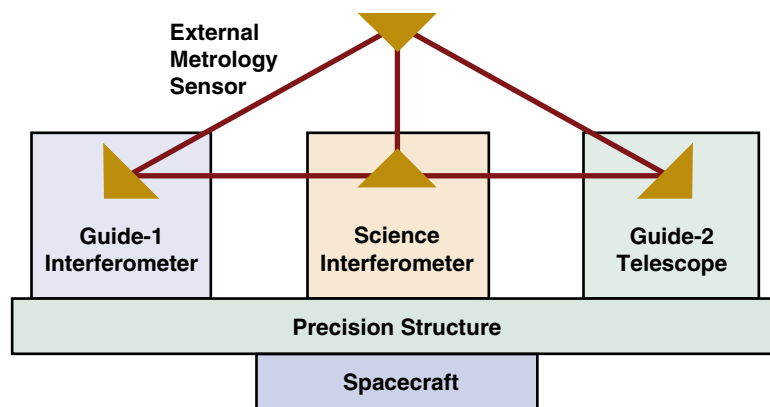
Figure 16-5. The geometry of SIM Lite's external metrology truss with respect to the science and guide sensors. The cylinders and cones represent the light paths of the interferometers and guide telescope.
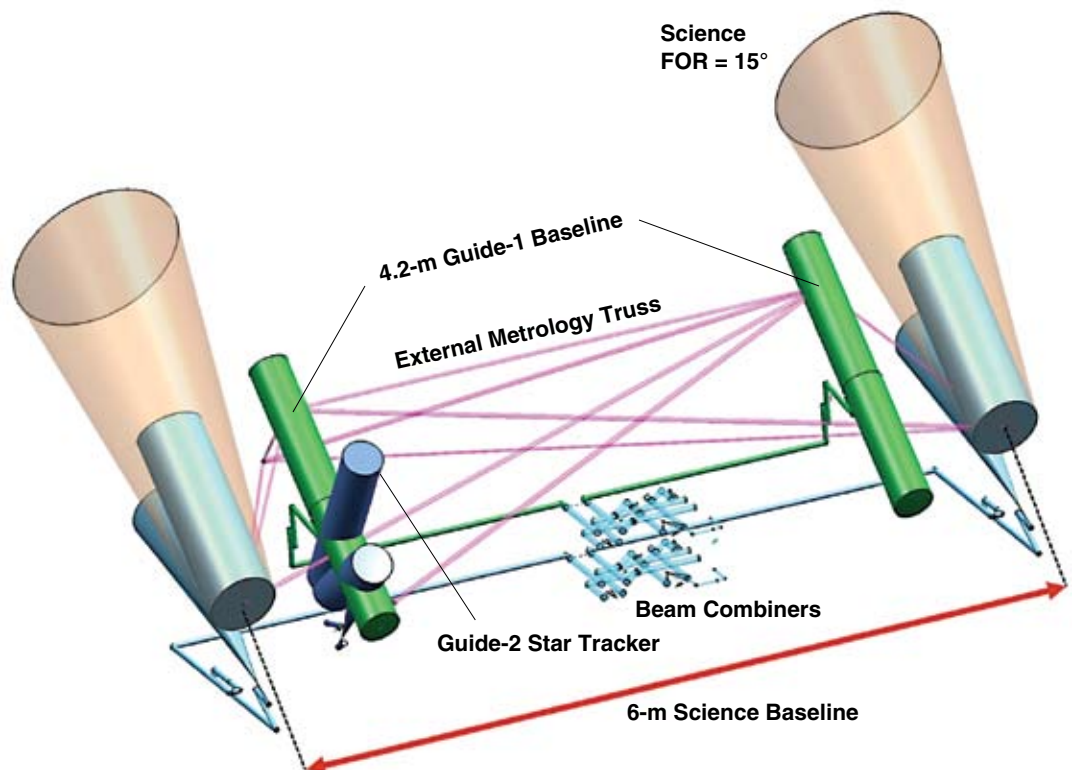
Figure 16-6. The narrow-
angle observing geometry
in three dimensions (a), and
projected onto the sky (b).
The gray vector in (a) shows
baseline motion $d\theta$ in the
direction observed by the
Guide-2 instrument.
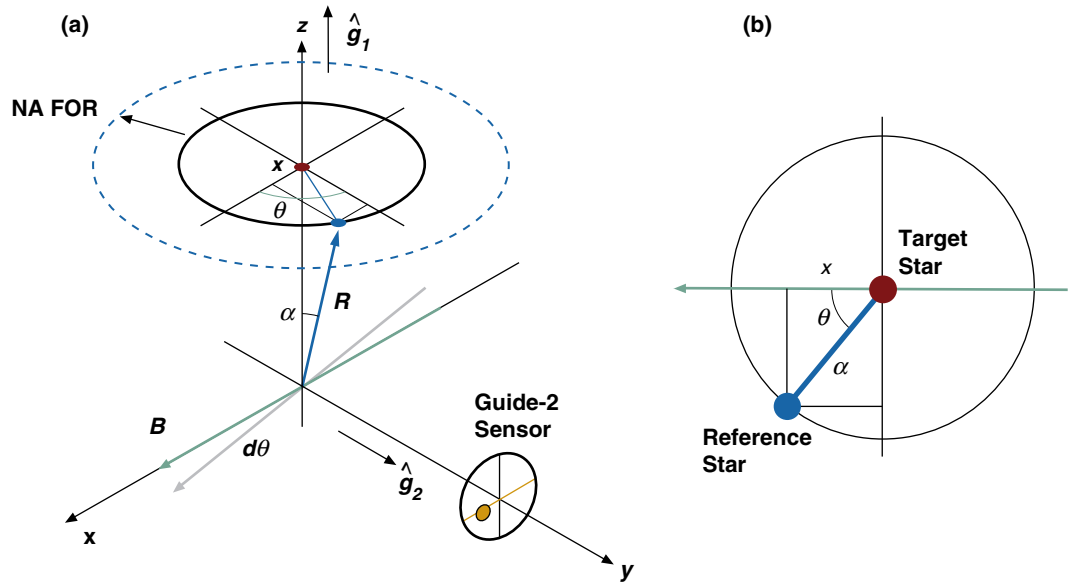
Figure 16-7. Guide-2
telescope schematic. The
pointing sensor is an angle
tracking camera. These
corner cubes (ACC, TCC,
and CCC) act as fiducial
reference points.
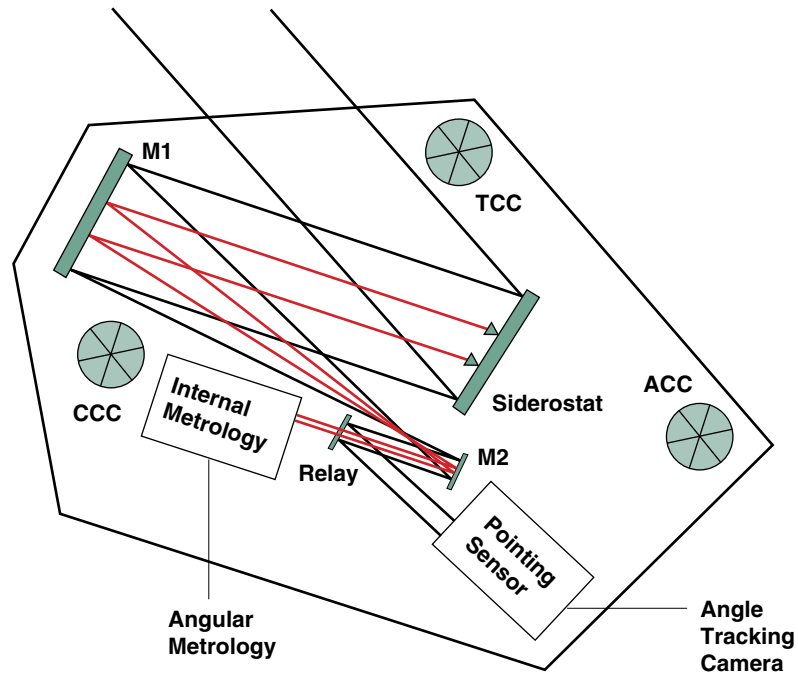
Shown schematically in Figure 16-7, the Guide-2 telescope uses an angle tracker camera and an an-
gular metrology system to tie its measurements to the rest of SIM Lite. To achieve the tie, fiducials are
mounted on the Guide-2 bench so that its motion can be monitored by external metrology. The tele-
scope images the guide star on its angle tracking camera. Using its siderostat fine stage, it maintains
its line of sight on the desired spot on the camera focal plane. The measurement of rotation is then
made using an angular metrology system that measures the tip/tilt of the siderostat relative to
the bench.

Observing with
17 SIM Lite
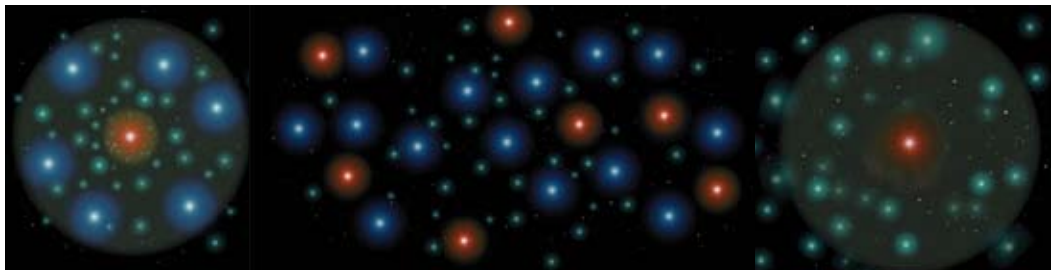
Stephen Unwin (JPL)

ABSTRACT

Making science measurements with a pointed astrometric instrument is very different from the observing modes of an imaging telescope or a spectrometer. Astrometric measurements are always made between objects, and the science is in the time-evolution of the astrometric signal. This chapter describes how the SIM Lite instrument is scheduled and operated. Astrometric observations must be carefully planned to make sure that the measurements are made between the appropriate target and reference objects, and that the observations are scheduled as part of a sequence that spreads over months or years to allow the astrometric signal to develop. Microarcsecond astrometry depends not only on optimizing observations for the desired signal, but also on scheduling the instrument in a way that minimizes systematic errors. A high-precision instrument must go hand in hand with careful experiment design.

17.1 Designing Astrometric Observations

The SIM Lite instrument makes sequential measurements of the positions of stars with the science interferometer. These measurements can be processed to represent angles on the sky projected along the interferometer baseline. All astrometric signals are two-dimensional on the sky, so every science measurement requires, at some later time, a repeated measurement with the baseline oriented approximately orthogonal. Since the orientation of the baseline may be determined by many factors, including the availability of guide stars and where the instrument was last pointed, the operations do not require that the nominally orthogonal observations be paired up nor must the position angles be repeated. This complicates the analysis of placing the data into a self-consistent frame, but is not fundamental to the measurement.

All SIM astrometric measurements are made within the framework of a basic unit of observation called a "tile." Individual stars are observed within a "tile" and the complete set of data on a given star will normally comprise many tens or hundreds of tiles. Observations of different stars are integrated at the level of tiles (from one to dozens of stars per tile) and then into campaigns of tiles. The construction of a tile is explained below.

17.2 The Tile Concept

Figure 17-1. A representation of the acquisition fields of regard (FORs) on the sky for the guide interferometer and Guide-2 telescope. Note that the center of the Guide-2 field is approximately 90 degrees from the tile center.

As explained in Chapter 16, the SIM Lite science interferometer makes sequential measurements of the path delay (through the instrument) of stars observed sequentially. Both during and between measurements, the science interferometer is held stable by continuous observations of guide stars. The guide interferometer observes a bright star in approximately the same direction as the science target. The Guide-2 telescope observes a second guide star, roughly orthogonal to the first. These two instruments observe continuously during a tile, sensing the pointing of the spacecraft, and providing corrections to the attitude of the science instrument (Figure 17-1). In this way, the science interferometer can be regarded as inertially fixed, to a precision better than the individual measurements, during and between science measurements. This leads naturally to the definition of the fundamental unit of observation — the tile.

FIELD OF REGARD WITH GUIDES

A tile is defined as the set of science observations performed while the guide interferometer and Guide-2 telescope remain "locked" onto guide stars.

This definition is not just a convenience. It is intimately coupled to the fundamental design of the instrument as a device that measures differential delays.

An observing campaign on a specific science target comprises the set of tiles that include that object. Depending on the science objective, these may be organized into "narrow-angle," "grid," or "wide-angle" campaigns. An individual tile may be a short as 10 minutes, or as long as a couple of hours. The gimbals of the science siderostats provide an FOR 15 degrees in diameter, centered on the guide interferometer boresight. Any target within 7.5 degrees of the center may be included in a tile.

A looser definition of a tile is the circular patch of sky 15 degrees in diameter centered on the guide boresight.

17.3   Target Acquisition Within a Tile

There is a sequence of activities that is executed for every tile, in order to set the instrument pointing in the desired direction and the science baseline stabilized ready to perform astrometric measurements. The slew to a new tile is done under control of the spacecraft using reaction wheels and a conventional star tracker. During slews, the science interferometer, guide interferometer, and Guide-2 telescope are not taking data.

They can, however, be prepositioned to minimize the acquisition time once they become active. First, the guide star in the guide interferometer is acquired (field of regard 40 arcseconds). The spacecraft rotates around the guide boresight until the Guide-2 star falls into the guide telescope's field of regard, which is also 40 arcseconds. Both the guide interferometer and the guide telescope at this point lock their respective pointing loops and track the centroids of the guide stars to their nominal positions. The guide interferometer uses its two Fine Steering Mirrors (FSMs) and the guide telescope uses the fine stage of its siderostat.

Science observations can begin once the guide interferometer has locked in both angle and fringe-track mode, and Guide-2 has its guide star stabilized.

17.4   The Astrometric Grid

Because SIM Lite can observe stars no further apart than 15 degrees — the maximum range of the siderostats — the measurement of wider angles involves the overlapping of tiles, with at least two "grid" stars in the overlap region. This is represented schematically in Figure 17-2. To minimize the overhead involved in slewing the spacecraft, the SIM Lite timeline is designed with most slews to adjacent tiles, so a typical slew is only about 5.5 degrees. Because most astrometric science depends on astrometric signals that evolve on timescales of weeks to years (exactly one year in the case of parallax), the timing of observations is very relaxed. Accordingly, the desire to minimize the slew angle can be met. The five-year observing scenario has a huge number of degrees of freedom. Finding the optimal solution (that minimizes slew time) may be almost impossible to determine. However, there exist a large number of solutions which are "very good" if not perfect.

The "grid" is a set of 1302 overlapping tiles that cover the entire sky (4π sr). Stars specifically chosen for the purpose of defining a wide-angle reference frame are termed "grid stars." With one grid star at

Figure 17-2. The straw-man
single-tile grid observation
scenario, showing how
wide-angle targets are
integrated with grid star
observations.
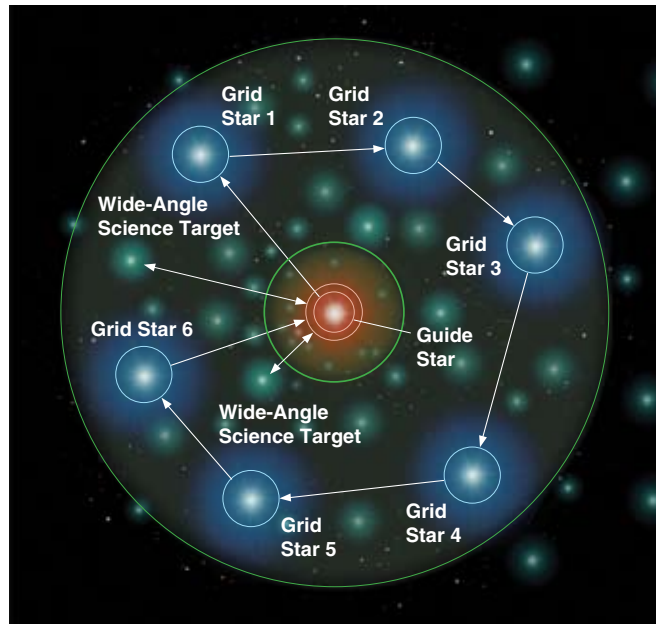
WIDE-ANGLE OBSERVATION

the center of each tile, the number of grid stars equals the number of tiles, namely 1302. The average separation is about 5.5 degrees, which means there are typically 6 to 7 grid stars per tile.

The SIM Project, after extensive simulation studies, selected galactic K-giant stars with a median magnitude V = 10.0 and median distance 700 pc for the grid. The primary requirement on a grid star is that its position and motion on the sky be well described by a model that includes five astrometric parameters: parallax and two components each of position and proper motion. Any (Galactic) star bright enough to be observed with SIM Lite will have a measurable parallax and proper motion, so the final reference frame must include measurements of these five parameters for every grid star. At any particular epoch, the grid is realized in terms of the positions computed from these five parameters. Ideally, these stars have no companions or other astrophysical effect which would cause "noise" in the five-parameter solution. The simulations showed that, with radial velocity (RV) screening, the K-giants will perform this task. Very few binary companions which might perturb the astrometric measurement will fail to be picked up by RV at modest precision (50 m/s). Those that "slip through" will have periods of 103 to 104 days and are not a problem for astrometry. The RV program needs three to four candidates for every star that is used in the final grid catalog.

17.5 Grid Observing Scenario

The astrometric grid comprises the global solution to measurements of the 1302 grid stars during the five-year mission. The grid observing scenario is designed to serve two functions:
- To provide the best estimates of the five-parameter solutions for the 1302 grid stars.
- To serve as a "framework" upon which to support the observations of science targets.

A typical tile can be viewed in either the sky domain or the time domain. Figure 17-2 shows a sketch of a grid tile, showing the sequential observation of grid stars. As indicated, science observations occur within the "framework" of the grid. The first grid star is chosen near the tile center and is re-observed at the end of the visit, allowing subtraction of a linear drift in the instrument delay during this period.

Figure 17-3. Schematic representation of how SIM Lite covers the sky in overlapping "tiles" in a schedule designed to minimize the time spent slewing the spacecraft.

OVERLAPPING TILES
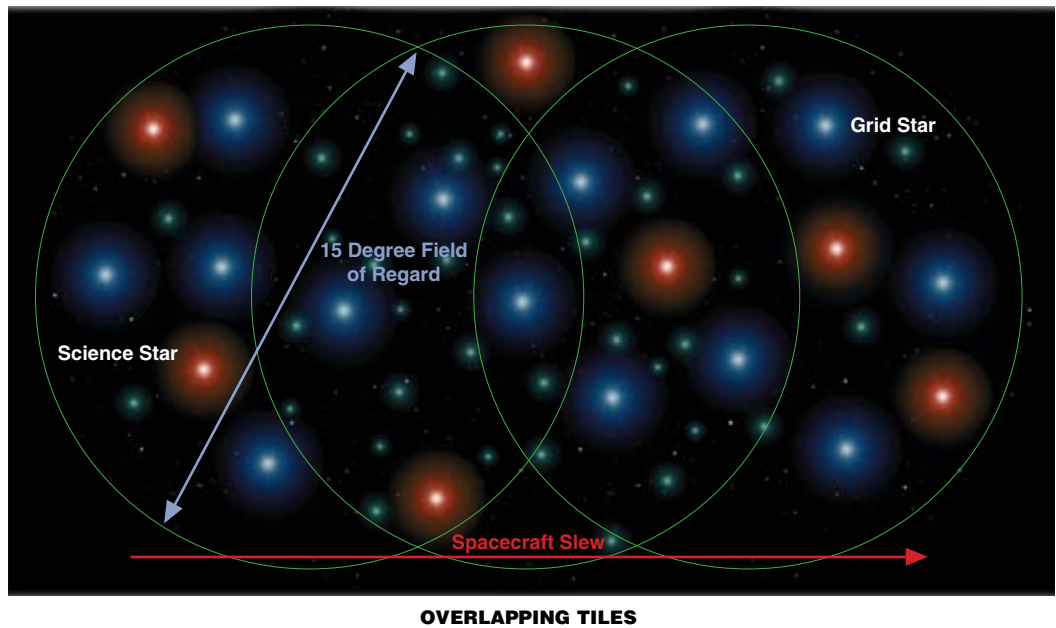
The wide-angle observing sequence for SIM Lite is built around the grid, with observations of science targets inserted into grid tiles. Normally, every grid star accessible to the instrument within a tile will always be observed. Science targets may or may not be observed, depending on the desired observing cadence and ultimate accuracy desired.

There are many ways to cover the sky efficiently (i.e., minimize the time spent slewing). One such scenario that has been studied extensively is the "orange peel." The scenario eventually used may differ, but will likely resemble this simple scheme. Optimization will be a task for project Phase C/D, implementation.

An orange peel (Figure 17-4) consists of sequential observations of 480 tiles, spaced approximately one tile radius apart, beginning in the anti-Sun direction and wrapping to the Sun's direction or vice versa. To minimize the effects of stray light, a solar exclusion zone on the sky forms the sunward boundary of each orange peel. As SIM orbits the Sun over the course of the mission, the solar exclusion zone moves accordingly, allowing the entire sky to be observable. The minimum radius of the solar exclusion zone is 49 degrees, making, at most, 83 percent of the sky available for observations at any given time.

The astrometric post-processing of grid star data solves for the astrometric parameters associated with each grid star as well as a number of instrument parameters (in effect calibrating the instrument). Over the course of the mission, there will be approximately 300,000 single-axis delay measurements covering 1302 grid stars. The number of measurements sufficiently exceeds the unknowns to allow solving for not only the five astrometric parameters per each grid star but also a number of key instrument parameters. Instrument parameters that are determined from the grid solution include the initial science baseline vector and the interferometer "constant" term at the start of each tile and the interferometer field-dependent term.

Additional instrument terms can be fitted out using this very large data set. For instance, the "field-dependent term" is a systematic bias over the science interferometer FOR and can be caused by a number of mechanisms. Since the domain of the field-dependent term is over a circle (the science FOR), it lends itself well to being described in terms of Zernike polynomials. Simulations have shown

Figure 17-4. Orange peel observation sequence for an instant in time. Each observation is indicated by a green mini-arrow showing the baseline orientation. During a year, the exclusion zone traverses the ecliptic.
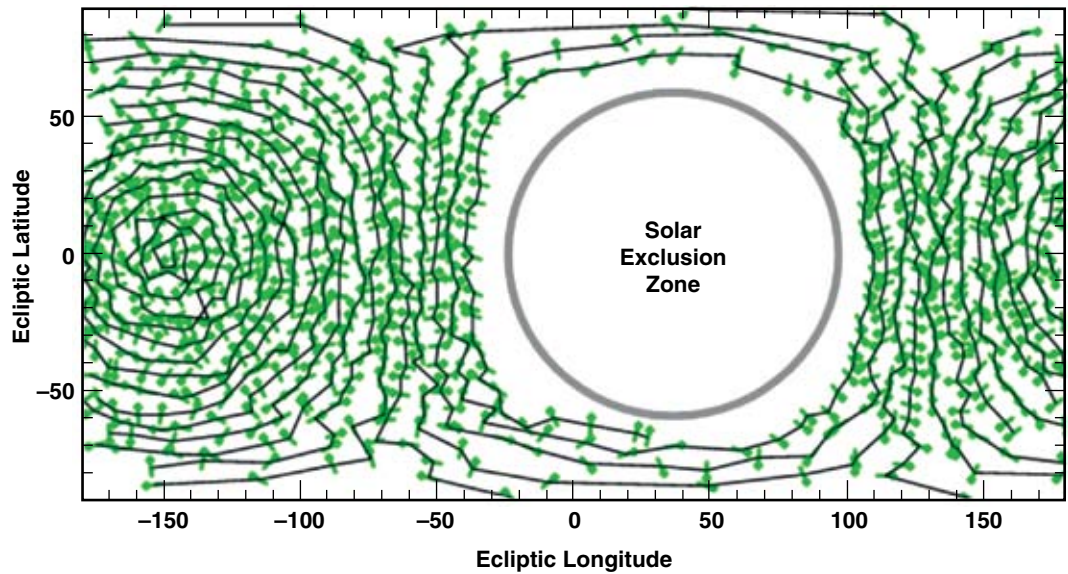
that the grid solution can be used to determine a piston (overall delay offset), tilt, and power error over the FOR of every tile, and higher order errors (up to fourth order in the radial component) over groups of approximately 50 tiles. Being able to calibrate these errors on the sky has allowed significant reduction of complexity, cost, and risk in SIM Lite.

17.6 The Narrow-Angle Observing Scenario

The narrow-angle (NA) observing scenario is used for the astrometric search for exoplanets and other investigations requiring the utmost performance of SIM Lite. NA observing is the most demanding of SIM Lite's astrometric applications. In this scenario, a target star's motion is measured against a set of reference stars across many visits.

As noted previously, the experiment design and instrument design are tightly coupled. In this case, the extreme astrometric accuracy is enabled by two design factors:
- Rapid switching between target and reference effectively eliminates errors cause by long-term (e.g., thermal) drifts. The relevant time scale for the instrument thermal stability is reduced to ~90 seconds.
- Differential measurements over small angles, and shared over several targets, eliminate a number of field-dependent errors that would be present in the wide-angle scenario.

The reference stars around each NA target are chosen to be astrometrically well described by position, proper motion, and parallax. As with the grid and wide-angle observations, the fundamental observing unit is a tile. Because of the demands of astrometric accuracy, tile construction must optimize the measurement sequence. Other science observations are inserted into the tile on a non-interference basis. The geometry of a typical NA visit is shown in Figure 17-5. (No other science targets are shown in this simple case.) To minimize systematic errors, the reference stars are chosen so that their individual locations and their collective barycenter are both as close as possible to the target star. On the other hand, to minimize random errors, the reference stars are allowed to be as far as one degree from the target star to increase the likelihood of brighter reference stars. During each visit, the baseline points in a single direction. In order to measure the target motion in two angles, successive visits use alternate (ideally orthogonal) baseline orientations.

Figure. 17-5. The narrow-
angle observing scenario with
a target star at the center of
the field of regard and refer-
ence stars within a circle of
1 degree radius. The baseline
orientation on a subsequent
visit would be orthogonal to
that shown here.

$$T - R1 - T - R2 - T - \ldots - T - R1 - T - \ldots - T - Rn - T$$

NA Chop

NA Visit
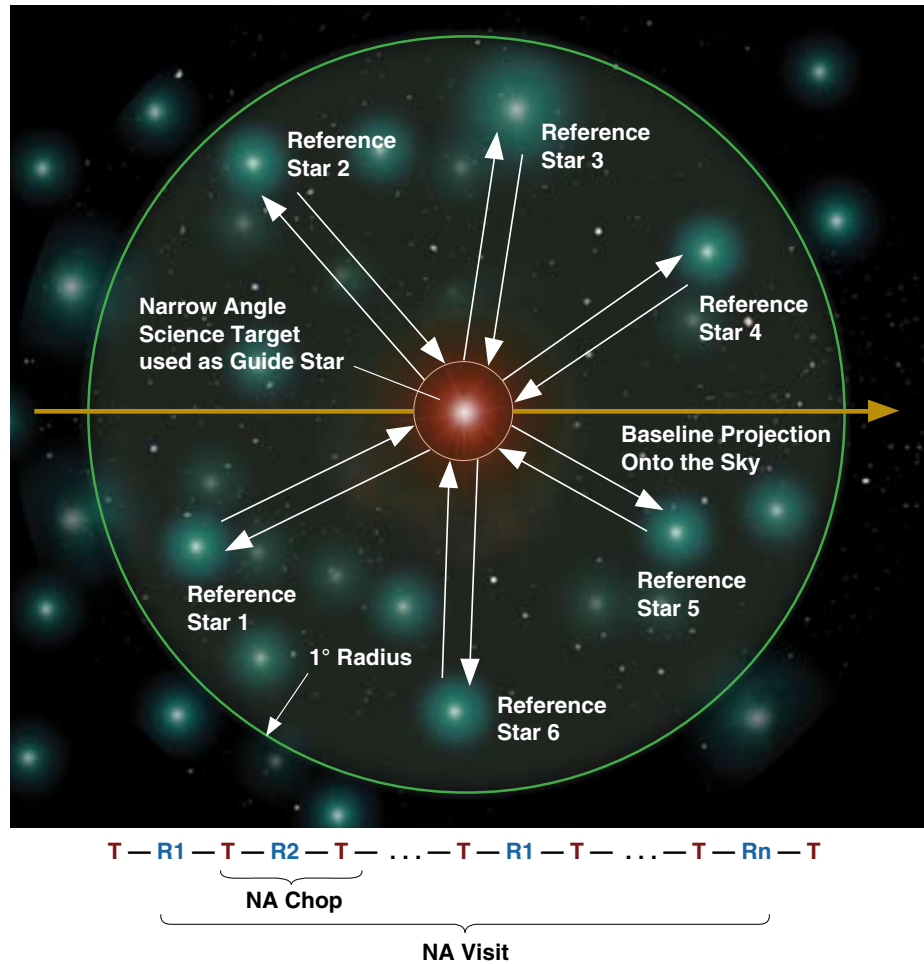
Reference stars are not, of course, perfect reference points because of astrophysical considerations. The reference stars, like the NA target, all have proper motions, parallax, and possibly "jitter" from unseen companions. More subtly, the localized frame they define has no constraint on scaling or rotation and no clearly defined origin of coordinates.

Jitter from unseen companions can be largely eliminated by two steps taken before launch. First, reference stars are preferentially selected to be K-giants, typically at distances of about 800 pc. Thus the jitter of reference stars will generally be negligible compared to that of narrow-angle targets, most of which are less than 10 pc from the Earth. Second, candidate reference stars are vetted using Earth-based radial velocity measurements. Stars with large planets or unseen companions can be identified and rejected. As with RV screening of grid stars (Section 17.4), this process is very effective. After launch, additional steps are taken. Separate solutions will be generated in which each reference star is separately treated as the "science target," while the other reference stars and the narrow-angle target are treated as "reference stars." Simulations have shown that unseen companions that escaped notice during Earth-based vetting can be detected in this way.

The proper motions and parallax of reference stars do not affect narrow-angle performance. We fit for the parallax of both the target and reference stars, and the net proper motion of the frame is absorbed into the proper-motion solution for the target. The definition of scale and elimination of rotation is

achieved by making additional observations to tie the reference stars to the SIM Lite grid. Finally, an origin of coordinates can be defined with respect to the reference stars themselves.

The basic NA measurement is the delay difference between the target and a reference star, and the analysis uses these measurements pair-wise. In the straw-man case, a target look is assumed to take 20 seconds, a reference look, 40 seconds, and the siderostat slew time from target to reference and vice versa is taken to be 15 seconds. The entire cycle of observations shown in Figure 17-5 is repeated during the visit, so that each reference star is measured three times. These are then averaged, forming a single, per-visit delay difference between the target and each reference star. The differences are collectively analyzed to determine the motion of the centroid of the reference stars relative to the local origin, which is defined to be the location of the target star. Thus, the signal is the relative motion of the centroid from epoch to epoch. For planet detection, the signal is in fact the acceleration measured across many epochs.

17.7 The Wide-Angle Observing Scenario

Observations of wide-angle targets are built upon the "framework" defined by the astrometric grid (see description above). Virtually all observations of wide-angle astrometry targets can be achieved by inserting those targets into grid tiles. Since all data within a tile are all referred to the same inertial science instrument baseline, the astrometric parameters extracted from the data set of wide-angle data are automatically referred to the grid. This is exactly what is needed for measurements of parallax and proper motion, for which the reference frame must be quasi-inertial.

Figure 17-6. Flowchart of wide-angle observations within a single tile, showing how grid stars, guide star, and science targets are sequenced.

Figure 17-6 shows the observing sequence as a flowchart, illustrating how the grid and wide-angle targets are assembled into a timeline. Key to the astrometric precision are the measurements, at the start and end of each tile, of the Guide-1 interferometer guide star by the science interferometer. Since the fields are independent, both instruments can observe the same star simultaneously. This ability will be important for performance assessment during initial checkout.
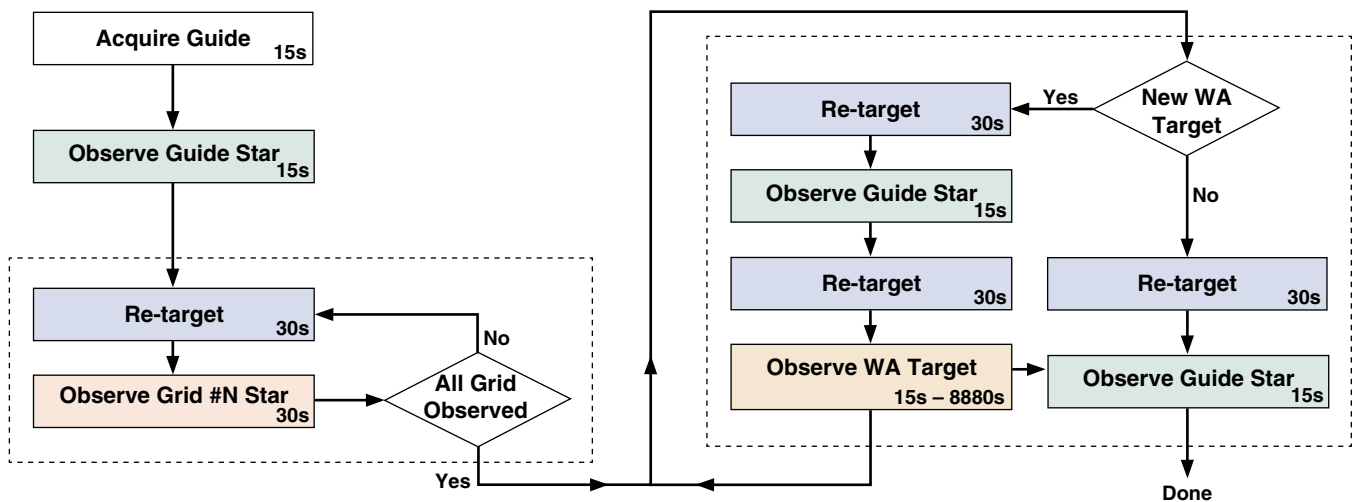
17.8 SIM Lite Mission Plan

17.8.1 Instrument Checkout and Science Verification

SIM Lite will be launched into an Earth-trailing solar orbit, lagging Earth by 0.1 AU/year. This orbit has been selected to minimize sky blockage and heat loading by the Earth and Moon. The trailing orbit enables one of the science experiments for SIM Lite, namely the gravitational microlensing experiment. Following launch there is a brief period, less than one month, of spacecraft checkout to ensure the health and satisfactory operation of the spacecraft component itself, followed by two months of instrument checkout. This is followed by four months for science verification, after which regular science observations begin.

The instrument checkout phase entails the initial power-up of the instrument, deployments, alignments, calibrations, and characterizations. Optics are exposed to space for the first time, after sufficient time has passed for structures to outgas to the vacuum. Initial alignment of the optics is commanded and target pointing is characterized. Tests are made of the instrument's thermal response and the effects of stray light. Exposure tables are verified.

After the instrument satisfactorily passes through checkout, science verification begins on SIM Lite. This is an intense period of testing the instrument and the spacecraft together to demonstrate they are ready for science operations. During this phase, narrow- and wide-angle astrometric measurements will be demonstrated. Differential wide-angle measurements will be made through the full orbit of a short-period binary star. Sample crowded fields will be observed, as will the effects on observations made close to Earth, the Moon, and Jupiter. By the end of this phase, the astrometric grid stars in about 75 percent of the sky will have been mapped three times (the missing portion residing in the solar exclusion zone until SIM Lite has moved through about 60 degrees of orbital longitude). This provides enough data to perform the first, very approximate, grid solution.

17.8.2 Observation Planning

Individuals and science teams wishing to obtain astrometric measurements from SIM Lite will begin the process well before launch. Working with the NASA Exoplanet Science Institute (NExScI), investigators will use estimation software to determine the number and frequency of measurements of their targets for the precision desired and submit their full sets for the mission to NExScI. NExScI will prepare a five-year schedule of observations, fitting observation requests, spacecraft maintenance, data downlinks, calibrations, and other flight activities into the schedule. After launch, during science verification, the astrometric software will be updated based on in-flight experience.

A six-week "sequencing" process is planned for SIM Lite operations spanning a two-week period. Several of these sequence planning processes will be ongoing, at different phases, throughout the mission. The initial four weeks are used by the mission operations team to prepare the science measurement commands for the instrument, calibration measurements, and spacecraft orientation commands. Additional spacecraft operations sequence commands are added by the flight team, including uplink/downlink, housekeeping, and general maintenance commands. This complete sequence is run through a spacecraft simulator for validation, then translated and uplinked to the spacecraft to begin operation a few days after receipt.

In the current plan for SIM Lite, missed observations will not be rescheduled, due to the expense of developing a scheduling and verification system capable of executing schedule changes robustly. Since most science programs involve repeated observations of each target, the loss of any particular observation will rarely be critical.

17.8.3 Data Downlink and Analysis

Science, metrology, and spacecraft data will be downlinked from SIM Lite in two eight-hour passes per week at Ka-band. All instrument data are downlinked through the high-gain antenna in no more than eight hours per week (end of mission). The remaining contact time uses the low-gain antenna for command upload, engineering telemetry, and Doppler ranging. The ranging data are required to determine spacecraft position and velocity for relativistic corrections to observed angles. The spacecraft memory volume is sized to hold data collected over a two-week period. In the event of a missed downlink, those data are preserved for repeat transmission up to two weeks after a lost downlink.

Once the data are "on the ground," they will be funneled through standard Deep Space Network processes and transferred to NExScI. At NExScI, the data will be processed using current calibrations, metrology at the time of the observation, and other correction routines. Aberration and general relativistic corrections will be made and the astrometric grid will be applied.

The astrometric grid will first be released about half-way through the mission. A final grid will be computed at the end of the mission and much of the data will be recomputed based on this improved grid at that time.

Rigorous definitions have been constructed for each phase of the data analysis, including data product levels. Access to the instrument "raw" data will be restricted, and in any case will be of little interest to typical users. In most cases, the lowest level data product will be "regularized delays." These data represent a self-consistent set of measurements in which the science interferometer is (effectively) fixed and known to µas precision relative to the astrometric grid. From these data, the user can derive the standard (five-parameter) astrometric quantities: mid-epoch position, proper motion, and parallax. Preliminary estimates will be provided to all users as part of the standard data products. For binary stars and planet searches, additional parameters defining the companions will be fitted to the data. These will be the responsibility of the individual investigators.

The level of science support, data product verification, visitor support, etc., for SIM Lite have yet to be determined in detail. Detailed plans for SIM PlanetQuest have already been developed, and these will be adapted to define the SIM Lite science operations system, with a view to providing science support at low cost.

The Astrometric Error Budget

18
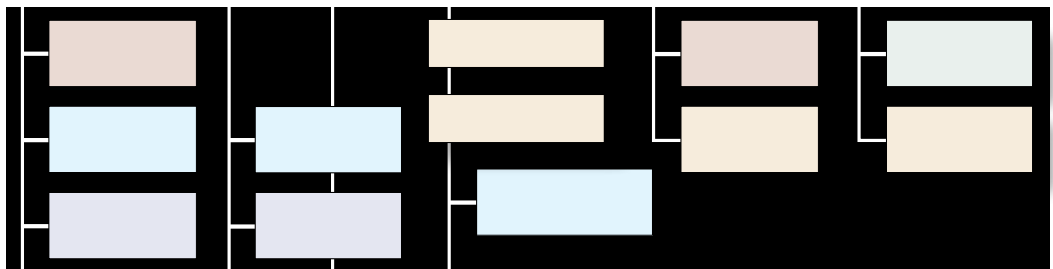
Bijan Nemati (JPL) and **Mauricio J. Morales** (JPL)

ABSTRACT

SIM Lite's performance is managed through the astrometric error budget. The astrometric error budget is designed to levy requirements on the various SIM Lite systems such as the metrology beam launchers, the astrometric beam combiners, and the delay lines. This performance model has been thoroughly validated using testbeds and more detailed models.

18.1   Introduction

Detecting the stellar wobble due to an Earth analog from a distance of 10 pc requires a per-visit astrometric accuracy of less than 1 µas. In Chapter 16 we saw that, with a 6 m baseline, this means that the external delay needs to be measured with a total error of less than 30 pm. Approximately half of this error is allocated to brightness-dependent errors, leaving only about 15 pm as the total allowable error in the science delay from all systematic sources. The dominant source of random errors is photon noise in the collected star light. Systematic errors arise from both extrinsic and instrument intrinsic sources.

SIM Lite's astrometric error budget (AEB) is a performance model designed to levy requirements and monitor the capability of the instrument in doing astrometry. It has received extensive testing and validation using testbeds and other models. In this chapter, we review the top-level structure of the AEB and discuss some of the more important error categories.

18.2   The Astrometric Error Budget

SIM Lite's AEB specifies the allowable error after a specified level of post-processing for each of two key observing scenarios: these are the grid and the narrow-angle scenarios. The grid scenario is a representation of a typical tile visit, including only the grid stars, while the narrow-angle (NA) scenario is designed to be a representation of a typical planet-finding visit. These two scenarios were chosen as drivers for the design because they are each key representatives of two different regimes of SIM Lite operations. Grid astrometry requires wide-angle operations and facilitates regularization and other essential calibrations of the instrument. Hence, it is the basis for all other astrometry. The search for exoplanets, on the other hand, is a key science objective and in many ways places the most demanding requirements on the instrument. Since the search for exoplanets is narrow angle in nature (less than one degree between any two stars measured), its error budget complements that of the wide-angle grid astrometry.

As with any form of astrometry, the final astrometric product is the result of extensive post-processing. The post-processing applies calibrations and combines all the measured quantities according to a detailed algorithm. Each observing scenario, whether searching for planets or measuring the astrometric grid, requires its own observation strategy and associated processing algorithm. These observing strategies aim to minimize the measurement error while at the same time also minimizing overall mission cost in terms of observation time.

Detailed observing scenarios and algorithms have been developed for SIM Lite's main observing modes. These have been tested extensively by modeling and have been validated in the various SIM Lite testbeds. Chapter 15 describes these observing scenarios in detail.

18.3   Grid AEB Top-Level Structure

The top-level grid error budget is shown in Figure 18-1. It is a performance model that captures the single-axis, mid-mission, grid star position error after the entire mission data set has been processed. Extensive mission observation and processing simulations have shown that the grid processing combines N_g separate measurements of each grid star to produce a grid with errors significantly less than the single-measurement error (note that we do not assume the errors scale as $1/\sqrt{N_g}$). The simulations predict that after the post-processing is complete, the mid-mission grid star position error is reduced by the "grid solution multiplier" of 0.25. The single-tile error is the position error per axis after only one tile of grid stars has been processed. It accounts for astrophysical errors including, in order of importance, stellar companions, stellar aberration, and gravitational perturbations.

Figure 18-1. The top-level
portion of the grid astromet-
ric error budget is based
on the end-of-mission perfor-
mance in measuring grid star
positions in each axis.
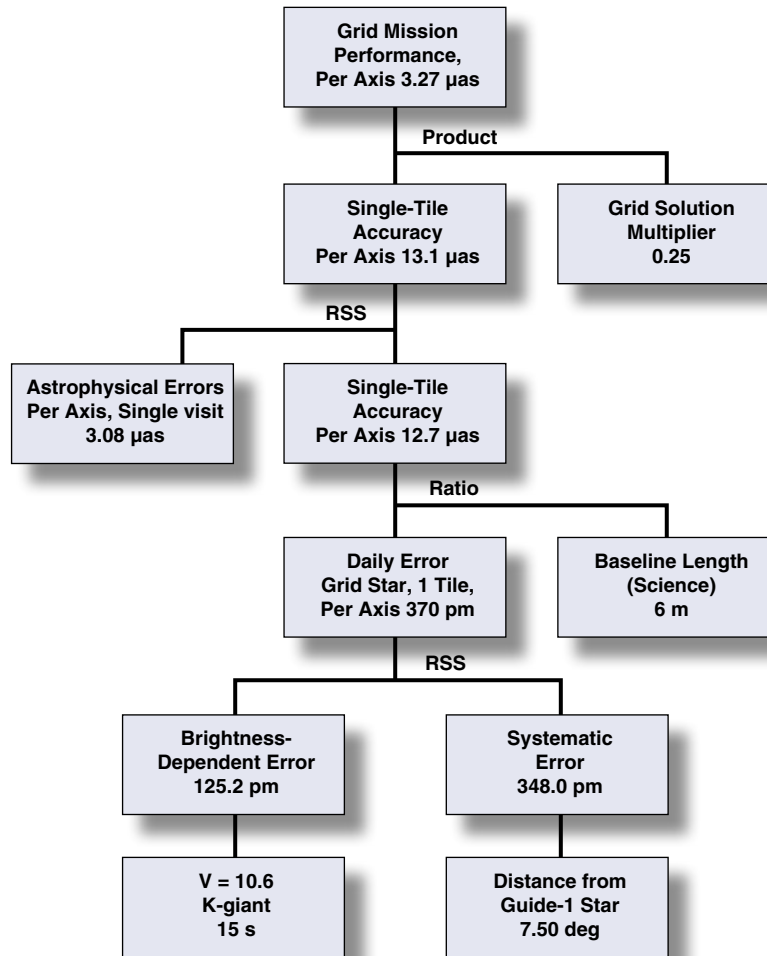
One level below, the error is expressed in pm of delay. Since the basic measurement of an astrometric interferometer is starlight delay, it is most convenient to specify instrument astrometric performance in units of allowable delay error. Instrument errors are divided into two major categories of brightness-dependent (random) errors and instrument systematic errors.

18.4 Narrow-Angle AEB Top-Level Structure

The top-level narrow-angle error budget is shown in Figure 18-2. Its performance metric is the single-visit, single-axis, effective single-measurement position error. To get the effective single-measurement error, the error budget assumes the target and reference star observations contribute equally to the differential astrometric error. Hence, it is set to equal the differential error divided by $\sqrt{2}$. The differential astrometric error includes contributions from astrophysical effects and non-ideal reference star geometry. One level below, the budget has two branches, one corresponding to errors from the target star and the other from the reference stars. Specific assumptions have to be made about the reference and target star brightness, spectral type, and observation durations. These, as mentioned above, are captured by the straw-man observing scenario. The breakdown below this level is similar to the grid error budget, with the branches being brightness-dependent and systematic errors.

Figure 18-2. The top-level portion of the narrow-angle astrometric error budget is based on the effective single-visit, single-measurement error under a planet-finding scenario.

Astrometric Error Per Axis, After 5 Yrs 0.049 µas

Eff. Single-Meas. Error Per Axis, Single Visit 0.99 µas

No. of Visits in 5 Yrs Per Axis 800

Astrometric Error Per Axis, Single Visit 0.40 µas

RSS

Astrometric Error Per Axis, Single Visit 0.17 µas

Astrometric Error Per Axis, Single Visit Ideal Ref. Star Locations 1.253 µas

Multiplier for Non-Ideal Ref. Star Geometry 1.10

RSS

Astrometric Error Per Axis, Science Star 0.83 µas, 4.00 prad

Astrometric Error Per Axis, Ref. Star 0.96 µas, 4.53 prad

Ratio

Ratio

Delay Error Science Star 24.0 pm

Baseline Length (Science) 6 m

Baseline Length (Science) 6 m

Delay Error Science Star 27.8 pm

RSS

RSS

Brightness-Dep. Error Science Star 4.0 pm

Systematic Error Science Star 23.7 pm

Brightness-Dep. Error Science Star 11.1 pm

Systematic Error Science Star 25.5 pm

BDE Budget

BDE Budget

6 Mag KOV 180 s

9 Mag KOIII 360 s

Distance from Guide-1 Star 1.00 deg

18.5   Brightness-Dependent Error

Brightness-dependent error (BDE) primarily arises from shot noise in the collected starlight, dark current in the detector, and read noise in the readout electronics. It is random in nature, and goes down with integration time. Figure 18-3 illustrates the important elements affecting BDEs.

In this figure, starlight from the two arms is combined, dispersed, and focused on the fringe detector. The light is converted to electrons according to the quantum efficiency of the detector. In SIM Lite, the fringe is formed temporally, as the delay is modulated. Since the fringe is dispersed across the detector, each pixel maps to a relatively narrow spectral channel.

Within each channel, the visibility of the fringe is given by:

$$V = \frac{I_{max} - I_{min}}{I_{max} + I_{min}} = \frac{a_0}{n_0} \qquad (1)$$

Figure 18-3. The brightness-dependent error fringe measurement is affected both by photon noise and detector noise.
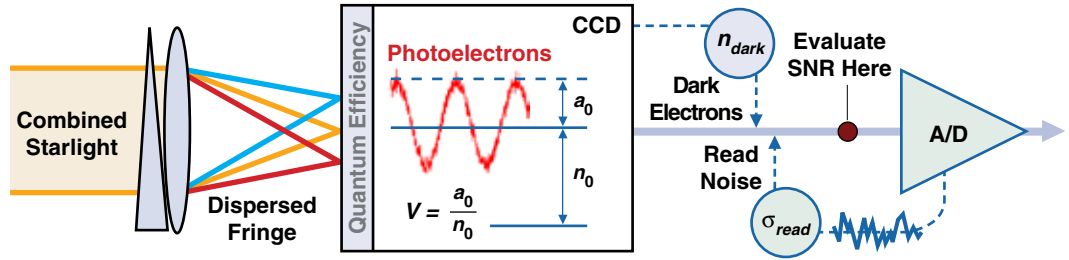
where I_{min} and I_{max} are the minimum and maximum intensity in the fringe, respectively, and alternatively a_0 and n_0 are the "ac" and "dc" levels of the fringe. The phase is best estimated near a "zero crossing" of the fringe.

The phase error is given by the reciprocal of the fringe signal-to-noise ratio (SNR) near the zero crossing:

$$\delta\phi = \frac{1}{SNR} = \frac{\sqrt{n_0 + n_{dark} + \sigma_{read}^2}}{V n_0} \tag{2}$$

where n_{dark} is the accumulated dark current, in electrons, and σ_{read} is the read noise, again in electrons. The brightness-dependent error is simply the phase error converted into pathlength. Putting it all together, the full expression for the brightness dependent error within a spectral channel is given by:

$$\sigma_{BDE} = \frac{\lambda}{2\pi} \cdot (\gamma\,\delta\phi) = \frac{\lambda}{2\pi} \cdot \gamma \frac{\sqrt{n_0 + n_{dark} + \sigma_{read}^2}}{V n_0} \tag{3}$$

where λ is the mean wavelength within the spectral channel and γ is a correction factor for the fact that the fringe has to be sampled at a number of points, not just the (ideal) zero crossings, before a phase estimate is obtained. We note that, as expected, the error goes down with integration time.

The BDE is an important error and drives the instrument in many very important ways. A cursory glance at Equation (3) immediately shows that the BDE has a first-order dependence on visibility. Visibility is wavelength dependent and ranges from about 0.7 to 0.9 over most of the spectrum covered by the fringe detector. Many attributes of the combined beams affect the visibility, with the most important being relative static wavefront, jitter in pathlength difference or tilt difference, and mismatch in footprint, polarization, or amplitude. The visibility requirements thus drive the instrument to have diffraction-limited optics, nanometer-class pathlength control, and mas-class jitter control. The STB-3 testbed described in Chapter 19 has demonstrated control at levels better than these requirements on a flight-like structure.

The BDE's next strongest sensitivity is to n_0, the total collected number of photons. This drives the instrument towards maximizing the collecting area and optical throughput.

Finally, the BDE also places requirements on the allowed dark current and read noise. The fringe detector in SIM Lite is specified to have a read noise of less than five electrons per read and dark current less than 0.01 e-/pixel/sec. With proper electronics and thermal design, both of these performance requirements are straightforward to accomplish.

18.6 Instrument Systematic Errors

The instrument systematics portion of the SIM Lite AEB is shown in Figure 18-4. At the highest level, each of the primary sensors is represented: the science and Guide-1 interferometers, the Guide-2 telescope, and the external metrology system. The errors from each of these sensors can in general be considered independent. The exceptions are captured in a separate branch called "second-order errors" and will be described separately. A more detailed instrument model, which includes effects to the second order, has validated this simple breakdown structure for the errors.

The values appearing in the boxes are the current best estimates of performance. The basis of most estimates ranges from actual performance measured in a prototype or testbed to engineering judgment based on previous work. As will be shown in Chapter 19, the algorithmic advances made alongside the

Figure 18-4. SIM Lite's instrument systematics error budget has been tested and validated against the independently developed and more detailed SIM Lite instrument model. The grid example is shown here.
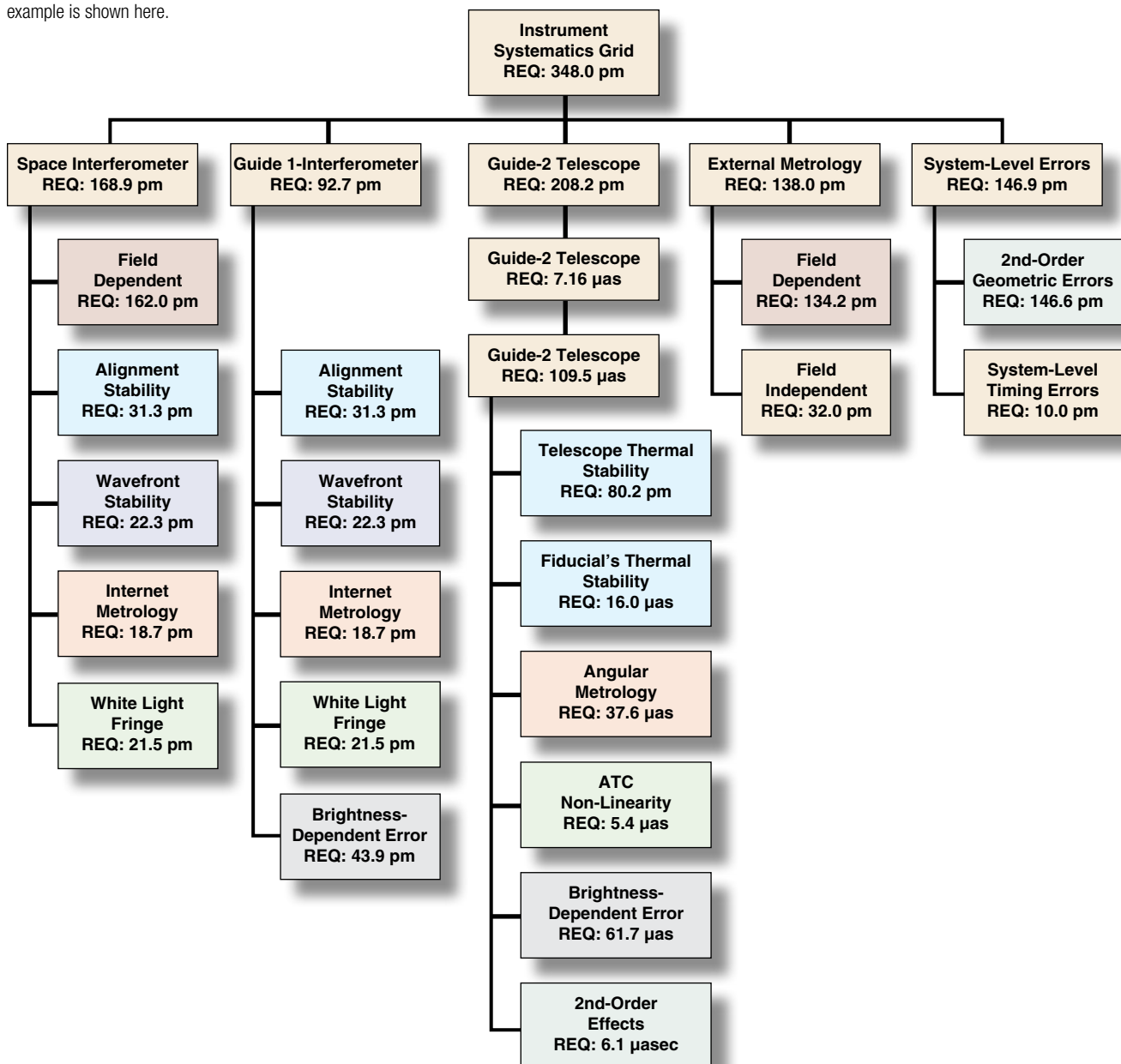
technology development have brought about a great deal of relaxation to the requirements at the hardware level. These algorithmic improvements usually fall into the categories of reduction and randomization of errors through strategic temporal programming of observations (such as chopping) and calibration of systematic effects using constrained fits to astrometric observations. The performance estimates in the error budget include the filtering effects of the processing algorithms.

18.6.1   Interferometer Errors

The science and Guide-1 interferometer systematic errors are similar, with the exception that the science interferometer has a siderostat which gives it a 15 degree FOR while the Guide-1 interferometer has a fixed collector. As a result, the entire category of field-dependent errors is absent for the Guide-1 interferometer. On the other hand, since the Guide-1 interferometer boresight is coincident with the center of the science FOR while the guide baseline is shorter than the science baseline, Guide-1 instrument errors are magnified by the ratio of the science baseline to the Guide-1 baseline. This makes Guide-1 requirements every bit as stringent as the science interferometer requirements.

We discuss the interferometer errors organized within the broader categories of the fundamental measurements: white light fringe delay, internal delay, and the baseline vector. Detailed mission modeling has verified that completeness at the topmost level is assured if these three fundamental measurements are captured.

18.6.2   Measuring the White Light Fringe

The total (internal plus external) optical pathlength difference (OPD) is given by the white light fringe phase. In SIM Lite, the fringe is temporal in nature, being observable by modulating the pathlength. It is also spectrally dispersed across a number of pixels using a prism, shown in Figure 18-5. The fringe phase is obtained by modulating the pathlength and recording the resulting photoelectron counts at each of a number of spectral channels. The white light fringe on the "minus" or "dark" side of the beam splitter is shown in Figure 18-5. The fringe on the other side would be bright at zero OPD, and is also used.

Pathlength modulation for measuring fringe phase is used in a number of commercial interferometers. None of the commercial interferometers have accuracy below 100 pm. By using a pm-accurate metrology system to measure the position of the pathlength modulator and using that information along with the CCD measurements in a least-squares estimate of the complex visibility, SIM Lite eliminates the largest and most common error in pathlength modulation interferometry.

At the subnanometer level, two types of systematic errors remain. Both of them are related to the fact that we are measuring the optical phase of a white light fringe rather than a monochromatic light source's fringe. As the interferometer is pointed at different stars with different spectral energy distributions, two sources of errors can arise. They are (1) dispersion and polarization in the optics, and (2) changes in the effective wavelength of the light. SIM Lite addresses these errors by calibrating the dispersion curve daily and measuring the spectrum of each observed star once during the mission. This approach is currently being refined using a testbed called the Spectral Calibration Development Unit.

Figure 18-5. Phase estimation using dithering is illustrated here; the response of four spectral channels is shown as the delay is dithered. The spectrally dispersed white light fringe is on the left. A, B, C, D are the integrated detector counts during each temporal quadrant of pathlength dither. With the aid of precision metrology, SIM Lite has successfully demonstrated pm-class fringe delay estimation.

$$\phi = \tan^{-1}\left[\frac{B-D}{A-C}\right] + \frac{\pi}{4}$$
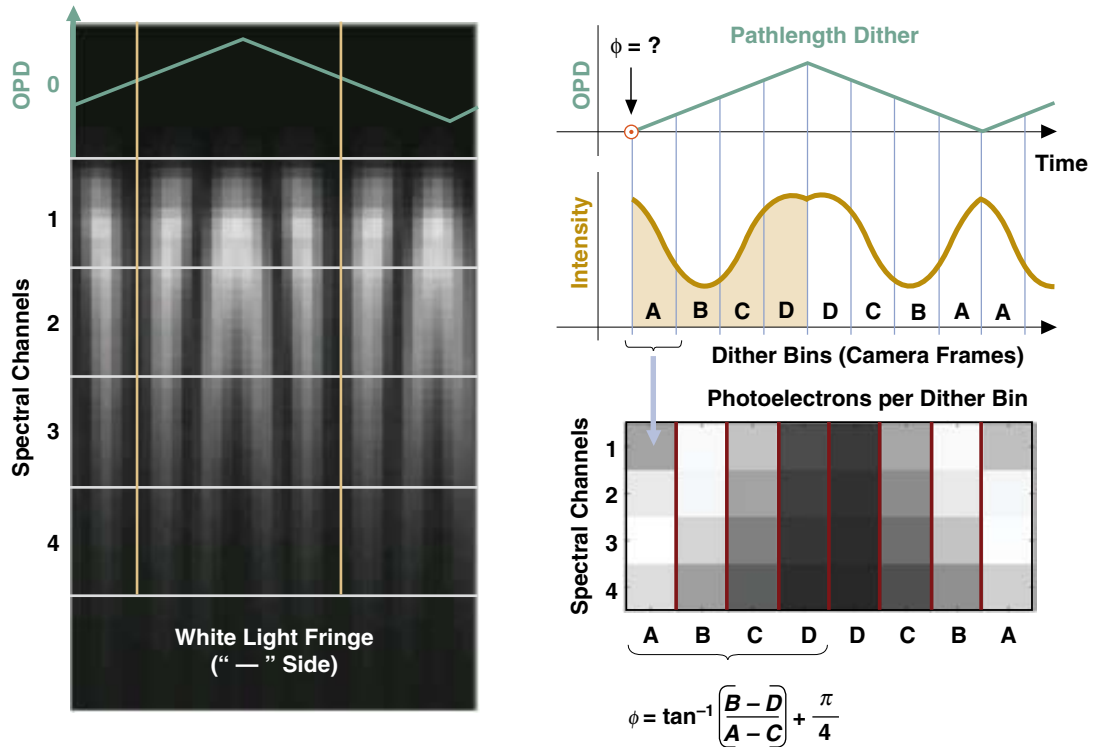
18.6.3 Measuring the Internal Delay

The starlight internal delay is measured using the internal metrology system. An infrared laser beam originates from a beam launcher and is separated into two beams by the beam combiner/splitter. The two beams make round-trip journeys to the two double corner cubes (DCCs, one at each siderostat) and return to the beam launcher with phase delay, which measures internal pathlength difference (Figure 18-6). The footprints of the two metrology beams are within the annular footprint of the starlight beam.

In the error budget, any deviation between what the starlight experiences and what the metrology measures is book-kept under internal metrology error. Since the metrology footprint is a small central region inside the annular starlight footprint, differences can arise between the two, leading to errors. For example, at the siderostat, the starlight bounces off the annular mirror while the internal metrology beam only senses the DCC mounted at the center. When the siderostat, with its DCC, is turned from one star to another, an error proportional to the offset between the vertex of the corner cube and the surface of the siderostat arises. This error will depend on the siderostat look angle within its FOR, and is hence called a field-dependent error (Figure 18-7).

Another source of field-dependent error lies within the optical delay line (ODL), which is the system that changes the internal delay to match pathlengths. As the instrument switches from star to star within its FOR, the delay can change by as much as 2 m. As the ODL compensates for this, the imperfections in the ODL mechanical structure will induce micron-level lateral motion (beam walk) of the light on the optics. Since the footprints of metrology and starlight are different, imperfections in the optics cause different delay changes between the two, leading to a field-dependent error.

The mitigation of these field-dependent errors requires a combination of tight tolerances on opto-mechanical parts and calibration of residual requirements using star observations. This approach has been validated using the Microarcsecond Metrology (MAM) testbed and SIM Lite mission modeling.

Alignment instability in the metrology beam can cause beam-walk errors as the diffracted metrology beam walks across the optics. Beam-walk errors have been tested both in the MAM testbed and the diffraction testbed. The results from these testbeds indicate that the beam-walk errors in SIM Lite are controllable to within error budget allocations.

Wavefront instability, mostly driven by thermal changes anywhere along the optical train, can translate into an effective metrology error, again due to the difference in the starlight and metrology footprints. SIM Lite's Thermo-Opto-Mechanical (TOM) testbed (described in Chapter 19) has demonstrated that, thanks to the thermal mass of the components involved, the thermal environment is sufficiently quiescent to keep the errors within the allocations.

Figure 18-6. The internal metrology gauge monitors the changes in the left-right optical pathlength difference in the interferometer at the pm level.
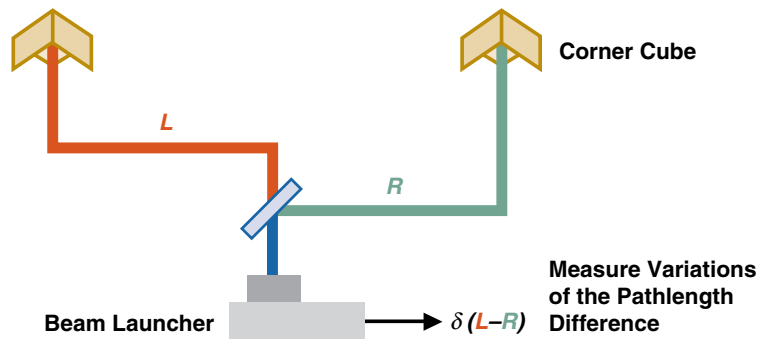
Figure 18-7. There are two ways metrology can be in error relative to starlight. Figure errors in the optics can result in sensitivity to beamwalk. Here, the starlight and metrology are "walking" together across the optic, resulting in a net OPD error. Alternatively, a change in the surface figure ("wavefront instability") can cause a difference between the metrology and starlight. These effects have been fully tested in a number of SIM Lite testbeds and shown to be controllable to within requirements.
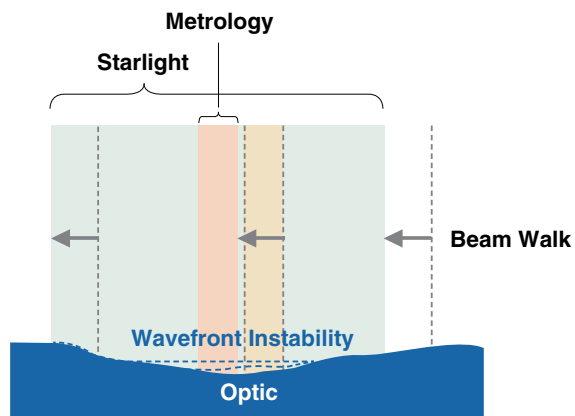
18.6.4 Guide-2 Telescope Errors

Another branch of the instrument systematics error budget (see Figure 18-4) is the Guide-2 telescope (G2T) branch. Converting the allocation to G2T's native units of attitude knowledge accuracy, the requirements on G2T are 50 and 100 µas for the NA and Grid scenarios, respectively. To get the level of centroiding accuracy needed to support these requirements, a pointing loop is used to maintain the line of sight (LOS) of the telescope on the "sweet spot" of the angle tracking camera (essentially the cross-hairs formed by specific pixel boundaries). Siderostat angular motions required to fix the star image on the angle tracking camera (ATC) are monitored using an angular metrology system. Angular metrology operates in a manner similar to internal metrology, except that it uses more beams so that it can perceive tip and tilt.

Ideally, G2T measures the rotation of the external metrology truss relative to inertial space. To make this tie, the telescope is mounted on a bench with fiducials that are monitored by external metrology beams. G2T's most important source of systematic error is thermally induced deformations. These deformations are broken down into two categories: the internal deformations of the telescope optics and motions of the fiducials with respect to the telescope.

It is useful to consider an example. If the thermal gradients induce a relative motion between the ATC and the siderostat, the star image would move in the ATC and the pointing loop would promptly rotate the siderostat to bring the image back to the nominal spot. At the same time, the angular metrology measurement would sense the correction and indicate a rotation relative to the star. This would be incorrectly perceived as an inertial rotation of the instrument.

The G2T error budget also includes the errors in measuring the centroid in the ATC. These include photon noise as well as nonlinearities in the centroiding algorithm arising from the finite sampling of the image by the CCD. These errors are minimized by driving the image to the "sweet spot" as mentioned before. Additionally, the G2T error budget includes the errors in measuring the tip/tilt of the siderostat with metrology beams. These include errors associated with knowledge of instrument geometry and metrology gauge errors.

Because the thermal errors are expected to be the largest contributors to the G2T errors, they have been given the highest allocation. These allocations were made consistent with the thermal deformations expected on orbit, using thermal models of SIM Lite under flight-like conditions.

To demonstrate that SIM Lite can meet these requirements, a new testbed called G2T has been built and is currently in operation. The testbed and the initial results are discussed in Chapter 19. So far, the results indicate that all the G2T requirements can be solidly met.

18.6.5 External Metrology Errors

All relative displacements between SIM Lite fiducials are measured using the external metrology system. The system is composed of beam launchers interposed between the fiducials, monitoring in each case a one-dimensional length. Each beam launcher is a miniature heterodyne laser interferometer with an accuracy of a few pm. Elements of a single link are shown in Figure 18-8.

External metrology errors are generally grouped into two main categories. These are one-dimensional gauge (field-independent) errors and field-dependent errors.

Figure 18-8. External metrology measures the distances between fiducials such as the double corner cube (DCC, left) using beam launchers (right). Noncommon vertex error (NCVE) is the distance between the two vertices of a DCC.
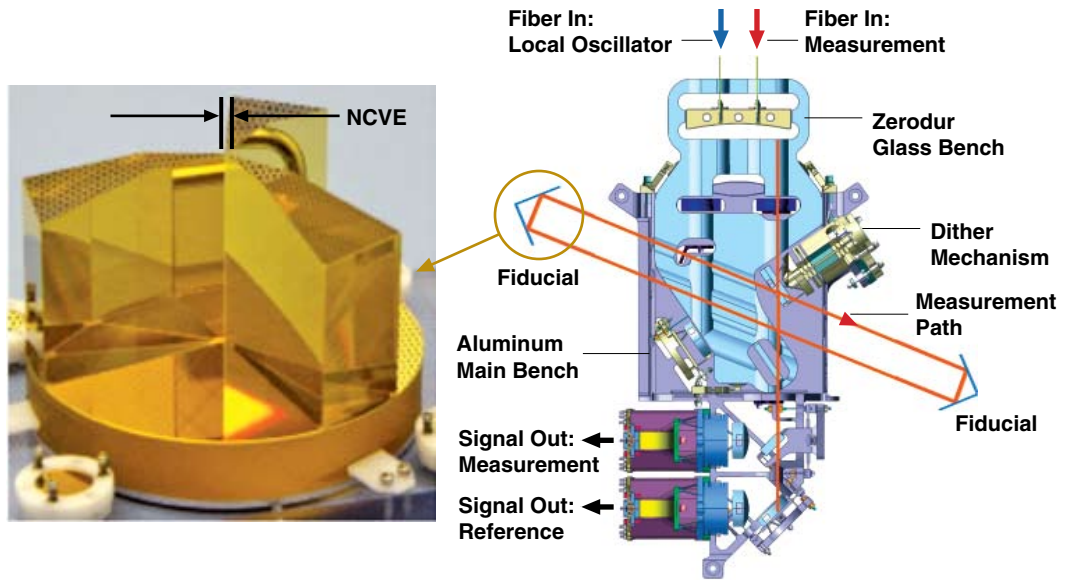
Field-independent errors primarily include gauge errors arising from crosstalk between laser metrology signals, thermal deformations within each beam launcher, alignment errors, and finite SNR in the detected laser signal. The metrology truss solution requires a micron-class survey of the instrument. This is done using beam launchers in two-color interferometry mode, which is dubbed "absolute metrology." Errors in the absolute metrology survey are also book-kept under field-independent errors.

As the siderostat with its DCC turns from star to star, the external metrology system incurs field-dependent errors due to a number of effects. First, we note that each fiducial is a multiple corner cube constructed in a way that the noncommon vertex error (NCVE, Figure 18-8) between its component corner cubes is as small as possible (less than a few microns). Even at this level, the noncommonality of the vertices in each DCC results in geometrical errors in the truss. Also, reflection phase shifts will be different on the different metrology beams that interrogate a given DCC. These beams will also be "walking" on the corner cubes. Any surface errors coupled with this beam walk result in errors. Finally, corner cube dihedral errors (deviation from orthogonality) cause additional field dependent errors.

SIM Lite's external metrology testbed, described in Chapter 19, was dedicated to demonstrating all of the technological aspects associated with external metrology. The results, discussed in Chapter 19, show that the technology to meet these external metrology requirements is at hand.

18.6.6 Second-Order Errors

The final branch to be discussed in the instrument systematics error budget concerns second-order errors. There are seven important second-order effects, and they are typically the product of a knowledge or measurement error and some motion. Figure 18-9 indicates all the second-order effects and highlights the ones that are significant.

They are all essentially residual errors that are beyond the reach of further calibration and enter into the astrometric measurement without further suppression. One example is the second-order error arising from the attitude control system (ACS) error (a motion) coupling with error in absolute metrology.

As mentioned in Chapter 16, by knowing the truss geometry and the measured ACS motion using the guide instruments, the science delay can be corrected for the science baseline motion. An error in the absolute metrology results in an error in the truss geometry knowledge, and hence an error in the corrected science delay.

This and all such errors are controlled by placing tight requirements on the motions in question and on the knowledge or measurement errors. These errors have been studied using instrument modeling and in testbeds, and their impact has been demonstrated to be tolerable.

Figure 18-9. Second-order instrument systematics errors involve a motion coupled with a knowledge or calibration error.
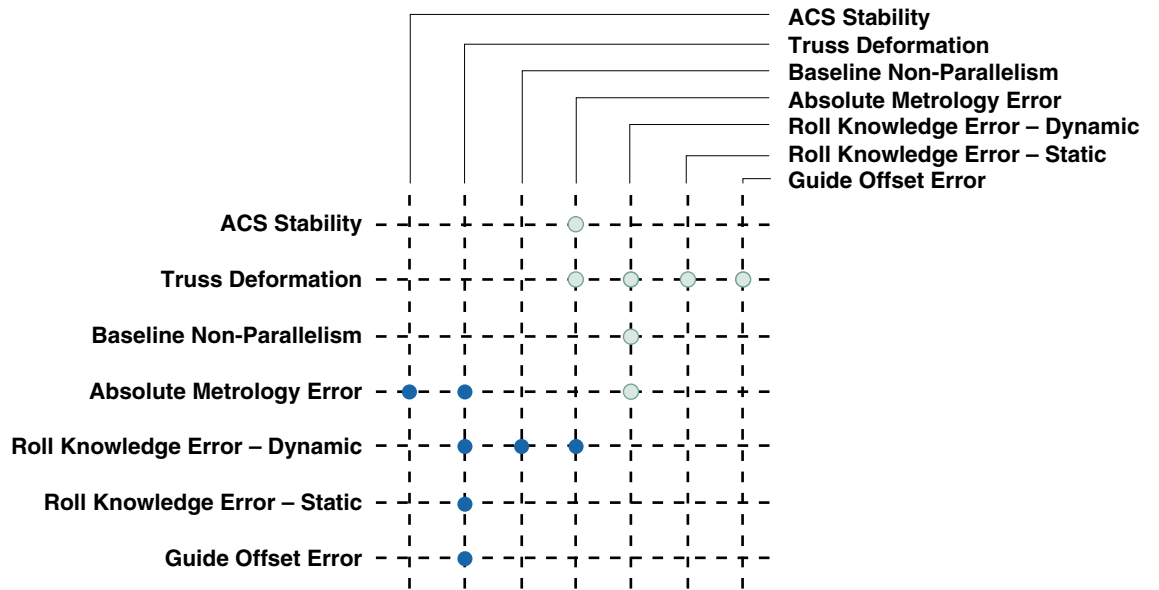
Technology Program
19 Accomplishments
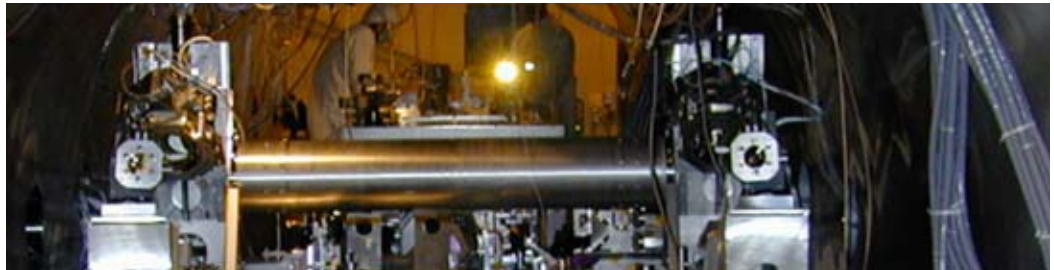
Bijan Nemati (JPL), **Inseob Hahn** (JPL), and **Oscar S. Alvarez-Salazar** (JPL)

ABSTRACT

Developed over the past 12 years, SIM Lite's spectacularly successful technology program has conclusively demonstrated that the era of sub-µas optical astrometry is at hand. Overall, SIM Lite's development has placed a high emphasis on retiring risks and ensuring completeness. This resulted in the successful completion of all of the NASA-required technical milestones. With many key brassboards already completed and submitted to environmental testing, and more presently under development, SIM Lite is ready for final design and flight implementation.

19.1 Technology Demonstrated Through Testbeds

For over a decade, the SIM Project has carried out an expansive and ambitious technology program to demonstrate the key technologies required in order to make sub-µas astrometry possible. The program has been a resounding success. Here we give a brief overview of the measurement approach, the technologies required, and the results obtained from SIM Lite's technology program.

The flowdown of the error budget showed, early on, that in many areas the technology for SIM Lite had yet to be demonstrated. Some of the most demanding technology included:

- Measurement of displacements within the instrument to picometers — 2 orders of magnitude better than the current state of the art.
- Pathlength stabilization to nanometers in the presence of various disturbances in the spacecraft environment.
- Nanometer pathlength stabilization when the star is so dim that the fringe position can only be estimated every few minutes.
- Millikelvin-level thermal stability for the collector optics.
- Building a star tracker with 50 µas accuracy — 3 orders of magnitude better than the state of the art.

This chapter highlights how these and other technology challenges were successfully met and retired by SIM LIte's technology program.

Broadly speaking, the SIM technology testbeds can be placed in two categories. The first is focused on whether the level of pm-level sensing required for SIM Lite astrometry can be achieved. Chief among these are the Microarcsecond Metrology (MAM), the external metrology (Kite), and the Guide-2 telescope (G2T) testbeds. The second category is focused on the environment under which these measurements need to take place. The primary concerns here are vibrations and thermal variations. To address the dynamics and controls issues, a series of system-level testbeds was created, culminating in the three-baseline System-Level Testbed (STB-3). Thermo-opto-mechanical (TOM) investigations were conducted with the TOM testbed. We will discuss STB-3 and TOM later in this chapter.

19.2 The Microarcsecond Metrology Testbed

The MAM testbed, shown in Figure 19-1, was designed to study specific errors expected in SIM Lite's pm-class interferometers. It demonstrates, at the system level, the essential technology for sensing the white light and metrology pathlength differences at the pm level. The MAM testbed tested most of the error budget allocations for the science and the guide interferometers at the system level.

The testbed, whose layout appears in Figure 19-2, is composed of two major parts: the test article and the pseudo star. The test article (TA) is an optical interferometer with internal metrology. The inverse interferometer pseudo star (IIPS) provides the test article with wavefronts consistent with a distant star. Starting from the IIPS source, broadband (600 to 1000 nm) light is injected from an optical fiber tip, then collimated and separated into two beams. The beams are steered to two coordinated stages and thence launched towards the test article siderostats as flat, coherent wavefronts. The stages are designed to provide simulated starlight for the test article over the range of angles that comprises SIM Lite's field of regard (FOR), a 15-degree-diameter circle on the sky. The wavefronts are not required to have the relative delay that corresponds to the angle of the star being simulated. The actual external delay generated by IIPS is monitored by its metrology system, and it is the job of the test article to measure this delay.

Figure 19-1. SIM Lite's MAM testbed, shown here in the 4-m-diameter vacuum chamber, has demonstrated goal-level performance (see text) in both narrow-angle and wide-angle regimes. (From Hines et al. 2003.)
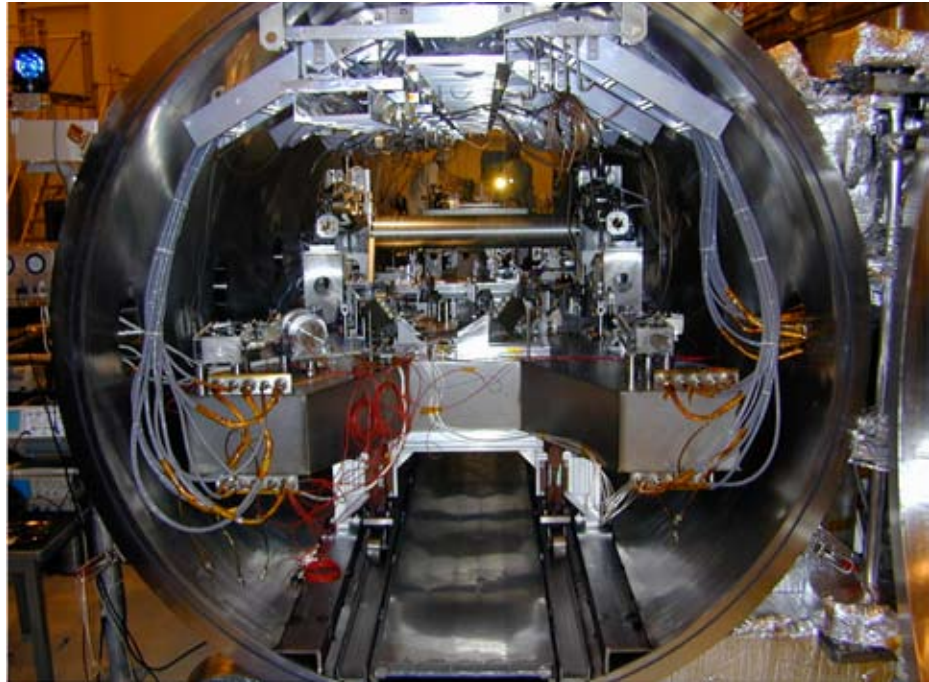
Figure 19-2. The MAM optical system captures the main elements of the SIM Lite science interferometer. (From Hines et al. 2003.)
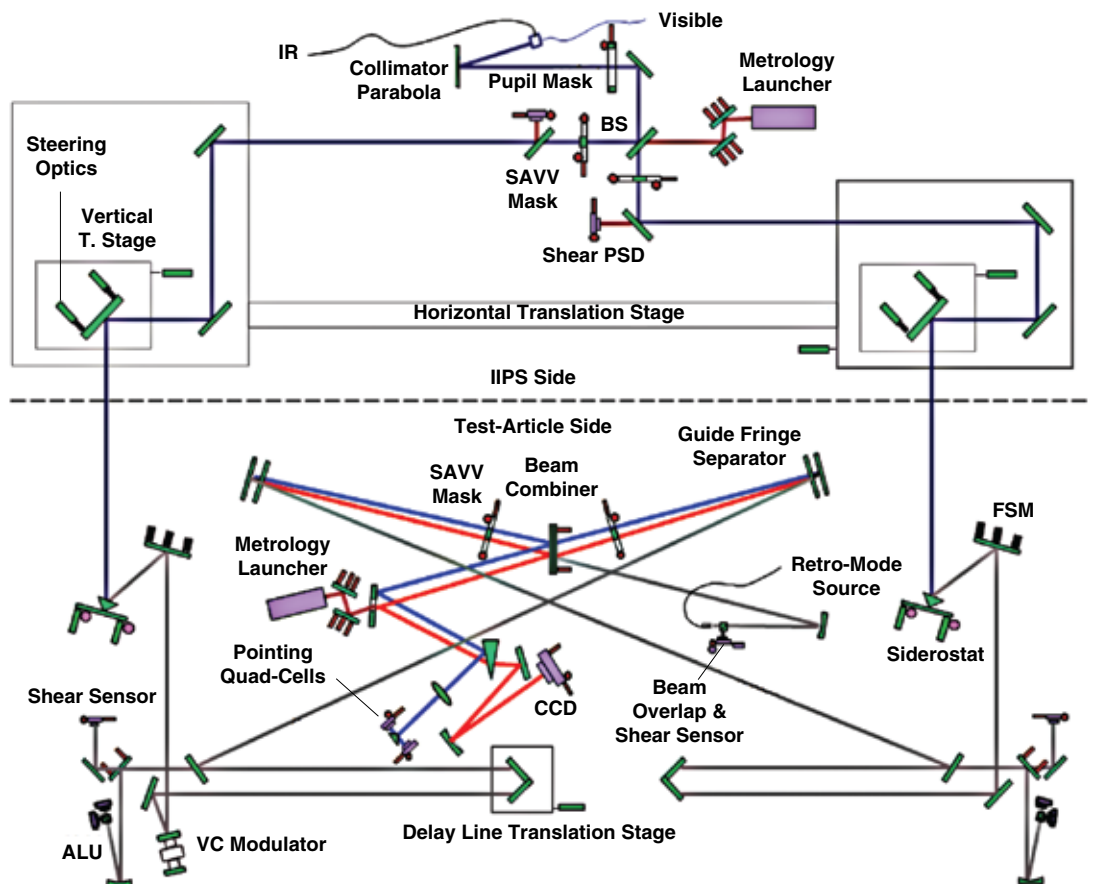
In the interferometer, the two "starlight" beams captured by the siderostats are steered to a beam splitter where they are combined and spectrally dispersed onto a CCD detector. The pathlength of one interferometer arm is modulated using a triangle wave resulting in an intensity modulation detected on the fringe tracking CCD. By proper detection and processing of this intensity signal, the phase of the white light fringe pattern can be measured at the pm level. Thus, the white light beams start at the IIPS beam splitter and terminate at the TA beam combiner. As in SIM Lite, the fundamental reference points of the TA interferometer are the vertices of the two corner cubes installed at the center of the two siderostats: all astrometric measurements are defined in terms of these two points.

Besides the white light, the same paths are also traveled by metrology, though not continuously. MAM uses prototype internal metrology launchers called SAVV (short for sub-aperture vertex-to-vertex). The experience gained from the SAVV launchers led to the development of the successful internal metrology brassboard beam launcher (Chapter 20). In MAM, a metrology launcher in the IIPS monitors the left-right path difference from the IIPS beam splitter up to the TA siderostat-mounted corner cubes (Figure 19-3). The TA internal metrology does the same thing starting from the TA beam combiner out to the siderostat corner cubes. A severe technical constraint on MAM, as on SIM Lite, is that the metrology and starlight paths have different footprints. The starlight beam footprint is an annulus around a central metrology footprint. Achieving pm-level internal metrology fidelity with respect to starlight in the presence of this constraint necessitates careful optical design and accurate alignment.

The MAM error metric is the difference between the total white light and metrology measurements:

$$E_{MAM} = \phi_{TA} - (M_{IIPS} + M_{TA}) \tag{1}$$

The TA fringe measurement gives the total pathlength difference from the IIPS beam splitter to the TA beam combiner [the conversion from phase to pathlength units is implied in Equation (1)]. The sum of the IIPS and TA metrology also gives a measurement of the total path difference. As usual, these are all variation ("relative") measurements over some given time span. Going from the error metric to the narrow-angle and grid performance metrics occurs by following the appropriate scenarios and their associated processing algorithms. Since the performance metrics are based on the instrument only, an adjustment of $1/\sqrt{2}$ is applied to the error metric. This factor assumes that the IIPS and TA interferometers have similar errors so that the variance of the error metric (Equation 1) is twice the variance of the TA portion.

In MAM's wide-angle (WA) runs, the pseudo star projects planar wavefronts at various angles consistent with SIM Lite's 15 degree FOR. The starting point is a star at the middle of the field. Over the course of a one-hour sequence of measurements representing a tile, the initial star is measured again at the middle of the hour and once more at the end. These three visits are used to remove the linear portion of any temporal drift in the data. In the MAM runs, certain stars in the field are designated as grid stars. These are used to calibrate out those trends in the field that the grid solution is expected to solve for. The MAM wide-angle metric is the root-mean-square (RMS) residual for stars not used to determine the field-dependent trend. The wide-angle error in MAM was measured to be under 260 pm, which is better than the goal performance for SIM Lite.

The geometry of a typical SIM Lite narrow-angle (NA) visit is shown in Figure 19-4. To minimize systematic errors, the reference stars are chosen so that their collective center of brightness (computed analogously to a center of mass) is as close as possible to the target star. On the other hand, to minimize random errors, the reference stars are allowed to be as far as one degree from the target star to increase the likely presence of brighter reference stars. During each visit, the baseline points in a single direction. In order to measure the target motion in two angles, successive visits use alternate (ideally orthogonal) baseline orientations.

Figure 19-3. The SAVV beam launcher, used for the first time in MAM, proved that pm-class internal metrology is feasible. It became the prototype for SIM Lite's brassboard beam launcher.
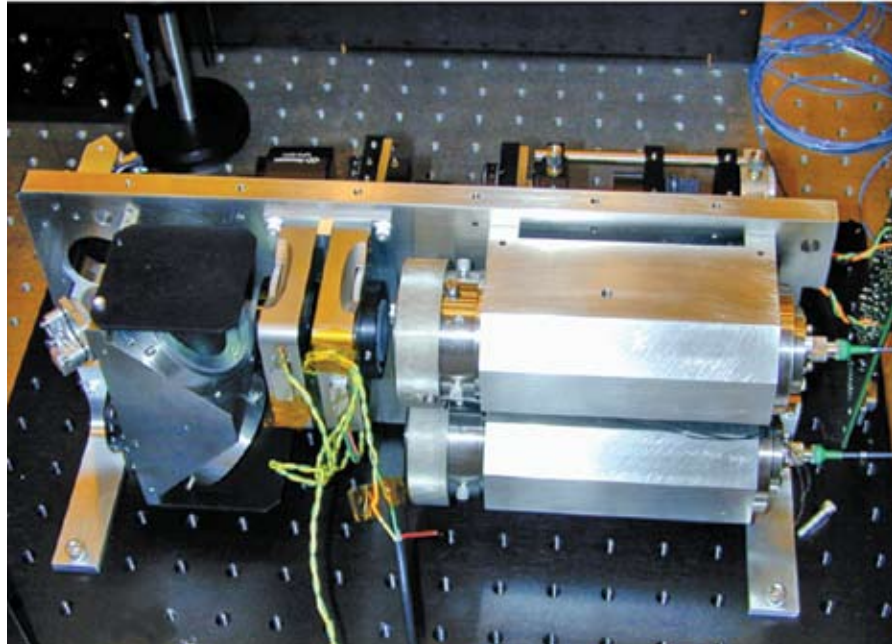
Figure 19-4. The narrow-angle observing scenario with a target star at the center of the field of regard and reference stars within a circle of one-degree radius. The baseline orientation on a subsequent visit would be orthogonal to that shown here.
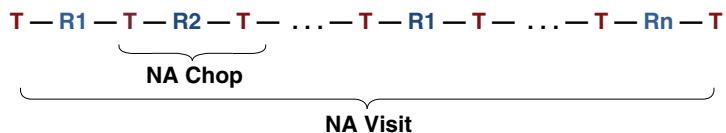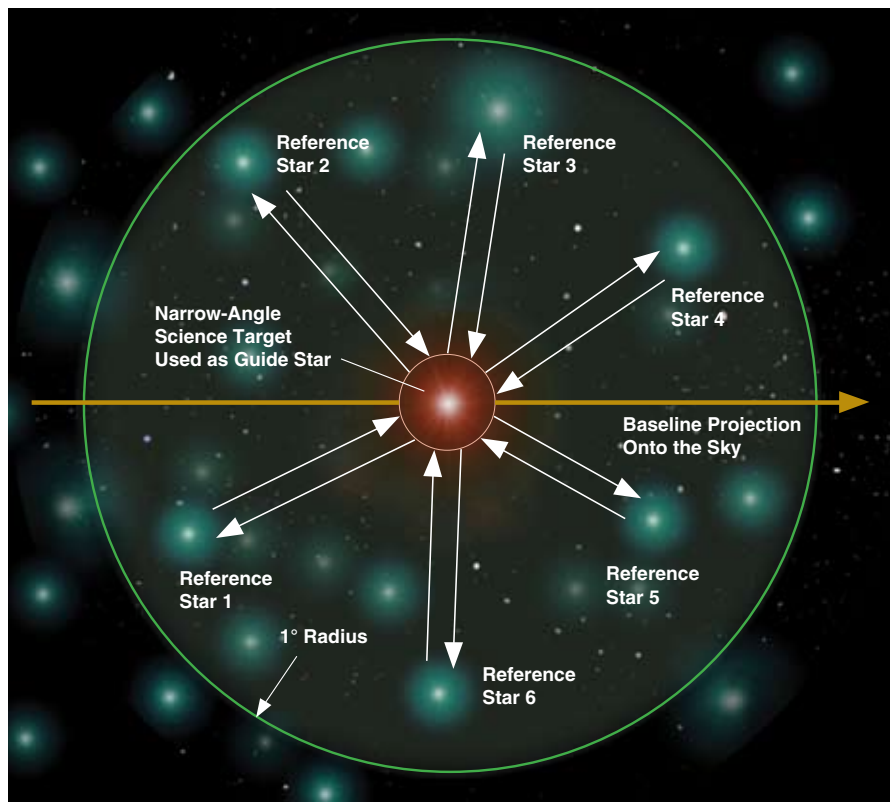
The basic NA measurement is the delay difference between the target and a reference star. In order to minimize the effect of instrument drifts, the instrument chops between the target and a reference and back to the target. The chopped delay difference is then given by:

$$d_i = x_R^i - \frac{x_T^{i-1} + x_T^{i+1}}{2} \qquad (2)$$

where x_R^i is the measured delay for reference star *i*. It includes corrections for proper motion and parallax effective at the measurement epoch. Similarly, x_T^{i-1} and x_T^{i+1} are the measured residual delays in the preceding and succeeding target looks, respectively. Depending on the brightness of the star, each observation is approximately 30 seconds long and the time to look from a target star to a reference star is approximately 15 seconds. The entire cycle of observations is repeated during the visit, so that each reference star is measured twice. These are then averaged, forming a single, per-visit delay difference between the target and each reference star. The differences are collectively analyzed to determine the motion of the brightness center of the reference stars relative to the local origin, which is defined to be the location of the target star. Thus, the signal is the relative motion of the reference star brightness center from epoch to epoch. For planet detection, the signal is in fact the acceleration measured across many epochs.

MAM NA visits involve four stars in a symmetric cross pattern. The goal-level NA performance for MAM, based on the SIM Lite error budget, is that the per-visit error be under 24 pm in at least 68.3 percent of the runs. In actual tests, the fraction of runs with performance metric under 24 pm was found to be 67.8 percent, implying performance just meeting the goal.

In a follow-on version of the MAM testbed, called Spectral Calibration Development Unit (SCDU), the field-independent portion of the NA performance was recently studied in a 230-hour quasi-static run. The data were divided up into segments ascribed alternately to target and reference star looks, as well as slew times between the looks where the data were not used. Chop differences in the manner of Equation (2) were computed. Figure 19-5 shows the effectiveness of averaging the chops. As can be seen in the figure, averaging continues to reduce the error until all available data are exhausted. Hence, no noise floor is reached using the total recorded data, dipping the error to below 17 nanoarcseconds after 71 hours of integration.

An important question in applying testbed results to SIM Lite is: How does the thermal behavior of the relevant parts of SIM Lite compare with the testbed? Figure 19-6 shows a comparison of the temperature power spectral densities (PSDs) as measured in the testbed and modeled for SIM Lite. The SIM Lite model is a 20-hour simulation with a few thousand nodes. The temperatures extracted are those associated with the beam combiner region, where the internal metrology beam originates. The relevant frequency range for planet finding and NA astrometry is near 1/90 s or about 0.01 Hz. Overall, the plot shows the expected thermal environment for SIM Lite to be no worse than that experienced by the testbed. Thus, the testbed shows end-of-mission error at or below 17 nanoarcseconds with thermal conditions more challenging than SIM Lite is expected to encounter.

19.3 The External Metrology Truss Testbed (Kite)

SIM Lite's external metrology truss testbed was built to demonstrate that an external metrology system with pm-level performance is feasible for SIM Lite. A metrology truss consists of a set of fiducials, typically hollow corner cubes, with metrology beam launchers interposed between them. Each beam launcher, along with its associated laser source and phase measurement electronics, comprises a

Figure 19-5. The narrow-angle chopping scheme is highly effective in randomizing the thermal error. The error behaves as white noise down, down to 17 nanoarcseconds after 71 hours of integration.
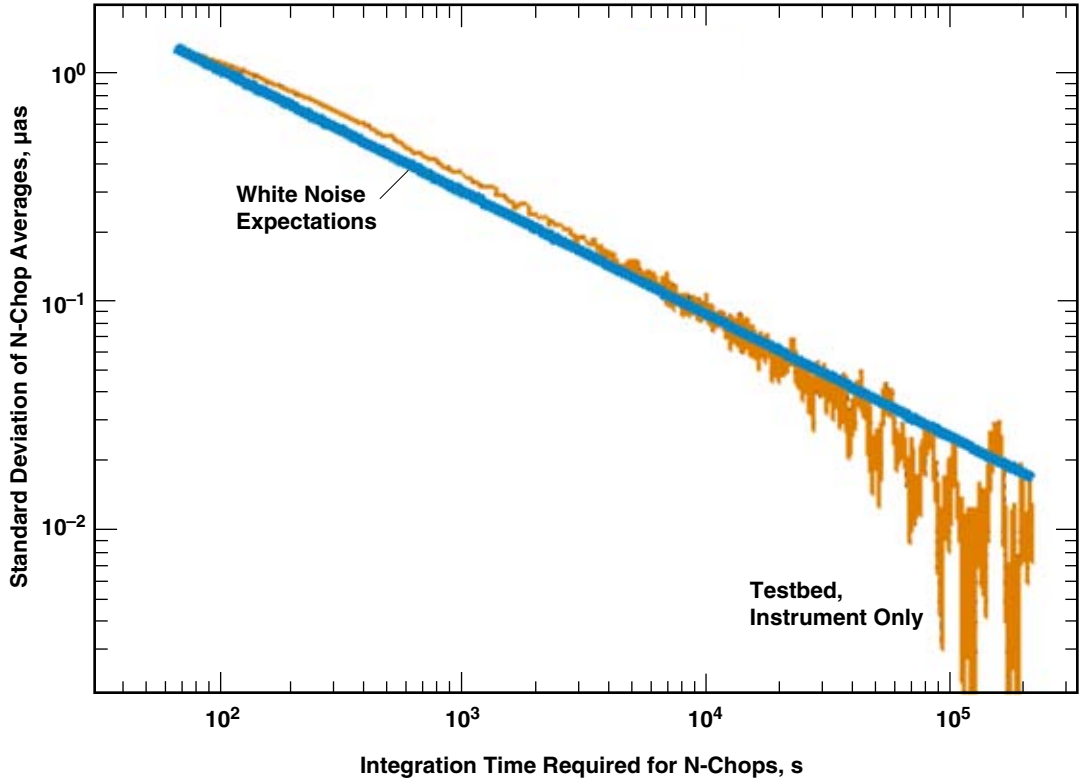
Figure 19-6. The SIM Lite expected thermal environment (blue) is quieter and more benign than the thermal environment encountered by the testbed (orange).
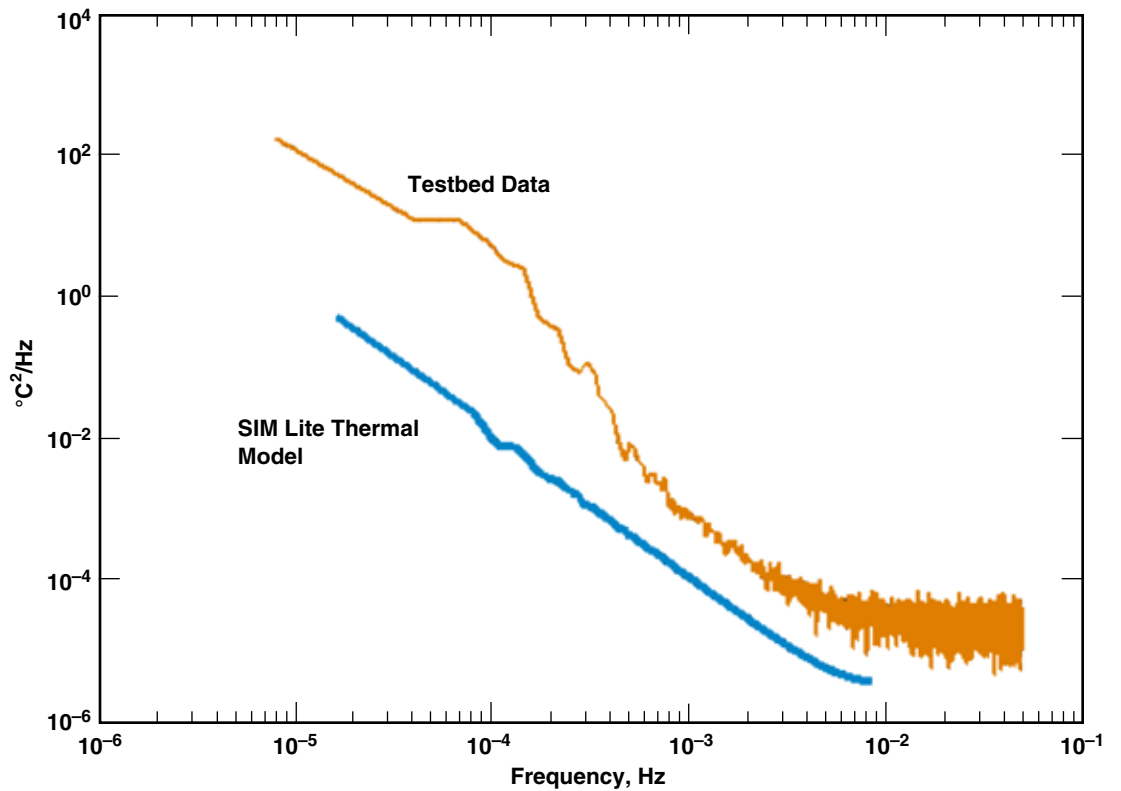
one-dimensional metrology gauge. The testbed featured a novel beam launcher, called QP for "quick prototype," in which the reference and probe beams were spatially separated (Figure 19-7). This innovation made possible the first feasible pm-class metrology gauges.

The minimal test configuration for point-to-point metrology is a two-gauge set-up, in which two metrology beam launchers simultaneously probe the same pair of corner cubes, as shown in Figure 19-8. Assuming the gauges are independent, the difference between their readings will have a variance that is twice the per-gauge variance. The two gauge set-up can be used to qualify individual launchers for most of the field-independent errors discussed in Chapter 18.

A real truss, however, will have errors beyond the reach of a two-gauge test. The entire class of field-dependent errors, as well as truss-only errors such as in the absolute metrology survey, needed to be investigated. For a truss with N nodes (fiducials), the number of possible links and the number of sensed degrees of freedom are given by:

$$n_{link} = \frac{N(N-1)}{2} \quad \text{vs.} \quad n_{dof} = \begin{cases} 2N-3 & \text{(2 dimensions)} \\ 3N-6 & \text{(3 dimensions)} \end{cases} \tag{3}$$

To have redundancy, i.e., $n_{link} > n_{dof}$, the minimal configuration is a two-dimensional truss with four nodes, where there are six links, or measurements, and five sensed degrees of freedom, or unknowns. Hence, the testbed was chosen as a planar truss with four nodes. Its original diamond shape led to the name "Kite." Figure 19-9 shows the testbed in its original configuration in the vacuum tank it shared with the MAM testbed. To achieve planarity, a theodolite was used to move one of the four corner cubes (called the planarity corner cube) into the plane defined by the other three. A planarity error of less than a few tens of microns is sufficient to keep the resulting truss error at the allocated level of a few pm.

To illustrate the testbed data and the impact of narrow-angle processing, a sample one-hour quasi-static run is shown in Figure 19-10. Quasi-static conditions imply that no intentional change or disturbance was introduced to the test set-up. The dominant sources of motion under these conditions are vibrations and ambient thermal variations. The sampling rate in the test shown here is 100 Hz, with 10 ms averaging of the metrology data prior to readout. The green trace, extending lower than all others, is telemetry from Gauge 2, or the test link. It shows a hash of about 30 nm RMS from vibrations on top of a slower trend of approximately 400 nm peak to peak from temperature change during this period.

The error metric for the truss testbed is the difference between the readings of Gauge 2 versus the prediction for that link using the other five gauges. This prediction will rely on a prior survey of the absolute lengths at the <10 μm level. The truss is operated in "absolute" mode periodically to obtain an up-to-date survey suitable for pm-level relative metrology. For this geometry, modeling shows that the per-link expected error is very nearly $1/\sqrt{2}$ of the metric error. The metric error is the black trace.

It is possible to use quasi-static data such as these to assess aspects of truss performance under various scenarios. For example, one can apply processing representative of the narrow-angle scenario. Figure 19-11 shows the error averaged down in 30-second intervals, resulting in the blue trace. The peak to peak variation in the averaged metric is seen to be about 400 pm over the hour. However, the timescale for a narrow-angle chop measurement is much shorter. The green trace shows the single-chop error over the same time span, with a standard deviation of 15 pm. Assuming four reference stars each visited twice, the effective random error is reduced by averaging, as shown by the red dots whose standard deviation is 8 pm.

In Kite's full narrow-angle tests, four reference stars are assumed to be symmetrically situated 1 degree away from the target star in a cross pattern. For the corner cube, this means rotations to 0.5 degree

Figure 19-7. The quick prototype (QP) beam launcher demonstrated for the first time that pm-level monitoring of relative displacements between two fiducials is feasible. It also demonstrated absolute metrology at the 10 micron level. In the figure, CC refers to corner cube.
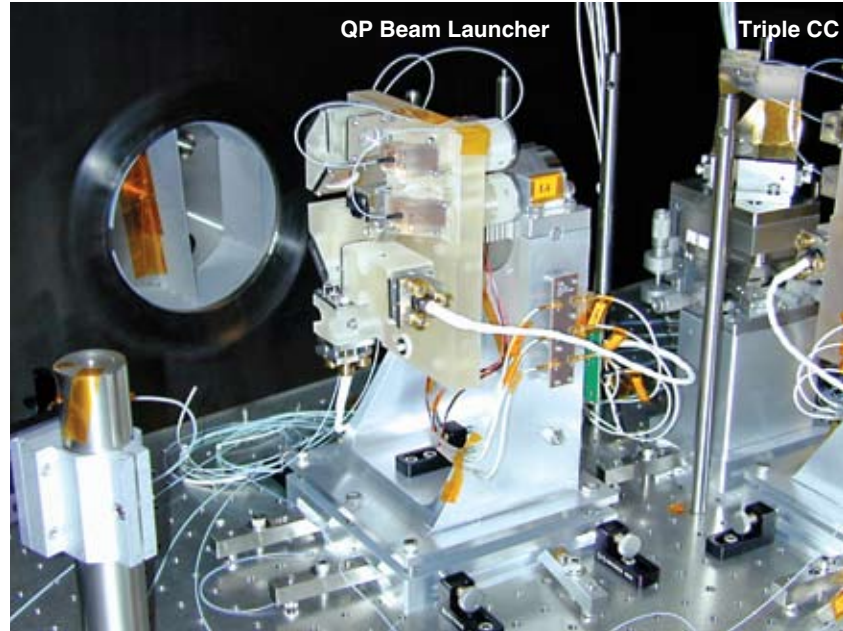
Figure 19-8. To accommodate a two-gauge test set-up, SIM Lite beam launchers are designed so that both have clear paths to the corner cubes.
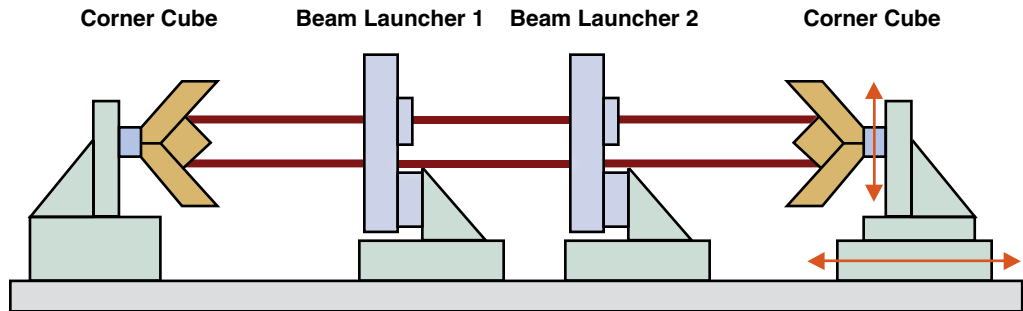
Figure 19-9. The Kite testbed shown here in the vacuum chamber, demonstrated that a collection of fiducials separated by many meters can be monitored with pm accuracy. (From Laskin 2006.)
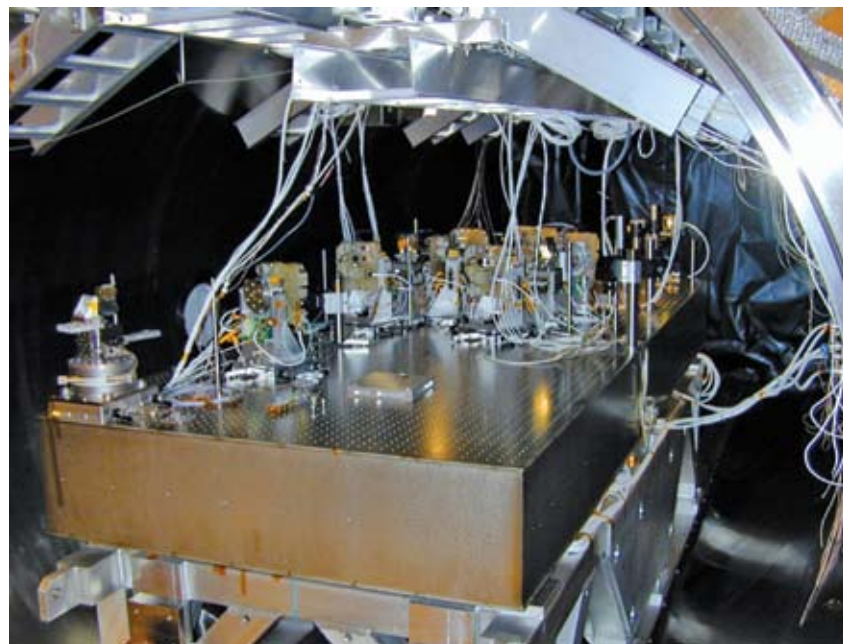
Figure 19-10. Kite's metrology gauges, shown here during a one-hour quasi-static run, are seen to be highly accurate, as evidenced by the black trace. The full extent of their unprecedented accuracy can be seen in Figure 19-11.

The Error Metric: $\Delta = L_2^{measured} - L_2^{Estimated}$
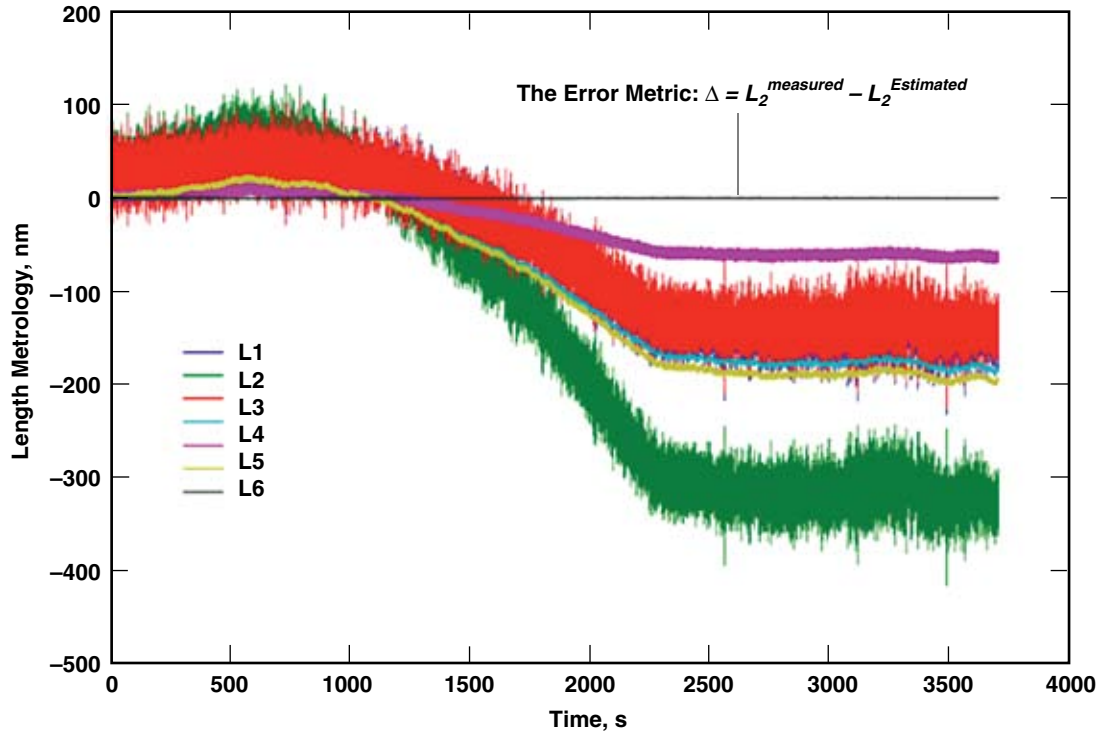
Figure 19-11. SIM Lite's chopping scheme is seen in this quasi-static test to be highly effective in bringing errors down to the required pm class.

30 s Average $\sigma = 130$ pm
Single Chop $\sigma = 15$ pm
8–Chop Average $\sigma = 8$ pm
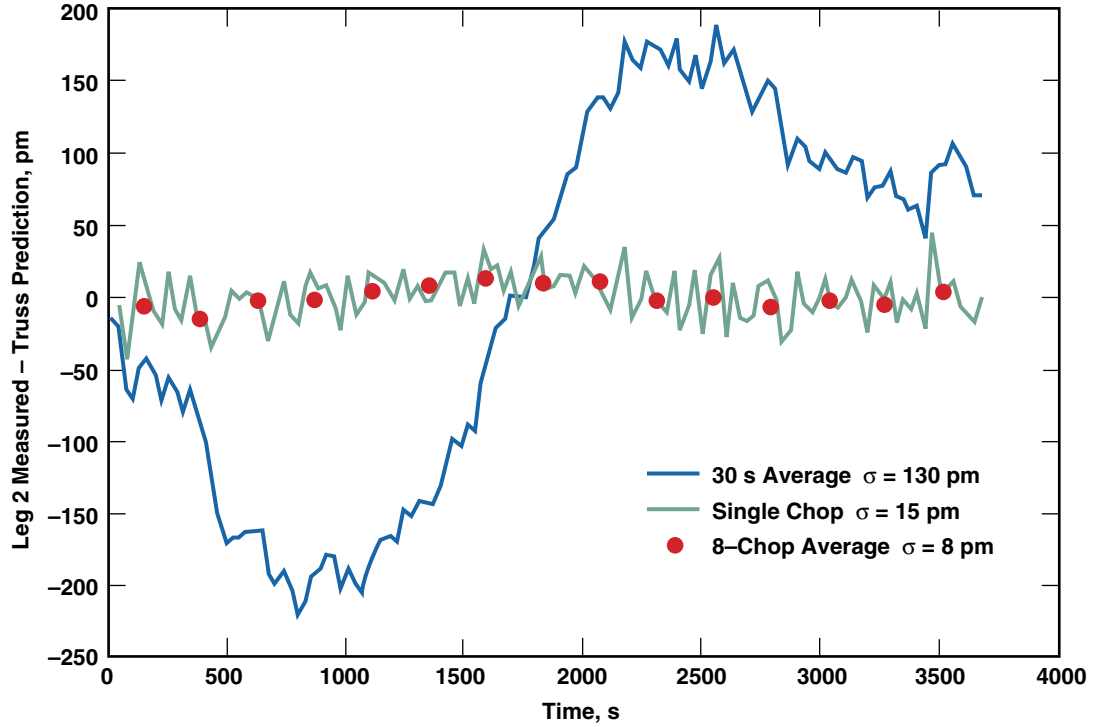
away and back. The Kite narrow-angle visits consist of two cycles of four chops each, with one reference star per chop. The RMS error for the eight-chop visit is measured to be 5.6 pm. This demonstrates that, even in the highly demanding circumstances of the narrow-angle observing scenario, the external metrology truss can meet its requirements.

19.4 The Guide-2 Telescope Testbed

One of the innovations that has enabled the lower-cost SIM Lite architecture is to use a precision star tracker to perform the Guide-2 function. To meet the requirements for µas astrometry, the Guide-2 telescope (G2T) must achieve an unprecedented 50 µas star-tracking capability. The greatest challenges to achieving this level of performance are expected to be (1) thermally induced deformations of the telescope system, and (2) measurement error in the angle metrology system. To develop this technology and demonstrate that such an instrument is feasible, the G2T testbed was built in the same vacuum chamber that had earlier contained the Kite testbed (Figure 19-12).

On SIM Lite, G2T consists of a 30 cm siderostat (Figure 19-13) and a 30 cm confocal beam compressor, similar to the other telescopes in both the science and Guide-1 interferometer. Starlight collected by G2T propagates directly to a CCD-based pointing sensor. As the attitude of SIM Lite changes in inertial space, the G2T siderostat mechanism tracks the guide star, maintaining the star spot at the optimal position on the CCD. An angle metrology gauge (aMet) tracks the siderostat motions required to keep lock. The star tracker output is the sum of the pointing sensor signal and the angle metrology.

The testbed layout is shown in Figure 19-14. White light is injected and collimated using an off-axis parabola and propagates through the beam compressor (7:1) to the siderostat in a retroreflecting position. The beam is returned to the fine-steering mirror (FSM) and focused on the pointing sensor. The optomechanical drift of the entire optical train is compensated by the FSM and measured by the aMet. By placing the siderostat in the retro configuration, G2T directly measures its own angular stability.

The angle metrology gauge is perhaps the most innovative feature of G2T. Figure 19-15 shows the aMet architecture. Based on the heterodyne metrology approach developed for internal and external metrology, aMet monitors the angle of a reflecting surface by probing the distance to three or four reference points (corner cubes) mounted on the surface (Figure 19-16).

In the initial phase of this testbed, the siderostat is not actuated. With the siderostat in retro position, the FSM is used to lock the artificial star (fiber tip) image on a fixed spot on the CCD pointing sensor. The aMet gauge tracks the tip/tilt of the FSM independently. In SIM Lite, the pointing detector and aMet readings together are used to provide the measurement of the G2T rigid-body rotations. In this testbed configuration, however, they measure the instrument's internal errors.

Figure 19-17 shows results from a typical G2T run, three hours in this case, under quasi-static conditions. The orange trace is the pointing sensor reading in real time under closed loop control. The blue trace is the aMet reading of the FSM position as it is controlled to lock the star image on the pointing detector. Together these two readings capture all the drift and noise in the system. In a recent 200-hour run processed according to SIM Lite's narrow-angle observing scenario, the measured G2T error was found to be less than 30 µas. This surpasses the required G2T performance for SIM Lite.

Figure 19-12. The G2T testbed, shown here in the vacuum chamber, has demonstrated star-tracking capability at an unprecedented 30 µas level. (Hahn et al. 2008)
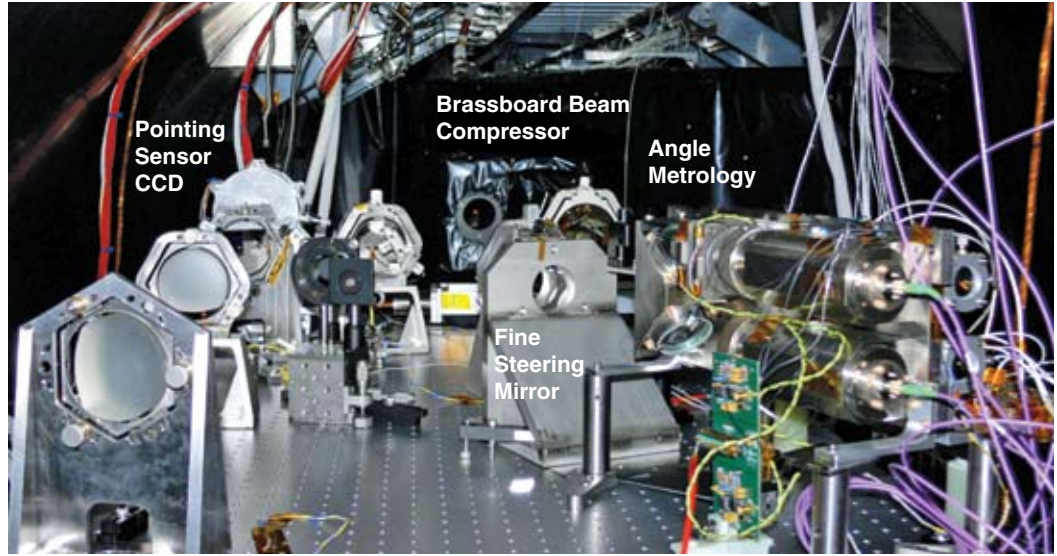
Figure 19-13. The brassboard siderostat in G2T uses a sophisticated corner cube design that allows µas level angle metrology. (Laskin 2006)
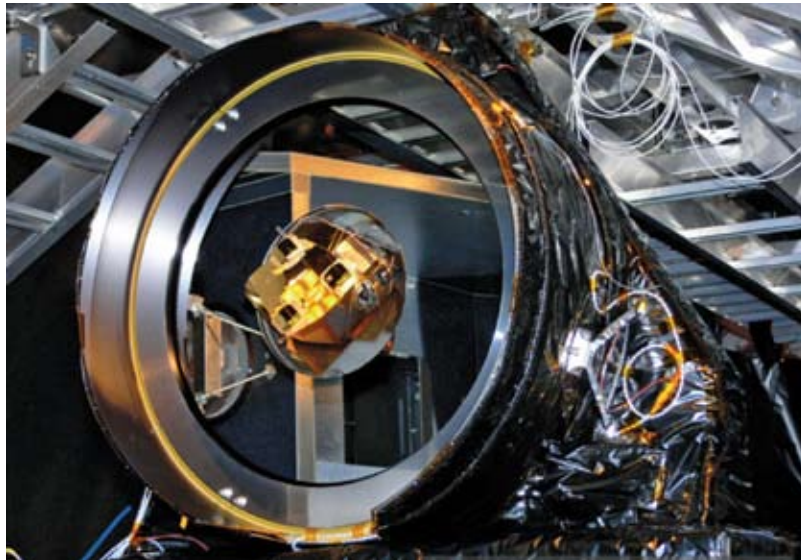
Figure 19-14. The G2T testbed has all the essential optical elements of the Guide-2 telescope, including a brassboard beam compressor and a brassboard siderostat. (Hahn et al. 2008)
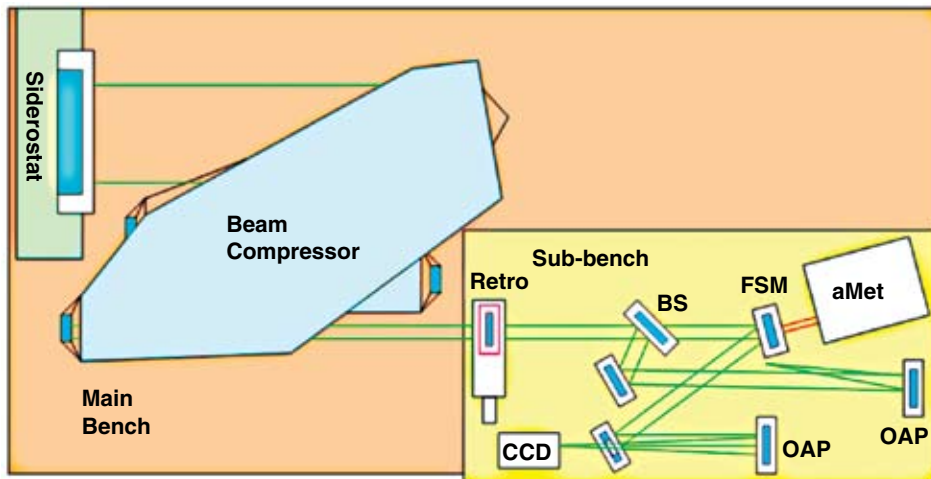
Figure 19 15. The angle metrology (aMet) system uses the proven heterodyne architecture of all SIM Lite metrology systems. (From Hahn et al. 2008.)
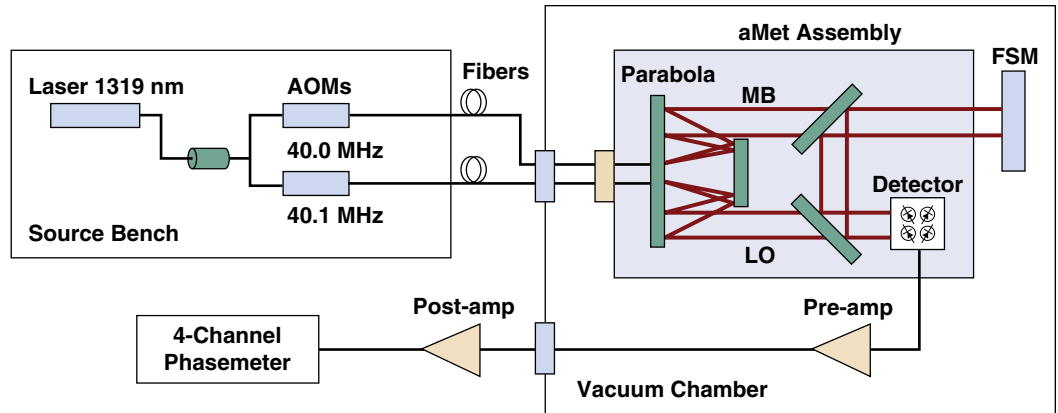
Figure 19-16. The aMet beam launcher is based on the internal metrology brassboard with a modified photo detector assembly (inset).
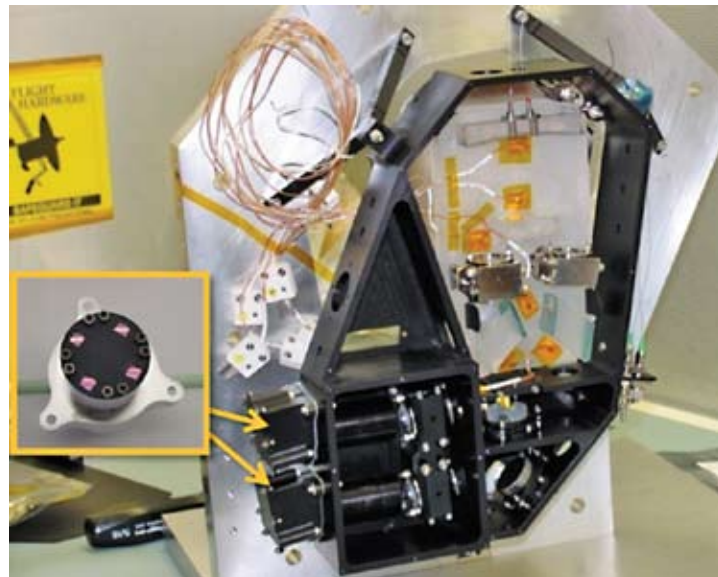
Figure 19-17. Pointing sensor and aMet angle measurements from a typical G2T run show that the FSM is effectively keeping the (orange) centroid locked on the CCD while the siderostat, under flight-like thermal conditions, undergoes mas level drift (blue).
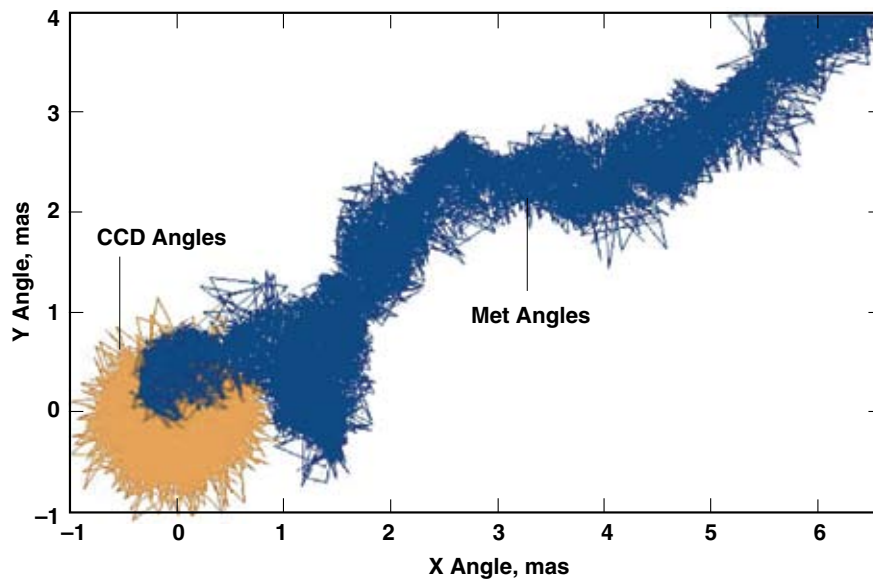
19.5 The Three-Baseline System-Level Testbed

As seen in Chapter 18, precision fringe measurement requires high fringe contrast or visibility. The dynamic contributions to a reduction of visibility are jitter in the relative path length and pointing of the combined beams. In particular, when the astrometric target is dim, active stabilization of the pathlength and pointing using conventional closed-loop techniques is not adequate due to photon noise. In these cases, other sensors are needed to predict the required pathlength and pointing corrections (so-called pathlength feed-forward and angle feed-forward) to be applied while the observation and integration of photons is in progress.

The STB-3 testbed was designed to capture the dynamics and control aspects of SIM. While the testbed was designed and operated prior to the innovations that led to SIM Lite, virtually all of the demonstrations and lessons learned are valid to the new design. STB-3 made it possible to develop the approach to pathlength and pointing control, as well as feed-forward, in the presence of disturbances higher than expected for SIM Lite. It also facilitated validation of a nm-level dynamics and control model for the instrument. Figure 19-18 shows the testbed with the collector bays on the near and far ends, and with the combiner bays in the center of the picture. The testbed is operated in air, since for control purposes nm-class performance is adequate.

Figure 19-19 shows the major system components of STB-3. The Precision Support Structure (PSS) is a 9-m-long, flight-like, flexible structure (longer than SIM Lite). It is capable of supporting an attitude control system (ACS) module, one of the main sources of jitter in the system. The two collector bays (east and west) are where the telescopes are housed, together with relay optics, fine-steering mirrors for pointing, and external metrology beam launchers. The beam launchers measure how the interferometer fiducials move relative to each other as a result of thermal drift and dynamic disturbances. The beam combiner pallets contain the combining optics, internal metrology, the delay lines, and the tracking cameras that monitor pointing.

Figure 19-19 also shows the pseudo star system. It is an inverse Michelson Interferometer that is used to generate collimated, in-phase wavefronts to both collector bays. A diffraction grating splits the pseudo star beam at each end into simulated wavefronts from three stars in the sky 15.4 degrees from each other: the science, Guide-1 and Guide-2 stars. The test article is mounted atop three, 1/2-Hz-class isolators designed to render the system quasi free-free in six degrees of freedom.

During SIM Lite science operations, fringe motion occurs when the attitude of the instrument varies within the deadband of the ACS and when the structure deforms as a result of varying thermal loads in normal operation. In SIM Lite, the fringe must be stabilized to less than 10 nm RMS or lower in order to reach μas-class accuracy in each visit. Modeling of the ACS system performance shows that a disturbance rejection of at least 40 dB (i.e., a factor of 100 in amplitude) is required in the frequency range 0.1 to 1 Hz.

To attain this level of suppression, SIM Lite will use a combination of passive and active methods. The passive method is dual-stage isolation of the reaction wheels in the spacecraft, which are the largest source of jitter (>10 Hz). The active method is a technique called pathlength feed-forward (PFF), mainly used to reject rigid body motion (<10 Hz) and thermal drift. The science interferometer itself cannot be used to compensate for these disturbances, as its targets are often too dim and generate photon rates that are too low for sufficient sensory bandwidth.

In the PFF technique, the guide instruments are used to pinpoint the attitude of the instrument with respect to the target star of interest. To account for jitter and thermal distortions among the instruments, the external metrology system is used to tie the guide data to the science interferometer.

Figure 19-18. The STB-3 testbed emulates the full SIM Lite instrument and features a flight-like flexible structure.
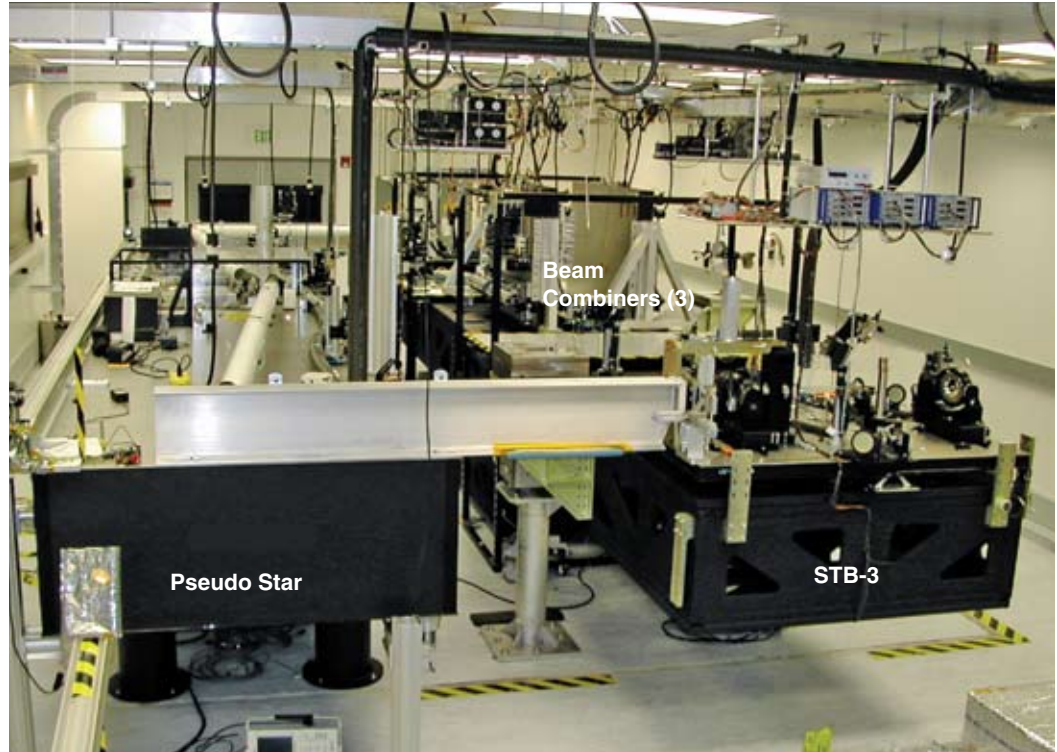
Figure 19-19. The STB-3 test set-up, shown here, allows for the illumination by three simulated stars so that full system-level tests can be conducted. (From Laskin 2006.)
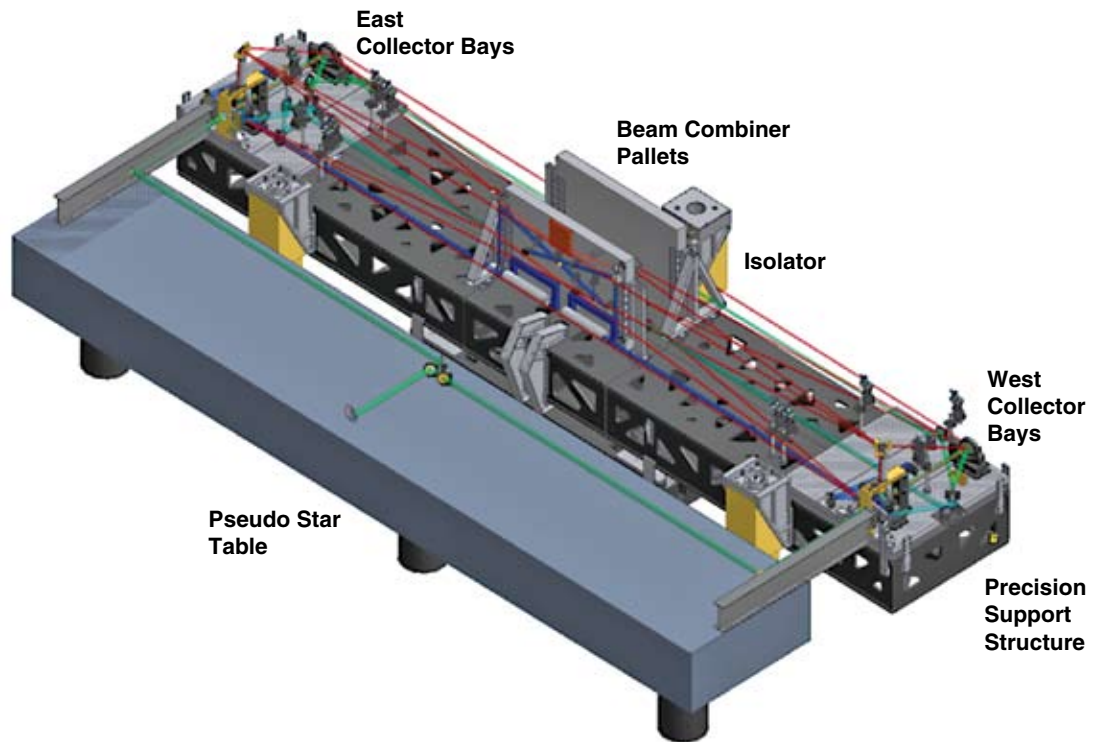
Figure 19-20 shows a 20-minute fringe-tracking experiment during which the ACS error simulator (a voice-coil acting against the structure) injected a harmonic ACS disturbance resulting in about 2200 nm RMS of science delay at 0.01 Hz (blue trace). The figure also shows the phase residual for the science interferometer under PFF control (green trace). To simulate the on-orbit situation, data from the science fringe detector are not used in tracking the fringe. The phase jitter over all frequencies is seen to be 38 nm RMS, including both drift and broadband contributions. The drift in the PFF residual contributes about 26 nm RMS to the total error, and it is largely due to drift in the internal metrology sources (all three interferometers in STB-3). The flight metrology design has been shown to have much less drift than this. The atmosphere's contribution to the low-frequency error (i.e., <1 Hz) is estimated to be in the neighborhood of 6 to 10 nm RMS (this estimate is actually based on external metrology data).

Figure 19-21 shows the power spectral density for the data. The disturbance applied at 0.5 Hz is seen to be rejected by 50 dB, better than the requirement. At 0.01 Hz, the rejection is about 60 dB. Here the experiment was limited by the laboratory ambient noise floor on the one hand and the maximum available ACS range on the other. The experiment clearly shows that the PFF performance exceeds all requirements (i.e., better than 40 dB of rejection at a frequency in the 0.1 to 1.0 Hz band). STB-3 has verified that the dynamics and control challenges of space-based stellar interferometry have been met and SIM Lite is ready for flight design.

19.6 The Thermo-Opto-Mechanical Testbed

The Thermo-Opto-Mechanical (TOM) testbed (Figure 19-22) was designed to demonstrate that SIM Lite's collectors can meet their stringent wavefront stability requirements under flight-like thermal conditions. Each collector includes a siderostat and a beam compressor. In the center of the siderostat is a double corner cube (DCC) that serves as a fiducial for the metrology system that determines the pathlength differences in the interferometer. The beam compressor (Figure 19-23) is an off-axis confocal telescope. Using brassboard versions of these components, the testbed has shown that SIM Lite will meet its unprecedented thermal requirements.

In SIM Lite's science and Guide-1 interferometers, the internal metrology footprint occupies the central region of each optic while the starlight occupies the surrounding annulus. This arrangement, which is optimal in many respects, does make the instrument sensitive to changes in wavefront error (primarily power/defocus) over the course of a measurement. In the case of the all-important siderostat, the central part contains a DCC. Any "piston" motion of the DCC relative to the siderostat mirror can cause an error. The optical path difference between starlight and metrology through the siderostat and the large compressor optics must be stable to tens or hundreds of pm, depending on the type of SIM Lite observation.

The primary source of wavefront instability in SIM Lite is thermal disturbance, and the main on-orbit thermal disturbance is expected to be from the change in the relative position of the Sun with respect to SIM Lite. The typical observational scenario will generate about 7 degrees of episodic spacecraft motion every hour in order to slowly scan the entire sky. The next most important thermal disturbance occurs with the change in the orientation of the siderostat relative to the rest of the collecting hardware when it is articulated. The siderostat will acquire light from stars anywhere in its 15 degree FOR. These two thermal disturbances are simulated in TOM using its liquid nitrogen thermal shroud. The temperature variations are produced by simulating the operational scenarios for the flight system and then generating thermal profiles for the shroud heaters that would produce a similar environment for the siderostat. The objective of the testbed is to show that the Science collector and Guide-1 collector, in the presence of flight-like thermal conditions, will not cause wavefront thermal instabilities that exceed the error budget allocations. Another important goal of the testbed is to develop an integrated thermo-opto-mechanical model and validate its predictions.

Figure 19-20. The STB-3 testbed demonstrates that pathlength feed-forward can suppress large fringe-delay errors (blue) down to the nm level (green). (From Laskin 2006.)
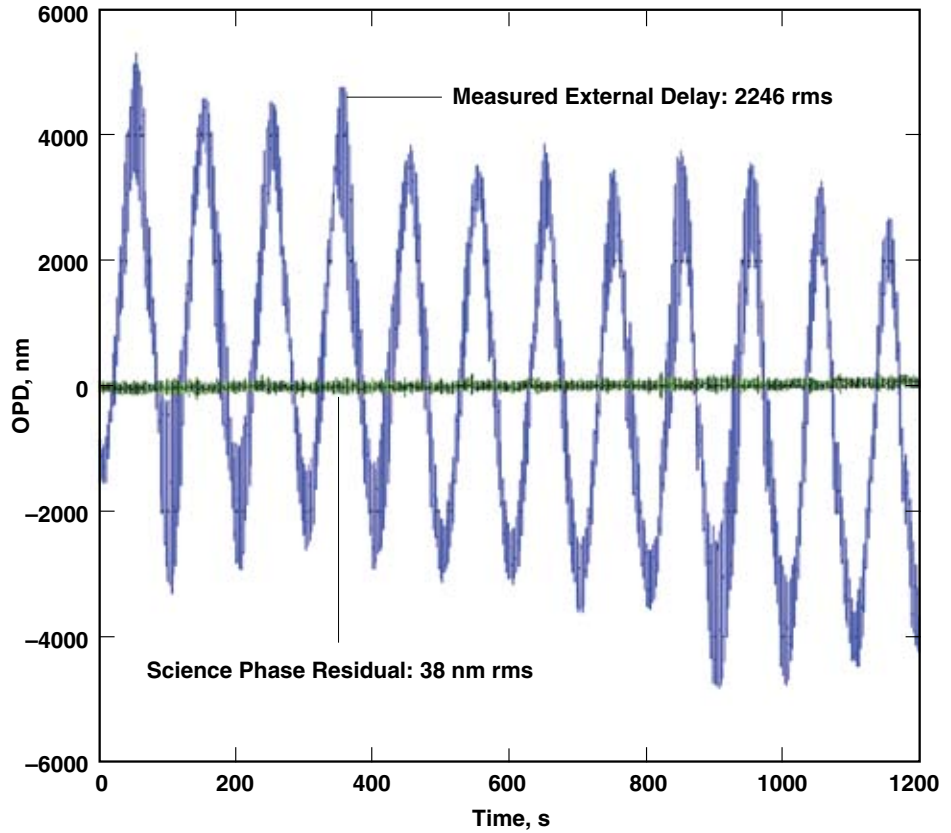
Figure 19-21. A power spectral density of STB-3 results shows the excellent rejection of disturbance in the region of greatest interest (>60 dB at 0.01 Hz to >50 dB at 1 Hz), surpassing SIM Lite's stabilization requirements. (From Laskin 2006.)
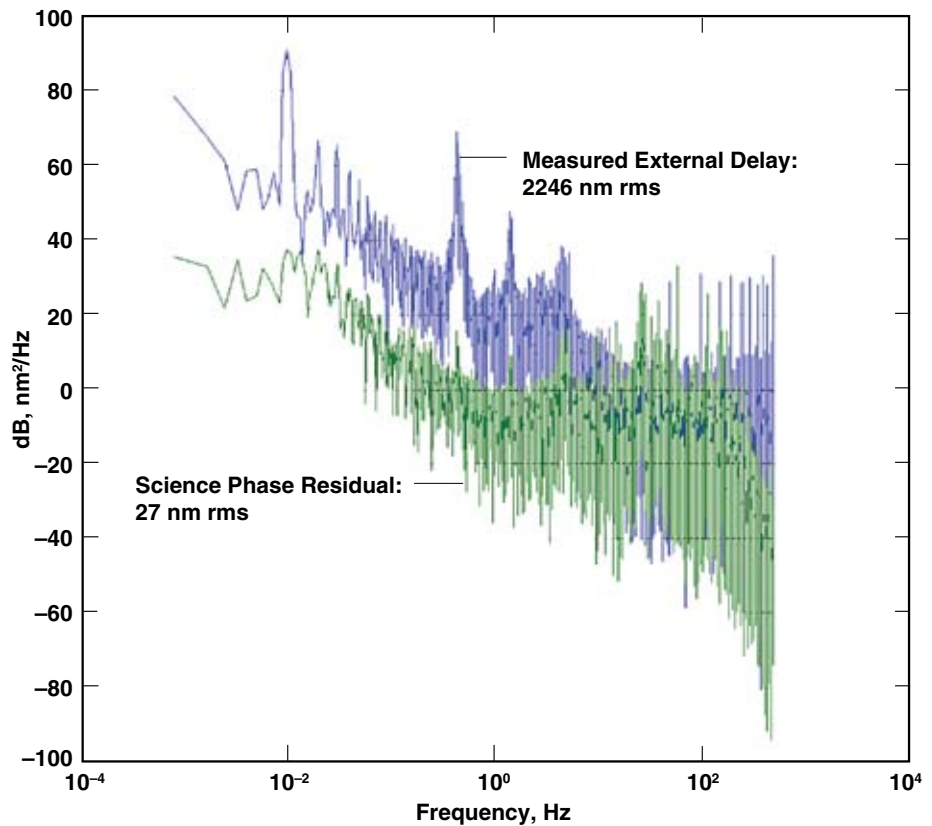
The test article includes a brassboard siderostat and brassboard beam compressor monitored by a highly precise multisensor metrology gauge called the Common Optical Path Heterodyne Interferometer (COPHI). COPHI was the original prototype metrology gauge that led the way to all the SIM Lite pm-class beam launchers. For this testbed, the COPHI detector was modified to monitor OPD errors over a number of points across the siderostat, including the DCC at its center. A schematic of the testbed and a view of some of the optics is shown in Figure 19-24.

TOM tests involved multihour runs where the testbed thermal environment was made similar to expected SIM Lite flight levels. The test metric is the average difference between the central metrology reading and nine annular readings (Figure 19-24).

For the Guide-1 collector test, the chopping fold mirror is in the retro position with respect to the COPHI sensor such that the beam compressor becomes the main test article. Figure 19-25 shows the result of a typical data run. One can see a strong correlation between the thermal variation and the optical response in the data shown in the figure. The slow downward drift and the diurnal cycle of the temperature suggest a 3 nm/K linear thermo-opto-mechanical sensitivity of the compressor (single path) that is consistent with the thermal model predictions.

The OPD was processed from the raw data according to the narrow-angle observing scenario (the more limiting scenario) and the narrow-angle error was found to be 5.4 pm. Separate testing showed that the number was in fact dominated by the error in the test set-up, rather than the test article itself. For example, COPHI's noise contribution was found to be 3 pm, leaving 4.5 pm as the measured thermal stability error of the Guide-1 collector. Thus the Guide-1 collector exceeds the SIM Lite wavefront thermal stability requirements.

For the science collector test, the COPHI sensor measured the OPD stability, including the siderostat together with the beam compressor. The results of tests suggested that the narrow-angle performance of the science collector at the inboard bay (nearest the rocket booster) of the SIM Lite structure is 9.5 pm, and 8.7 pm for the case of outboard bay. These testbed performances are near the required levels for the SIM Lite mission. Further testing indicated that the stability of the COPHI measurement system (which is ground-support hardware) limited the ultimate performance test of brassboard hardware. In these tests, the system was thermally overdriven and the results confirmed that the test article's true thermal sensitivity is significantly better than SIM Lite requirements.

Beyond the direct performance tests, TOM was also used to validate SIM Lite's integrated thermo-opto-mechanical model. The overdrive tests were used to correlate the model with the raw data. Figure 19-26 shows the typical results from a 16-hour data run. The TOM-measured OPD is shown in dark blue (the spikes in the data are glitches in COPHI and not physical). The OPD measurements showed a strong temperature dependence, as expected. The other traces are integrated model calculations with various conditions. Three varieties of modeling are shown in the figure: fully modeled (orange), in which thermal model predictions were put into the structural model to generate OPD outputs; partially modeled (red), in which an empirically measured sensitivity of the OPD to the siderostat temperature (dOPD/dT) was used; and empirically modeled (green), in which the measured dOPD/dT number (6 nm/K) was simply multiplied by the measured temperature changes.

The thermal models using the best available inputs predicted the relevant parameters (peak-to-valley temperature change and rate of change) to within 60 percent prior to any attempts to adjust uncertain model parameters to fit the experimental data. For most components of interest, except for the DCC, the model over-predicted the temperature swings and rate of change. The over-prediction is preferable to under-prediction because it provides margin against design or modeling errors.

Figure 19-22. The TOM test-bed includes a brassboard siderostat and double corner cube (gold colored) centered in the siderostat mirror. (From Laskin 2006.)
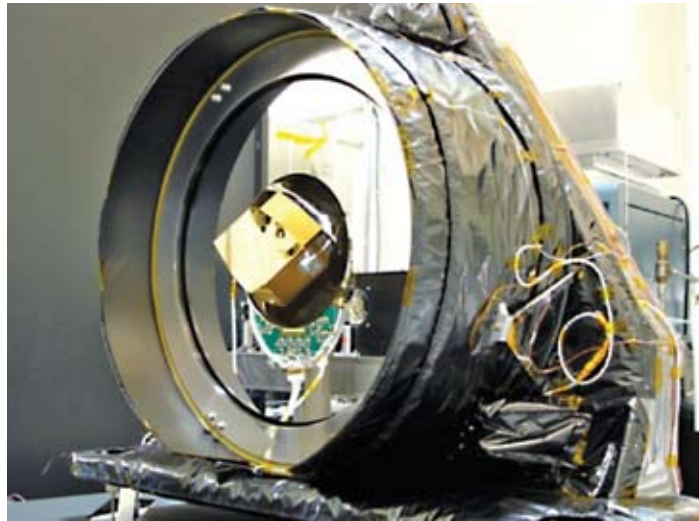
Figure 19-23. The brassboard beam compressor used in TOM has shown excellent wavefront stability.
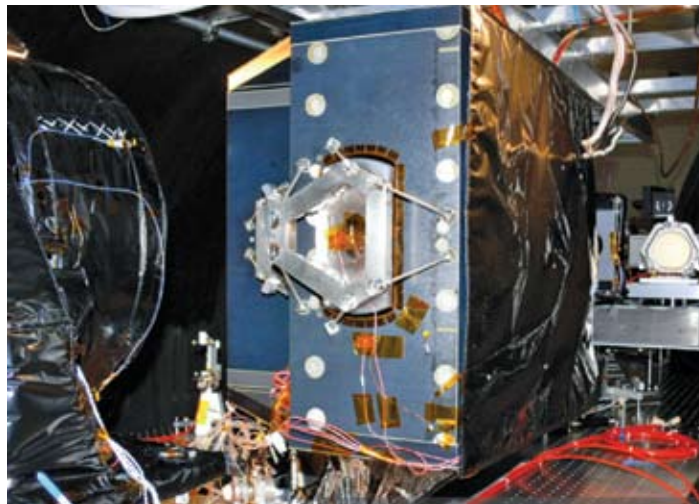
Figure 19-24. The TOM testbed layout (left) and view from the fold mirror (right).
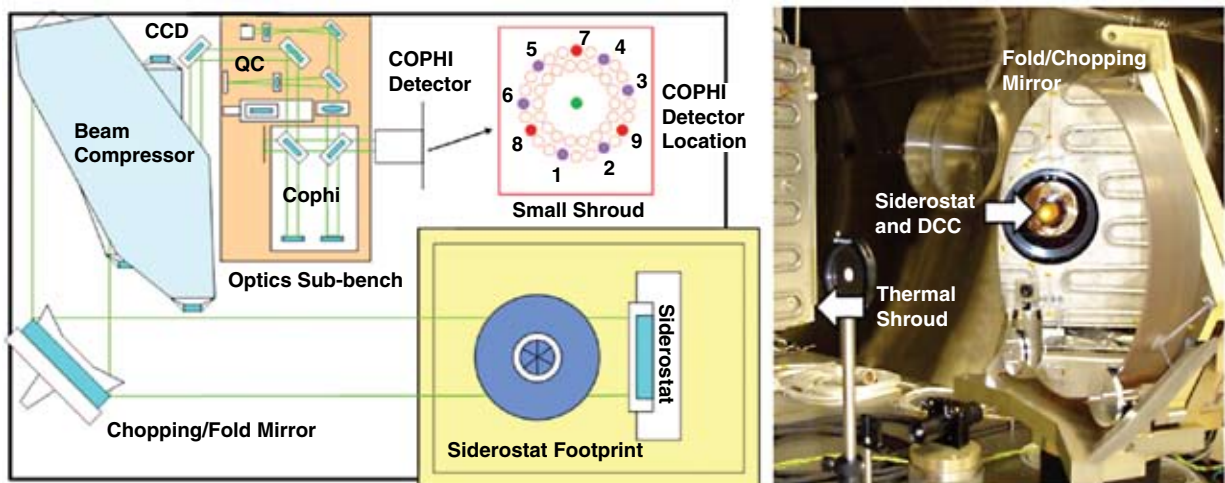
Figure 19-25. The OPD versus temperature (magenta circles) measurement correlates well with the temperature profile (all other traces) and is indicative of the Guide-1 collector performance. M1, M2, and M3 re the three main mirrors in the beam compressor; COB stands for collector-outboard side.
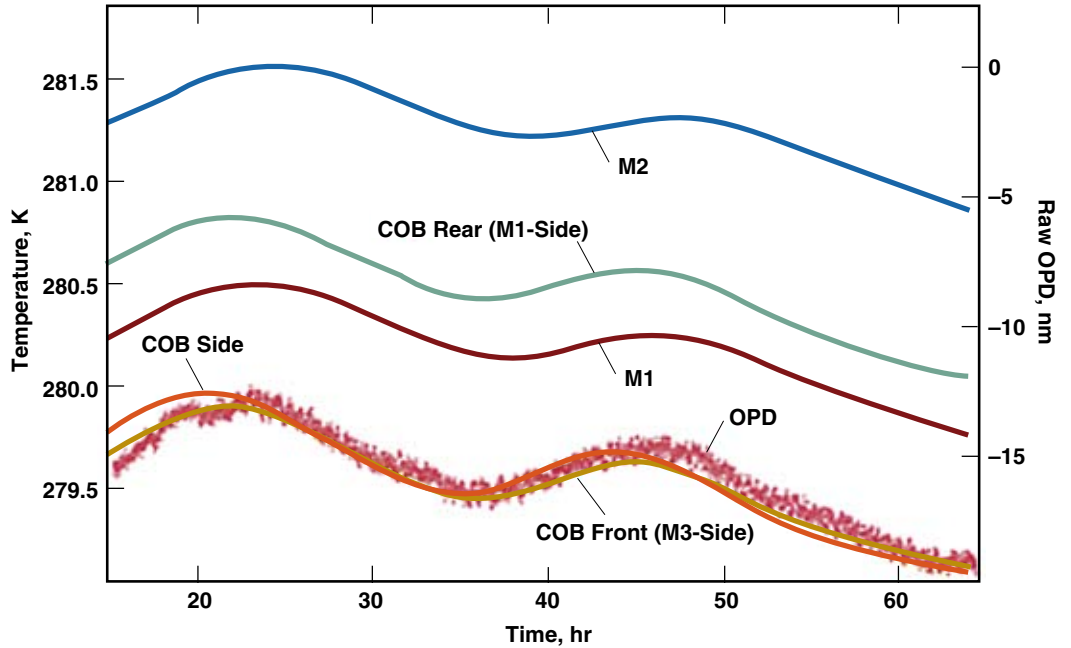
Figure 19-26. The SIM Lite integrated thermo-opto-mechanical models perform well in predicting the dependence of OPD on temperature. (From Laskin 2006.)
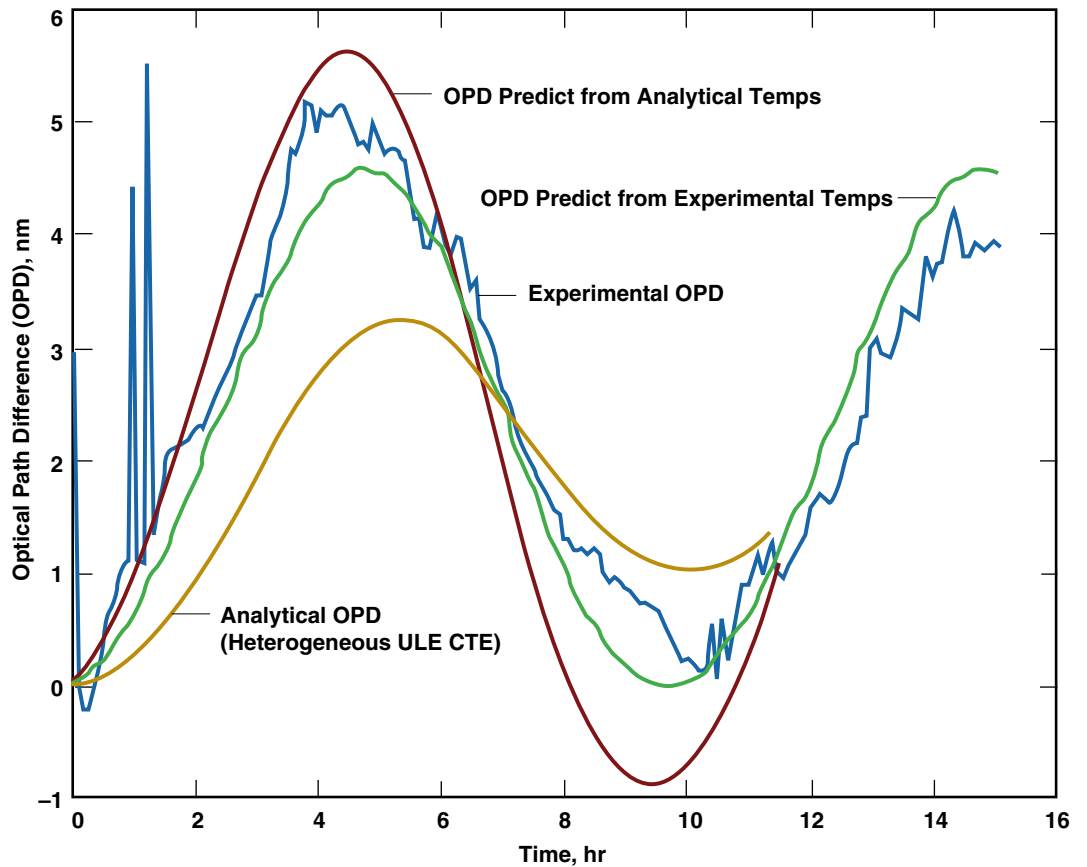
The structural models, though fairly sensitive to accurate knowledge of material parameters, particularly the coefficient of thermal expansion (CTE), provide valuable performance predictions for flight development. Prior to model correlation, the structural model of the siderostat under-predicted by a factor of about three. After modifying the CTE of the ultra-low-expansion (ULE) glass in the model to be more consistent with the properties of the real glass, including inhomogeneity, the model under-predicted by a smaller factor of about 1.6. Understanding the modeling uncertainty factor is important for developing design margins for the flight system.

Overall, the TOM testbed consistently demonstrated performance close to or better than the goal levels of the Science and Guide-1 collectors. In all cases, the test results appear to be limited by the noise floor of the ground support measurement system rather than the actual performance of the flight-like test articles.

19.7   Completeness

The ultimate test of completeness is a full-up test article that matches the operation of the flight article in all its details in an environment that is completely flight-like. With SIM Lite, as with all the next generation large instruments, this is an ideal increasingly impossible to realize. SIM Lite has benefited from an impressive array of testbeds, only a few of which have been highlighted in this book. These testbeds have come very close to reaching the ideal at the level of the instrument's fundamental sensors. That is, MAM replicates all the complex operations involving a single, pm-class stellar interferometer; Kite does the same thing for the external metrology system, and G2T captures the most important, previously untested aspects of the Guide-2 telescope sensor. TOM shows that the all-important thermal errors are well handled by the SIM Lite design. STB-3 shows that the control authority exists to stabilize the fringe to the levels required for pm fringe measurement. Together these testbeds have made a strong case, confirmed by a very thorough and independent technical review process, that the technology for each of the sensors is at hand. The same review process also examined the entire SIM Lite approach, asking whether any "holes" might exist in considering the performance of the full instrument. What follows is a result of this examination, which took place over the last few years.

At the heart of SIM Lite's architecture is a provision to minimize the number and impact of "holes" by requiring that the instrument sensors obey the principal of separability. This means that if the each of the four fundamental sensors work to the levels required by the error budget, the whole instrument shall meet its mission goals. There are a number of situations where separability can in principle be violated. These ultimately all involve pure sensing errors. SIM Lite addresses these cases through measurement, calibration, and placement of tight requirements on mechanisms that feed any of these violations. The three categories of situations where separability can be violated are:

I. Second-order errors involving a motion and a knowledge error.
II. Instrument fiducials being sensed inconsistently by different sensors.
III. Cross-talk or corruption of one sensor due to another sensor.

Second-order errors were discussed in the error budget, Chapter 18. These are arguably the most important violators of separability. The approach to minimize these errors involves tight requirements on the motions involved, and calibration of the parameters whose errors can contribute to a given second-order error. For the example described in Chapter 18, the error due to the coupling of ACS motion and baseline nonparallelism is brought within allocations by placing tight ACS deadband requirements (<0.2 arcseconds over 10 minutes) and at the same time placing tight absolute metrology requirements (<3 μm absolute error per metrology link).

The second category of separability violators involves the instrument's fiducials. The double corner cubes, in particular, are the most fundamental reference points on the instrument since they define the ends of the science baseline. However, the very fact that they are double cubes means that the science interferometer sensor's internal metrology probe sees one cube, while the external metrology system sees another. Since it is not practical to make the distance between the vertices of the two corner cubes zero, a motion of the DCC during retargets from one star to another couples to this non-common-vertex error (NCVE) to create a type of second-order error. (This error happens to be book-kept in the error budget under external metrology's allocation. Otherwise it would naturally belong under second-order errors.) A specific testbed called NCVE showed that submicron absolute measurement of the NCVE is feasible. Later, analysis and modeling showed that on-sky calibrations can also provide this important parameter, so that this source of separability can meet its allocation using the simpler approach.

The final category of separability violators involves crosstalk between the sensors. This is only a significant issue between internal metrology (part of the Science and Guide-1 interferometer sensors) and external metrology. Here the heterodyne laser beam from internal metrology could potentially leak into the external metrology beam launcher's detector, and vice versa. To ensure this error is small, a specific test was done that mimicked the geometry of a typical external metrology link with respect to an internal metrology beam incident on the same corner cube. The measured cross-talk was found to be significantly smaller than the allocation. Had this cross-talk been a significant issue, a relatively simple mitigation approach would have been to use different heterodyne frequencies for internal and external metrology, taking advantage of filtering in the electronics to eliminate this error.

To summarize the answer to separability, SIM Lite, through an extensive and independently reviewed technical program has shown that the individual sensors meet their requirements (the pm technology testbeds) and further that the areas where errors could occur in the interplay of the sensors are each mitigated through tests, measurements, and calibrations.

A final note is appropriate on the important question of the SIM Lite data flow and its processing to create a complete astrometric result. SIM Lite has developed an extensive array of modeling tools that have been validated using the testbeds. These primarily include the instrument model and the SIM Lite mission simulator (SIMsim).

The instrument model captures outputs from all sensors and motions in the fundamental fiducials of the instrument. It uses testbed data to create empirical pseudo data with correct noise characteristics, and flows the data into telemetry. It simulates its subsequent processing up to the point of arriving at regularized delays. Using the delays, the instrument model applies realistic observing scenarios to show that the predicted instrument performance is consistent with testbed results in affirming that error budget allocations can be met.

SIMsim is a computer model that starts at the level of individual telemetries and simulates the entire mission, including actual star characteristics and locations from star catalogs, Sun and Earth exclusion, slew times, and calibration-related observations. It simulates the complete calibration and post-processing to the level of final astrometric products such as position, proper motion, and parallax. SIMsim was instrumental in identifying zonal astrometric errors and verifying that the use of quasars was effective in minimizing them. It also is an indispensable tool in determining the schedule of observations and the optimization of the schedule for maximum observing time and minimum calibration errors.

Overall, SIM Lite's development has placed a high emphasis on retiring risks and ensuring completeness. The full array of tests and modeling that has led to successful completion of all of the NASA-required technical milestones is described in the SIM technology plan volumes submitted to NASA.

At the heart of SIM Lite's architecture is a provision to minimize the number and impact of "holes" by requiring that the instrument sensors obey the principal of separability. This means that if the each of the four fundamental sensors work to the levels required by the error budget, the whole instrument shall meet its mission goals.
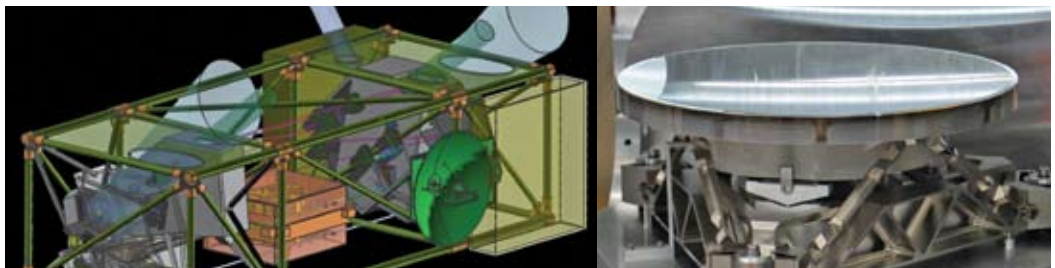
References

Hahn, I., Sandhu, J., Weilert, M., Smythe, R., Nicaise, F., Kang, B., Dekens, F., and Goullioud, R., 2008, Proc. SPIE Vol. 7013, 70134W.

Hines, B. E., Bell, C. E., Goullioud, R., Spero, R., Neat, G. W., Shen, T. J., Bloemhof. E. E., Shao, M., Catanzarite, J., and Regehr, M., 2003, Proc. SPIE, Vol. 4852, 45.

Laskin, R.A., 2006, IAC-06-A3.P.1.05.

SIM Lite
20 Flight System Design

Frank G. Dekens (JPL), **Bijan Nemati** (JPL), **Rolf Danner** (NG), and **Fabien Nicaise** (JPL)

ABSTRACT

The SIM Lite instrument comprises a 6-m-baseline astrometric interferometer with 50 cm collecting apertures. The science baseline vector is monitored using two guide instruments and an external metrology system. A truss structure supports the instrument, and a "back-pack" mounted space-craft allows for a compact overall flight system. Given the complex nature of interferometry, SIM Lite's design seeks reduction of cost and risk by maximizing the reuse of components within the system, minimizing mass and volume, and using a proven and simple truss structure. Overall, the system design represents a great degree of optimization, maximizing performance while minimizing cost.

20.1 Overview of the Instrument Design

The SIM Lite science instrument is a 6-m-baseline Michelson stellar interferometer with 50-cm entrance apertures. A guide interferometer and a high-accuracy guide star-tracking telescope, tied to the science interferometer by an external metrology truss, measure the changes in the science baseline vector. When this architecture is implemented into a cost, volume, and mass-optimized optomechanical design, the boundaries between the fundamental sensors blur to some extent and it becomes more appropriate to describe the overall system based on its structural units. In this view, the instrument consists of several "benches" or large assemblies. Each bench holds various repeating subassemblies or components, such as siderostats, fine-steering mirrors (FSM,) and astrometric beam combiners (ABCs). We begin this overview by describing, still within the "sensor" paradigm, the salient features of the four fundamental sensors. Following this top-level introduction, we adopt the structural-unit view as we describe the contents and features of the various benches that comprise the instrument. We end with a brief description of the structure and the spacecraft.

The layouts of the guide and science interferometers are very similar. The two interferometers are co-aligned so that at the start of an observing sequence they are pointed at the same star. The light paths of the two interferometers differ only in the addition of delay lines in the science interferometer, which are needed to achieve the larger science field of regard (FOR). Compared with the guide interferometer, the science interferometer features larger collecting apertures, longer baseline length, and a much larger FOR. The overall layout of the optics is shown in Figure 20-1, where blue is used for the science interferometer and green for the guide interferometer. Figure 20-2 shows a more detailed view of the science and guide collector optics.

.

20.1.1   The Science Interferometer

The science interferometer collects light from two 50-cm siderostats separated by a 6-m baseline. The siderostats articulate over an angular range of ±3.75 degrees, giving the science interferometer a 15-degree-diameter FOR. Once they are pointed at a star, these actuators are locked in place for the duration of the observation. In the optical train beyond the siderostat, each beam is compressed to a diameter of 4 cm using a confocal beam compressor. Next in the path is the FSM, which, compared to the siderostat, has a smaller range of motion but a much higher pointing resolution. It is used to track the star as the instrument attitude changes. The pathlength optic mechanism (POM) then folds the beam into the delay lines. The POM scans and stabilizes the starlight fringe by applying fine and relatively small delay modulations. Both the FSM and the POM are momentum-compensated in order to not disturb the interferometer while observing. The delay line provides the coarse correction to the optical path difference between the two arms, with a 40 cm range. With one such delay line at each collector, a total path difference of 80 cm can be produced between the two sides, enabling interferometry with the 15 degree FOR. The delay line only moves during retargeting to a new science object and is then locked into place. Finally, the beam is folded towards the center of the instrument where the two sides are combined to form fringes inside the ABC.

20.1.2   The Guide-1 Interferometer

The design of the Guide-1 interferometer is similar to the science interferometer, although it has less stringent requirements. First, because the spacecraft points the entire instrument to the Guide-1 star each time, there is no need for Guide-1 siderostats and delay lines. Hence, the first Guide-1 optic is the

Figure 20-1. SIM Lite's four fundamental sensor systems are illustrated here: the science interferometer, the Guide-1 interferometer, the Guide-2 telescope, and the external metrology. The starlight is always first compressed to 4 cm beams, and then transported to be combined at the center of the interferometers, or focused onto the CCD in the Guide-2 case. The metrology truss tracks the motions of the baselines. (From Goullioud et al. 2008.)
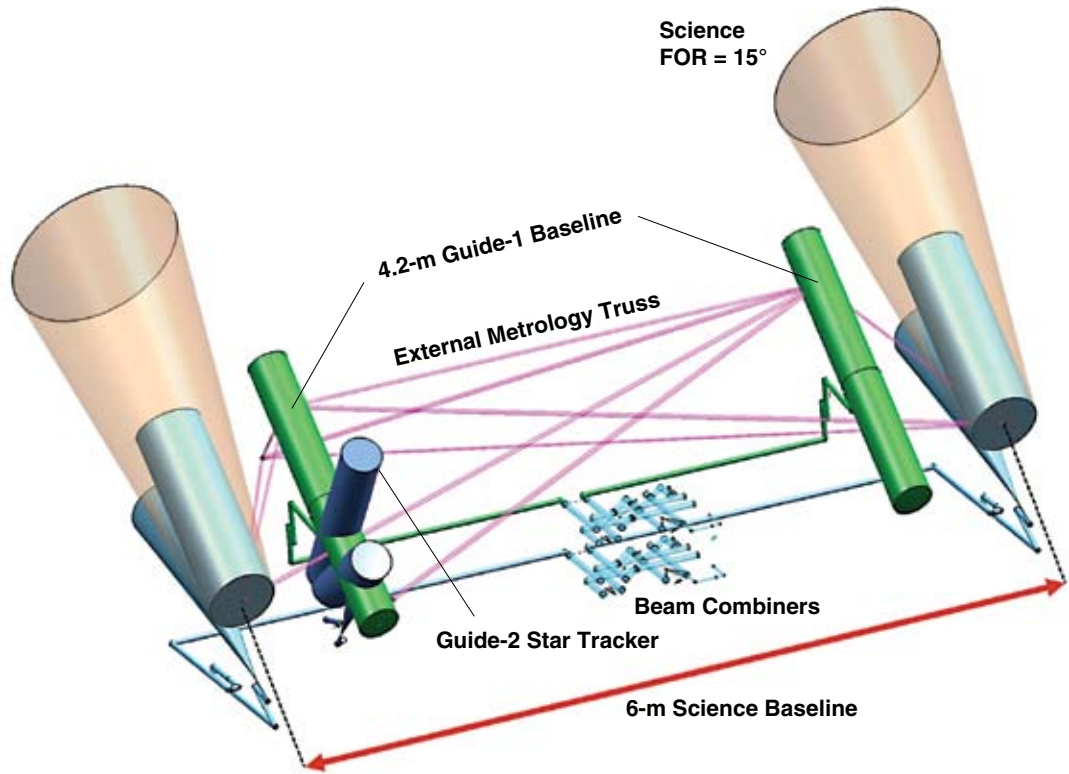
Figure 20-2. CAD drawings of the optical components in the science (left) and guide (right) collectors.
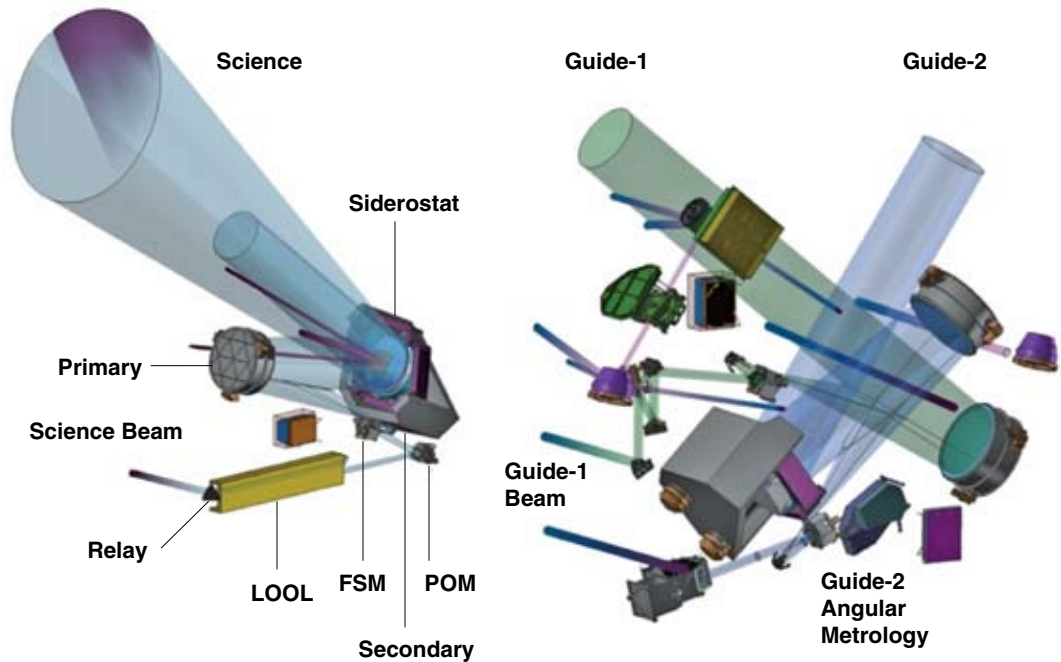
primary mirror of the confocal compressor. Second, the Guide-1 star is often much brighter than the science target, so a 30-cm Guide-1 collecting aperture is adequate. The optical compressor reduces the beam size by a factor of 7.5 so that the downstream optics have the same clear aperture of 4 cm as the science interferometer. Due to packaging constraints, the Guide-1 baseline is reduced to 4.2 m. Finally, in Guide-1 the optical delay is corrected using a single mirror on a coarse motor stage, since only 1 mm of travel is needed.

20.1.3 The Guide-2 Telescope

The Guide-2 telescope monitors the roll of the spacecraft about the vector pointing to the Guide-1 star. This roll is primarily caused by the drift of the attitude control system (ACS). A schematic layout of the star tracker was shown in Figure 17-6. It is mounted on the same bench as one of the Guide-1 telescope collectors, and the beam path is shown in blue in Figure 20-2. The allowable Guide-2 star location is within a 1 degree radius of a vector that is 90 degrees away from Guide-1, in the place orthogonal to the science baseline. Thus, Guide-2 has a siderostat with a small, 2 degree range but with higher pointing resolution to track the star while the ACS is drifting. The siderostat design is similar to the science siderostat, but smaller (30 cm instead of 50 cm) and the actuator has a fine and a coarse stage. The coarse stage acquires and then locks, just as in the science siderostat. Then the fine stage takes over the role of the FSM in the interferometers. This approach results in fewer reflections and fits more readily on the already crowded bench.

The Guide-2 compressor is identical to Guide-1. After the compressor, there is a mirror with a hole to let through a metrology beam that interrogates the pointing of the siderostat while folding the starlight beam onto an angle tracking camera. The detector arrangement of the angle metrology system for the Guide-2 telescope is a variant of the interferometer's internal metrology gauge, allowing it to measure tip-tilt instead of piston. As the attitude of SIM Lite changes in inertial space, the fine stage of the siderostat mechanism locks onto the Guide-2 star, keeping the star image within a few mas of the intersection of four pixels in the pointing camera. Meanwhile, the angle metrology sensor measures the siderostat rotations required to keep this lock, compensating for spacecraft attitude changes (about 1 arcsecond). This technique transfers the bulk of the angle tracking to the much more linear metrology sensor, while keeping the camera image in the more accurate region near the cross-intersection of four pixels. Both the CCD-based pointing sensor and the metrology system tracking the angular position of the siderostat have accuracy close to 20 μas over short time periods (Hahn et al. 2008).

20.1.4 The External Metrology Truss

The external metrology system is needed to monitor the relative positions of SIM Lite's fiducials, four of which define the science and guide baselines. The measurements are made using heterodyne metrology beam launchers using the same principles employed in internal metrology. However, rather than measure the path difference between the left and right arms of the interferometers, the external metrology beam launchers monitor the direct distance between each pair of fiducials. They send the light beam on a round trip, in a race-track fashion, between two corner cubes (fiducials). Nine beam launchers are used to monitor the external metrology truss, which has five fiducials. Two of these are double corner cubes (DCCs), which define the science baseline. Two of the fiducials are triple corner cubes, which define the Guide-1 baseline. The fifth fiducial is the apex corner cube and is used to monitor the out-of-plane motion of the truss. Finally, there is a tenth metrology gauge, which monitors a sixth fiducial (the clocking corner cube) used to measure drift of the Guide-1 and Guide-2 bench.

20.1.5 The Precision Support Structure, Spacecraft, and System Layout

The precision support structure (PSS) is a highly stable structure accommodating the instrument components. It is the primary load-carrying member of the SIM Lite flight system, and interfaces directly to the launch vehicle payload adapter. Beyond supporting the instrument subsystems, it maintains the thermal environment and provides solar shield and contamination protection. The PSS is a tubular truss-structure built up from carbon fiber reinforced plastic (CFRP) longerons and custom-designed titanium fittings.

The spacecraft, in a side-mounted graphite bus structure, provides all the infrastructure and services needed by the instrument, including power, three-axis attitude control, and command and data handling. It also provides omnidirectional low-gain antennas, a body-mounted 1.5-m high-gain antenna, and an articulated solar array. For cost effectiveness, the spacecraft only includes high-heritage components with minimal customization.

An overview of the SIM Lite flight system configuration is shown in Figure 20-3. The mechanical layout consists of five benches, each attached to the PSS with six struts. The electronics and spacecraft bus are configured as "backpacks" that are attached on the outside of the PSS. Each of the two interferometers requires three mechanical benches: one bench at each end of the instrument contains the collecting apertures and one in the center accommodates the beam-combining optics. The two sets of beam-combining optics, the ABCs, are stacked vertically and share what is collectively called the central bench. In Figure 20-3, they are identified by the label "D."

20.2 Collecting Bench Assemblies

In Figure 20-3, the two benches on either side of the astrometric beam combiner are the guide benches. These contain the guide-collecting optics. The bench closest to the spacecraft bus also contains the Guide-2 star tracker. The layout of the latter bench is shown in Figure 20-2. The two outer benches, just outside of the guide benches, contain the science interferometer collecting optics. The layout of that bench is shown in Figure 20-2. All of these are attached to the PSS so that they are kept aligned both through launch and as the thermal loads on the spacecraft change. Among the four benches, many of the components are copies or near copies of one another, keeping the design and development costs to a minimum. In the discussion that follows, the components are described in the order of the path starlight takes.

20.2.1 Siderostat

Each science siderostat with its mount is the heaviest single component of SIM Lite, with a mass of about 190 kg. The siderostat assembly is shown in Figure 20-4.

A bezel ring design for the mirror mount allows the pivot point of the siderostat to be adjusted to within 100 μm of the DCC vertex. The bezel also holds thermal control hardware in order to keep the siderostat at 20 degrees Celsius, maintaining and stabilizing the wavefront. In order to accommodate a clear aperture of 50 cm for all angles of incidence, the science siderostat mirror is made with an actual diameter of 55 cm.

The Guide-2 siderostat, although smaller in diameter, features both a fine and a coarse stage and hence is somewhat more complex mechanically. The design of this item was only recently begun, and as of this writing, is still in progress.

Figure 20-3. All key elements of the SIM Lite flight system are designed and the most challenging components have undergone lifetime and flight-qualifying tests at the brassboard (BB) level. These substantial investments have made SIM Lite a well-understood system with low implementation risks.
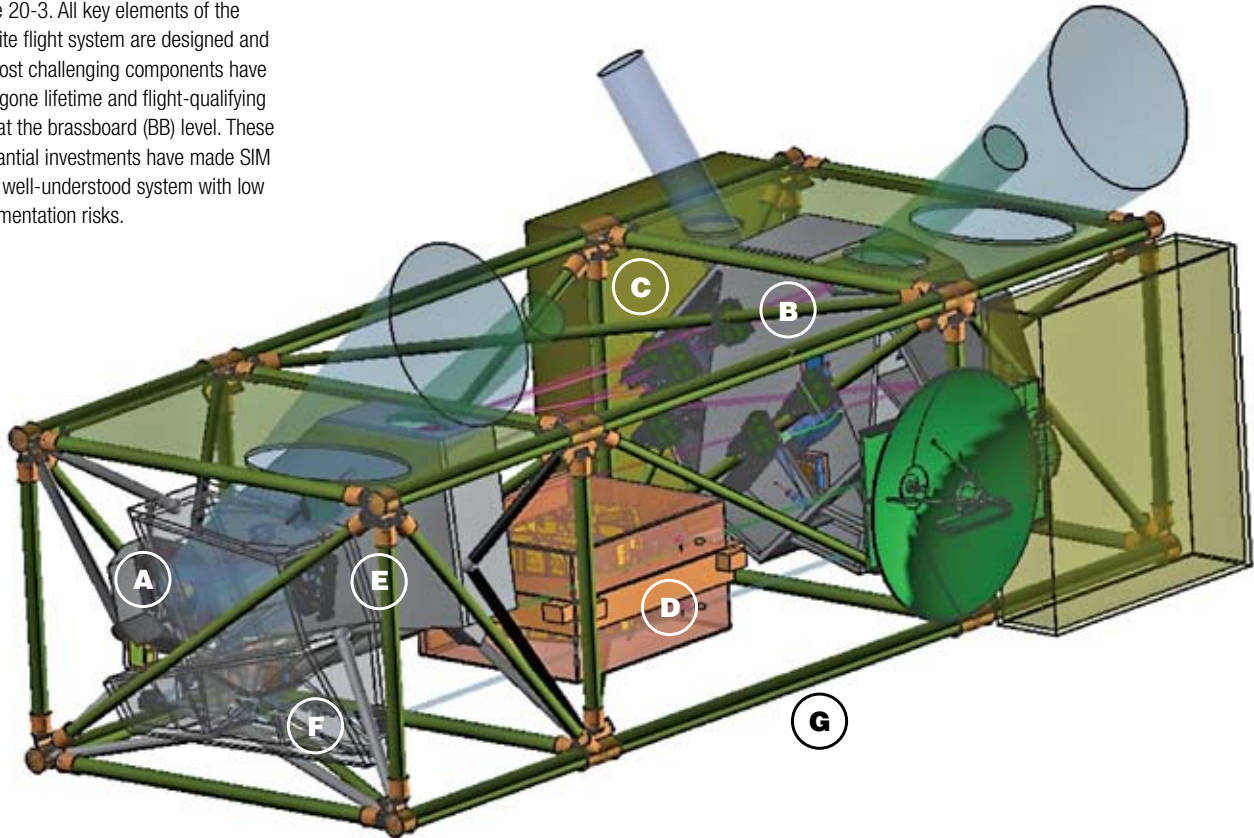
A

BB siderostat mechanism (SID). Complete design will be done by the end of 2008.

Prototype siderostat mirror (SID): non-articulating siderostat mirror. Successfully passed thermal stability tests in the TOM3 testbed.

Brassboard double corner cube: build by CSIRO and used in the JPL Kite testbed. Successfully passed optical prescription and stability requirements.

Prototype ball-screw actuator. It passed resolution and accuracy requirements and is now being used for a life-test, and has reached over 300,000 cycles.

B

Fiber In: Local Oscillator
Fiber In: Measurement
Zerodur Glass Bench
Dither Mechanism
Fiducial
Measurement Path
Aluminum Main Bench
Fiducial

Phase difference between these two 20 kHz signals gives pathlength change.

Signal Out: Measurement
Signal Out: Reference

Brassboard external metrology beam launcher: successfully passed vibration and thermal tests; passed optical metrology stability and cyclic error requirements at the 4 pm level.

C
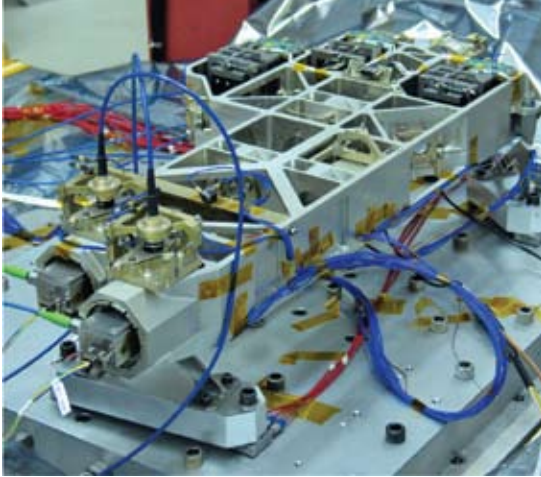
Brassboard laser source bench: successfully passed vibration and thermal tests; passed optical throughput, optical power stability, and chopping requirements.

D

Brassboard internal metrology beam launcher: successfully passed vibration and thermal tests; passed metrology stability and cyclic error requirements at the 3 pm level. Will be integrated into the ABC in 2009.
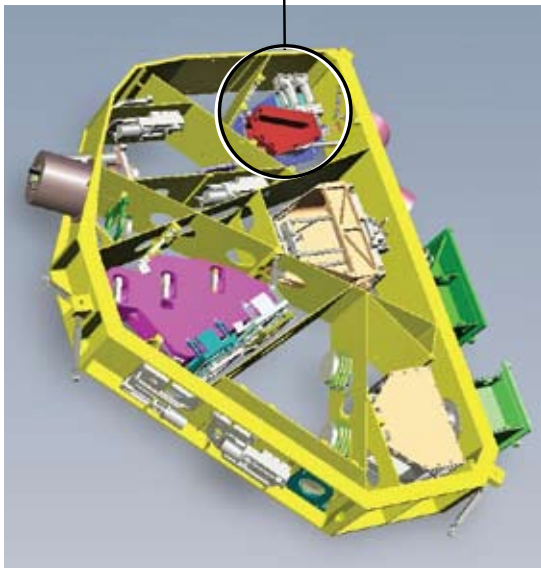
Brassboard astrometric beam combiner (ABC): currently in the design phase. Long-lead items are on order. Brassboard will be built in 2009.

E

Prototype primary mirror assembly (M1): figured and mounted a 300 mm lightweight mirror with 5.7 nm RMS wavefront error. Successfully passed both vibration and thermal tests.

F
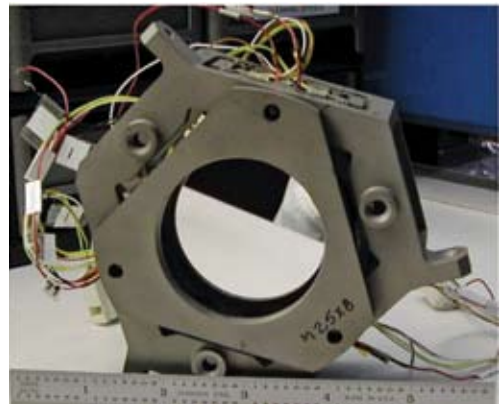
Prototype fast-steering mirror: prototype is being used in the Guide-2 testbed. Brassboard versions will be build by end of 2008 for thermal and vibration tests. PZTs are undergoing life-tests, and currently have over 26 billion cycles.

G
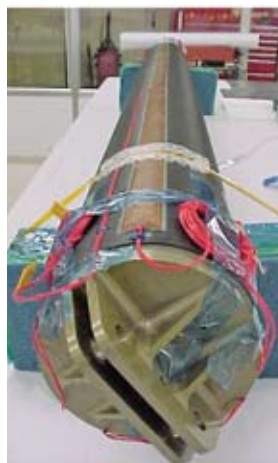
Prototype single-strut test article (SSTA): built by NG. A prototype graphite truss component passed thermal control and thermal expansion tests.

20.2.2 Beam Compressor

Among the cost-saving simplifications that have led to the current SIM Lite design has been a relaxation of the field of view requirement for all the beam compressors down to only 40 arcseconds. This has allowed for a simpler design, so that each of SIM Lite's compressors now consists simply of two off-axis parabolas. The compressor reduces the beam size by a factor of 12.5 for the science interferometer and a factor of 7.5 for the Guide-1 and Guide-2 instruments.

An important aspect of a beam compressor is its thermal stability. As described in Chapter 19, a brassboard beam compressor was constructed and used in the TOM testbed (Figure 20-5). Though more complex than the current design and hence more susceptible to thermal errors, the brassboard has already demonstrated thermal stability that meets SIM Lite's requirements.

Another important requirement for the beam compressor is that its large precision optics can be mounted in such a way that they, on the one hand, can survive launch loads, and on the other hand, are not significantly deformed in the mounting process. This was demonstrated with the M1 primary mirror, which is shown in Figure 20-3 (inset E). This mirror, which has a 34.3 cm diameter, has an allocation of only 8 nm RMS including mounting errors. With this lightweight version, an RMS wavefront error of 6.3 nm RMS was achieved. The mirror and mount also successfully passed the thermal cycling and vibration tests needed for SIM Lite without any degradation to the wavefront. (Bloemhof et al. 2008)

20.2.3 Fine-Steering Mirror

The FSM is a 5 cm optic that is used primarily to compensate for the slow attitude drifts of the spacecraft. The brassboard FSM is shown in Figure 20-3 (Inset F) and a CAD drawing of the flight design assembly appears in Figure 20-6.

The FSM's fine resolution is accomplished using piezoelectric transducers (PZTs), supplied redundantly to ensure reliability. The mount mechanism is momentum compensated so that its motion does not disturb the rest of the instrument. The FSM has a single-step resolution of 13 mas (mapped onto the sky) and a total range of 40 arcseconds, covering the entire instantaneous field of regard. The resolution is slightly better on the science interferometer because of the larger compression ratio, at the expense of a smaller field. But this is acceptable for the science interferometer because of the existence of its siderostat. The FSM's PZT actuators have strain gauge encoders in order to linearize their motion. This feature is used when the science interferometer is observing very dim objects, at which point the ACS error will be too large for the interferometer to track using the centroid on the CCD. Instead, the measured motion from the Guide-1 FSM will be used to control the science FSM. After sufficient integration time on the science angle tracker camera, a direct pointing measurement becomes available, providing a closed-loop correction on the slower time scale. This control scheme, called angle feed-forward, has already been successfully demonstrated in SIM Lite testbeds.

20.2.4 Delay Line

One of the original challenges that optical interferometry faced was the need to control delay from meters down to nanometers. The dynamics and control challenges posed by this requirement necessitated an early proof of concept for this aspect of SIM Lite. A significant effort early on resulted in a brassboard beam delay line that delivered, in three stages, the nine orders of magnitude of dynamic range required. The brassboard delay line was taken through full qualification-level vibration and thermal vacuum testing. Before and after such testing it was able to meet the demanding nanometer control requirements, with a pathlength stabilization performance of 1.4 nm.

Figure 20-4. SIM Lite's science siderostat assembly (brassboard on left; flight version CAD drawing on right) uses a flight-proven actuation approach. The DCC at the center of the siderostat is mounted on a post made of the same materials as the siderostat, minimizing changes in the offset between the vertex of the DCC and the plane of the siderostat.
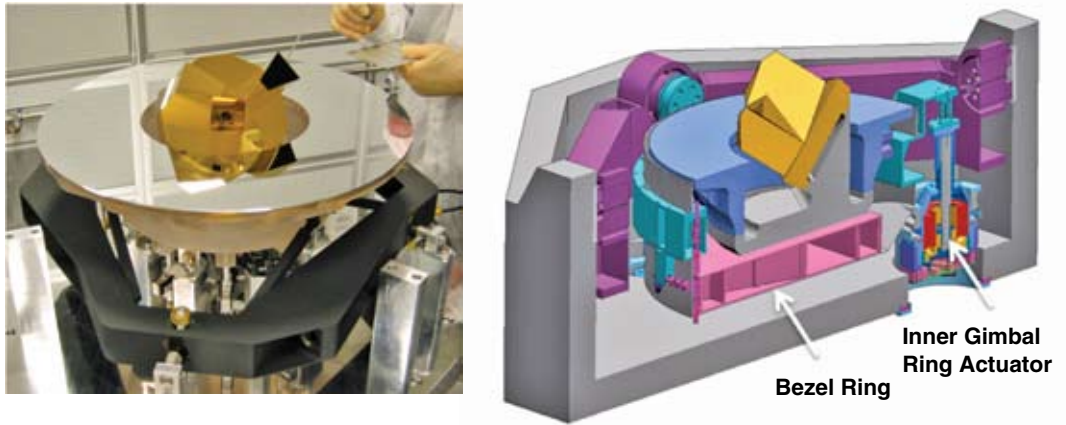

Inner Gimbal Ring Actuator

Bezel Ring

Figure 20-5. The brassboard compressor demonstrated the thermal stability of the optomechanical structure and the optics themselves. The SIM Lite mounts and structures will therefore be similar to this one. (From Laskin 2006b.)
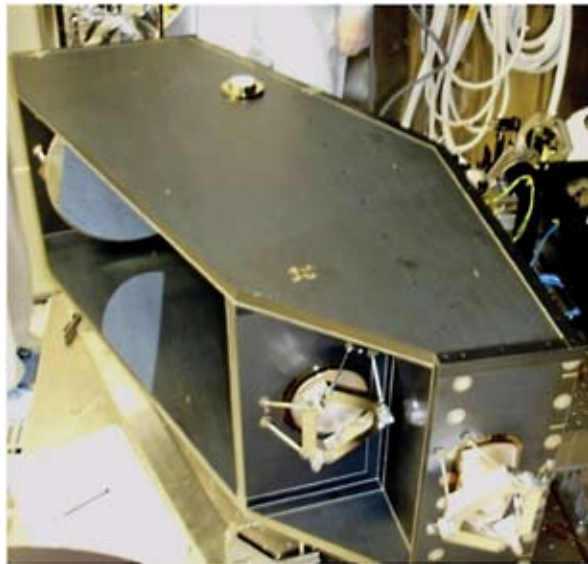
Figure 20-6. The fine-steering mirror actuator, shown in this CAD drawing in its flight mount, has been built as a brassboard (Figure 20-3, inset F) and will be flight-qualified in 2009.
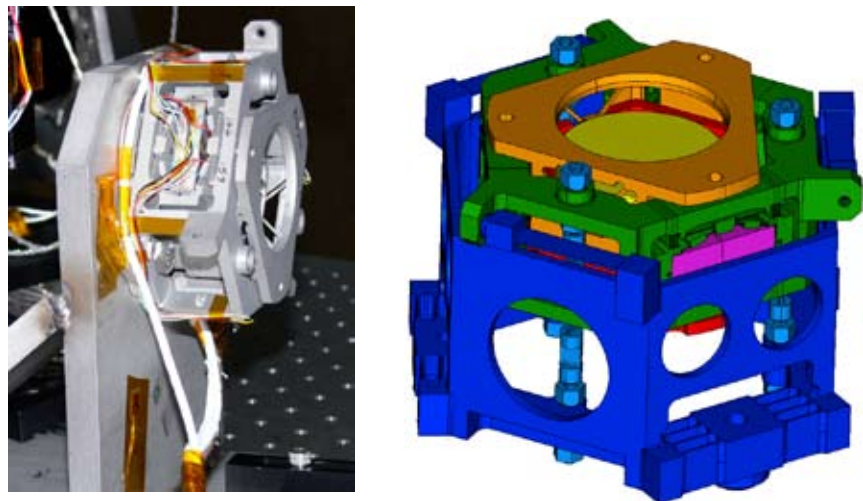
More recently, as part of the aggressive cost-cutting measures to make SIM Lite possible, a significantly simpler, lighter, and more distributed design has been adopted. The new delay line in many other respects inherits the innovations proven by the delay line brassboard. It also incorporates a better optical design, avoiding the cat's eye employed in the brassboard, and thereby reducing the sensitivity to beam-walk errors. In the new design, a ball-screw mechanism pushes a three-mirror optical assembly that in effect forms a corner cube.

Figure 20-7 shows the original brassboard delay line and its simplified version as will be implemented in SIM Lite. There are two delay lines in the science interferometer, each with 40 cm of travel. The design is simple and precise, but less compact than seen in many ground-based interferometers, because of the required accuracy to match the internal metrology and starlight paths.

As with the siderostat, the delay line does not move during observing; it only slews while acquiring a new star and is then locked into place. During an observation, the pathlength optic mechanism (POM), also shown in Figure 20-7, is responsible for correcting the optical path changes.

20.3   Astrometric Beam Combiner

At the heart of the instrument lies the ABC. This is where the starlight interferes and is measured. As the name implies, the ABC receives the starlight from both sides of the interferometer and combines it to form fringes. Figure 20-3 (inset D) shows a CAD drawing of the ABC, which is currently under construction. An optomechanical representation showing the light paths can be seen in Figure 20-8.

The entrances into the ABC are on the lower left, receiving collimated starlight from the two arms. The beams maintain a 4 cm outer diameter until reaching the fringe and angle tracking cameras. The beams split off for angle tracking are imaged onto the angle tracking camera (ATC) CCD. Also integral to the ABC is the internal metrology gauge, which tracks pathlength changes of the interferometer arms at the pm level.

20.3.1   Fringe Tracking Camera (FTC)

Starlight from both arms is combined at the main beam splitter of the ABC, yielding two combined beams, sometimes referred to as A and B. One side is folded so both beams end up traveling to the right in Figure 20-8. They are then compressed to 4 mm diameter and, using a Wollaston prism, each is separated into S and P polarizations. The reason for separation by polarization is that there will inevitably be some phase dispersion in the interferometer and it will be different for S- and P-polarized light. Since the incoming starlight may be slightly polarized, and the polarization can be different from one star to another, there can result significant polarization-dependent phase measurement errors. By resolving the beams into the S- and P-polarized parts, separate, polarization-specific delay difference measurements can be made of the stars, mitigating the polarization-dependent error (Figure 20-9).

The resulting four beams (two for each side of the beam splitter) are spectrally dispersed using a prism and imaged across 80 pixels in the CCD. The FTC uses an 80 × 80 E2V CCD, shown schematically in Figure 20-10. The choice of spectral resolution is an optimization between readout speed (2 kHz) on the one hand and spectral information on the other. The spectral window extends from 450 to 950 nm. The number of spectral channels is variable from the full 80 down to 4, useful for increasing the SNR on the dimmest objects.

Figure 20-7. The brass-board delay line (left) successfully demonstrated nm-class performance after flight-level vibration and thermal testing. The modified SIM Lite delay line (right) uses some of the same mechanical features as the brassboard with the nanometer stage separated into a simpler mechanism called the pathlength optic mechanism (POM). A brassboard POM is currently under fabrication.
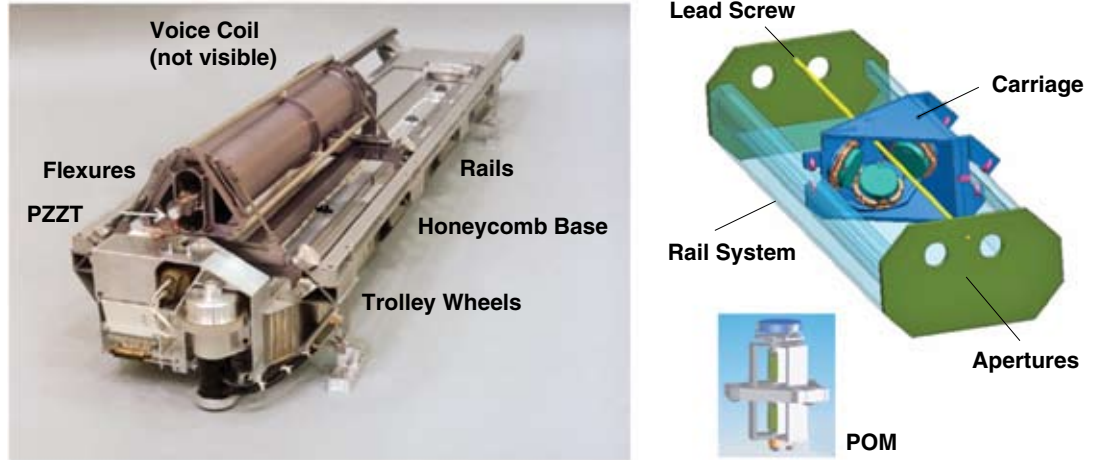

Figure 20-8. The ABC is the heart of the interferometer, housing the fringe and angle tracking cameras and the internal metrology beam launcher. It also contains a stimulus to calibrate the interferometer. (From Dekens et al. 2008.)
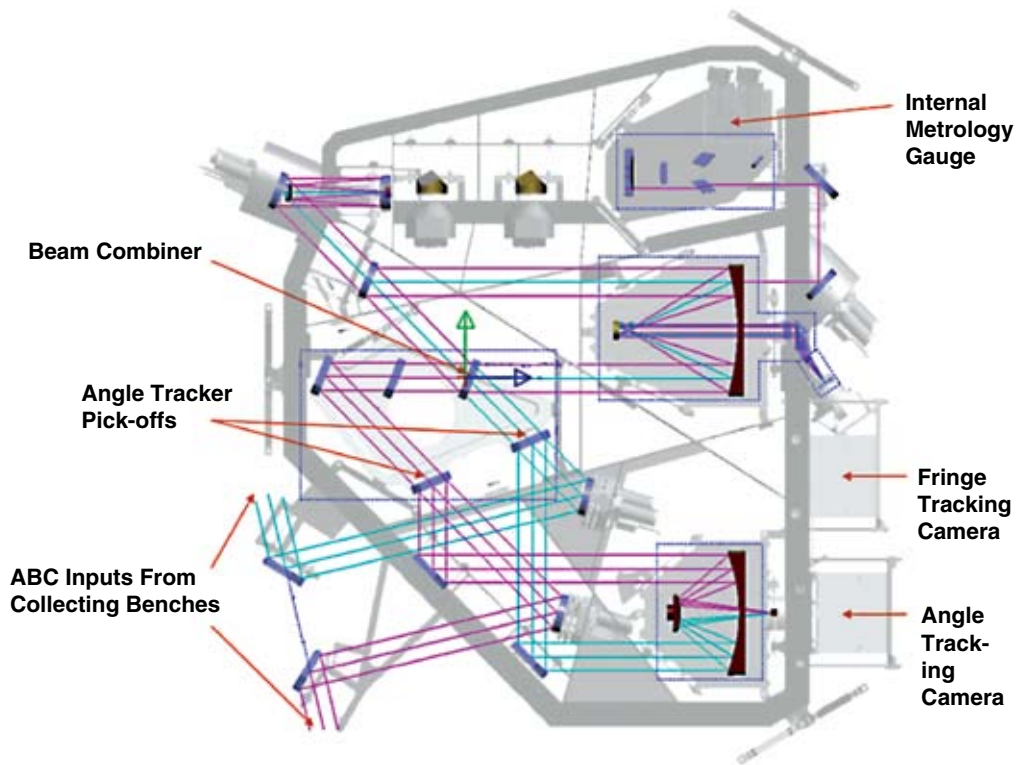
Figure 20-9. SIM Lite's fringe tracker assembly (left) and camera (right). The camera, which uses an 80 × 80 E2V CCD and is operated at –110 ºC, will have dark current below 0.01 e-/pixel/second. (From Jeganathan et al. 2008.)
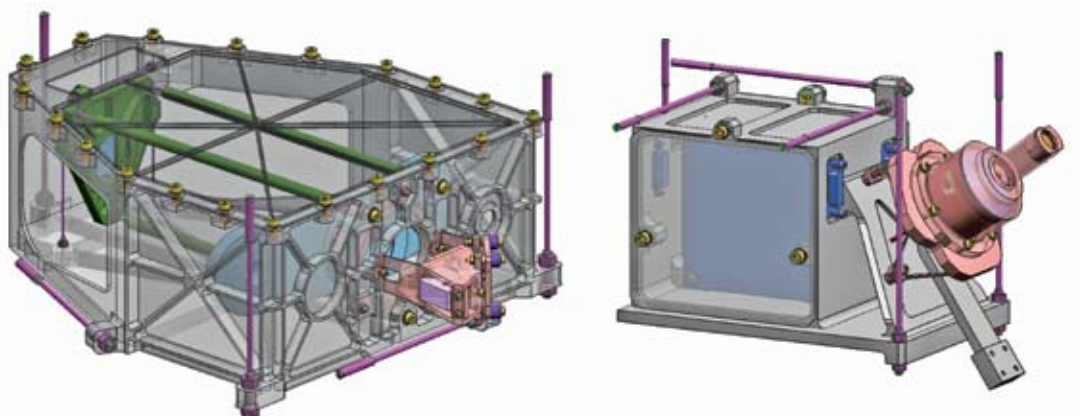
20.3.2 Angle Tracking Camera

Prior to being combined, 25 percent of each of the incoming beams is split off in the ABC and imaged on the ATC focal plane, which also uses an 80 × 80 E2V CCD. By applying a pointing offset via the folding mirrors, two star images are formed in two different quadrants of the CCD, as seen in Figure 20-10. The spots provide a measure of the pointing of the starlight beams in the two arms of the interferometer. The two quadrants are read out and fed back to the pointing control, which actuates the fine steering. The plate scale is 1 arcsecond per pixel for the guide interferometer (and slightly smaller for the science interferometer, since it has a larger compression ratio), making it easy to position the star with the 5 arcsec attitude control system provided by the spacecraft. The plate scale gives sufficient resolution to point the beams properly and obtain high-visibility fringes on the FTC (Figure 20-11).

20.3.3 Internal Metrology Beam Launcher

The internal metrology beam launcher is located within the ABC (upper right in Figure 20-8 and Figure 20-12). The measurement beam consists of four 3 × 3 mm "pencil" beams, two per side of the interferometer. Masks in the FSMs and within the beam launcher define the two pencil beams used for each of the arms. Metrology light is fed in from the metrology source via two fibers, carrying 1.3 µm laser light separated by a heterodyne frequency of 100 kHz. The beam launcher optical bench is made of low-expansion glass, with dispersion carefully balanced between the two arms to minimize sensitivity to thermal drifts.

The brassboard internal metrology beam launcher was designed and fabricated using many of the same design tools, materials, and parts qualities as will be used for the flight units. Two brassboard beam launchers have been built. One was used to conduct both stand-alone pm performance tests and system-level tests in the MAM testbed and the other was used to conduct environmental tests with pre- and post-environmental stand-alone pm performance tests. More recently, the latter beam launcher has been modified into the angle metrology (aMet) beam launcher of the Guide-2 telescope (G2T) testbed.

The internal metrology launcher design has been driven by the performance requirements under the narrow-angle scenario. The requirement is 3.5 pm of error and the brassboard has achieved 3.1 pm. The wide-angle requirement is 46 pm, and the beam launcher has achieved 41 pm.

Overall, the internal metrology beam launcher has successfully passed both stand-alone and system-level performance tests, as well as the environmental (thermal cycling, vibration) tests. Having met all of its requirements, the next step for the brassboard internal metrology beam launcher is its integration into the ABC brassboard currently under construction.

20.4 Guide-2 Telescope

The Guide-2 telescope (G2T, Figure 20-13) collects starlight using a scaled-down version of the science siderostat. At the center of the G2T siderostat are four small corner cubes rather than a large DCC, since here the metrology is used to measure the siderostat's tip and tilt. The reflected starlight goes through a 30 cm compressor, which is a copy of the Guide-1 compressor, and then onto a 5 cm annular mirror that allows the metrology beams to pass. The reflected annular starlight beam continues on to a focusing mirror and is imaged on a CCD, which is a copy of the ABC's angle-tracking camera.

As the attitude of SIM Lite changes in inertial space, the fine stage of the siderostat mechanism tracks the Guide-2 star. This makes it possible to keep the Guide-2 star locked on the pointing camera, at the

Figure 20-10. The angle and fringe tracker cameras, both use the 80 × 80 E2V CCD, which has dark current under 0.01 e-/pix/s under SIM Lite operating conditions.
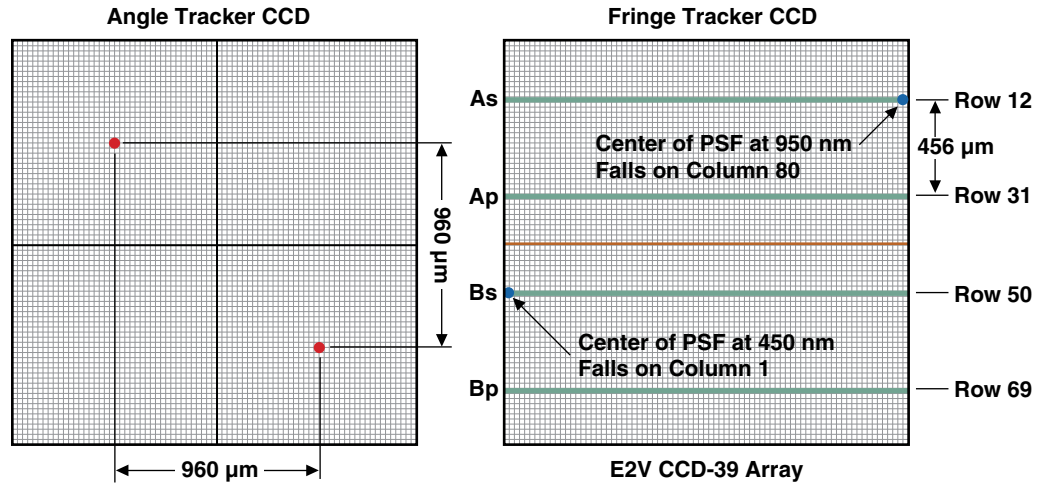

Figure 20-11. Left: Angle tracker assembly with primary and secondary optics. Right: ATC with camera head and electronics. The two will be mounted to a common structure and aligned and tested as a single unit. (From Jeganathan et al. 2008.)
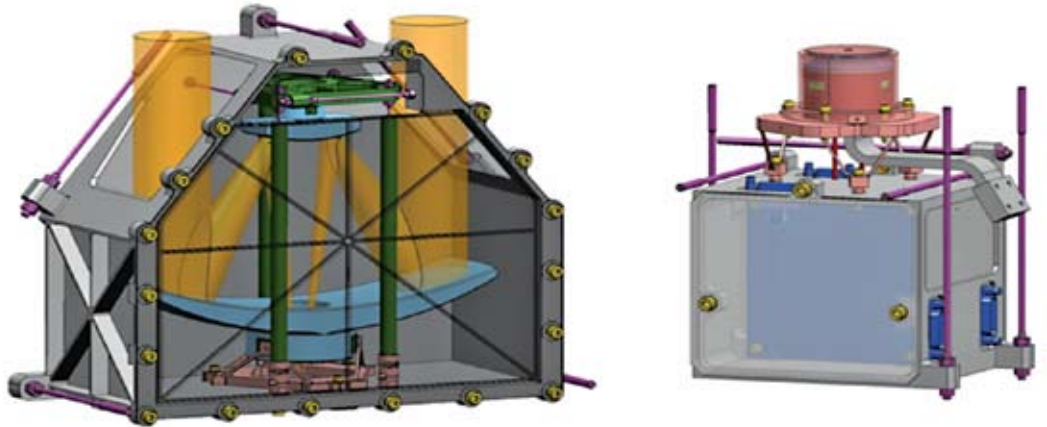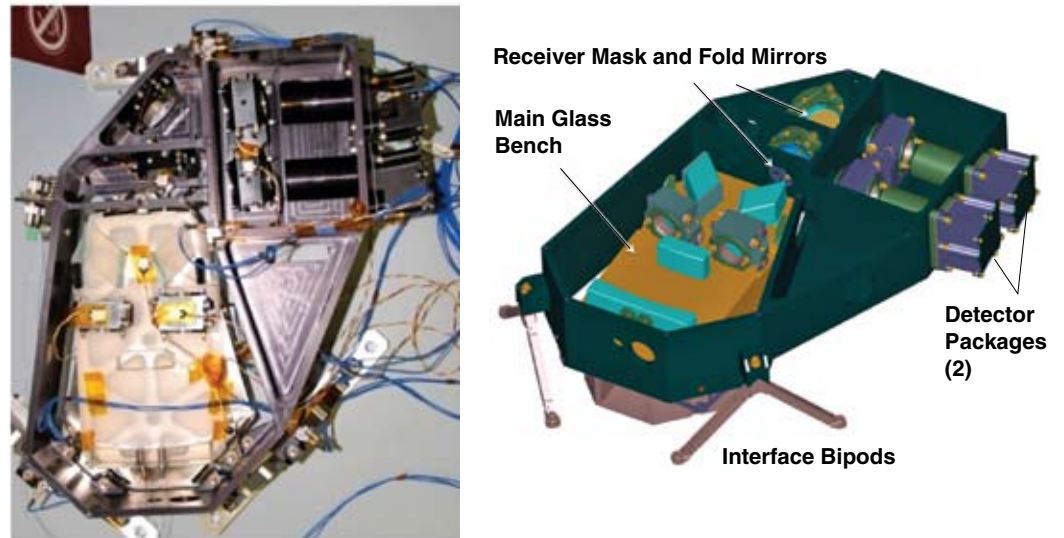

Figure 20-12. The internal metrology beam launcher brassboard has successfully met all flight requirements.

intersection of four pixels within a few mas, while measuring the larger dynamics of the spacecraft attitude change (about 1 arcsecond) with the metrology sensor. Both the CCD-based pointing sensor and the metrology system tracking the angular position of the siderostat have accuracy close to 20 μas over short periods of time. The G2T testbed, described in Chapter 19, is meeting its performance requirements and confirming that the flight implementation will be successful.

20.5   External Metrology System

Optically, the external metrology sensor comprises a set of fiducials, a number of beam launchers, and a metrology source.

20.5.1   External Metrology Beam Launchers

The brassboard external metrology beam launcher can be seen in Figure 20-14. It met nearly all the requirements. The driving requirement is narrow-angle performance of 3.0 pm; the performance was measured to be 3.5 pm. Even though the impact of this on the overall performance of SIM Lite is minimal (~1 percent), the design improvements needed to ensure meeting flight goals have already been identified. The wide-angle performance, measured to be 14 pm, is significantly better than the wide-angle goal of 42 pm and improves SIM Lite's expected wide-angle performance by 2 percent. The beam launcher has also demonstrated pointing stability and tracking performance meeting flight requirements. Finally, one of the beam launchers was subjected to flight-qualification-level vibrations and thermal cycling spanning 10 to 45 degrees C. Afterward, it showed no degradation in performance.

20.5.2   Fiducials

The fiducials that are needed for SIM Lite are challenging to build because they must satisfy many tight optical tolerances. Two of the fiducials require two corner cubes, and two require three corner cubes to be fashioned in such a way that their vertices coincide to <6 μm. A double corner cube (DCC) version was built and tested in the external metrology testbed Kite (Laskin 2006). The testbed passed its milestones using the DCC shown in Figure 20-15, showing the fiducial can be built to the SIM Lite specifications. The wavefront error of the base plate is required to be 3 nm, and that of the wedges 6 nm. Further testing by Australia's Commonwealth Scientific and Industrial Research Organization (CSIRO), which manufactured the brassboard, has shown that the optical bonds in the DCC meet flight strength requirements (Burke et al. 2008).

20.5.3   Metrology Source

The metrology source (MetSource) provides all the optical inputs required for the external metrology and internal metrology sensors described in the previous sections. The fiber-optic cables transport the 1.319 μm light throughout the SIM Lite structure to the external and internal metrology beam launchers. The MetSource optical bench is the opto-electro-mechanical assembly that physically contains all the necessary devices (laser heads, laser switches, absolute metrology switches, frequency shifters, and power monitor detectors) and components (lenses, beam-splitters, mirrors, half-wave plates, polarizers, and associated mounts) required to provide the desired output beams. The MetSource brassboard bench can be seen in Figure 20-16.

Figure 20-13. The Guide-2 telescope, currently being developed in the G2T testbed, will deliver an unprecedented 50 µas star-tracking precision. (From Goullioud et al. 2008.)
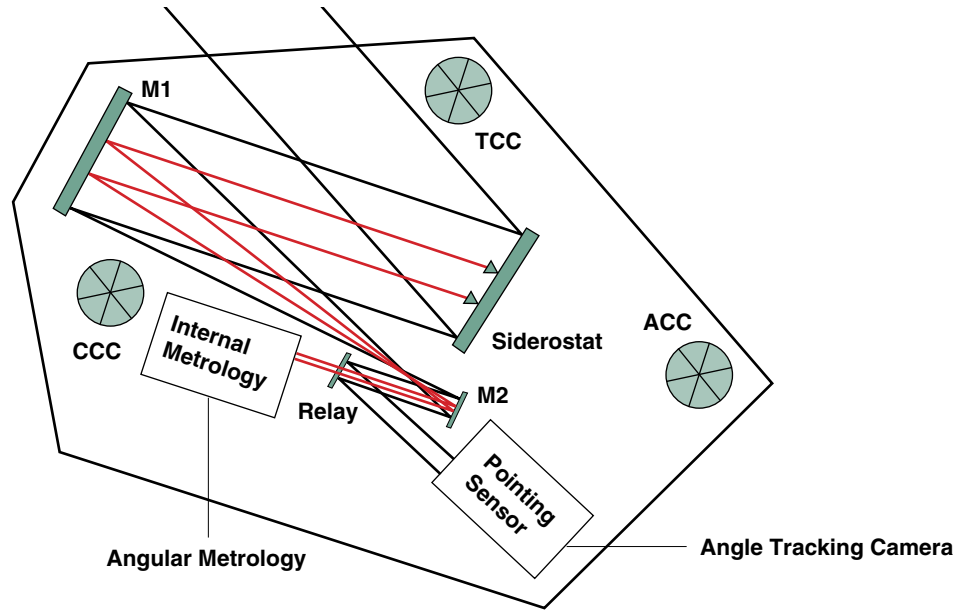

Figure 20-14. The brassboard external metrology beam launcher, shown with its interfaces, monitors the distance between SIM Lite's fiducials. (From Jeganathan 2007.)
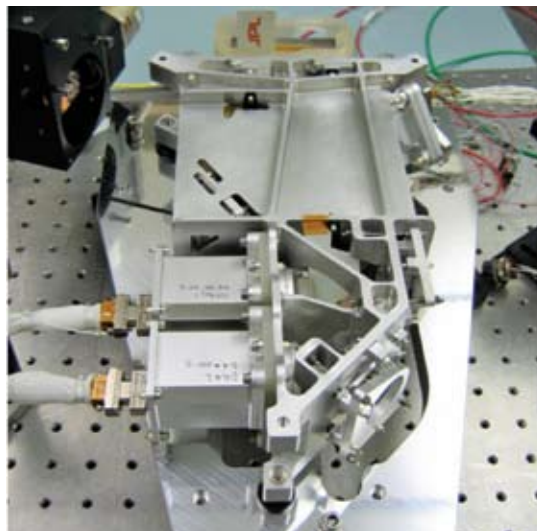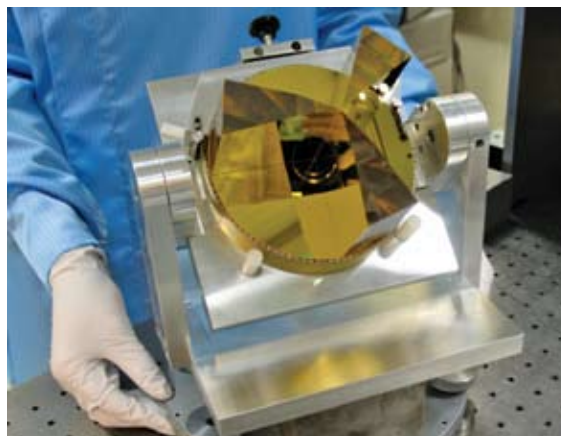

Figure 20-15. The brassboard double corner cube has successfully passed its performance requirements in the Kite testbed. (From Laskin 2006b.)

To accommodate "absolute metrology" mode (measuring a link's absolute length to a few microns), the metrology source contains two 1.319 μm NdYAG nonplanar ring oscillator (NPRO) lasers operated at optical frequencies offset by 15 GHz. The single laser head can be seen in Figure 20-17. In absolute metrology, acousto-optic modulators (AOMs) alternate between the two laser outputs as the carrier light for metrology. The switch rate is 250 Hz, chosen as high as possible in order to minimize the sensitivity of the absolute metrology measurement to fiducial vibrations. In the "relative metrology" mode, the switching is stopped, and one of the AOMs continuously selects only one laser to feed the system with heterodyne light.

The entire metrology source (including the pump diodes, electronics, and thermal control) is located in one of the electronics backpacks.

20.6 Precision Support Structure

The precision support structure (PSS) acts as the optical bench that houses the collector bays, astrometric beam combiners, external metrology, and other associated hardware of the SIM Lite instrument (Figure 20-18). Together with the thermal insulation and control system, the PSS maintains a stable environment for all optical components. The PSS is also the primary load-carrying member of the SIM Lite flight system and interfaces directly to the launch vehicle adapter.

The PSS is a tubular truss constructed of graphite tubes (Figure 20-19) and titanium nodal fittings. In some locations, diagonal struts are replaced by graphite sheer panels to avoid blockage of the siderostat field of views.

The PSS is being developed in close collaboration between Northrop Grumman and the instrument design team at JPL. The design and verification efforts will draw on the Northrop Grumman experience from the precision thermal, distortion, and dynamic disturbance control achieved on the Chandra X-Ray Observatory and other programs. All thermal-control components, including heat pipes, heaters, thermistors, and insulation blankets have flight heritage. The CFRP materials, lay-ups, and procedures have been proven in the Single-Strut Test Article (SSTA) testbed in 2006.

The purpose of the SSTA was to mitigate technical development risks relative to the PSS structural and thermal control design and to provide a partial pathfinder for flight manufacturing. The testbed employed a building-block approach using component level test articles — material, joint, and substructure. The SSTA characterized thermal response of a CFRP strut tube and clevis fitting, measured the end-to-end CTE, and verified joint capability. The test coupon was dried to a constant temperature prior to testing and was tested in a vacuum environment to prevent moisture absorption. Test results showed that the test article met all test requirements. More coupon testing to verify procedures and workmanship are anticipated prior to manufacturing.

20.7 Spacecraft

The SIM Lite spacecraft (block diagram, Figure 20-20) is a three-axis stabilized, zero momentum platform. Using Northrop Grumman heritage components and software, it provides the standard spacecraft functions of attitude control, electrical power, thermal control, data management, telecommunications, and software.

Figure 20-16. The brass-board metrology source has successfully met its requirements. (From Dekens et al. 2008.)

Figure 20-17. SIM Lite's brass-board NPRO laser, shown with thermal enclosure, has met the frequency stability requirements for pm metrology. (From Dekens et al. 2008.)
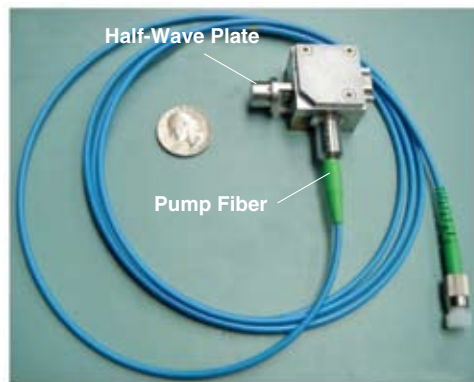

Figure 20-18. The precision support structure carries all instrument components, the instrument electronics compartments, and the spacecraft compartment, as well as the high-gain antenna and thrusters. (From Goullioud et al. 2008.)
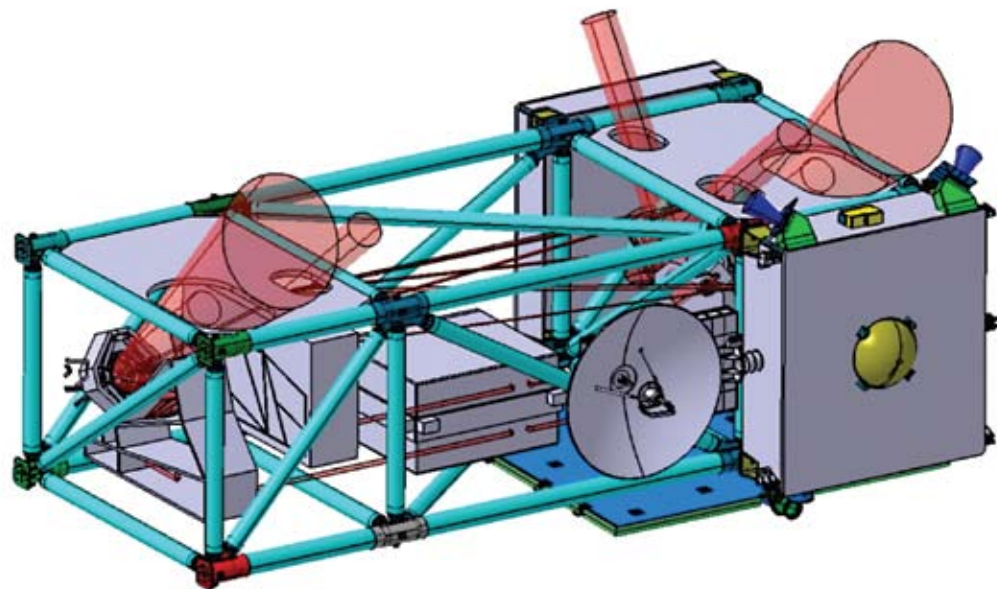
Figure 20-19. In 2006, a representative element of the precision support structure, the single strut test article, met all test requirements. (From Dekens et al. 2008.)
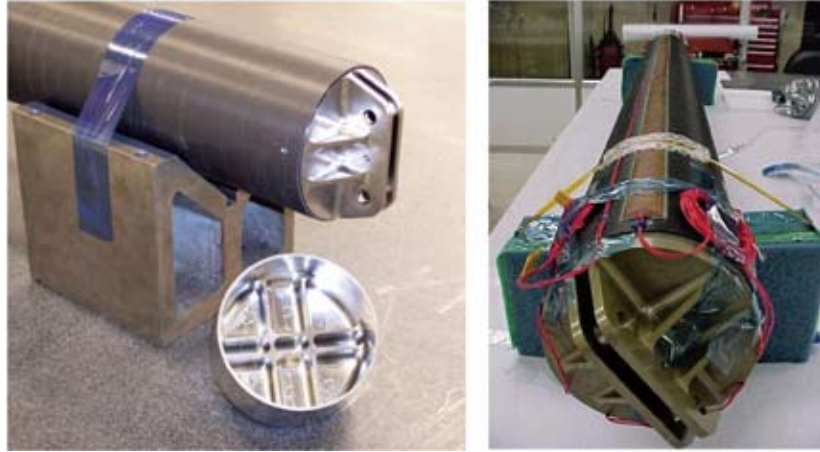
The spacecraft structure is a 195 × 210 × 60 cm graphite honeycomb structure shaped like an open bookshelf. It houses the propellant tank in the center with all the other components mounted on its faces. The open side faces the PSS and is thermally isolated from it with multilayer insulation (MLI).

The attitude control subsystem (ACS) provides space vehicle maneuvering to position the instrument with knowledge and stability of 0.1 arcsecond to support the science mission. Its four Teldix reaction wheels and inertial reference unit (IRU) have heritage from the National Polar-Orbiting Operational Environmental Satellite System (NPOESS), and its Galileo Star Trackers will be flying on the Lunar Crater Observation and Sensing Satellite (LCROSS). Momentum unloading is achieved via four Northrop Grumman dual-thruster monopropellant modules. Identical designs have been flown on the Earth Observing System (EOS). The thrusters are oriented and operated such that no delta-V is imparted during momentum wheel desaturation. Two-stage vibration isolation on the reaction wheels reduces jitter to the levels required by the interferometer.

The redundant command and data handling subsystem uses a Rad 750 processor board with 36 MB of RAM manufactured to host the flight software and control the spacecraft. The 96 Gbit (single side) onboard data storage system is almost twice the required 50 Gbit/week memory for science data. The units are manufactured by Northrop Grumman Technical Services and will be flying on LCROSS.

Communication is via X-band low-gain omni-directional antennas for both uplink and downlink for command and telemetry. Science data are downlinked using the Ka-band high-gain body-mounted antenna. No science operations will be scheduled during science downlinks, as the spacecraft needs to point the high-gain antenna at Earth during this time. However, the bandwidth is scoped so that science data downlink will require a maximum of eight hours per week at the end of the mission (at maximum communication distance), keeping impact on observing time to a minimum. X-band can be switched to the high-gain antenna if the need arises. All units are redundant and cross-strapped. Data rates are 10 bps to 6.4 Mbps in Ka-band and 10 bps to 3.48 Mbps in X-band through the high-gain antenna. Doppler ranging will be performed via the X-band uplink/downlink or X-band uplink/Ka-band downlink. Differential one-way (DOR) ranging is also supported via X-band or Ka-band.

Spacecraft power is provided via a single-wing, dual-gimbaled, triple-junction GaAs solar array and Saft lithium ion batteries. The 96 Ahr battery's main function is to provide power during launch and from launch vehicle separation to solar array deployment with some limited capability during safe modes. During normal operation, the 4400 W (end of life) solar array provides all onboard power. The end-of-life capability of the power system includes a 30 percent contingency on the current best estimate of the payload power.

Figure 20-20. Spacecraft block diagram.
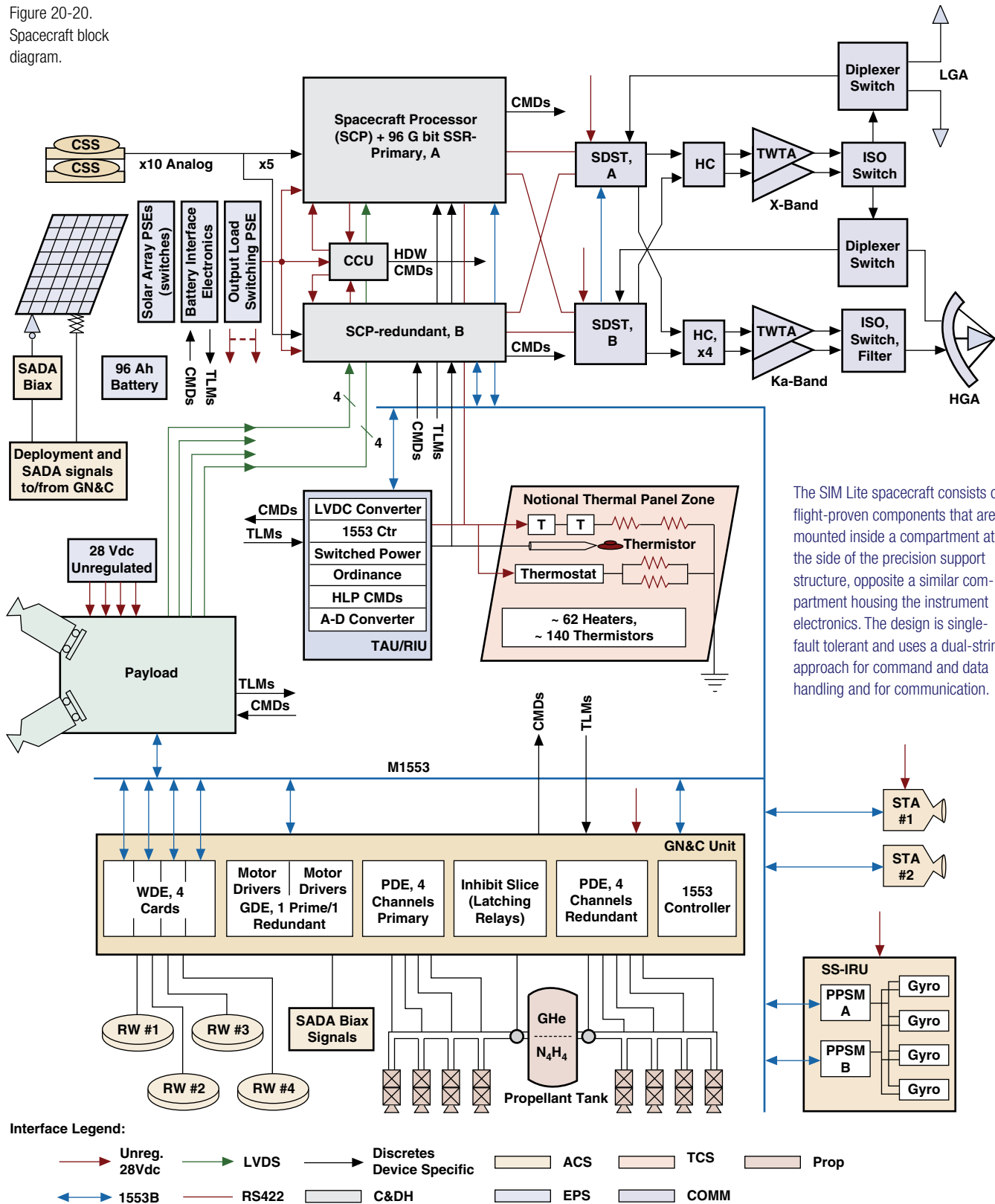
The SIM Lite spacecraft consists of flight-proven components that are mounted inside a compartment at the side of the precision support structure, opposite a similar compartment housing the instrument electronics. The design is single-fault tolerant and uses a dual-string approach for command and data handling and for communication.

Interface Legend:

→	Unreg. 28Vdc	
↔	1553B	
→	LVDS	
—	RS422	
→	Discretes Device Specific	
	C&DH	
	ACS	EPS
	TCS	COMM
	Prop	
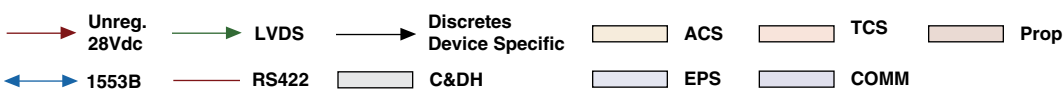
Acronyms:

CCU: Configuration Control Unit
GN&C: Guidance, Navigation, and Control
PDE: Propulsion Deployment Electronics
PSE: Power Supply Electronics

STA: Star Tracker Assembly
HGA: High-Gain Antenna
LGA: Low-Gain Antenna

TWTA: Traveling-Wave-Tube Amplifier
SADA: Solar Array Drive Assembly
SDST: Small Deep Space Transponder

TAU: Telemetry Acquisition Unit
RIU: Remote Interface Unit
CSS: Coarse Sun Sensors

References

Bloemhof, E. E., Lam, J. C., Feria, V. A., and Chang, Z., 2008, Proceedings of SPIE 7013, 3L.

Burke, J., Green, K. L., Raouf, N., Seckold, J. A., and Oreb, R. F., 2008, in Schöller, M., ed., Optical and Infrared Interferometry, 7013, 159.

Dekens, F. G., Bloemhof, E. E., Dubovitsky, S., Eldred, D., Goullioud, R., Jeganathan, M., Nicaise, F. and Zhao, F., Proc. SPIE vol. 7013, 70134U.

Goullioud, R., Catanzarite, J. H., Dekens, F. G., Shao, M., and Marr-IV, J. C., 2008 Proc. SPIE Vol. 7013, 70134T.

Hahn, I. et al., 2008, in Schöller, M., ed., Optical and Infrared Interferometry, 7013, 154.

Jeganathan, M., 2007 SIM Technology Expo, JPL.

Jeganathan, M., Kuan, G., Rud, M. Lin, S., Sutherland, K.,, Moore, J., and An, X., 2008 Proc SPIE, vol. 7013, 10134X.

Laskin, R., 2006a, in Advances in Stellar Interferometry, Monnier, J. D., Schöller, M., Danchi, W. C., eds., Proceedings of the SPIE, vol. 6268, 23.

Laskin, R. A., 2006b, IAC-06-A3.P.1.05.

Astrometry

A Precision Tool for the 21st Century

To many astronomers, astrometry is merely a necessary step toward other goals in astronomy. Only a minority really savor this important work and appreciate the fundamental nature of determining the positions of stars to higher and higher precision as the years pass. They glean parallaxes, yielding distances, and proper motions, which ultimately help define the general behavior of the stars in the Milky Way. A larger group of astronomers applies such measurements directly to the problems of astrophysics, a field recognized for only about 150 years, though its roots are much deeper. They determine the masses of binary stars' visible and invisible companions and reflect on their results in the context of theoretical predictions.

An astrometric observatory is a different "animal" than most astronomers are used to, and using one effectively requires a different mindset. There aren't going to be pretty pictures or high-resolution spectra for interpretation. There will be little instant gratification since many astrometric results require years (which could be the full duration of a space mission) to acquire the necessary data.

So many problems in astrophysics are addressed by the results from SIM Lite that anyone with an interest in planets, stars, star clusters, galaxies, quasars, or the Universe will find its investigations to be valuable. That includes just about everyone from professional astronomers to school children.

SIM Lite promises results that aren't just fundamental, but foundational. They will strengthen the whole edifice of astronomical science. In a different context but entirely appropriately, William Thompson (Lord Kelvin) expressed it well:

> "When you can measure what you are speaking about, and express it in numbers, you know something about it; but when you cannot measure it, when you cannot express it in numbers, your knowledge is of a meager and unsatisfactory kind: it may be the beginning of knowledge, but you have scarcely, in your thoughts, advanced to the state of science."

The technology necessary to make these measurements is impressive — control of the separation of optics at the nanometer level and knowledge at the picometer level. SIM Lite has demonstrated these measurements in the laboratory, and it has demonstrated all the technologies needed to make these precision measurements with SIM Lite in the space environment.

We know planets orbit other stars, and in a few cases we can actually see them directly or by silhouette. But we don't know their masses. We don't know if there are Earth-like planets. Do the planets we know about and the ones SIM Lite will find orbit in systems like the Sun's? Are there variations on this one scheme we are intimately familiar with? How do systems of planets change from formation to maturity? Do they survive the deaths of their parent stars?

Inside stars, nuclear reaction rates are dependent on the core temperature. The core temperature is dependent on the mass of the star. Except in a handful of cases, the masses of stars are known no better than to 10 percent, much too uncertain to distinguish between energy generation processes across the Hertzsprung-Russell diagram or to make the best use of the mass-luminosity relation, and in both of those the third dimension of metallicity lurks to confound results. How massive are the most massive O stars? How massive are the red dwarf stars that are just across the boundary from brown dwarfs? How

massive are stellar remnants like white dwarfs, neutron stars, and black holes in the Milky Way? SIM Lite data will yield masses at the 1 percent level. And SIM Lite's measurements of the luminous centroid of microlensing events, impossible in any other way, can be combined with observations made from the ground to address the unknown population percentages of stars, planets, and stellar remnants orbiting the Milky Way between the Sun and the nucleus of the Galaxy.

Star clusters are interesting in themselves, and offer clues to broader questions. How do stars behave dynamically within a young open cluster compared to an old globular cluster? SIM Lite will measure the distances and proper motions of individual cluster members. What does this behavior tell us about the ages of those stars, and what do the ages of the clusters tell us about the age of the Galaxy?

The motions of the Galaxy's dwarf spheroidal companions and their star streams, its globular clusters, and its halo stars help address a pressing mystery: dark matter. What is its distribution in the Milky Way? How much is there? What hints are there to its actual composition? SIM Lite's measurements can be expanded to many other members of the Local Group to address dark matter and its effects on galaxy motions within the Group.

Looking further afield, the processes ongoing in the extreme environment of the cores of galaxies are sure to expand our understanding of physics and the life cycles of galaxies. SIM Lite's resolution and measurements of events around the black holes there will clarify the processes behind the optical- and radio-activity in these tiny volumes.

Finally, one of the most exciting prospects for SIM Lite is "opportunity." This is a flexibly scheduled instrument that can be pointed at targets as faint as $V = 20$, with astrometric precision of a few microarcseconds. This capability, as with any fundamentally new instrument, offers the opportunity for unexpected discovery. One Science Team member summed it up this way:

> "As an astronomer, if you can't think of something truly interesting to do with SIM Lite, you should go back and think harder, because the opportunities are out there."

Many of the questions posed in this book recapitulate questions asked when astrophysics was just beginning, and in the case of planets, by some shepherd on a hilltop lost in antiquity. We have the opportunity to be the first to answer these questions both to a depth and across a breadth that will test the best theoretical models and that will leave a lasting foundation and legacy for the researchers who follow us.

Stephen J. Edberg

Stephen J. Edberg
SIM Lite System Scientist

Jet Propulsion Laboratory,
California Institute of Technology
Pasadena, California
January 2009

Acronyms and Abbreviations

ΛCDM	Lambda Cold Dark Matter
µas	microarcsecond
ABC	Astrometric Beam Combiner
ACS	Attitude Control System
AEB	Astrometric Error Budget
AGB	Asymptotic Giant Branch star
aMet	Angle Metrology
AO	Announcement of Opportunity
AOM	Acousto-Optic Modulator
ATC	Angle Tracking Camera
AU	Astronomical Unit
BB	Brassboard
BBB	Big Blue Bump
BD	Brown Dwarf
BDE	Brightness-Dependent Error
BH	Black Holes
BN	Becklin-Neugebauer star
CCD	Charge-Coupled Device
CFRP	Carbon-Fiber Reinforced Plastic
CMB	Cosmic Microwave Background
CMD	Color-Magnitude Diagrams
COMBO-17	Classifying Objects by Medium-Band Observations (a spectrophotometric 17-filter survey)
COPHI	Common Optical Path Heterodyne Interferometer
CSIRO	Commonwealth Scientific and Industrial Research Organization
CTE	Coefficient of Thermal Expansion
cTTs	Classical T Tauri stars

D	Distance
DCC	Double Corner Cube
DEBs	Detached Eclipsing Binaries
DETF	Dark Energy Task Force
DM	Dark Matter
DOR	Differential One-Way Ranging
DRM	Design Reference Mission
dSph	Dwarf Spheroidal galaxies

EB	Eclipsing Binary
EHZ	Earth Habitable Zone
EOS	Equation of State; Earth Observing System

FAP	False-Alarm Probability
FGLR	Flux-weighted Gravity Luminosity Relation
FOR	Field of Regard
FSM	Fine-Steering Mirror
FTC	Fringe Tracking Camera

G2T	Guide-2 Telescope
GEMS	Galaxy Evolution from Morphology and Spectra
GO	General Observer
GR	General Relativity
GTO	Guaranteed Time Observers

HB	Horizontal Branch
HMXB	High-Mass X-ray Binary
HRD	Hertzsprung-Russell Diagram
HST	Hubble Space Telescope
HVS	Hypervelocity Star
HZ	Habitable Zone

ICRF	International Celestial Reference Frame
IHZ	Inner Habitable Zone
IIPS	Inverse Interferometer Pseudo Star
IMF	Initial Mass Function
IMXB	Intermediate Mass X-ray Binary
IRU	Inertial Reference Unit
ISCO	Innermost Stable Circular Orbit
ISM	Interstellar Medium

JDEM	Joint Dark Energy Mission
JWST	James Webb Space Telescope

kpc	kiloparsec

LCROSS	Lunar Crater Observation and Sensing Satellite
LMXB	Low-Mass X-ray Binary
LOS	Line of Sight

MAM	Microarcsecond Metrology
mas	milliarcsecond
MASSIF	Masses and Stellar Systems with Interferometry
MLI	Multilayer Insulation
MLR	Mass-Luminosity Relation
MMR	Mean Motion Resonances
Mpc	Megaparsec
MS	Main Sequence
MSC	Michelson Science Center
MSTO	Main Sequence Turn Off

NA	Narrow Angle
NCVE	Non-Common Vertex Error
NExScI	NASA Exoplanet Science Institute
NPOESS	National Polar-orbiting Operational Environmental Satellite System
NPRO	Non-Planar Ring Oscillator
NS	Neutron Star
NYMG	Nearby Young Moving Groups

ODL	Optical Delay Line
ONC	Orion Nebula Cluster
OPD	Optical Pathlength Difference

pc	parsec
PFF	Pathlength Feed-Forward
PL	Period Luminosity
PMS	Pre-Main Sequence
PN	Planetary Nebula
POM	Pathlength Optic Mechanism
PPN	Parameterized Post-Newtonian
PSD	power spectral densities
PSF	point spread function
PSS	Precision Support Structure
PZT	Piezoelectric Transducer

RECONS	Research Consortium on Nearby Stars
RFP	Request for Proposal
RGB	Red Giant Branch
RLQ	Radio-Loud Quasars
RMS	Root-Mean-Square
RP	Rotational Parallax
RQQ	Radio-Quiet Quasars
RS	Schwarschild Radius
RV	Radial Velocity

SAVV	Sub-Aperture Vertex-To-Vertex
SB	Spectroscopic Binary
SCDU	Spectral Calibration Development Unit
sdO/B	Subdwarf O-type and B-type stars
SED	Spectral Energy Distribution
SIM	Space Interferometry Mission
SMA	Single-Measurement Accuracy

SMBH	Supermassive Black Hole
SME	Single-Measurement Error
SNR	Signal-to-Noise Ratio
SSTA	Single-Strut Test Article
STB-3	Three-Baseline System-Level testbed

TA	Test Article
TDI	Time Delay Integration
TOM	Thermo-Opto-Mechanical testbed
TOO	Target of Opportunity

| VLBI | Very Long Baseline Interferometry |

WA	Wide Angle
WD	White Dwarf
WIMP	Weakly Interacting Massive Particle
WLR	Wind-momentum Luminosity Relation
WR	Wolf-Rayet star
wTTs	Weak-lined T Tauri stars

ACKNOWLEDGMENT

Search for Habitable Worlds

Reveal the population, masses, and orbits of terrestrial and giant planets around nearby stars and the formation, evolution, and architecture of planetary systems.

Dark Matter and Galaxy Assembly

Determine the age of and probe the hierarchical formation history of the Milky Way. Map the distribution of local dark matter and place limits on the mass of the dark matter particle.

Precision Stellar Astrophysics

Ultraprecise measurements of the masses and luminosities of the highest- and lowest-mass stars allow testing of models of stellar evolution, from brown dwarfs to black holes.

Supermassive Black Hole Astrophysics

Understand how black holes accelerate jets, from stellar masses to galaxy central engines.

For more information about the SIM Lite Astrometric Observatory, visit our Web page at — sim.jpl.nasa.gov